

**Modelling infection risk due to  
environmental contamination in hospital  
single and multi-bed ward  
accommodation**

Marco-Felipe King

Submitted in accordance with the requirements for the degree of

*Doctor of Philosophy*

University of Leeds

School of Civil Engineering

July 2013



---

## *Intellectual Property and Publication Statements*

The candidate confirms that the work submitted is his own, except where work which has formed part of jointly authored publications has been included. The contribution of the candidate and the other authors to this work has been explicitly indicated below. The candidate confirms that appropriate credit has been given within the thesis where reference has been made to the work of others.

The work in Chapter 4 of the thesis has appeared in publication as follows:

M-F. King, M.A. Camargo-Valero, C.J. Noakes and P.A. Sleigh. CFD validation of controlled bioaerosol release for simulating droplet transmission of live pathogens. *Indoor Air Conference, Austin, Texas*, June 11th-18th, 2011

M-F. King, M.A. Camargo-Valero, C.J. Noakes and P.A. Sleigh. Bioaerosol Deposition in Single and Two-Bed Hospital Rooms: A Numerical and Experimental Study. *Building and Environment*, 59:436-447, 2013

I was responsible for planning and execution of the experiments, the CFD and the analysis of the data. The contribution of the other authors was advice in planning experiments and manuscript editing.

The work in Chapters 5, 6 and 7 of the thesis has appeared in publication as follows:

M-F. King, C.J. Noakes and P.A. Sleigh. Can single rooms reduce the risk of hospital-acquired infection? *Bioaerosols and the Built Environment Conference, University of Leeds*, June 26th - 27th, 2013.

I was responsible for planning and execution of the observational study and the data analysis. The contribution of the other authors was advice and manuscript editing.

This copy has been supplied on the understanding that it is copyright material and that no quotation from the thesis may be published without proper acknowledgement.

© 2013 The University of Leeds and Marco-Felipe King.

The right of Marco-Felipe King to be identified as Author of this work has been asserted by him in accordance with the Copyright, Designs and Patents Act 1988.

## *Acknowledgements*

I would like to extend my sincere gratitude to my supervisors Dr. Catherine Noakes and Dr. Andrew Sleigh for their vibrant enthusiasm for this research project. Their continued mentoring, involvement and invaluable suggestions have been vital motivating factors. I am also glad to have had the opportunity to work with ARUP under the guidance of Mr. Phil Nedin, Dr. Jake Hacker and Dr Kat Roberts - whose expertise, support and patience have been indispensable. My gratitude is also due to Dr. Carl Gilkeson, Dr. Miller Camargo-Valero and Dr. Amir Khan for their continuous mentoring, helpful suggestions, logistics and guidance.

Most importantly I truly value the love, support and understanding of my patient love Fiona, who is by now no doubt, also an eminent expert in CFD, stochastic modelling and pathogen transfer. Underlining my work throughout, and for which I am eternally grateful, is the unconditional love and support from Mama and Papa, both of whom have spent countless hours with me, pondering the finer details of Markov chain modelling.

And last, but not least, my thanks to the [TEX.stackexchange.com](https://www.tex.stackexchange.com) forum and community for their invaluable help in formatting this thesis.

## *Abstract*

This research considers whether hospital single rooms are better than multi-bed accommodation at reducing the risk of healthcare-acquired infections. The focus is to provide a mathematical model which quantifies the contamination levels of healthcare workers' (HCW) hands from surfaces within rooms. This is achieved through a multidisciplinary approach involving computational fluid dynamics (CFD) and biological experimental techniques coupled with clinical observation and Markov Chain Monte-Carlo modelling.

Spatial deposition of aerosolised bacteria was measured in a test room under different layouts: An empty room, a single-bed and a two-bed room. Comparison with CFD demonstrates realistic predictions of spatial deposition, and a Reynolds Stress turbulence model yields superior results compared to other models.

An observational study of patient care at a Welsh hospital showed that hand hygiene choice and frequency varied strongly. HCWs performing short episodes of care had a predilection for alcohol rub. In other care types the usage of alcohol rub or soap and water was 50/50.

HCW surface contact patterns in rooms were modelled by a Markov chain and fed into a mathematical model to calculate the pathogen colonisation level on hands after patient care. A parametric study highlights the differences between care type and colonisation. Results indicate that hand hygiene carried out by nurses may need to be rethought.

The model was applied using CFD predicted spatial contamination levels, in both multi-bed and single rooms. When ventilation rates were equal, hand colonisation differences were small. Results demonstrate that this depends on care type, the number of surface contacts and in particular on the distribution of surface pathogens. Contamination on the HCWs' hands decreases monotonically after care in single rooms; however increases during contact with subsequent patients in multi-bed rooms. Enforcing hand hygiene due to the knowledge of an infectious patient makes single rooms significantly less risk prone.

# Contents

<b>Acknowledgements</b>	<b>iv</b>
<b>Abstract</b>	<b>v</b>
<b>List of Figures</b>	<b>xiii</b>
<b>List of Tables</b>	<b>xix</b>
<b>Abbreviations</b>	<b>xxi</b>
<b>Symbols</b>	<b>xxiii</b>
<b>1 Introduction</b>	<b>1</b>
1.1 Overview	2
1.2 Health Care Acquired Infections (HCAI), What Are They?	3
1.2.1 Prevalence of HCAI	4
1.2.2 Why Are HCAI So Dangerous?	6
1.3 Disease Transmission Routes	7
1.3.1 Contact Transmission	7
1.3.1.1 Environmental contamination	8
1.3.2 Airborne and Droplet Transmission	9
1.3.3 Common Vehicle and Vector Borne Transmission	10
1.4 Hospital Room Design	10
1.5 Infection Transmission Modelling	12
1.5.1 Contact Transmission Models	12
1.5.2 Airborne Transmission Models	13
1.5.3 Importance of Airflow Patterns	14
1.6 Aims and Objectives	15
1.6.1 Hypothesis	15
1.6.2 Objectives and Research Methodology	17
1.6.3 Layout of This Thesis	19
<b>2 Hospital room design</b>	<b>23</b>
2.1 General Overview of Hospital Room Design	23
2.1.1 A Brief History of UK Ward Types	28
2.1.2 Evidence Based Design	29

2.1.3	Patient Centered Design: Patient Choice . . . . .	31
2.1.4	HBN04-01: In-Patient Accommodation . . . . .	32
2.1.4.1	Multibed-rooms . . . . .	33
2.1.4.2	Single Rooms . . . . .	34
2.1.4.3	Bevan-Ward research project . . . . .	38
2.2	Heating, Ventilation and Air-Conditioning (HVAC) Guidelines . . . . .	40
2.2.1	Mechanical Ventilation . . . . .	43
2.2.1.1	Mixing and displacement ventilation . . . . .	44
2.2.2	Natural Ventilation . . . . .	46
2.2.3	Advanced Passive Ventilation . . . . .	48
<b>3</b>	<b>Infection transmission pathways and modelling approaches</b>	<b>52</b>
3.1	Understanding Infection Transmission Pathways . . . . .	52
3.1.1	Contact Transmission . . . . .	53
3.1.2	Airborne Particles, Droplets and Bioaerosols . . . . .	55
3.1.2.1	Droplet vs. Airborne transmission . . . . .	56
3.1.2.2	Aerial transmission of HCAI . . . . .	59
3.1.3	Environmental Factors Influencing Pathogen Viability . . . . .	60
3.1.3.1	Environmental surface contamination . . . . .	62
3.1.3.2	Cleaning procedures . . . . .	63
3.2	Mathematical Epidemiology and Quantitative Infection Risk Modelling . . . . .	64
3.2.1	Population Models and the Epidemic Threshold: $R_0$ . . . . .	65
3.2.2	Compartmental Models . . . . .	66
3.3	Stochastic Transmission Effects . . . . .	69
3.3.1	Markov Chains . . . . .	71
3.3.1.1	Discrete time Markov chains (DTMC) . . . . .	71
3.3.1.2	Calculating $n^{th}$ step transitions . . . . .	73
3.3.2	Airborne Transmission Models . . . . .	75
3.3.2.1	General assumptions . . . . .	76
3.3.3	Unsteady Quanta Production . . . . .	77
3.4	Modelling Individual Patient Risk . . . . .	80
3.4.1	Single-Hit Dose-Response Models . . . . .	80
3.4.1.1	Exponential Model . . . . .	82
3.4.1.2	Beta-Poisson Model . . . . .	83
3.4.1.3	Beta-Binomial Model . . . . .	84
3.4.1.4	Infection Heterogeneity: Statistical non-identifiability . . . . .	84
3.4.2	Cumulative Dose-Response Models . . . . .	85
3.5	Computational Fluid Dynamics: Modelling Airborne Particles in Buildings . . . . .	88
3.5.1	CFD Approaches to Model Bioaerosols . . . . .	89
3.5.1.1	Passive scalar transport . . . . .	89
3.5.1.2	Lagrangian particle tracking . . . . .	92
3.5.2	Other CFD and Experimental Approaches . . . . .	93
3.5.2.1	Schlieren or shadowgraph photography . . . . .	95
3.5.2.2	Small- and large-scale models . . . . .	95
<b>4</b>	<b>Bioaerosol deposition: Experimental and CFD comparison</b>	<b>100</b>

4.1	Experimental Methodology . . . . .	101
4.1.1	Overview of Experimental Scenarios . . . . .	101
4.1.1.1	Heated mannequin . . . . .	105
4.1.2	Characterising the Airflow Patterns . . . . .	106
4.1.3	Bioaerosol Generation . . . . .	106
4.1.4	Bioaerosol Collection . . . . .	107
4.1.5	Data Analysis . . . . .	110
4.2	CFD Methodology . . . . .	112
4.2.1	Turbulence Modelling . . . . .	112
4.2.1.1	Two equation Eddy Viscosity Model $k-\epsilon$ . . . . .	113
4.2.1.2	Seven equation Reynolds' Stress Model . . . . .	115
4.2.1.3	Large eddy simulation . . . . .	116
4.2.1.4	Choosing a turbulence model . . . . .	116
4.2.2	Artificial Viscosity . . . . .	116
4.2.3	High Resolution Schemes . . . . .	117
4.2.4	Defining Ventilation Diffusers . . . . .	119
4.2.4.1	Velocity prescription . . . . .	119
4.2.4.2	Momentum Method . . . . .	120
4.2.4.3	Box Method . . . . .	121
4.2.4.4	Turbulence intensity . . . . .	121
4.2.5	Instruments and Instrumentation Error . . . . .	122
4.2.6	Boundary Conditions . . . . .	123
4.2.7	Modelling Particle Deposition . . . . .	125
4.2.7.1	Discrete random walk: DRW . . . . .	125
4.2.8	Mesh Generation . . . . .	127
4.2.8.1	Mesh refinement . . . . .	128
4.2.9	Preliminary Mesh-Independence . . . . .	129
4.2.9.1	Particle-mesh independence . . . . .	131
4.2.9.2	Convergence criteria . . . . .	131
4.3	Results and Discussion . . . . .	132
4.3.1	Scenario 1: Empty Room . . . . .	132
4.3.1.1	Airflow patterns . . . . .	132
4.3.1.2	Bioaerosol deposition . . . . .	136
4.3.2	Scenario 2: Single Patient Room . . . . .	141
4.3.2.1	Airflow patterns . . . . .	141
4.3.2.2	Bioaerosol deposition . . . . .	143
4.3.3	Scenarios 3 and 4: Double Patient Room . . . . .	145
4.3.3.1	Airflow patterns . . . . .	146
4.3.4	The Effect of a Curtain Partition . . . . .	149
4.3.4.1	Bioaerosol deposition . . . . .	151
4.4	Conclusions . . . . .	155
4.4.1	Implications of Results . . . . .	156
<b>5</b>	<b>HCW behavioural and observational study</b>	<b>158</b>
5.1	Background . . . . .	159
5.1.1	Hand Hygiene . . . . .	160

5.1.1.1	Guidelines . . . . .	161
5.1.1.2	Types of hand hygiene opportunities . . . . .	163
5.1.1.3	Personal protection equipment (PPE) usage . . . . .	164
5.1.2	Hand Hygiene Compliance . . . . .	164
5.2	Observational Study: Ysbyty Aneurin Bevan (YAB) . . . . .	166
5.2.1	Objectives . . . . .	166
5.3	Methodology . . . . .	167
5.3.1	Definition of Activities . . . . .	167
5.3.2	Definition of Surface Categories . . . . .	168
5.3.3	Observational Strategy . . . . .	169
5.3.4	Statistical Analysis . . . . .	171
5.4	Results & Discussion . . . . .	172
5.4.1	Surface Contact Distributions . . . . .	173
5.4.1.1	Activity profile . . . . .	173
5.4.1.2	High contact surfaces . . . . .	174
5.4.1.3	Surface contact distribution by surface category . . . . .	176
5.4.1.4	Contact frequency distribution . . . . .	179
5.4.1.5	Duration of care . . . . .	182
5.4.2	Quantitative Analysis of Hand Hygiene . . . . .	185
5.4.2.1	Probability of hand hygiene . . . . .	185
5.4.2.2	Preference for hand antiseptics type . . . . .	187
5.4.2.3	Influence of patient contact on hand hygiene . . . . .	188
5.5	Summary . . . . .	190
5.6	Implementation of the Results . . . . .	190
<b>6</b>	<b>Pathogen accretion model: PAM</b> . . . . .	<b>191</b>
6.1	Introduction to Dermal Models . . . . .	192
6.1.1	Background . . . . .	195
6.2	Overview and Objectives of the Dermal Model . . . . .	197
6.3	Model Structure and Approach . . . . .	197
6.3.1	Simulating an Individual HCW . . . . .	198
6.3.1.1	Method 1: Empirical marginal frequency density ( $\hat{P}$ ) . . . . .	198
6.3.1.2	Method 2: The Markov Chain . . . . .	200
6.3.1.3	Bootstrapping, Laplace smoothing and confidence intervals of $\hat{P}_{ij}$ . . . . .	202
6.4	Model Development: PAM . . . . .	205
6.4.1	Model Input: Contact Surface Area ( $A$ ) . . . . .	206
6.4.2	Model Input: Surface Pathogen Load ( $V$ ) . . . . .	207
6.4.3	Model Input: Surface-To-Hand Transfer Efficiency ( $\lambda$ ) . . . . .	209
6.4.4	Model Input: Hand-To-Surface Transfer Efficiency ( $\beta$ ) . . . . .	213
6.4.5	Model Input: Antisepsis Efficacy ( $h$ ) . . . . .	214
6.4.5.1	Gloves . . . . .	214
6.4.5.2	Hand washing . . . . .	216
6.4.5.3	Alcohol rub . . . . .	219
6.4.5.4	Summary . . . . .	220
6.5	Preliminary Results and Validation . . . . .	220

6.6	Model Sensitivity Analysis . . . . .	222
6.6.1	Methodology . . . . .	224
6.6.1.1	Effect of unobserved Markov chain transitions . . . . .	224
6.6.2	Pearson Correlation Analysis . . . . .	225
6.6.3	Sobol Indices $S_i$ . . . . .	229
6.6.4	The Total Effect $S_{Ti}$ . . . . .	231
6.6.5	Linear Loading of CFU (Y) Without Deposition . . . . .	232
6.7	Uncertainty Analysis and Parametric Study . . . . .	234
6.7.1	Care Type . . . . .	234
6.7.2	Increasing Hand-Hygiene Probability . . . . .	236
6.7.3	Increasing Surface Cleanliness ( $V$ ) . . . . .	237
6.8	Summary . . . . .	238
<b>7</b>	<b>Application of PAM and Quantification of Risk</b>	<b>240</b>
7.1	Scenario Description and CFD Case Set-Up . . . . .	241
7.1.1	Single Patient Room: YAB . . . . .	242
7.1.1.1	Model set-up . . . . .	242
7.1.1.2	Mesh generation . . . . .	243
7.1.1.3	Bioaerosol injection . . . . .	243
7.1.2	HBN04-01 Four-Bed Patient Room . . . . .	244
7.1.2.1	Model set-up . . . . .	244
7.2	CFD Results and Discussion . . . . .	247
7.2.1	Airflow Pathways . . . . .	247
7.2.2	Bioaerosol Deposition . . . . .	247
7.3	Application of PAM to YAB Single Room and HBN04-01 Multi-Bed Accommodation . . . . .	257
7.3.1	HCW Behaviour in the HBN04-01 Four-Bed Ward . . . . .	257
7.3.2	PAM Results and Discussion . . . . .	258
7.3.2.1	Single bed room: YAB . . . . .	258
7.3.2.2	Combined single and multi-bed room comparison . . . . .	260
7.4	Quantifying Patient Risk and Application of an Exponential Dose-Response Model . . . . .	263
7.4.1	Relative Risk . . . . .	265
7.4.1.1	Prior knowledge of infection . . . . .	269
7.5	Summary . . . . .	271
<b>8</b>	<b>Implications of results, conclusions and further research</b>	<b>272</b>
8.1	Key Findings . . . . .	272
8.1.1	Bioaerosol Deposition: Experimental and Numerical Approaches . . . . .	273
8.1.2	HCW Behavioural and Observational Study . . . . .	274
8.1.3	Quantification of Risk and Application of PAM . . . . .	275
8.2	Future Research . . . . .	277
8.2.1	Experimental and Numerical Particle Deposition . . . . .	277
8.2.2	Clinical Observational Studies . . . . .	278
8.2.3	Pathogen Accretion Models . . . . .	279
8.3	Implications of the Study and Conclusions . . . . .	279

<b>A Appendix A</b>	<b>281</b>
<b>B Appendix B</b>	<b>285</b>
<b>Bibliography</b>	<b>287</b>



# List of Figures

1.1	Venn diagram showing overlapping of each discipline involved in creating a multidisciplinary approach. . . . .	3
1.2	Percentage distribution of HCAI in the USA [1]. . . . .	5
1.3	Bacterial resistance to $\beta$ -lactam antibiotics [2]. Reproduced courtesy of the American Society of Microbiology. . . . .	7
1.4	Transmission pathways set out by the CDC [3]. . . . .	8
1.5	NHS poster reproduction of gentleman sneezing, courtesy of The Stationery Office, UK. . . . .	9
1.6	Flowchart of typical disease transmission dynamics in an SEIR model. Bullet points show important environmental factors affecting transfer from category <i>Susceptible</i> to <i>Exposed</i> . Equally they depict control parameters dictating the rate of progress from <i>Infectious</i> to <i>Removed</i> . . . . .	13
1.7	Flowchart of model development. . . . .	22
2.1	University College Hospital, London, UK. Image Copyright Nigel Chadwick. This work is licensed under the Creative Commons Attribution-Share Alike 2.0 Generic Licence. . . . .	24
2.2	Percentage spending of GDP on health care by EU countries between 2000 and 2012, source OECD [4]. . . . .	25
2.3	Four tenets of design for hospitals in the UK according to HBN04-01 [5]. . . . .	27
2.4	General UK ward design types reproduced, with permission, from Alalouch et al. [6]. . . . .	29
2.5	Examples of hospital multi-bed ward design evolution ca. 1870-2010. . . . .	30
2.6	Patient preference for bed positioning. +++ = Most preferred location, - - = least preferred. (Star = nurse station). Adapted from Alalouch et al. [6]. . . . .	32
2.7	Typical room layout of the four-bed patient accommodation in the UK [5]. . . . .	34
2.8	HBN04-01 single room. . . . .	35
2.9	Bevan Ward project comparison of ward layout and room design. . . . .	38
2.10	Ventilation guidelines for hospital and clinical areas. . . . .	40
2.11	Mechanical ventilation of hospital cross-section. Adapted with kind permission from [7]. . . . .	44
2.12	Mechanical ventilation: Mixing and displacement methods. . . . .	46
2.13	Passive ventilation strategies and implementation. . . . .	47
2.14	Passive ventilation examples. . . . .	48
2.15	Example air streamlines of buoyancy driven natural ventilation at Alt-nagelvin Area Hospital, Northern Ireland. [8]. . . . .	49
2.16	Advanced natural ventilation, adapted from Lomas et al. [9]. . . . .	50

2.17	Examples of advanced building design for mitigating the effects of climate change. . . . .	51
3.1	Mortality rate plotted against year in the obstetrics ward at the <i>Wiener Allgemeine Krankenhaus</i> [10]. . . . .	54
3.2	Horizontal transmission diagram including endogenous and exogenous transmission routes. . . . .	55
3.3	Diameter ranges in $\mu\text{m}$ of some commonly found indoor particles [11]. . . . .	56
3.4	Wells' original evaporation curve representing particles falling 2m in quiescent air. Adapted from Xie et al. [12]. . . . .	57
3.5	Percentage of times transfer from the originating surface was detected through swabbing. Adapted from Duckro et al. [13] . . . . .	63
3.6	Non-dimensionalised SIR model with $R_0 = 2.133$ . . . . .	67
3.7	Flow diagram of the SEIR model . . . . .	68
3.8	Non-dimensionalised SEIR model, $N=100$ , $R_0 = 2.133$ . . . . .	69
3.9	SIS model comparing stochastic vs. deterministic solutions, adapted from Allen et al. [14]. . . . .	75
3.10	Threshold vs non-threshold concept of infection probability. Adapted from Sze et al. [15]. . . . .	80
3.11	A typical dose-response curve for norovirus, adapted from Pujol et al. [16]. . . . .	81
3.12	Stochastic cumulative dose model by Pujol et al. [16] . . . . .	87
3.13	Tracer spread within a hospital isolation room. Adapted from work by King [17]. . . . .	91
3.14	Example of multiple particle tracks coloured by residence time within an enclosed environment. . . . .	93
3.15	Use of mannequins for tracer gas techniques and CFD comparison. . . . .	94
3.16	Schlieren set-up and photography of a breathing subject reproduced with kind permission from Tang et al. [18]. . . . .	95
3.17	Water bath model of tracer escaping from an isolation, reproduced from of Eames et al. [18], courtesy of the Royal Society Publishing. . . . .	96
3.18	Mechanically ventilated experimental facilities of different types. . . . .	97
4.1	PaCE chamber geometry . . . . .	102
4.2	Single room set-up . . . . .	103
4.3	Double patient room . . . . .	104
4.4	Heated mannequin thermal image . . . . .	105
4.5	Airflow measurements within the PaCE chamber . . . . .	106
4.6	Scenario 1: Isotropic release from inside red diffuser ball in centre of room . . . . .	107
4.7	Location of settle plates in the empty chamber scenario with photograph showing a sampling point with a typical group of 5 plates (scenario 1) . . . . .	109
4.8	Single-bed room experimental set up. Petri dishes were located on surfaces representing the Bed, Chair, Table and Sink . . . . .	109
4.9	Double-bed room experimental set up Petri dishes were located on surfaces representing the Bed, Chair and Table for each patient and the Sink. . . . .	110
4.10	Representation of a discontinuity via an upwind scheme . . . . .	117
4.11	Second order upwind scheme . . . . .	118
4.12	Typical four-way diffuser (0.5m x 0.5m) . . . . .	120
4.13	Simplified diffuser geometry . . . . .	120

4.14	Diffuser opening . . . . .	120
4.15	Measurement surfaces away from the grille . . . . .	121
4.16	A single surface showing 9 measurement points . . . . .	121
4.17	Hypothetical plot of fluctuating velocity along time-averaged velocity . . . . .	122
4.18	Anemometry measurements of inlet diffuser air velocity . . . . .	124
4.19	Particle tracking within a room showing the effects of modelling the dispersion with and without DRW . . . . .	126
4.20	Hexahedral meshing within the single room . . . . .	127
4.21	Hexahedral meshing within the single room . . . . .	128
4.22	Hexahedral mesh refinement from bulk flow area to boundary wall highlighting the cell size reductions in red . . . . .	129
4.23	Anemometry comparison against three hexahedral mesh sizes for the empty chamber (Scenario 1). Errorbars represent one standard deviation either side of the mean. . . . .	130
4.24	Particle deposition percentage on all surfaces within Scenario 1: The empty room . . . . .	131
4.25	Velocity vectors 0.001-0.07(m/s) plotted on planes within the empty room . . . . .	133
4.26	Anemometry comparison against k- $\epsilon$ RNG and RSM turbulence models for the empty chamber (Scenario 1). Errorbars represent one standard deviation either side of the mean. . . . .	134
4.27	Representative images from <i>scenario 1</i> . . . . .	136
4.28	Comparison between experimental data and numerical deposition predicted by the two turbulence models. Errorbars represent one standard deviation either side of the mean. . . . .	137
4.29	Scatter plots showing correlation between experimental data and numerical deposition predicted by the two turbulence models . . . . .	138
4.30	Velocity vectors (0.001-0.07m/s) superimposed onto temperature contours in single room. . . . .	142
4.31	Comparison between numerical and experimental deposition on furniture surfaces in the single patient room. Errorbars show one standard deviation either side of the mean. . . . .	143
4.32	Velocity contours (0.001-0.07m/s) superimposed onto temperature contours. No intervention scenarios 3a 3b. . . . .	147
4.33	Velocity contours (0.001-0.07m/s) superimposed onto temperature contours. Partial partition scenarios 4a and 4b . . . . .	148
4.34	Influence of curtain and source location on experimentally measured deposition. Errorbars represent one standard deviation either side of the mean. . . . .	149
4.35	Particle tracking for scenarios 3a,b,4a and b. Coloured by residence time (s). . . . .	152
4.36	Influence of curtain and source location on experimentally measured deposition compared to numerical results. Errorbars show one standard deviation either side of the mean. . . . .	153
4.37	Comparison between scenarios 3 and 4. Spatial comparison of particle deposition with and without a permanent partial partition . . . . .	154
5.1	Venn diagram showing the distribution of average contact counts per episode of care as observed by Hayden et al. [19]. . . . .	160

5.2	5 moments of hand hygiene in the NHS, reproduced with kind permission from the WHO. . . . .	162
5.3	Room surface layout of YAB single room. . . . .	169
5.4	Ordered surface contacts for any care type. . . . .	175
5.5	Average surface contacts for both patient and other environmental surfaces, categorised for care type. Errorbars represent one standard deviation either side of the mean. . . . .	175
5.6	Episodes of care containing patient and/or environmental contacts. . . . .	176
5.7	Surface contact distribution subdivided by care type. . . . .	177
5.8	Probability density histograms of surface contact counts broken down by care type. . . . .	178
5.9	Surface contact frequency categorised by care-type. Where Eq. stands for equipment. . . . .	180
5.10	Contact duration categorised by care-type. Errorbars represent one standard deviation either side of the mean. . . . .	182
5.11	Total surface contacts for each type of care plotted over time. . . . .	184
5.12	Cumulative probability of hand hygiene category subdivided by care type. .	186
5.13	Probability of hand hygiene by surface contact count subdivided by care type.	187
6.1	Stages involved in pathogen transfer reproduced from Pittet et al. [20]. . . .	193
6.2	Example of surface contacts of HCW #50 performing a standard episode of care. . . . .	202
6.3	Bootstrap confidence intervals for $\tilde{P}_{\text{personal care}}$ . . . . .	204
6.4	Probability density function of hand surface area contact parameter $A$ . . . .	207
6.5	Empirical CFU values for test case PaCE chamber single room parameter $V$ .	209
6.6	Empirical comparison between transfer of bacteria to porous and non-porous surfaces $\lambda$ . Data reproduced from Lopez et al. [21]. . . . .	211
6.7	Comparison between a non-porous surface-to-hand and hand-to-surface transfers . . . . .	214
6.8	Distribution of CFU adhering to nurses' hands after care, comparing gloved vs. ungloved hands. Data reproduced from Pittet et al. [22]. . . . .	215
6.9	Hand hygiene efficacy of antibacterial soap comparing resident vs. exogenous microflora reduction (data from Montville et al. [23]). . . . .	217
6.10	Hand hygiene efficacy of three different types of hand-antiseptics. Data from Montville et al. [23]. . . . .	221
6.11	Scatter plot of CFU ( $Y$ ) against patient contact for <i>direct care</i> . . . . .	221
6.12	Q-Q plot of published empirical data from Pittet et al. [22] against modelled data by PAM. . . . .	223
6.13	Confidence intervals representing the percentage difference between mean $Y$ values calculated by the maximum likelihood estimates $\hat{P}$ , and those calculated by $\tilde{P}_{\text{lower}}$ and $\tilde{P}_{\text{upper}}$ . Errorbars represent one standard deviation either side of the mean. . . . .	225
6.14	Visual inspection of input parameters plotted against output $Y$ . . . . .	227
6.15	Conditional variance of $Y$ within the red box representing a specific value $X_i = x_i^*$ . . . . .	230
6.16	Comparison between unidirectional and bi-directional transfer of CFU . . .	233
6.17	CFU count by care type before and after hand-hygiene . . . . .	235

6.18	Comparison of CFU values due to improved hand hygiene. Errorbars represent one standard deviation either side of the mean. . . . .	237
6.19	Comparison between model or empirical derived CFU counts and the baseline quantity proposed by Dancer et al. [24] . . . . .	238
7.1	Photo of inside a single room at YAB. . . . .	242
7.2	YAB single room layout and CFD geometry. . . . .	244
7.3	Photo of Bradford Royal Infirmary 4-bed maternity ward. . . . .	245
7.4	Bradford Royal Infirmary multi-bed room. . . . .	245
7.5	Close-up of surfaces within a patient cubicle in the multi-bed room. . . . .	246
7.6	Velocity magnitude contours and vectors on horizontal ( $y=1.5\text{m}$ ) and vertical ( $x=2\text{m}$ ) planes within the YAB single room. . . . .	248
7.7	Velocity magnitude contours and vectors on horizontal plane ( $y=1.5\text{m}$ ) within HBN04-01 4-bed room. . . . .	249
7.8	Particle tracks by colour ID within the single room. . . . .	250
7.9	Particle tracks coloured by particle ID, when released from all infectious patients within the multi-bed room. . . . .	251
7.10	Particle deposition on surfaces within both YAB single room and HBN04-01 4 bed accommodation. Displayed as percentage deposition. Multi-bed release positions 1-4. Comparison shown between $4 \text{ ac.h}^{-1}$ and $6 \text{ ac.h}^{-1}$ for each case. . . . .	252
7.11	Particle deposition quantities on horizontal surfaces within the YAB single room displayed as $\text{CFU}/\text{cm}^2$ . Legend: E=Equipment, P=Patient, H=Hygiene Products, N=Near-bed surfaces, F=Far-bed surfaces. . . . .	253
7.12	Particle deposition quantities on horizontal surfaces within the HBN04-01 4 bed accommodation. Displayed as $\text{CFU}/\text{cm}^2$ . Multi-bed release positions 1-4. Comparison shown between $4 \text{ ac.h}^{-1}$ and $6 \text{ ac.h}^{-1}$ for each case. Legend: E=Equipment, P=Patient, H=Hygiene Products, N=Near-bed surfaces, F=Far-bed surfaces . . . . .	254
7.13	Adjusted HCW behaviour based on ward observations by Smith et al. ([25] and private communication). Patient charts become near-bed surfaces in the multi-bed scenario instead of the far-bed surfaces in the single room. . . . .	258
7.14	Boxplots showing normalised CFU values for YAB single room, comparing 4 and $6 \text{ ac.h}^{-1}$ . . . . .	259
7.15	Comparison of normalised CFU values (Y) against YAB single room <i>direct care</i> after hand hygiene: YAB single room vs HBN04-01 4-bed room. . . . .	260
7.16	Comparison of normalised Y values between single room (red) and cumulative sum for each release location within the multi-bed room (black). . . . .	264
7.17	HCW route for all care types except <i>miscellaneous care</i> within both the YAB single room and HBN04-01 4 bed room. Star indicates infectious patient location in the first scenario. . . . .	265
7.18	Boxplots show normalised Y values after an episode of <i>direct care</i> following care of one infected patient. . . . .	266
7.19	Comparing average risk during care to 3 uninfected patients within single and multi-bed room relative to <i>direct care</i> . $\alpha = 0.069$ . Where infection status of all patients is unknown. Errorbars represent one standard deviation either side of the mean. . . . .	268

- 7.20 Comparing average risk during care to 3 uninfected patients within single and multi-bed room relative to *direct care*. Antisepsis is enforced after care with the infectious patient.  $\alpha = 0.069$ . When infectious patient is identified. Errorbars represent one standard deviation either side of the mean. . . . . 270

# List of Tables

2.1	Health Building Notes guidelines as of 2013. . . . .	26
2.2	Perceived and potential advantages and disadvantages of hospital single rooms according to York HEC [26]. . . . .	33
2.3	Single room construction from HBN04-01:In-patient accommodation. . . . .	36
2.3	(continued) Single room construction from HBN04-01:In-patient accommodation. . . . .	37
2.4	Reported advantages and disadvantages in the Green, Lilac and Blue single rooms from the Bevan ward experiment 2009. . . . .	39
2.5	Ventilation strategy as set out in Appendix 2 of HTM03-01 for some example health care facilities. S=Mechanical supply, E=Mechanical extract, N=Natural ventilation. . . . .	41
3.1	Droplet sizes and definitions. . . . .	58
3.2	Viability of some Department of Health (UK) surveillance microorganisms. . . . .	61
3.3	Examples of some pathogens and their cited modes of transmission . . . . .	62
3.4	Transition states for the stochastic model by Pujol et al. [16] . . . . .	86
3.5	Advantages and disadvantages of some airflow visualisation techniques. Adapted from Tang et al. [18]. . . . .	98
4.1	Experimental case scenarios, single and double-room particle deposition . . . . .	102
4.2	Dimensions of surfaces and items in the double room . . . . .	105
4.3	Correlation between CFD and experimental results for both turbulence models. The p-value corresponds to the Wilcoxon-Ranksum test comparing median differences between ranks. . . . .	139
4.4	Statistical analysis of correlation between experimental deposition and CFD for scenarios 3 and 4. p-values do not reject null-hypothesis of 0 median differences between ranks. . . . .	154
5.1	Fulkerson scale ranking hand hygiene [27]. . . . .	162
5.2	Hand-washing opportunities from Epic2: 5 moments [28] . . . . .	163
5.3	Care type and examples of each. . . . .	168
5.4	Room surface categorisation . . . . .	168
5.5	Observed activities or care types at YAB. . . . .	173
5.6	Breakdown of the number of surface contacts sample mean $\bar{x}$ and deviation $s$ for care types observed at YAB. . . . .	179
5.7	Correlation coefficients and p-values for time versus surface contacts. Where $\dagger$ represents a statistically significant value. . . . .	183

5.8	Correlation coefficients and p-values for hand washing probability versus surface contacts. Where † represents a statistically significant value at the 10% level. . . . .	187
5.9	Care type categorised by hand hygiene opportunity. . . . .	188
5.10	Probabilities of patient contact influencing hand hygiene for each care type given with the standard deviation. Where † represents a statistically significant value. D.C.=Direct care, H=housekeeping, M.T.=Mealtimes, M.R.=Medication rounds, M=Miscellaneous, P.C.=Personal care. . . . .	189
6.1	Probabilities for surface contacts based on care type and surface category. . . . .	199
6.2	Directed probabilities of moving from surface $i$ to surface $j$ . . . . .	201
6.3	Published data on percentage transfers ( $\lambda$ ) from surfaces onto hands . . . . .	213
6.4	Literature for % transfer through clinical permeable gloves onto hands. . . . .	216
6.5	Literature for $\log_{10}$ reductions of CFU for hand-washing. Where i=in-vivo and t=in-vitro, and CHG denotes chlorhexidine gluconate. $N \sim (\mu, \sigma)$ represent the normal distribution with parameters $\mu$ and $\sigma$ . . . . .	218
6.6	Literature for $\log_{10}$ reductions of CFU for waterless alcohol rub, displayed as a continuous distribution or as a range. Where i=in-vivo and t=in-vitro testing. . . . .	219
6.7	Pearson correlation coefficient comparing Y against the different variables. * indicates inclusion of probability of hand-antisepsis not just efficacy. . . . .	228
6.8	First order and total sensitivity factors for each input factor for PAM . . . . .	232
6.9	Average decontamination of hands for all care types and rankings from best to worst performers. † lower ranking is better. Higher $\log_{10}$ reduction is better. All hygiene types are included. . . . .	235
7.1	CFD case names and layout. . . . .	241
7.2	Boundary conditions for YAB single room. . . . .	243
7.3	Boundary conditions for the multi-bed room . . . . .	246
7.4	Wilcoxon rank test p-values for particle deposition distribution comparison between 4 ac.h <sup>-1</sup> and 6 ac.h <sup>-1</sup> . † denotes significant difference at the 10% level . . . . .	256
7.5	Ranking by mean and maximum of care types (lower is better, meaning cleaner hands) after hand hygiene in YAB single room. . . . .	259
7.6	Comparison of infectious patient location by ranking via mean, median and maximum. A higher rank is better. † indicates a tied rank. . . . .	262
7.7	Comparison of CFU values after hand hygiene between YAB single room and HBN04-01 4-bed room via a one-sided non-parametric Wilcoxon ranksum test hypothesising that 50% of the values obtained from the multi-bed room are higher than those from YAB while performing the same activities. * denotes significant results at 2.5% level. † denotes significant values at 5% level. . . . .	263

# Abbreviations

<b>ACE</b>	<b>A</b> ir <b>C</b> hange <b>E</b> ffectiveness
<b>ACH</b>	<b>A</b> ir <b>C</b> hanges per <b>H</b> our
<b>ARO</b>	<b>A</b> nti-biotic <b>R</b> esistant <b>O</b> rganism
<b>ANV</b>	<b>A</b> dvanced <b>N</b> atural <b>V</b> entilation
<b>ASHRAE</b>	<b>A</b> merican <b>S</b> ociety of <b>H</b> eating, <b>R</b> efrigerating and <b>A</b> ir-conditioning <b>E</b> ngineers
<b>CDC</b>	<b>C</b> entres for <b>D</b> isease <b>C</b> ontrol
<b>CFD</b>	<b>C</b> omputational <b>F</b> luid <b>D</b> ynamics
<b>CFU</b>	<b>C</b> olony <b>F</b> orming <b>U</b> nits
<b>CHG</b>	<b>C</b> hlorhexidine <b>G</b> luconate
<b>CIBSE</b>	<b>C</b> hartered <b>I</b> nstitution of <b>B</b> uilding <b>S</b> ervices <b>E</b> ngineers
<b>DH</b>	<b>D</b> epartment of <b>H</b> ealth
<b>DIN</b>	<b>D</b> eutsche <b>I</b> nstitut für <b>N</b> ormung
<b>DRW</b>	<b>D</b> iscrete <b>R</b> andom <b>W</b> alk
<b>EPA</b>	<b>E</b> nvironmental <b>P</b> rotection <b>A</b> gency
<b>HBN</b>	<b>H</b> ealth <b>B</b> uilding <b>N</b> ote
<b>HCAI</b>	<b>H</b> ealth <b>C</b> are <b>A</b> ssociated <b>I</b> nfection
<b>HCW</b>	<b>H</b> ealth <b>C</b> are <b>W</b> orker
<b>HPA</b>	<b>H</b> ealth <b>P</b> rotection <b>A</b> gency
<b>HVAC</b>	<b>H</b> eating <b>V</b> entilation <b>A</b> ir <b>C</b> onditioning guide
<b>ICT</b>	<b>I</b> nfection <b>C</b> ontrol <b>T</b> eam
<b>ID</b>	<b>I</b> nfection <b>D</b> ose
<b>HTM</b>	<b>H</b> ealth <b>T</b> echnical <b>M</b> emorandum
<b>MRSA</b>	<b>M</b> ethicillin- <b>R</b> esistant <b>S</b> taphylococcus <b>A</b> ureus
<b>NAO</b>	<b>N</b> ational <b>A</b> udit <b>O</b> ffice
<b>NHS</b>	<b>N</b> ational <b>H</b> ealth <b>S</b> ervice

---

<b>RNG</b>	<b>Re-Normalisation Group</b>
<b>RSM</b>	<b>Reynolds Stress Model</b>
<b>SARS</b>	<b>Severe Acute Respiratory Syndrome</b>
<b>SBS</b>	<b>Sick Building Syndrome</b>
<b>SEIR</b>	<b>Susceptible Exposed Infectious Removed</b>
<b>SIR</b>	<b>Susceptible Infectious Removed</b>
<b>SIS</b>	<b>Susceptible Infectious Susceptible</b>
<b>SSI</b>	<b>Surgical Site Infection</b>
<b>UTI</b>	<b>Urinary Tract Infection</b>
<b>VRE</b>	<b>Vancomycin Resistant Enterococci</b>
<b>WHO</b>	<b>World Health Organisation</b>
<b>YAB</b>	<b>Ysbyty Aneurin Bevan</b>

# Symbols

$A$	Surface area	$\text{m}^2$
$\text{ac.h}^{-1}$	Air changes per hour	$\text{ac.h}^{-1}$
CFU	Colony forming units	CFU
$C_c$	Cunningham slip-correction factor	-
$C_i$	Normalised CFU count	CFU
$D$	Inoculum	CFU/ml
$d$	Particle density	$\text{kg/m}^3$
$E$	Discretisation error	-
$F_i^L$	Lift force	N
$G$	Gaussian white noise	-
$g$	Gravity	$\text{m/s}^2$
$h$	Hand hygiene efficacy	-
$k$	Turbulence kinetic energy	J/kg
$\dot{m}$	Mass flow rate	kg/s
$n$	Surface contact count	-
$n_i$	Brownian forces	N
$P$	Pressure	Pa
$\hat{P}$	Maximum likelihood estimate matrix	-
$\tilde{P}$	Bootstrapped maximum likelihood estimate matrix	-
$Q$	Volume flow rate	$\text{m}^3/\text{s}$
$r$	Refinement ratio	-
$R_0$	Reproductive ratio	-
Re	Reynolds' Number	-
$s$	Sample standard deviation	-
$S$	Particle/Fluid density ratio	-

$S_i$	First order Sobol index	-
$S_\phi$	Source term of $\phi$	kg/kg
$S_{Ti}$	Total Sobol index	-
T	Temperature	°C
t	Time	s
$\mathbf{U}$	Velocity vector( $u, v, w$ )	m/s
$u_p$	Particle velocity	m/s
$u'$	Instantaneous velocity	m/s
$\bar{u}$	Average velocity	m/s
V	Surface contamination quantity	CFU/m <sup>3</sup>
$v_t$	Terminal velocity	m/s
$\bar{x}$	Sample mean	-
Y	Normalised CFU by <i>direct care</i> in single room at 6 ac.h <sup>-1</sup>	-
$y^+$	y plus	-
$\alpha$	Probability of infection	-
$\beta$	Hand-to-surface transfer efficiency	-
$\Delta$	change	-
$\epsilon$	Air change effectiveness	-
$\epsilon$	Turbulence dissipation rate	m <sup>2</sup> /s <sup>3</sup>
$\Gamma$	Coefficient of diffusion	m <sup>2</sup> /s
$\mu\text{m}$	Microns	$\mu\text{m}$
$\lambda$	Surface-to-hand transfer efficiency	-
$\mu$	Population mean	-
$\mu$	Kinematic viscosity of air	Pa s
$\phi$	Scalar quantity	-
$\rho$	Density of air	kg/m <sup>3</sup>
$\rho_p$	Density of particle	kg/m <sup>3</sup>
$\forall$	For all values	-
$\delta$	Small change	-
$\delta_{ij}$	Kronecker delta	-
$\in$	Element of	-

$(a, b]$	The set of $a$ to $b$ including $a$ but not $b$	-
$\infty$	Infinity	-
$\sum^i$	Sum over $i$	-
$\prod$	Product	-



# Chapter 1

## Introduction

### Contents

---

1.1	Overview . . . . .	2
1.2	Health Care Acquired Infections (HCAI), What Are They? . .	3
1.3	Disease Transmission Routes . . . . .	7
1.4	Hospital Room Design . . . . .	10
1.5	Infection Transmission Modelling . . . . .	12
1.6	Aims and Objectives . . . . .	15

---

This multidisciplinary research deals with the global question of whether hospital single rooms show any advantage over multi-bed accommodation at minimising the spread of infection between patients. Some of the therapeutic value of single room spaces is well known but the scientific evidence is still weak. This thesis considers the potential for airborne dispersal of pathogenic microorganisms which leads to environmental contamination and explores how surface pathogen loading, room design and the health care process may influence propagation of infection. This research combines computational fluid dynamics (CFD) with mathematical pathogen exposure models and a behavioural study of health care workers (HCW) within their work environment to gain a robust understanding of the potential mechanisms of infection transmission, whereby improving patient centered evidence based design. This chapter outlines the research methodology in a succinct manner and concurrently consolidates the aims and objectives.

## 1.1 Overview

Health Care Acquired Infections (HCAIs) are a major concern, costing the UK over £ 1,000 million per annum [29]. As well as causing misery to affected patients, they also impact on hospital management by increasing the duration of patient stays, constraining nursing activities, adding to the diagnostic workload and restricting visitor access [30]. At the close of the fiscal year of 2012, the UK deficit stood at £ 126 billion [31]. Therefore understanding, predicting and curtailing how this phenomenon develops and spreads throughout a hospital is of paramount importance. An understanding of how pathogens behave in the indoor environment is critical to developing appropriate infection control strategies. It is therefore important for research to involve the multidisciplinary interaction of microbiology, engineering methods of ventilation and room design alongside, human intervention.

This research has risen from the need for combining the largely disjoint areas of CFD models of environmental infection spread within hospital buildings and mathematical modeling to evaluate infection risk as in Figure 1.1. Although it has previously been thought that direct contact between patients and health care workers contributed most significantly to the route of infection [28, 32], recent studies suggest that surface reservoir contamination and airborne transport are also highly important [25, 33, 34, 35].

The key question and research aim is to evaluate and quantify the pathogen transport risk via hands between patients and health care workers (HCW) by comparing the standard UK hospital single room against the hospital four-bed ward accommodation. The risk of hand contamination has received much attention within the agricultural and chemical industry [36], where molecules can easily be absorbed by the skin, but the study of microbial load on hands (adsorption) within the hospital environment has lagged behind. This research seeks to develop a framework methodology to predict HCW hand contamination, focusing on environmental reservoir sources. To accomplish this in any logical and rigorous manner it is vital to include real-life data of HCW behavioural patterns along with surface contact frequencies. This will lay the foundations to incorporate the spatial deposition of particles within the hospital environment predicted by CFD and latterly to quantify the risk of pathogen accretion under different care activities.

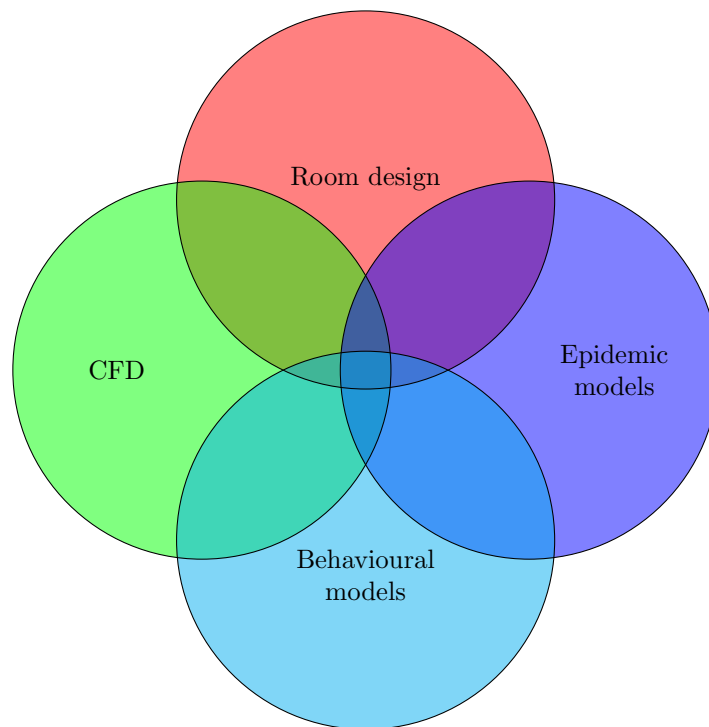


Figure 1.1: Venn diagram showing overlapping of each discipline involved in creating a multidisciplinary approach.

## 1.2 Health Care Acquired Infections (HCAI), What Are They?

A suitable place to begin is with one of the most famous quotes in British nursing history and quite possibly that of health care in general:

“It may seem a strange principle to enunciate as the very first requirement in a hospital that it should do the sick no harm. It is quite necessary, nevertheless, to lay down such a principle, because the actual mortality in hospitals, especially in those of large crowded cities, is very much higher than any calculation founded on the mortality of the same class of diseases among patients treated out of hospital would lead us to expect.” *Florence Nightingale, Notes on Nursing, 1883.* [37]

Nosocomial or health care acquired infections (HCAIs) are those acquired whilst staying, visiting or working in a health care facility, whereby increasing patient morbidity, mortality and additional medical costs [38]. Within this context the causal pathogens can be classified into two categories:

**Pathogenic microorganisms** are those that are harmful to healthy human beings. A wide range of potentially pathogenic microorganisms is associated with HCAIs, many of which are considered as ‘opportunistic’.

**Non-pathogenic microorganisms** may or may not be native to the patient’s microflora but do not pose a health risk to even immunocompromised humans.

Within these categories are two sub-sets:

**Endogenous** microorganisms belong to the patient’s own microflora, such as *Staphylococcus aureus*.

**Exogenous** microorganisms are not native to the patient’s own microflora, but may be prevalent in the patient’s environment.

Opportunistic microorganisms fall into the first category; these pathogens target patients who have weaker immune-systems, open wounds from surgical operation, or a depleted intestinal flora usually occurring as a result of antibiotic therapy [2].

### 1.2.1 Prevalence of HCAI

The risk of acquiring nosocomial infections is omnipresent in health care facilities worldwide. Globally, it is estimated that 1.4 million people are suffering from such an affliction at any one time [39], ranging from a mild bladder infection resulting from bacterial build-up on a catheter to life-threatening *Tuberculosis*. In the USA for example, the National Nosocomial Infections Surveillance (NNIS) calculated that approximately 1.7 million patients were infected by HCAIs and 99,000 attributable deaths were reported in 2002 [1]. The European counterpart (Hospital in Europe Link for Infection Control through Surveillance - HELICS) considers the figure of affected patients to be around 5 million in Europe [39]. Differences in benchmarking of surveillance data often make comparisons difficult on an

international level however the significance of the problem is undisputed. While the transmission routes for some diseases are well documented, the precise mode of transmission is uncertain for many infections, particularly for those pathogens that cause HCAs. Although it is highly likely that the majority of transmission occurs via a contact route [39], there is evidence suggesting that a proportion of HCAs potentially could have arisen from an environmental reservoir [40]. Figure 1.2 shows the percentage prevalence of HCAI in the USA. UK data is similar [41].

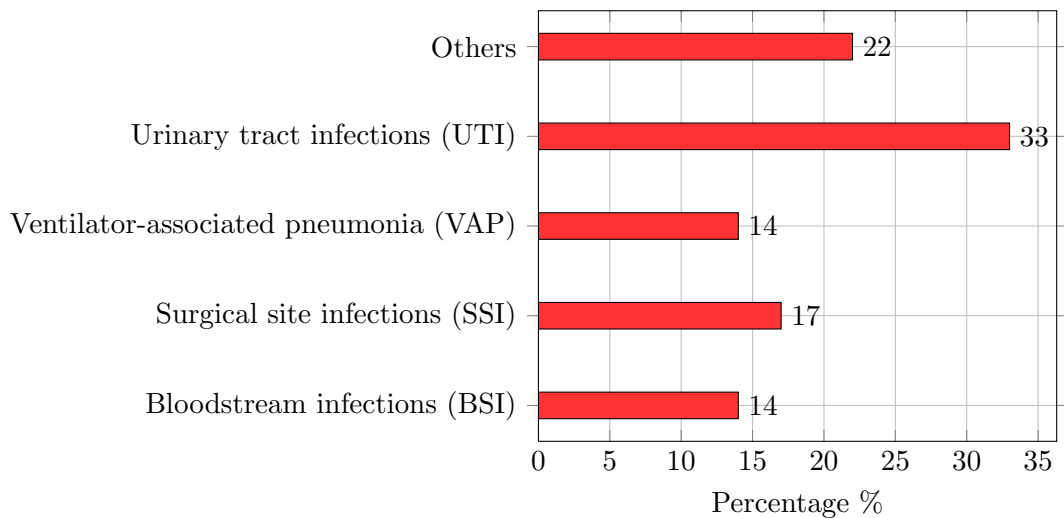


Figure 1.2: Percentage distribution of HCAI in the USA [1].

In 2001 the UK's chief medical officer [42] introduced a mandatory survey within health care facilities which recorded cases of patients who contracted nosocomial infections. Following this, several guidelines were introduced in 2003 and consequently a performance indicator of hospitals in respect to HCAs was created [42]. Subsequently in 2006 a code of practice was introduced that aims to provide a framework for hospitals to help minimise the risk of infection [43]. With antibiotic resistant microorganisms on the rise, surveillance became mandatory for surgical site infections and *Multi-drug resistant Staphylococcus aureus* (MRSA) in 2001, with the introduction surveillance for *Clostridium difficile* in 2003. HCAs have seen a steady decline from these sources since 2004 and continue to fall as of March 2013 [44]. Despite the eradication of opportunistic HCAs being nearly impossible Harbarth et al. [40] estimated conservatively that at least 20% of these infections could be avoided.

### 1.2.2 Why Are HCAI So Dangerous?

*“In 20 years time we could have an ‘apocalyptic scenario’ [where people going for simple operations could die] because we have run out of antibiotics.”* Dame Sally Davies, UK Chief Medical Officer, 2013.

Antimicrobial resistance (AMR) is defined as the resistance of a microorganism to an antimicrobial medicine to which it was previously sensitive. Resistant organisms which include bacteria, viruses and some parasites, are able to withstand attack by antimicrobial agents such as antibiotics, antivirals, and antimalarials, rendering standard treatments ineffective. As a consequence, infections persist until the body’s white blood cells overcome it or the patient dies. AMR is a direct result of the (ab)use of antimicrobial medicines and develops when a microorganism mutates or through gene transfer [2]. Microorganism populations are largely heterogeneous where some members are naturally hardier or more resistant to a particular antimicrobial medicine. These individuals persist and confer their immunity not only to their offspring but to other members of their own and other species through a process called horizontal gene transfer [2].

This then requires a change of treatment for the patient, often to more expensive drugs and the cycle may repeat itself.  $\beta$ -lactam based medicines are a large class of potent antibiotics. Resistance to these is rising continuously, where an example of which can be seen increasing exponentially of the last 40 years in Figure 1.3. Eventually a microorganism may become insensitive to all currently available antimicrobial drugs and no defence is left in the arsenal [45]. In such a scenario, Dame Sally Davies’ quote may not be quite so apocalyptically unthinkable as first thought. If AMR does continue to this point then potentially infection control through design of the environment becomes even more important.

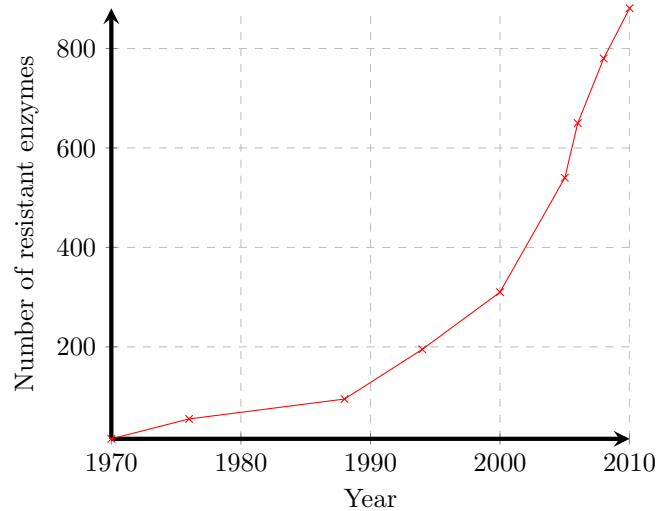


Figure 1.3: Bacterial resistance to  $\beta$ -lactam antibiotics [2]. Reproduced courtesy of the American Society of Microbiology.

## 1.3 Disease Transmission Routes

Since the early nineteenth century, where doubt was cast over the existence of invisible organisms to the naked eye [10], there has been much controversy regarding the spread of diseases. Today, five main transmission routes are identified and shown in Figure 1.4:

### 1.3.1 Contact Transmission

Direct contact transmission between health care staff and patients is often considered to be the primary route by which many health care acquired infections are spread within and between wards [32]. Human behaviour has been established as playing a vital and, by and large, unpredictable link in the infection transmission chain [19]. Hand hygiene is therefore considered as critical to curtailing infection spread [32, 46, 47]. As well as the hands of the HCWs, infection by contact may occur due to the use of medical devices such as contaminated catheters, intravenous feeding lines, and respiratory aids [28].

Indirect contact transmission involves an intermediary object such as a room surface or medical implement which acts as a latent object in the transmission pathway.

### 1.3.1.1 Environmental contamination

Recent attention has focussed on environmental surface contamination as a reservoir and potential infection risk hazard [48]. Patients and staff are likely to supply most of this, but if allowed, environmental surfaces can harbour viable microorganisms for prolonged periods [20, 48, 49, 50]. Therefore the process of decontamination and sanitation has been the subject of much contention. “*Mopping up hospital infection*” by Dancer et al. [24] highlights the struggle to implement efficient cleaning procedures despite their accepted importance in infection control. Particular difficulties can be seen when terminal cleaning is incomplete as shown by over 50% of rooms in a study by Bhalla et al. [51].

While much of the surface contamination may be from hand contact, deposition of pathogens may prove to be an issue too. In particular, many microorganisms expelled in these droplets, such as respiratory viruses, remain viable in droplet form that settle on objects in the immediate environment of the patient. While falling through the air droplets evaporate leaving a dry nucleus. Viruses, bacteria and fungi can survive long enough in a desiccated state on surfaces to be picked up on the hands of patients or personnel [52, 53]. Microorganisms may then be transmitted by inoculation of these membranes by contaminated hands in a process known as indirect transfer [54]. In depth characterisation of this phenomenon is given in Chapter 3 Section 3.1.1.

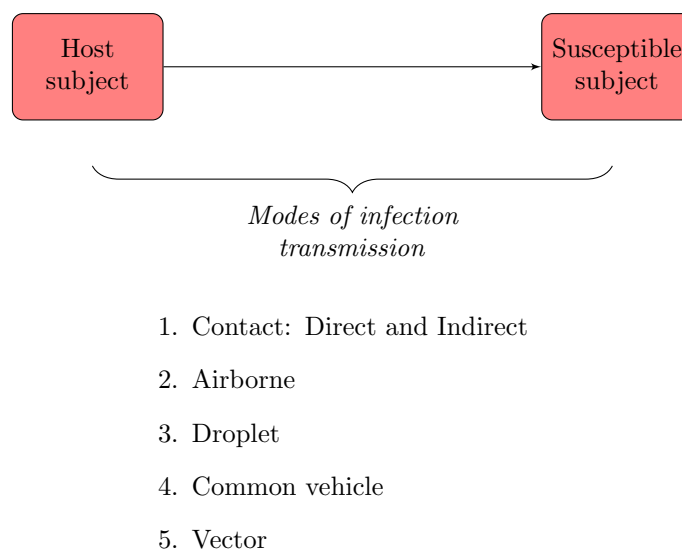


Figure 1.4: Transmission pathways set out by the CDC [3].

### 1.3.2 Airborne and Droplet Transmission

Airborne droplets of biological origin can range in size from  $\sim 1\text{-}100\mu\text{m}$ . These refer to an aqueous suspension of pathogenic material, such as in Figure 1.5. Respiratory illnesses are the first example that spring to mind, where large quantities of bioaerosols are produced but operations involving bronchoscopies, cutting or drilling produce even greater quantities [55]. Larger ( $>5\mu\text{m}$ ) droplets are thought not to remain suspended in the air for more than a few minutes [18].

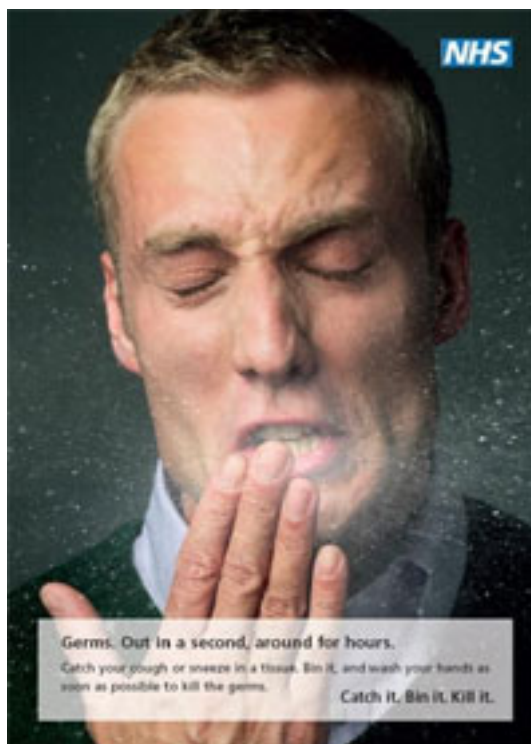


Figure 1.5: NHS poster reproduction of gentleman sneezing, courtesy of The Stationery Office, UK.

Aerosolisation of bioaerosols is the most formal definition of airborne infection. Airborne transmission occurs via the dissemination of droplet nuclei ( $<1\mu\text{m}$ ) from evaporated droplets containing the infectious agent. The microorganisms are transported through the air and can, depending on their size, remain suspended for many hours [53, 56]. Sub-micron sized particles may remain airborne for many hours undergoing the process of desiccation [57] which, to a great extent, delays their deposition.

The microorganisms can be widely dispersed by air currents and contagion occurs by inhalation of infectious particles, causing infection starting in the lung or respiratory

tract [58]. Consequently, special control of airflow is recommended for the prevention of the spread of this type of transmission [59]. Patients known to be infected by a microorganism with an accepted airborne transmission component, including measles, chickenpox or TB, are suggested to be quarantined in a negatively pressurised room as a formal recommendation [60].

### 1.3.3 Common Vehicle and Vector Borne Transmission

Common vehicle refers to transmission via a single contaminated source such as: Food, water, medications, intravenous fluid or equipment that serves to transmit infection to multiple hosts. Control is through maintenance of appropriate standards in the preparation of food, medications, and the decontamination of equipment. Vector borne diseases such as malaria are transmitted indirectly between humans by vector agents, mostly insects or parasites. This phenomenon is a less frequent method of transmission in the health care setting of most developed nations.

Although the transmission mechanisms for many diseases are still poorly understood it is important to be able to categorise the pathways into broad routes of infection. Indeed, to improve success in reducing the prevalence of HCAI, the surveillance systems put in place by the Health Protection Agency (now part of the Public Health England) must monitor the efficiency of any intervention measures by means of infection route.

## 1.4 Hospital Room Design

The year 2008 marked a milestone event in the history of the National Health Service (NHS), not just for its 60th birthday occasion but also in the way that it was fundamentally going to change. Whitehall saw the NHS as a dichotomous, underfunded 1940s organisation lumbering into the 21st century. It was intrinsically inclusive and goal driven; lacking patient comfort [61]. The report “*High quality care for all*” [62] commissioned by Lord Darzi laid out the foundations of health care devolution, which gave back to GPs and patients greater autonomy and choice. An increase in funding was signed, bringing it up to the European average which guaranteed amongst other things, an increase in hospital single rooms. By 2013 50% of new rooms were to be single beds.

Hospital design guidelines in the UK have relied either explicitly or implicitly on the four tenets of design: Comfort/practicability, cost-effectiveness, infection control [63] and latterly energy efficiency [64]. Often, the former two dominate requirements. Within the Department of Health design framework: The Health Building Note 04-01 [5] allows for some scope regarding decisions made by architects, estates, clinicians and infection control groups with regards to the design of new buildings. However, only minimum room sizes are stipulated [5]. The therapeutic benefits of single patient rooms are known to some extent [65], where better rest directly results in reduced morbidity and shorter patient stays [41]. Privacy and dignity rank continuously high on patient questionnaires [41] which begs the question: Why shouldn't all rooms be single rooms? Nevertheless, there is an increasing body of evidence which points towards a relationship between the effect of design and infection control [49, 66, 67, 68]. Research has attempted to discover and establish a causal link between the use of multi-bed rooms and the increase in infection risk to patients [30, 41, 69]. Indeed, many private and PFI hospitals built in Europe and the USA are tending towards single room preference [70]. However, the UK is still some way behind with 50% targeted provision as of 2013. Furthermore, hospital room layout may also influence other infection control procedures such hand hygiene compliance. It has been shown that the physical barrier exercised by a single room, provides a mental stimulus, promoting the improved adherence to hand anti-sepsis [19, 22, 49].

Over the last two centuries hospitals have been built based on constantly evolving design guidelines [71]. Throughout this time, the emphasis has shifted away from large airy Nightingale wards, naturally ventilated by means of floor to ceiling windows [72], to smaller, mechanically ventilated rooms based on the Health Technical Memorandum [73]. The motivation in most cases was the cost of the buildings and the patient comfort. However, the effects of infection spread has not been, until recently, an uppermost priority [74, 75]. Amongst the measures to prevent cross-transmission of pathogens, European authorities recommended single rooms, aimed at enhancing compliance with infection control measures, in the design of intensive care units [41, 69, 76, 77]. This current research deals with the global question of whether single rooms can reduce the risk of spread of infection through indirect transmission.

## 1.5 Infection Transmission Modelling

*“A mathematical model is like a cartoon, it depicts the dynamic world in as much detail as the artist desires.”* Author’s own thoughts.

In the face of unreliable or scarce data, mathematics is a critical tool for formulating hypotheses, informing data-collection strategies, and discriminating between competing hypotheses [78].

Predicting infection spread and the possibility of epidemics has occupied mathematical epidemiologists for nearly a century. Particularly difficult is finding the causal agent which is responsible for the frequency of epidemic waves. Kermack and McKendrick [79, 80, 81] laid down the foundations of the so-called Susceptible-Exposed-Infected-Recovered (SEIR) mathematical model, which compartmentalised Susceptible, Infectious and Quarantined/Dead/Recovered members of a population (see Figure 1.6). This type of simplistic model treats infection transmission modes as a homogeneous phenomenon and does not account for heterogeneous properties of environmental factors, population or infection rates. Instead, it relies on average rate coefficients of transmission probability and time remaining infectious to describe the progression of a disease. The threshold value, commonly referred to as reproductive number ( $R_0$ ) corresponds to the tipping point [82] within a population where a disease will spread to become an epidemic or will die out. This can be considered an environmental factor which roughly estimates the contact rate between individuals in a population. The concept applies to both diseases in which recovery from infection conferred immunity against re-infection and for diseases in which recovered individuals are susceptible to re-infection [78]. The ability to apply such a model relies on determining appropriate rate constants to define contact rates between infectious and susceptible people and disease progression rates within a population.

### 1.5.1 Contact Transmission Models

A certain quantity of pathogenic material will transfer to the HCW’s hand through each contact with a contaminated surface [20, 22, 25]. This is a dynamic process in which multiple factors will vary. Considered by the US Environmental Protection Agency (EPA) to be two of the most important: both contact frequency and hand movement during

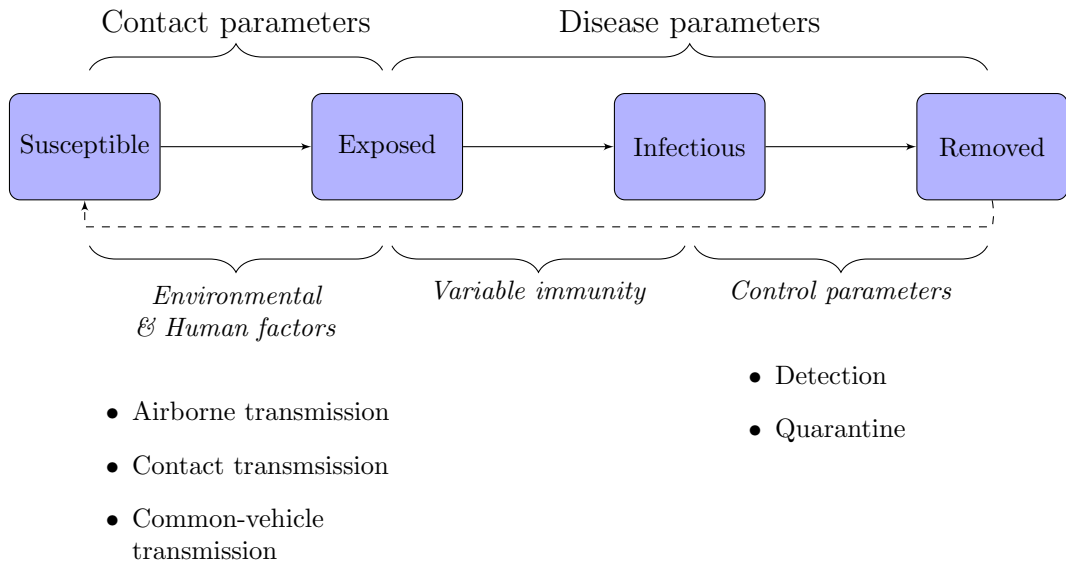


Figure 1.6: Flowchart of typical disease transmission dynamics in an SEIR model. Bullet points show important environmental factors affecting transfer from category *Susceptible* to *Exposed*. Equally they depict control parameters dictating the rate of progress from *Infectious* to *Removed*.

contact can be individual and job specific, while contact pressure may be more controlled. In their published guidelines [83], the EPA propose evaluation of dermal accretion of hazardous materials through hand-to-surface contact to be deterministic and linear in nature. However, reality is slightly different [36, 84, 85] and stochastic effects play an important role in determining pathogen accretion on skin.

## 1.5.2 Airborne Transmission Models

Wells and Riley [60, 86] proposed a model based on a Poisson probability distribution which considers the airborne transmission of pathogens. This model first introduced the term ‘quantum of infection’ which is an averaged virulence of the pathogen and hence intrinsically includes the level of reaction from a human immune system. This then may be considered a ‘disease parameter’ and, broadly speaking, represents the dose required to infect 66.7% of the population. One of the major disadvantages of this type of model are the averaged parameters which, although improved in a transient model by Gammaitoni [87], assume a homogeneous human population. A major simplification considers full and random mixing of the air volume. Hospital wards are highly dynamic even with

the most efficient ventilation systems and hence it is questionable at best whether this assumption is generally applicable [88].

Further questionable assumptions [89, 90] made within this standard accepted model include:

1. Homogenised pathogen distribution within the room air volume, hence not taking into consideration the proximity of individuals or spatial distribution.
2. Single parameters of transmissibility not allowing for variations between individual populations.
3. Requires a large population (>20) sample for Poisson probability distribution to be appropriate.
4. Periods of incubation required to be much longer than the time step involved in the simulation (e.g. TB)

Qian et al. [89] employed a spatially heterogeneous Wells-Riley model in the Prince of Wales Hospital in Hong Kong with the aid of Computational Fluid Dynamics. This combats the first assumption of a fully mixed air space which, up until recently could not be fully addressed due to computing power restrictions. Nevertheless a deterministic approach is still used and assumes a statistically sufficiently large population. Such a problem is considered by Noakes et al. [90] by the introduction of the stochasticity of infection possibility.

### 1.5.3 Importance of Airflow Patterns

Understanding the role that ventilation airflow and ward design play in the dispersion and deposition of infectious bioaerosols is tantamount to assessing airborne and pathogen exposure risk. With the difficulties in aerosolising microorganisms in hospital settings, many studies have turned to inert particle tracers [55, 67] or CFD models to infer bioaerosol behaviour in air and surface deposition [91]. In 2008 the H1N1 SARS *corona virus* sparked a renewed surge in funding for airborne disease modelling. As highlighted by Hathway et al. [46] direct comparison between CFD models and bioaerosol experiments are

sparse. Wong et al. [92] undertook a small scale experimental/numerical comparison using bioaerosol deposition within a climatically controlled enclosure in 2010 which lay the ground for the publication resulting from this current research [93].

Since CFD relies on high computing power, it has been used up until recently somewhat sparingly with respect to hospital designs. Most of the effort has gone into predicting steady state flows within operating theatres and isolation rooms [94, 95, 96, 97, 98]. These studies placed an emphasis on the health risk of the airborne bacteria released from the surgical team on the patient, and vice versa.

More recently, and with the ever increasing available computational power, CFD has been used to model both the bulk air flow and particle deposition of skin squamae within whole wards [12, 57, 99, 100]. Targeting of specific airborne pathogens including respiratory infections including Severe Acute Respiratory Syndrome (SARS) [101, 102] and Tuberculosis (TB) [103] have been the main focus of some later studies.

## 1.6 Aims and Objectives

### 1.6.1 Hypothesis

*“I propose that hospital single rooms provide improved protection against the spread of HCAI to patients in comparison to their multi-bed ward counterparts.”*

The aims of this research are two-fold: Firstly to develop a mathematical framework which will calculate the pathogens accrued on HCWs’ hands from surface contacts during patient care. Secondly the aim is to utilise this model to quantify the relative risk of infection in single and multi-bed hospital accommodation, with particular focus on transmission related to surface contamination through airborne dispersal of pathogens. This is tackled by examining the effect of room design and ventilation strategy to determine environmental pathogen contamination. Subsequently, the influence of HCW surface contact patterns is examined to investigate the opportunities for infection transmission.

*“The traditional process of scientific progress is to observe a phenomenon, hypothesize an explanation and then devise an experiment to test the hypothesis.”*

Brauer et al. [78]

---

This research aims to incorporate the field of computational fluid dynamics (CFD) into that of infection modelling whereby providing improved detail on the effects of room layouts and, in particular, the effects of single rooms over multi-bed wards. Principally it will establish and validate the most appropriate computational approach to model the spatial deposition of airborne bioaerosols within the hospital room environment. Real life behavioural data on HCW movements and surface contacts are fed into a custom-written pathogen accretion model, which gives insight into the risk associated with certain care types and, indirectly, the advantages of one room design over another. This is intentionally an inclusive modelling attempt such that it should combine the four aspects of design in Figure 1.1.

## 1.6.2 Objectives and Research Methodology

Objectives within this research are:

1. Establish the routes of transmission of HCAI between patients via HCW and how this is currently considered in hospital design. This background study is carried out to assess the requirements of the modelling technique to be employed, involving:
  - Investigate the variable factors involved in quantifying infection transmission.
  - Evaluate direct and indirect contact transmission routes and the techniques required to quantify these.
  - Review current guidance on UK health care design and the political, scientific and economic drivers behind it.
2. Demonstrate the most applicable CFD method for predicting spatial deposition of bioaerosols:
  - Gain a robust understanding of the factors which influence aerial dissemination.
  - Literature search evaluating validated techniques for bioaerosols transport via CFD and their scope.
  - Characterisation of appropriate flow parameters including turbulence models via anemometry and balometry of airflow patterns within a controlled experimental environment.
  - Comparison of the modelling techniques via Lagrangian particle deposition models against bioaerosol experiments for deposition in a controlled environment.
3. Quantify frequencies of health care worker (HCW) surface contacts by:
  - Conducting an observational study on an hospital ward comprised of single rooms to record HCW surface contacts during different types of care.
  - Generating probability mass functions representing the probabilities of contact with each surface type.
  - Generating maximum likelihood estimators for directed Markov chains and evaluating their performance against observations.

4. Develop a probabilistic pathogen accretion model (PAM) to evaluate the contamination levels of HCW hands within a defined scenario by:
  - Conducting a literature review for environmental parameters which have been experimentally evaluated e.g. hand surface contact area, pathogen transmission efficiency from surface to skin and hand hygiene efficacy.
  - Conducting a sensitivity study to evaluate the most appropriate mathematical representation of the pathogen pick-up process onto HCWs' hands.
  - Incorporating the Markov chain methodology of behavioural modelling, forming the basis of HCW surface contact frequency
5. Use the developed model to assess health care episodes in single and multi-bed scenarios by:
  - Applying CFD to single and multi-bed scenarios to obtain spatial deposition patterns to feed into the probabilistic model.
  - Assessing the sensitivity of the model and demonstrating the application and limitations within hospital accommodation.
  - Evaluate pathogen loading of HCWs' hands and compare different room scenarios.
  - Assess the risk attributed to each care type and scenario.

This research uses a multidisciplinary approach to combine two parallel studies (see Figure 1.7) to accomplish the objectives above.

The emphasis within the first part (see Chapter 4) is placed on using CFD to predict the deposition patterns of biologically active aerosols, which allows for the visualisation and quantification of contaminant transport through hospital settings. Initially, an experimental comparison will be made under strict controlled environmental condition within the University of Leeds aerobiology facilities to validate the techniques used. By monitoring aerosol deposition experiments within a test environment, the precise release method and location is maintained. Hence, by reducing the number of varying external factors, the influence of unpredictable variables can be minimised. This set of experiments will release a benign bioaerosol (*Staphylococcus aureus*) in different room layouts to determine spatial deposition patterns. Petri dishes will be placed on room surfaces for the resulting deposited

colonies to be counted. Comparison with CFD simulations using Lagrangian particle tracking will be made and, in particular, stressing the comparison between a Reynolds Stress (RSM) turbulence model and the abundantly used  $k-\epsilon$  RNG model. Subsequent modelling of hospital scenarios can then be carried out without the need for intrusive or hazardous experimental apparatus.

The second part of the research centres on observing HCWs in a hospital setting and recording both the frequency and order of surfaces touched during episodes of patient care. This study is particularly useful in identifying the activities that represent the greatest risk of surface contact but also to differentiate hand hygiene frequencies. Statistical analysis will be used to highlight differences and allow for distribution fitting to HCW behavioural patterns. Subsequently, probability density functions will be used through a process of Monte-Carlo sampling to mimic HCW behavioural patterns. This will then be compared with a Markovian approach and used to simulate surface contacts. By feeding in model parameters accrued from both the experiments described above and literature searches, further Monte-Carlo sampling will allow risk distributions to be created for each type of care activity performed.

### 1.6.3 Layout of This Thesis

A brief introduction to chapter layout is given in what follows:

**Chapter 1: Background** Here the concept of pathogen transmission is explained, highlighting the aim and objectives which the study intends to fulfil as well as the context within which it will be carried out. Discussion is then centred on the airborne and contact transmission routes. Current availability of hospital isolation rooms is known to be low and hence the focus is made on both single and multi-bed wards. The research perspective is multidisciplinary, aiming to quantify the risk that HCW contact with contaminated environmental surfaces poses to susceptible patients.

**Chapter 2: Hospital layout** This chapter reviews the current guidelines surrounding hospital design and layout followed by the importance of HCAs. This is analysed from the medical perspective and the economic impact is shown.

**Chapter 3: Infection transmission modelling** Here emphasis is made on the investigation of both contact and airborne transmission routes, when quantifying infection risk. Historical background is given on compartmentalised Kermack-McKendrick type SEIR models [79] and how the effects of small populations can significantly influence disease spread. Therefore, the rationale for focussing on the individual HCW as a vector of transmission is explained from the perspective of stochastic modelling. This is then introduced along with the foundation principles of constructing such models.

**Chapter 4: Bioaerosol deposition: Experimental and CFD validation** This chapter considers the ability of CFD simulations to accurately predict spatial distributions of bioaerosol deposition in indoor environments and explores the influence that different room layouts have on deposition patterns. Spatial deposition of aerosolised *Staphylococcus aureus* is measured in an aerobiology test room arranged in three different layouts:

1. an empty room
2. a single-bed
3. a two-bed hospital room.

Comparison with CFD simulations using Lagrangian particle tracking demonstrates that a realistic prediction of spatial deposition is feasible, and that a Reynolds Stress (RSM) turbulence model yields significantly better results than the  $k-\epsilon$  RNG turbulence model used in most indoor air simulations.

**Chapter 5: Observational study at Ysbyty Aneurin Bevan** Here it is shown how human behaviour in the health care environment, due to nursing activities, may result in exposure to pathogens described in Chapter 2. This chapter underpins the methodology on obtaining real data on hand-to-surface contact frequencies in a community hospital during different health care activities. This data is subsequently used to show how behaviour can be modelled realistically by probabilistic methods.

**Chapter 6: Infection risk modelling: Model development** This chapter describes the methodology behind the development of a probabilistic model for pathogen accretion on HCWs' hands. The main aim of this model is to provide a framework

which will allow the quantitative comparison of hospital room design, in particular, single vs. multi-bed rooms by means of an indirect metric.

**Chapter 7: Application of the model** Here, the results obtained from the observational study at YAB and presented in Chapter 5 form the basis for the behaviour of the personnel tending to patients. CFD models for proprietary single and generic multi-bed rooms are created and a parametric study shows the differences between particle deposition patterns in both. These results are used in conjunction with the hand-to-surface contact frequency model to predict a risk distribution for each type of health care performed. Hence, indirectly, the room layouts are compared between the two scenarios. A standard exposure risk model is used as a quantification of contact transmission risk towards subsequent patients in both scenarios.

**Chapter 8: Conclusions and Further Work** This final chapter presents the general conclusions from the study and potential areas for further investigation.

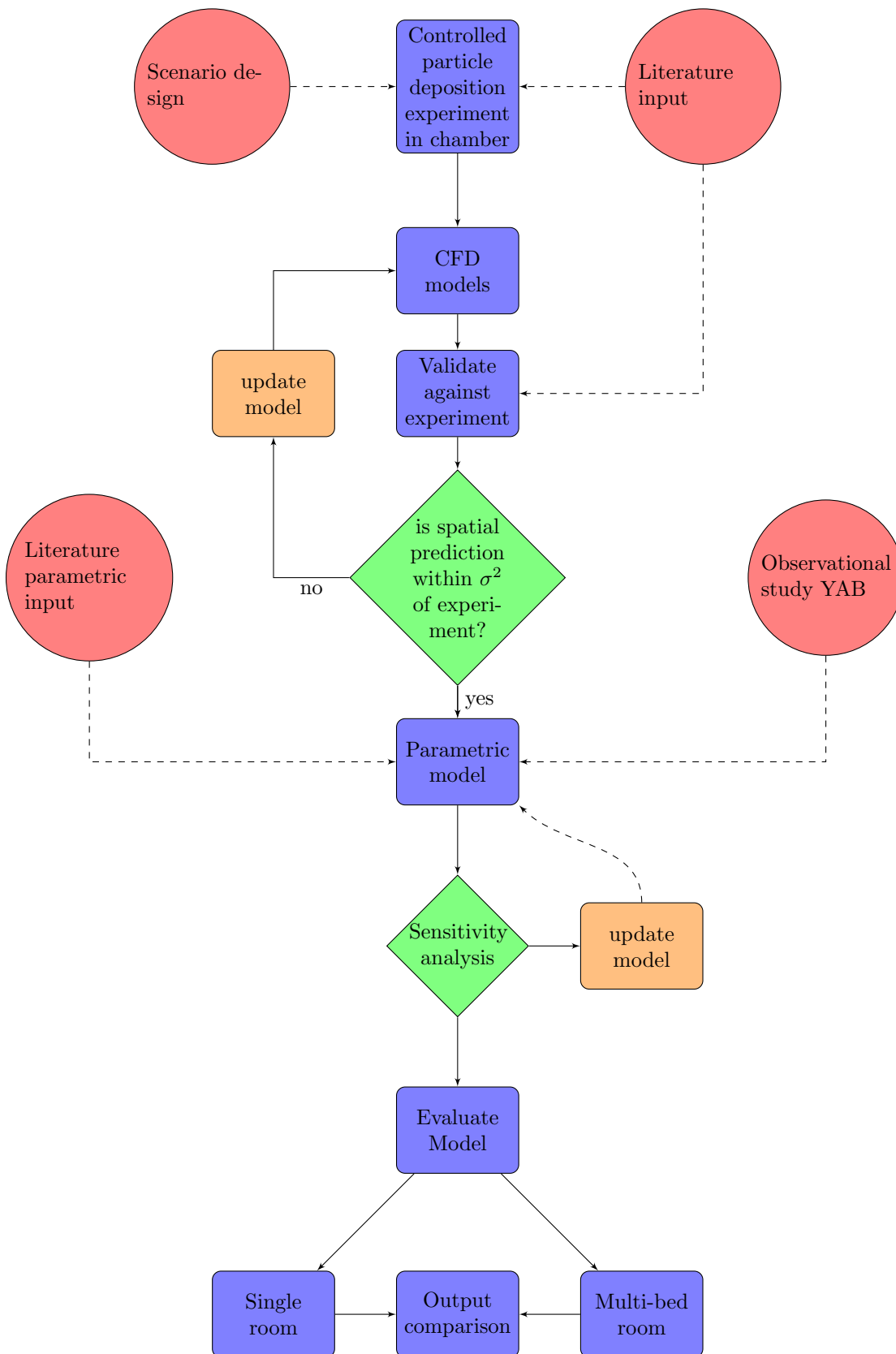


Figure 1.7: Flowchart of model development.

## Chapter 2

# Hospital room design

### Contents

---

<b>2.1</b>	<b>General Overview of Hospital Room Design . . . . .</b>	<b>23</b>
<b>2.2</b>	<b>Heating, Ventilation and Air-Conditioning (HVAC) Guidelines</b>	<b>40</b>

---

This chapter explores the driving forces behind the design of the modern hospital room; with particular focus on the UK. Historical perspective is drawn from early designs of rooms throughout the last two centuries and how the evolution of a modern health care system is imposing energy efficiency looking forward into the future. Ventilation guidelines are permanently under scrutiny and with resilience to climate change high on the agenda, novel ideas and innovative design are increasingly important.

## 2.1 General Overview of Hospital Room Design

*“Health care requirements are changing rapidly and these changes will have a major financial and operational impact on the existing health care estate. Not only are costs increasing, but there are pressures on estates to reduce costs, reduce size, become more specialised, integrate more with the community and reduce energy and carbon emissions.”* (Phil Nedin, Global Health Care Leader, Arup)

At its inception in 1948, the National Health Service (NHS) inherited an albeit architecturally beautiful, but already aging building stock. Some of the finest examples date back

to early Victorian designs: The University College Hospital, London in Figure 2.1, being a good example. Accelerated change and modernisation are at the epicenter of a developing National Health Service, forcing its archaic building stock kicking and screaming into the 21st century.



Figure 2.1: University College Hospital, London, UK. Image Copyright Nigel Chadwick. This work is licensed under the Creative Commons Attribution-Share Alike 2.0 Generic Licence.

Hospitals are complex multidisciplinary organisms; formed by a *mélange* of stakeholders, each with varying degrees of input and interest, all within a constantly developing health care environment. In 2010 the average government spend (see Figure 2.2) of GDP on health systems in the EU fell for the first time since 1975 [4]. Coupled with that, the burgeoning health complications relating to an aging population, chronic heart disease and uncontrolled diabetes, hospital design can no longer take a back seat. This could be seen as the NHS’ *‘golden opportunity’* to provide energy efficient buildings for the next 25 years [104].

Hospitals represent some of the most complex building types in existence and design over the last century has varied continuously, not just aesthetically but functionally. Such is the case that they represent a network of delicately interrelated functions requiring constant movement of people and goods [105]. “*Building a 2020 Vision: Future Health Care Environments*”, appeared in 2001 [61] and culminated research funded by the Nuffield Trust and RIBA Future studies to outline a roadmap for the NHS over the next twenty years;

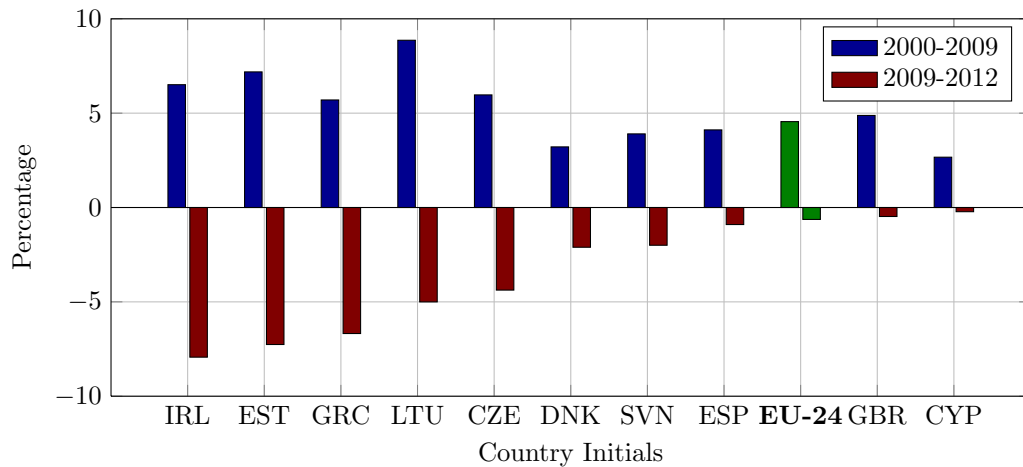


Figure 2.2: Percentage spending of GDP on health care by EU countries between 2000 and 2012, source OECD [4].

particularly with respect to customer expectation: The patient. Indeed, patients are becoming ever more discerning, expecting high standards of customer service including lower waiting times, better food, more personalised care and fully private accommodation [62].

In the UK, the Hospital Division of the Ministry of Health (now Department of Health) recognised a need to collate and standardise guidance for hospital and ward design. Common standards and provisions were set out initially in 1961 forming a collection of *Hospital Building Notes*, that became the foundation of today's *Health Building Notes*:

- HBN1: Building for the Hospital Service
- HBN2: The Cost of Hospital Buildings
- HBN3: The District General Hospital

Today these have evolved into sixteen separate guidance documents as set out in Table 2.1.

These HBNs provide guidance on a range of elements of hospital design from room sizing to window features. Alongside these documents are a second series of documents, *Health Technical Memoranda* (HTMs) which set out guidance on specific aspects of health care building design services provision. For example: *HTM03-01 "Specialist Ventilation for Healthcare Premises"* [73] deals with all aspects of ventilation systems from general ward

Health Building Note	Series title
Health Building Note 00	Core elements Support-system-based
Health Building Note 01	Cardiac care Care-group-based
Health Building Note 02	Cancer care Care-group-based
Health Building Note 03	Mental health Care-group-based
Health Building Note 04	In-patient care Generic-activity-based
Health Building Note 05	Older people Care-group-based
Health Building Note 06	Diagnostics Generic-activity-based
Health Building Note 07	Renal care Care-group-based
Health Building Note 08	Long-term conditions/long-stay care Care-group-based
Health Building Note 09	Children, young people and maternity services Care-group-based
Health Building Note 10	Surgery Generic-activity-based
Health Building Note 11	Community care Generic-activity-based
Health Building Note 12	Out-patient care Generic-activity-based
Health Building Note 13	Decontamination Support-system-based
Health Building Note 14	Medicines management Support-system-based
Health Building Note 15	Emergency care Care-group-based
Health Building Note 16	Pathology Support-system-based

Table 2.1: Health Building Notes guidelines as of 2013.

areas through to operating theatres, while *HTM07-01 “Safe Management of Healthcare Waste”*[106] covers the facilities and procedures to deal with clinical waste.

Design principles have also recently evolved in response to the climate and energy agenda. The year 2009 saw carbon dioxide (CO<sub>2</sub>) emissions become priority and are now a central pillar to modern NHS building and estate design. Guidelines are set out in the *NHS Carbon Reduction Strategy for England: Saving Carbon Improving Health* [64]. This aims to officially reduce carbon output over the following decade, particularly through cutting down on clinical packaging but also making building and estate design increasingly more

efficient.

Design of a hospital, due to the services it must provide, is complex in nature. The designing project group formed by experts from varying backgrounds must take into consideration and accordingly balance four tenets of hospital design as seen in Figure 2.3. From 2002 Infection Control Teams (ICT) officially take an active and important part in the project group throughout the planning stage and construction [107]. Prior to this, ICT and microbiologists had been mainly consultants, and it proved difficult for their recommendations to be implemented at any early design stage. In the majority of cases from 1950 until 1990, hospital design remained strongly in the domain of architects where cost effectiveness and patient comfort prevailed [75]. Clinician input was scarce and changes in ‘best-practice’ recommendations were often implemented retrospectively, incurring high costs and poor performance [108].

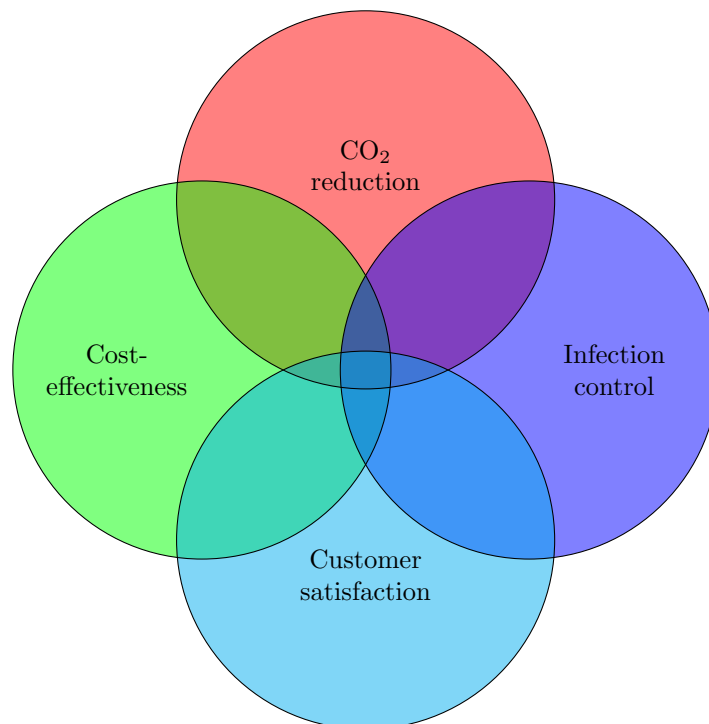


Figure 2.3: Four tenets of design for hospitals in the UK according to HBN04-01 [5].

Stockley et al. [63] highlight the importance of including experienced microbiologists and ICT at every stage of the commissioning of a new hospital. Stockley’s experiences are practical, gained from numerous new hospital developments. They have shown that ICT

are a vital component offering a counter weight perspective to engineers or architects who often have no training in hospital infection control. Wilson et al. [109] reviews Stockley's methods through a retrospective commentary of the building of the University College London Hospital, highlighting how the infection control team integrated into the design project. Reality appears to be somewhat different, with clinicians still being excluded during early discussion or their requirements not heeded [104].

### 2.1.1 A Brief History of UK Ward Types

Historically (1800-1940) in the UK, physicians primarily visited wealthy patients at home. Open ward accommodation originated as part of offering hospitalisation for injured military personnel and later the poor [104]. As such, this was and still is, seen as being inclusive and non-discriminatory. Single patient or side-rooms appeared through one of two reasons: Quarantine measures, or to cater for terminally ill or wealthy patients. The influence of the latter disappears with the inception of the NHS in 1948.

Since hospitals must house goods, services and people the design of patient wards is clustered around spaces contained within. As such, patient spaces, nurses stations and staff space and the combination of layouts of these three areas can be reduced to the resulting five ward types displayed in Figure 2.4. The Nuffield trust in 1955 [110] summarised these as simple open or *Nightingale* ward (Figure 2.4b), *duplex* or *Nuffield* ward (Figure 2.4a), *racetrack* or double corridor ward, *cruciform* or cluster ward (Figure 2.4c) and the *hub and spoke* or *radial* form (Figure 2.4d).

Nightingale wards such as the one in Figure 2.4b and Figure 2.5a with high ceilings and tall windows formed the staple backbone of hospital design from 1861 until the start of World War II [111]. These offered nurses visibility over 24-36 side-by-side patients, affording high air change rates through floor to ceiling windows [112]. Ironically, patients scored these often as being more private than the smaller wards which superseded them in the mid 20th century. An example of which is a six bedded room in Figure 2.5b. Logic alone would dismiss this claim, but high noise levels appear to appease the feeling of isolation [104]. With improvements to building envelope sealing, rooms had to be made smaller in order to maintain mechanical ventilation rates and consequently the standard UK multi-bed ward became the four bed room depicted in Figure 2.5c.

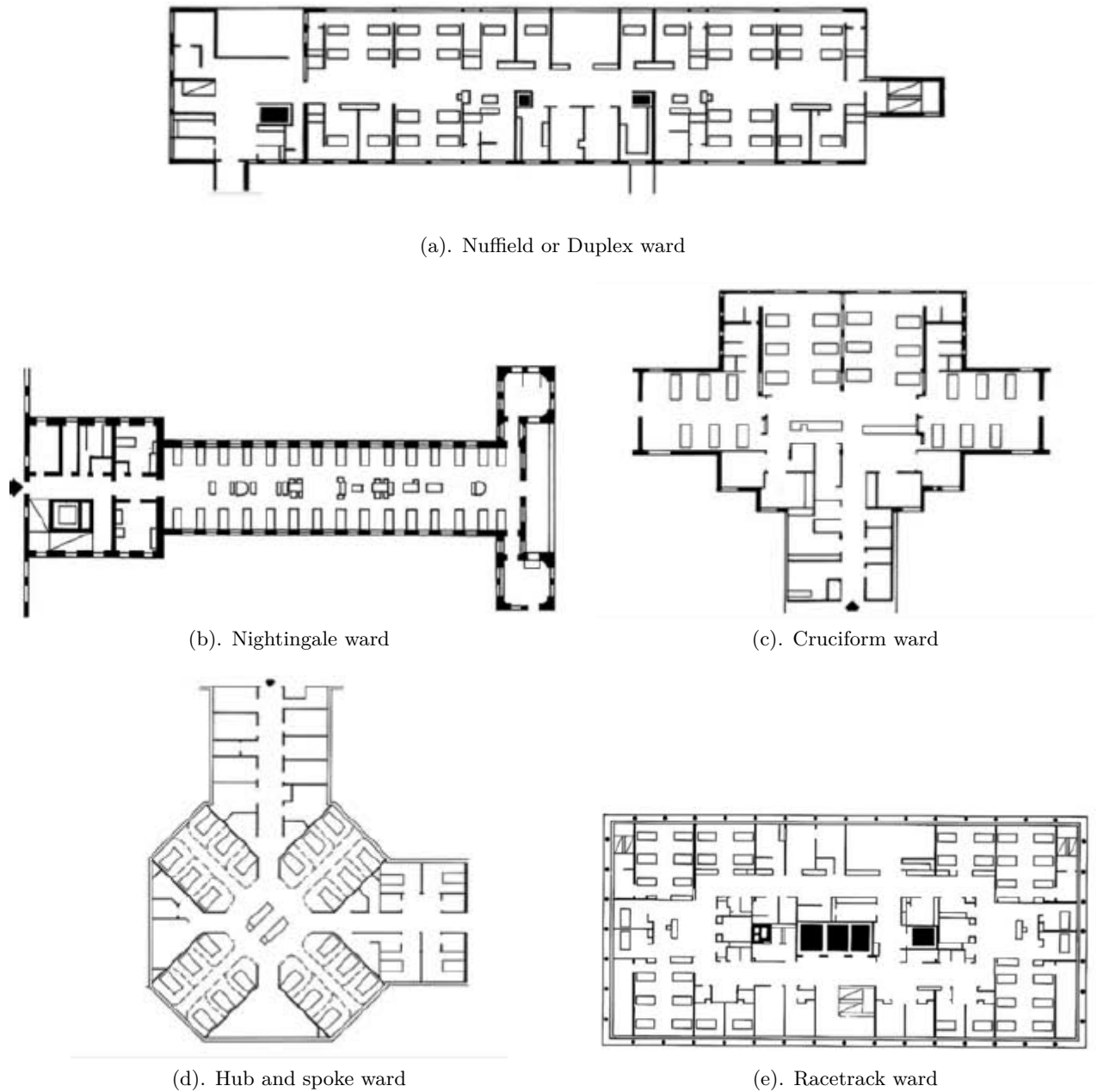


Figure 2.4: General UK ward design types reproduced, with permission, from Alalouch et al. [6].

### 2.1.2 Evidence Based Design

Evidence Based Design is popular in the health care sector relying on best-practice and credible scientific evidence that designing the built environment in such a way can result in patient and staff well-being, promote patient healing and cross-infection rate reduction [113].

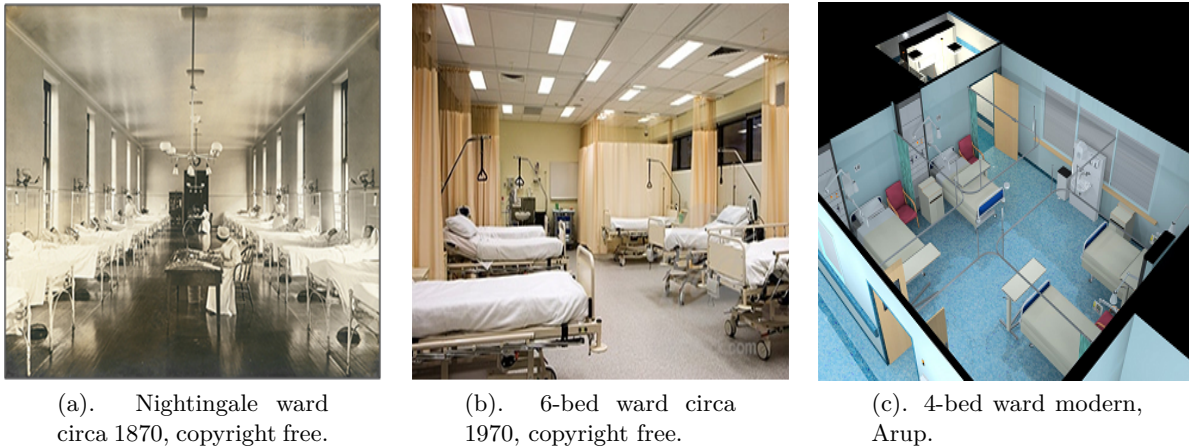


Figure 2.5: Examples of hospital multi-bed ward design evolution ca. 1870-2010.

The wealth of knowledge surrounding evidence based health care design has expanded rapidly in recent years with the York Health Economics Consortium (York HEC, UK) identifying the main aspects influencing a patients' hospital stay:

- Infection rates
- Length of stay
- Medication errors
- Patient satisfaction

Several literature review articles have tentatively supported the association between single-bed rooms and reduced infection rates, including Dettenkofer et al.'s [114] review on the relationship between architectural design and HCAI and Ulrich et al.'s [41] review on the advantages and disadvantages of single versus multi-bed accommodations. Others for example: Chaudhury et al.'s [69] have been more cautious, citing the scarcity of meta-analysis or truly randomised trials to uphold any general conclusions. However, perception between health care professionals does appear dichotomous with 67% of UK nurses considering infection risk to be low or medium and only 11% to be high within single rooms. The converse applies to double or multi-bed accommodation [113].

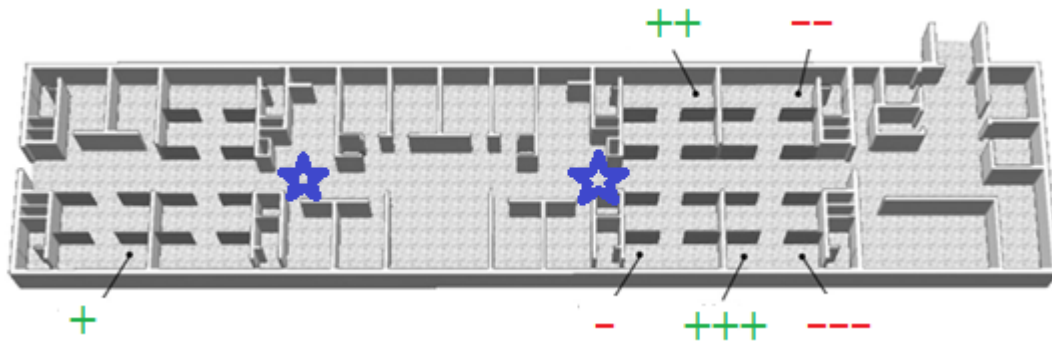
### 2.1.3 Patient Centered Design: Patient Choice

*“If ever there was a time when it was acceptable to treat a patient in the presence of others [patients], that time has long since passed”.* (Baron Ara Darzi of Denham, Chairman of the Institute for Global Health Innovation at Imperial College and world leading surgeon.)

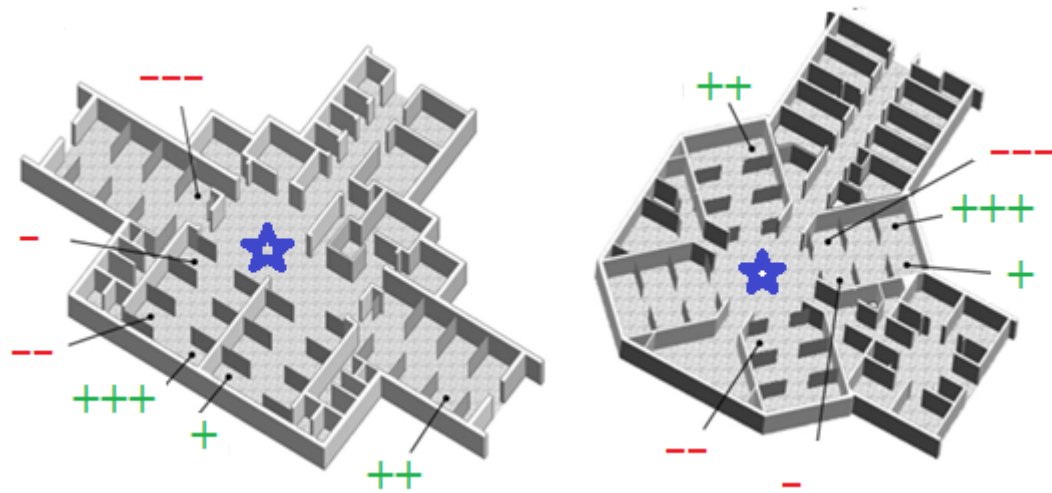
Today, patients are seen increasingly more as active stakeholders in the process of their own health care [104]. Patient privacy and dignity has become ever more prominent and into the forefront of the design process. The early 1990s showed the emergence of concepts such as patient-centered care and ‘*healing environments*’ [115]. Ever greater emphasis is placed on the impact of the patient’s physical and psychological well-being on healing and satisfaction. Therapeutic examples include lighting, sound, natural ventilation, views of nature, ergonomics, good food and privacy [113].

The lack of privacy in multi-bed ward appears to negatively affect the overall satisfaction of the patients and is something that has always been questioned [113]. Choice of room type appears on the surface, to be largely a generational choice with older or geriatric patients preferring multi-bed rooms and the younger patients often preferring a single bed room [111]. However, the choice may be a lot more fundamental. Alalouch et al. [6] suggest that formal quantification by means of spatial layout and integration of bed location can influence preference. They deduce through both computer simulation of patient visibility by nursing staff and questionnaires that patients of any age prefer a bed (regardless of room type) showing low integration and low control as dominant factors. That is to say they wanted to be easily visible to staff but in wards that are not too busy. This translates in the case of multi-bed rooms, to periphery beds in direct line of sight of the nursing station. In single bed rooms this would be homologous to beds with large windows to the corridor close to the nursing station [116]. Figure 2.6 shows three types of wards highlighting average patient choice according to nurse location (starred).

Advantages and disadvantages of single rooms were found to exist for both patients and staff and were collated in the York Health Economics Consortium report of 2005 [26]. Table 2.2 summarises these, and highlights that overall patient satisfaction increased due to improved privacy. However there are clearly some reservations concerning the potential lack of patient visibility by nursing staff. Current UK specification requires a minimum of



(a). Nuffield/duplex ward



(b). Cruciform ward

(c). Hub and spoke ward

Figure 2.6: Patient preference for bed positioning.

+++ = Most preferred location, --- = least preferred. (Star = nurse station).

Adapted from Alalouch et al. [6].

50% single bed rooms within all newly constructed and existing hospital wards [62]. Construction has already begun to deploy and or retrofit 45,000 single rooms within hospitals, costing a minimum of 1,500 million GBP over a five year period.

#### 2.1.4 HBN04-01: In-Patient Accommodation

The *Health Building Note 04-01: Inpatient accommodation* [5] is a Department of Health guidance document that lays out the minimum single room and multi-bed room sizings within the UK. It stipulates that each patient bed should contain access to five zones, namely: Bed space, WC/shower facilities, clinical support zone, social/family support zone and nurses' workstation. Minimum bed space for any type of hospital accommodation is

3.6m×3.7m, space which must be kept clear at all times to allow for free circulation of nursing staff and equipment.

#### 2.1.4.1 Multibed-rooms

Figure 2.7 is a typical minimal example layout for a multi-bed ward in the UK. It shows a four-bed room with an assisted shower room and a second semi-ambulant WC, both en-suite. Full details of these en-suite facilities are contained in *Health Building Note 00-02* - ‘*Sanitary spaces*’ [117].

Type	Example
<b>Perceived</b>	
<i>Advantages</i>	<ul style="list-style-type: none"> <li>-increased patient privacy, dignity and comfort and less disruption from other patients</li> <li>-improved control over their environment, enhanced sleep, enhanced contact with families</li> <li>-increased patient satisfaction</li> </ul>
<i>Disadvantages</i>	<ul style="list-style-type: none"> <li>-reduced social interaction and thus patient isolation</li> <li>-less surveillance by staff</li> <li>-increased failure to rescue and increased rates of slips, trips and falls</li> </ul>
<b>Potential</b>	
<i>Advantages</i>	<ul style="list-style-type: none"> <li>-more personalised patient contact</li> <li>-fewer interruptions with medical storage in rooms</li> <li>-a decreased chance of prescribing errors</li> <li>-less walking for nurses</li> </ul>
<i>Disadvantages</i>	<ul style="list-style-type: none"> <li>-increase in staff travel distances</li> <li>-adjustments to staff skill-mix</li> </ul>

Table 2.2: Perceived and potential advantages and disadvantages of hospital single rooms according to York HEC [26].



accommodation as per Figure 2.8 lays out the five-stage make-up of a typical ‘*best-buy*’ single room. Table 2.3 gives a description of the individual sections within the room.

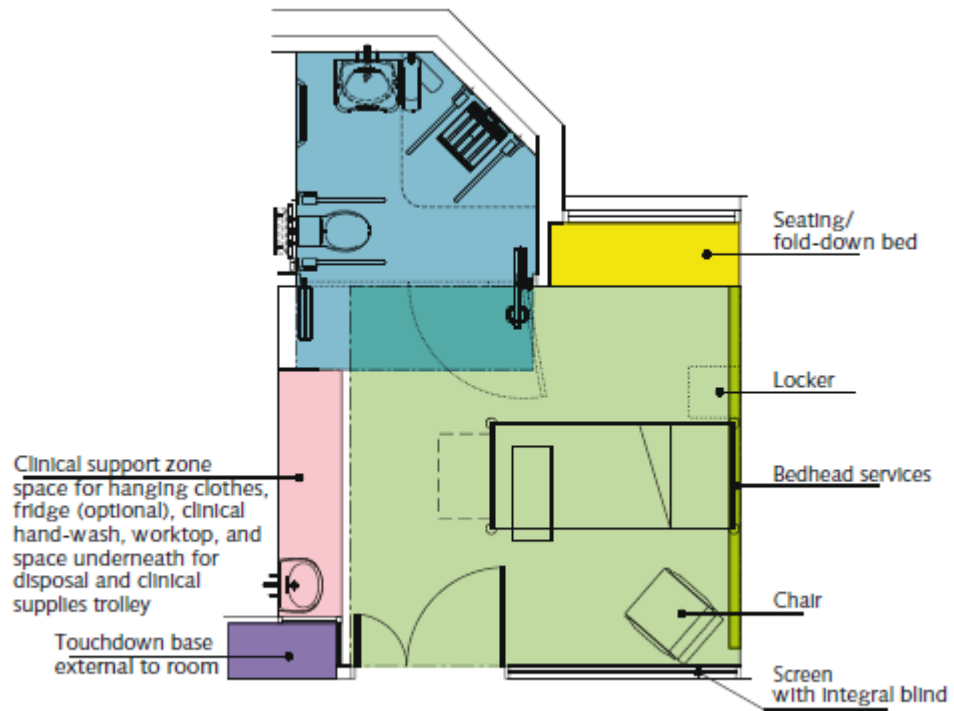


Figure 2.8: HBN04-01 single room.

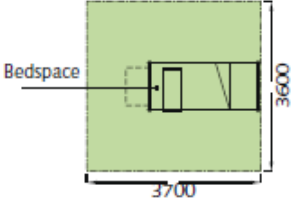
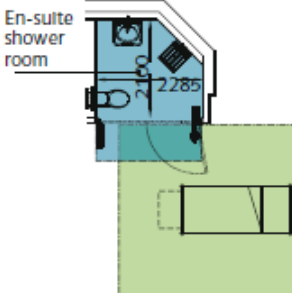
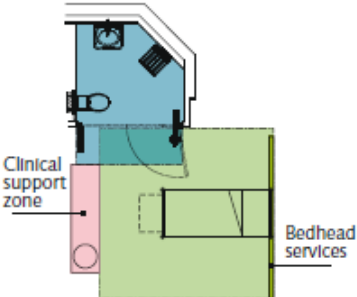
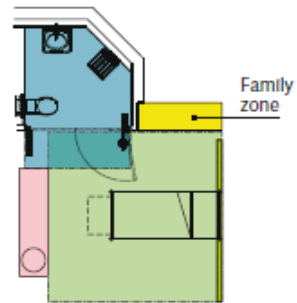
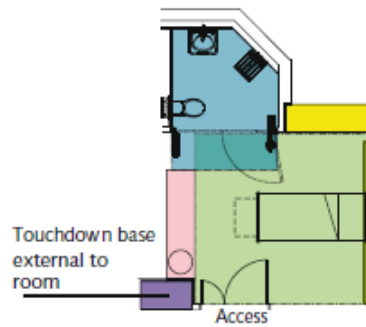
Room feature	Comment
	Bed space 3.6m × 3.7m
	Clear space around the bed + ensuite WC/hand-wash basin/shower (4.5 m <sup>2</sup> ) and clinical workstation, storage and overnight stay facility (up to 3 m <sup>2</sup> )
	Clinical support hand-washing, built-in storage and space for movable equipment such as supply or disposal trolleys. Typical total room area is 23.5 m <sup>2</sup> allowing circulation within the room

Table 2.3: Single room construction from HBN04-01:In-patient accommodation.



Accommodation for visitors should not impede access to bedside



Touchdown bases are located near to room entrances so that it is possible to observe the patient from outside the room

---

Table 2.3: (continued) Single room construction from HBN04-01:In-patient accommodation.

### 2.1.4.3 Bevan-Ward research project

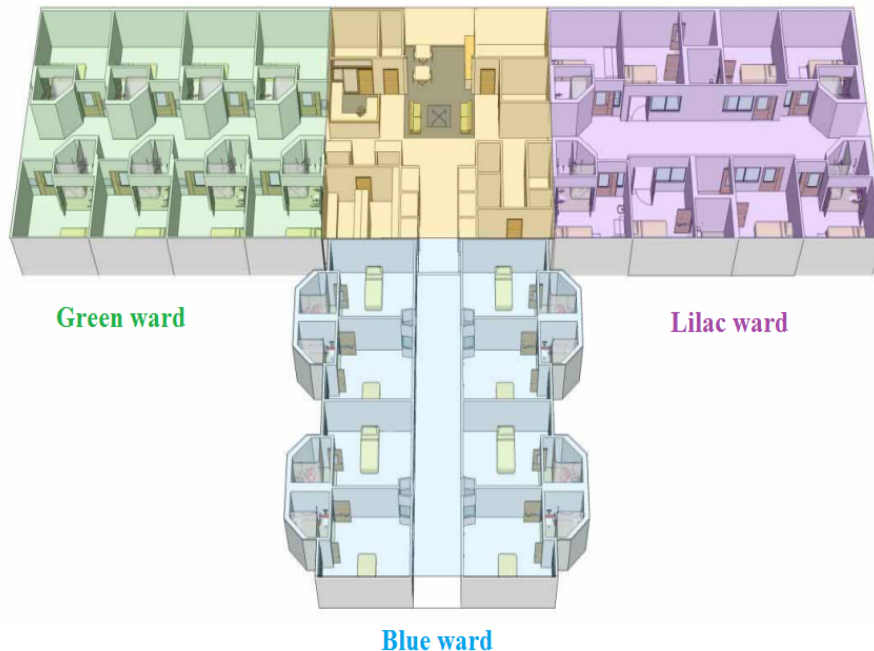


Figure 2.9: Bevan Ward project comparison of ward layout and room design.

Following the Darzi report, layout of single rooms has received a lot of recent attention. With 29% of the NHS estate pre-dating 1948, the Bevan Ward research project (unpublished 2009) set out, as part of establishing the costs and benefits of 100% single bed accommodation, to identify a layout of ward and room that promoted both patient and staff satisfaction. The study was based on a nine month analysis of 1,289 patients in gastroenterology, haematology and general medicine wards. Twenty four rooms comprised in three connected wards (blue, green and lilac) of differing layout were used by patients for six months as an annex to Hillingdon Hospital, UK (see Table 2.4). The design combinations were tested on a number of criteria with the primary aim to collate and investigate by means of observations as well as patient questionnaires:

1. Views and opinions of patients
2. Views and opinions of staff
3. Implications for clinical staffing and costs
4. Implications for non-clinical staffing and costs (e.g. cleaning)

## 5. Clinical outcomes of patients

Conclusions suggest that rooms with high HCW-patient visibility (**Lilac Room** in Table 2.4) were most preferred. An important corollary results from the positioning of the WC either side of the room rather than within the corridor space or on the exterior façade wall. This allows for large windows both into the corridor and outside. It also reduces the room cost due to lower exterior surface area materials used.

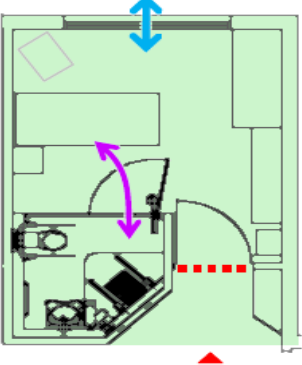
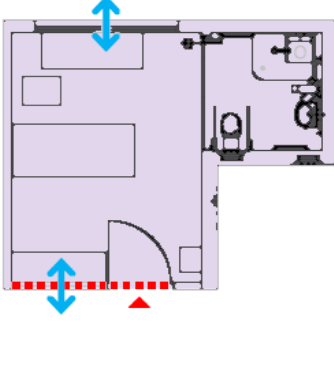
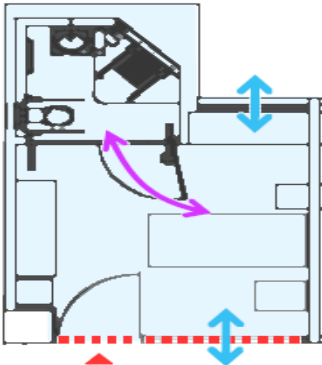
Green Room	Lilac Room	Blue Room
		
<ul style="list-style-type: none"> <li>• <b>Reduced</b> visibility from corridor</li> <li>• <b>Good</b> views outside</li> <li>• <b>Private</b> for patients</li> <li>• <b>Easy</b> access to en-suite</li> </ul>	<ul style="list-style-type: none"> <li>• <b>High</b> visibility to corridor and outside</li> <li>• <b>Less</b> patient privacy, controllable with blinds</li> <li>• <b>Flexible</b> bed location</li> </ul>	<ul style="list-style-type: none"> <li>• <b>High</b> visibility to corridor</li> <li>• <b>Limited</b> views outside</li> <li>• <b>Less</b> patient privacy, controlled by blinds</li> <li>• <b>Poor</b> access to en-suite due to door position</li> </ul>

Table 2.4: Reported advantages and disadvantages in the **Green**, **Lilac** and **Blue** single rooms from the Bevan ward experiment 2009.

## 2.2 Heating, Ventilation and Air-Conditioning (HVAC) Guidelines

“To keep the air he [the patient] breathes as pure as the outside air; without chilling him.” (Florence Nightingale, Notes on Nursing - What is and what is not, 1860.)

The ventilation strategy and energy consumption are key choices in hospital design. Although the ventilation approach is affected by the climate, it has a direct effect on the building form and the running cost of the hospital [118].

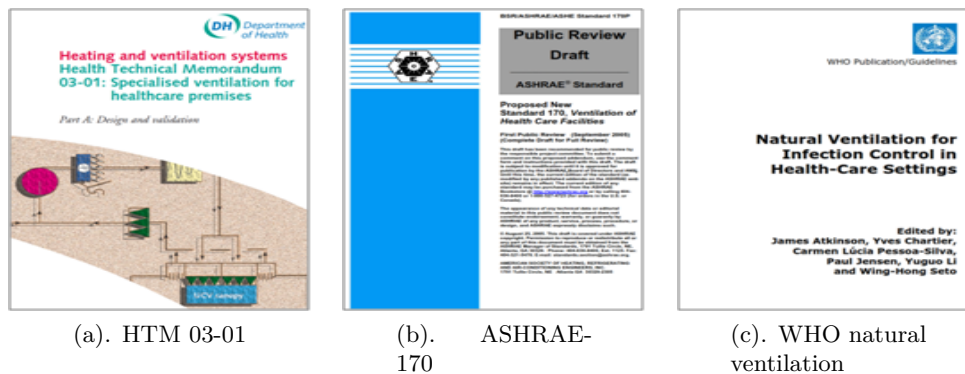


Figure 2.10: Ventilation guidelines for hospital and clinical areas.

Heating, Ventilation, Air-Conditioning and Refrigeration (or HVAC-R) refers to the treatment of air within a building. UK health care facilities come under the Chartered Institute of Building Engineers’ umbrella of guidance upon which ventilation design, or more commonly known *CIBSE guide B* is based. This a comprehensive text which outlines both strategy and calculation methodology for building ventilation principals. Health-Technical Memoranda (HTM) focus this guidance into health care specific elements of standards, policies and up-to-date established best practice. In particular the Heating and Ventilation Systems guidelines are set out in the: HTM03-01 (see Figure 2.10a), which give “comprehensive advice on the design, [...] installation and operation of specialised building and engineering technology used in the delivery of health care” [73].

The CO<sub>2</sub> reduction agenda has prompted heating and refrigeration to become a significant issue showing room for improvement and consequently room design [118]. Indeed the efficiency of heat distribution and management is consequently affected [104]. The *HTM*

*07-07:sustainable health and social care buildings* calls on NHS organisations to achieve targets of 35-55 GJ/100 m<sup>3</sup> for new buildings, and 55-65 GJ/100 m<sup>3</sup> for less intensive refurbishments of existing facilities [64].

Guidelines on how and where ventilation should be achieved are rather vague, particularly for general ward areas. Minimum threshold ventilation rates are given in terms of air changes per hour ac.h<sup>-1</sup> with most spaces assuming dilution (or mixing) ventilation. However, expert opinion suggests that actual air handling systems, particularly older installations, may well be under-performing. Gilkeson et al. [112] conduct ward-wide ventilation testing and highlight that through building leakage air change rates are highly variable.

Spaces are differentiated in terms of clinical need and risk when prescribing ventilation provision, as set out in Table 2.5. HTM03-01 also indicates a recommended types of ventilation system for each clinical and non-clinical room; mechanical supply, extract or natural ventilation. In ward areas, guidance suggests natural ventilation is appropriate, however many designers opt for mechanical or hybrid systems as it is easier to demonstrate the ventilation rate is achieved [104].

Room type	Ventilation	ac.h <sup>-1</sup>	$\Delta P$	Temp. °C
General ward	S or N	6	-	18 - 28
Communal toilet	E	6	-ve	-
Single room	S,E or N	6	0Pa or -ve	18 - 28
Single room WC	E	3	-ve	-
Isolation room	S, E	10	-5Pa	18 - 28
Operating theatre	S,E	25	+25Pa	18 - 25
Critical care areas	S	10	+10Pa	18 - 25

Table 2.5: Ventilation strategy as set out in Appendix 2 of HTM03-01 for some example health care facilities. S=Mechanical supply, E=Mechanical extract, N=Natural ventilation.

Evidence based rationale for the chosen values in Table 2.5 is quite scarce, relying mainly upon metrics of indoor air quality such as CO<sub>2</sub> levels and temperature [118]. However, it should be acknowledged that the guidance does include an element of a safety factor.

The USA and many other countries rely on a counterpart document produced by the American Society of Heating, Refrigerating and Air-Conditioning Engineers: *ASHRAE-170, Ventilation of Healthcare Facilities, 2011* [119]. Hospital ventilation systems are prescribed as mechanical ventilation for all clinical areas, suggesting a value between 60-80 L/s of air per person. The basis for this value appeared in the 1989 edition and was suggested to maintain indoor CO<sub>2</sub> levels around or below 1,100ppm to maintain occupant comfort, but has since vanished in later editions. A requirement of at least 2 ac.h<sup>-1</sup> from external air with the remaining quantity made up of recirculated and filtered air is also stipulated. This supplementation is understandable when considering deep-plan, energy intensive hospital designs that have prevailed up until very recently in the USA [104].

As summarised by Sundell et al. [120] the establishment of ventilation requirements for occupied spaces has a long history. Several literature reviews have been published on the effects of ventilation on health. Their common conclusion is that lower ventilation rates can significantly aggravate health outcomes, namely sick building syndrome (SBS). However, only one longitudinal study conducted by Menzies et al. [121] in a hospital deduces conclusively that the incidence of TB amongst health care workers is indirectly tied to the ventilation rate. They conclude that air change rates lower than 2ac.h<sup>-1</sup> were associated with higher incidences of TB. This was supported by a retrospective study in a Hong Kong hospital conducted by Li et al. [122] following the SARS outbreak in 2003. Noakes et al. [118] suggest that the lowest permissible turn over rate, based on cost-analysis, should be at least 4ac.h<sup>-1</sup>.

Indeed, current ventilation guidelines are based primarily on data that pertain to occupants' perception of indoor air quality such as stuffiness and temperature, rather than on risk-related aspects of indoor pollutant exposure. Extending ventilation standards to more explicitly include health risks as well as perceived air quality requires scientific knowledge; knowledge that is scarce. Whyte et al. [123] set the precedent for clean air supplies within operating theatres in their study arguing that an average value of 0.5 pathogenic microorganisms /m<sup>3</sup> corresponds to an acceptable clean air sample. In parallel to the previous study, the importance of airborne infection and the protective functions of ventilation systems were demonstrated by Lidwell et al.[124] in a controlled trial on patients having joint replacement operations. Both this and Drake's [125] work in Australia based around similar premises, prompted the HTM and ASHRAE to employ a standard 12-25 ACH with

+25Pa pressurisation within their operating theatres. However, nothing is mentioned with respect to general patient rooms. The following constitute the HTM03-01's primary list of important ventilation factors:

1. Human habitation (minimum fresh-air requirement based on CO<sub>2</sub> background levels of 350ppm)
2. The extraction of odours, aerosols, gases, vapours, fumes and dust - some of which may be toxic, infectious, corrosive, flammable, or otherwise hazardous (Control of Substances Hazardous to Health (COSHH) Regulations)
3. Dilution and control of airborne pathogenic material
4. Thermal comfort
5. The removal of heat generated by equipment (for example catering, wash-up, sterilising areas, electrical switchrooms, and some laboratory areas)
6. The reduction of the effects of solar heat gains

The World Health Organisation (WHO) also provides some guidance (see Figure 2.10c) with respect to designing natural ventilation systems in health care facilities, although this is more aimed at hospitals in developing countries. They recommend clinical areas should be mechanically ventilated providing between 160-180L/s for air per person within isolation rooms. Natural ventilation systems are preferred for non-critical or non-clinical areas, for example providing 2.5L/s/m<sup>3</sup> in corridors.

### **2.2.1 Mechanical Ventilation**

The provision of the air change rates stipulated by the HTM03-01 and laid out in Table 2.5 can be achieved in at least two different ways according to the room type. Clinical environments should be at least partially supplemented by an active mechanical ventilation system, to ensure constant turnover. For example within this category, clean rooms refer to areas which must remain aseptic such as pharmacies and packing rooms in sterile services departments, and consequently must be provided with a supply of clean air. Extracts are typically via pressure stabilisers. Conversely *dirty* rooms such as sanitary facilities,

dirty utilities and rooms where odorous but non-toxic fumes are likely; should be under negative pressure and so require extract ventilation. Patient bathrooms also fall in this category but do not require special treatment of the extracted air. Figure 2.11 shows a representative hospital cross-section.

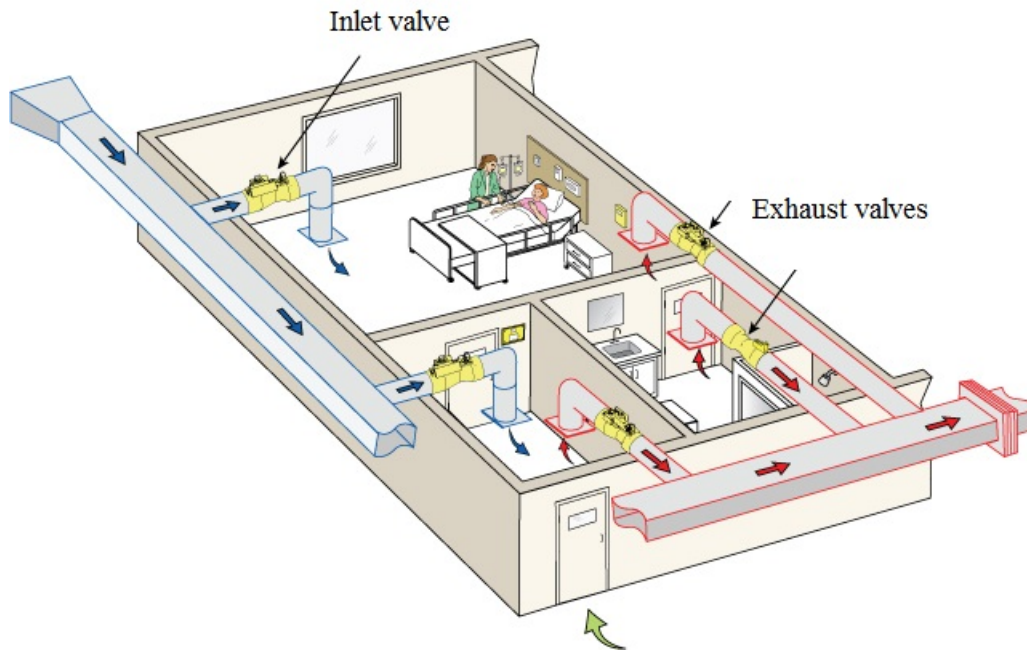


Figure 2.11: Mechanical ventilation of hospital cross-section. Adapted with kind permission from [7].

The HTM03-01 suggests that hospital corridors (Table 2.5) should largely be at a higher positive pressure than the adjoining single rooms, whereby attempting to prevent cross-contamination from one patient room into another. Ward design varies greatly and so does the ventilation provision, often with supply coming from ceiling diffusers and extracts being located in the WCs. Increasingly common are hybrid systems that rely on mechanical ventilation but openable windows supplement the fresh air supply [8]. Often standalone fans provide extra air movement during the summer months [46] but the extent to which they influence the spread of airborne infections is still unclear [120].

### 2.2.1.1 Mixing and displacement ventilation

Indoor air quality can be measured by  $\text{CO}_2$  levels and a metric  $\epsilon$  has been found to represent the air change effectiveness (ACE) of a ventilation system [126]. One way of

looking at ACE is by means of the age of air  $\tau$ . This is the total time a small *packet* of air has spent in a room from the moment it entered. Calculating this relies on a tracer gas such as CO<sub>2</sub>, SF<sub>6</sub>, or NO<sub>2</sub> injected into the ventilation shaft, the concentration of which can be analytically monitored throughout the room:

$$\tau = \frac{1}{C(t_{\text{end}})} \int_0^{t_{\text{end}}} C(t_{\text{end}}) - C(t) dt, \quad (2.2.1)$$

$$\text{ACE} = \frac{\tau_{\text{return air}}}{\tau_{\text{breathing level}}}, \quad (2.2.2)$$

where  $C(t)$  is the concentration at the point in question,  $C(t_{\text{end}})$  is the steady state concentration, and  $t$  is the time elapsed since the start of tracer gas injection. ACE is then the ratio between the age of the exhaust-air and that of the average air where occupants breathe. A short circuiting flow pattern decreases the exhaust-air age and causes the ACE to be smaller than unity. Perfect mixing results in an ACE of one. This can be represented also through the concentration of tracer gas at the inlet, outlet and any recycled or return air:

$$\epsilon = \frac{\text{CO}_{2\text{return air}} - \text{CO}_{2\text{in}}}{\text{CO}_{2\text{in}} - \text{CO}_{2\text{out}}}, \quad 0 \leq \epsilon \leq 1 \quad (2.2.3)$$

$$(2.2.4)$$

Short circuiting ( $\epsilon < 1$ )     $\leq$  Fully mixed ( $\epsilon = 1$ )     $\leq$  Piston displacement ( $\epsilon > 1$ )

Idealised ventilation acts like a piston, flushing out old air ahead of incoming air [127] such as in Figure 2.12b. This is referred to as displacement ventilation with a corresponding  $\epsilon$  value greater than one. Fully mixed air (Figure 2.12a) can be represented by a value of  $\epsilon = 1$  where CO<sub>2</sub> concentrations are homogeneous within the room. In reality, contaminations in indoor air tend to be inhomogeneous in nature, lingering in certain locations. Sometimes this is a sign of ventilation short-circuiting showing an  $\epsilon$  value of  $< 1$ .

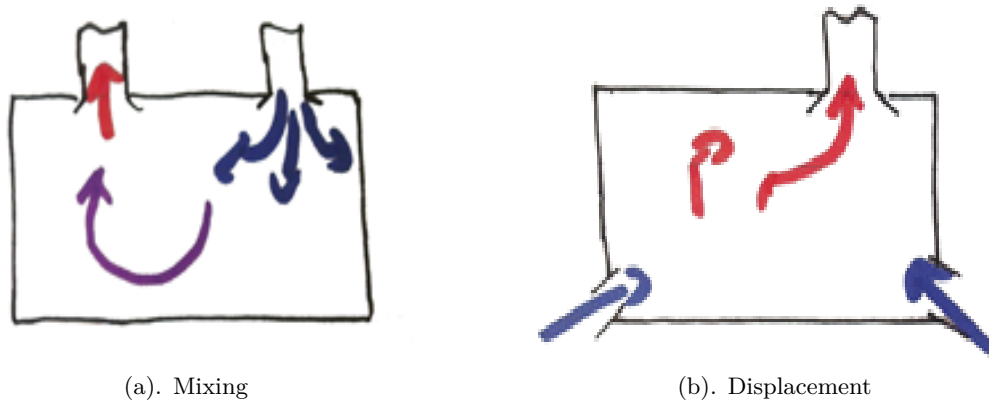


Figure 2.12: Mechanical ventilation: Mixing and displacement methods.

Positioning of supply and extract diffusers has become an increasingly important area of research, with much contention over the appropriate location, shape and size of these. Obscuring the outlet by furniture is not only bad practice but potentially can cause under performance the system or recirculation zones [8]. Questions are also being raised as to whether inlets should be positioned at low level [12], with high level extracts or vice-versa and which provides the best performance.

### 2.2.2 Natural Ventilation

Ventilation of fresh air into the room from outside can be induced via temperature differences denominated *buoyancy* or *stack driven* methods, (Figure 2.13a) or through the natural force of the wind: *Wind driven* methods. Both of these are widely used in hospital design [112], particularly within large open Nightingale style wards (Figure 2.13b). However, improved envelope sealing of new buildings has reached the point that infiltration through building leakage can no longer be relied upon to provide sufficient air flow and hence design should make explicit provision for ventilation [73]. Both windows and louvres offer a low cost method of ventilating non-critical patient rooms and non-clinical areas [8].

Natural ventilation methods can achieve much higher air change rates than their mechanical counterparts in an energy-efficient manner, many times the above prescribed values [112]. While natural ventilation is promoted by the NHS for non-critical spaces such as wards and offices [128], there are perceived barriers: Concerns about infection control. There are few examples of natural ventilation/passive cooling strategies being

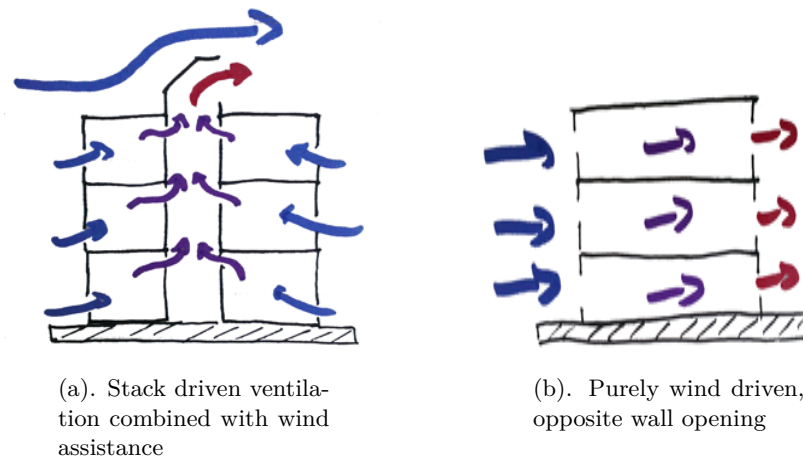


Figure 2.13: Passive ventilation strategies and implementation.

used in hospital buildings that allay these fears, although recent research through the De<sup>2</sup>RHECC (Design and Delivery of Robust Hospital Environments in a Changing Climate, UK) shows that innovative simple modes are indeed, not only possible, but mutually compatible with the HTM03-01's  $6\text{ac.h}^{-1}$  and the HTM07-07's  $55\text{-}65\text{GJ}/100\text{m}^3$  energy consumption [118, 129, 130]. Adamu et al.'s [131] comparison by numerical modelling of natural ventilation strategies for a single room highlight the potential impact that these will have on patient satisfaction. However, Short et al.[130] do note that it is unlikely that current technology in passive ventilation would suffice far into the future without the necessary installation of an adjuvant mechanical ventilation system further down the line. In particular Gilkeson et al. [112] argue that when carefully coupled with extractor fans, such hybrid systems can stabilise the unreliability of wind speed and direction, hence working in tandem.

Positioning openings or windows within hospital rooms can be tricky, not least to maintain correct pressures but to ensure constant supply and extract. Figure 2.14 shows five different examples of these positions. Nightingale wards take advantage of cross ventilation with their tall windows on opposing walls [112, 129]. Single patient rooms cannot implement this type of strategy in the same way, often having to combine a natural stack effect with a single or double opening on the same exterior wall. Low wind speeds coupled with small temperature difference can mean that air changes are too low at times. In this vein, the ASHRAE-170 [119] suggests that rooms that are 3m or deeper should not rely on this method alone.

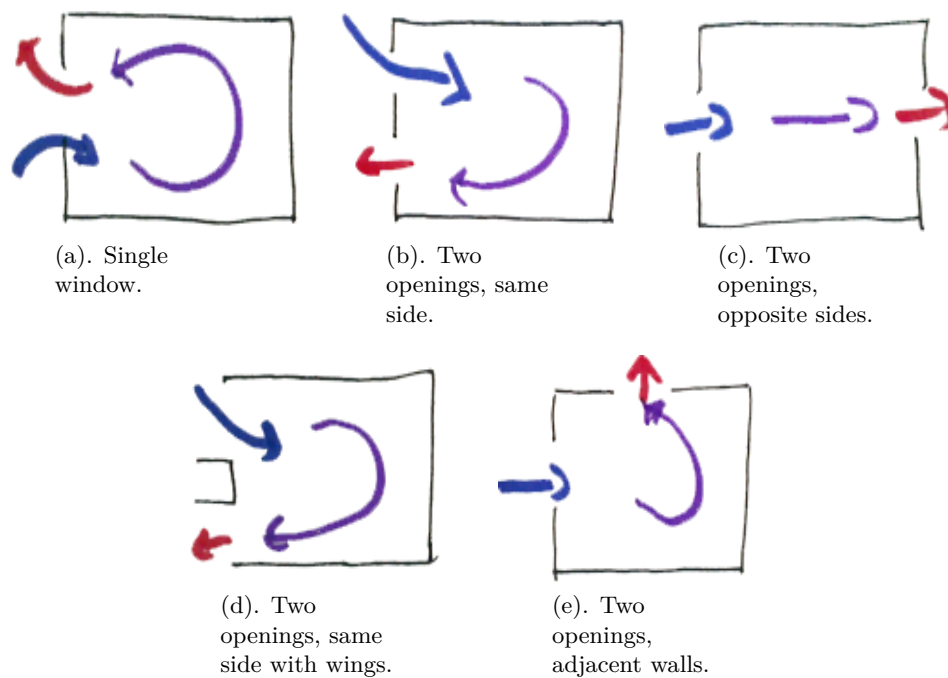


Figure 2.14: Passive ventilation examples.

Figure 2.15 shows the natural ventilation of a hospital room at Altnigelvin, NI, through a large windowed façade. This is an example of single sided, double opening ventilation which relies on buoyancy and can be effective all year round. A maximum window opening distance of 10cm within patient reach is an added restriction however, promoting the use of mechanisms such as trickle vents. CIBSE's Application Manual AM10 - '*Natural ventilation in non-domestic buildings*' suggests that wind driven methods are more reliable throughout the year than their temperature driven counterparts. However, since the wind is naturally a highly variable phenomenon, it can not be relied upon either within clinical areas and so should be supplemented by mechanical ventilation. This is then denominated *mixed mode ventilation*.

### 2.2.3 Advanced Passive Ventilation

In the post-2008 economic climate it is unlikely that the NHS will attempt a wholesale replacement, looking closely at retrofitting, shoehorning and refurbishing of their aging building stock. With increasing pressure to combine low-cost, highly resilient ventilation designs, architects and building services modellers are increasingly focussed on staving off the omnipresent effects of global warming. The UK can suffer from cold winters and very

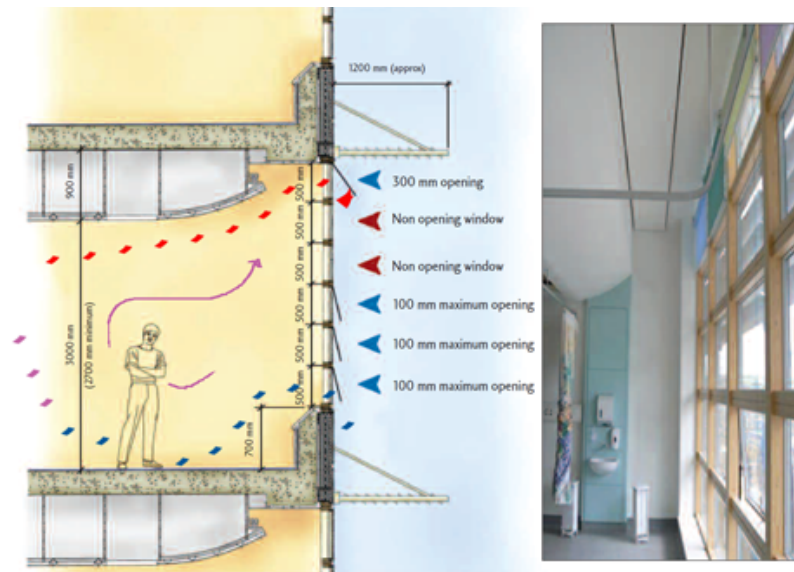


Figure 2.15: Example air streamlines of buoyancy driven natural ventilation at Altnagelvin Area Hospital, Northern Ireland. [8].

warm summers, with the heat wave of 2003 becoming increasingly a more frequent event by 2050 [132]. The shoehorning of mechanical cooling into existing patient areas appears to be an unavoidable recommendation from the NHS patient safety risk assessments but the carbon implications would undoubtedly undermine the NHS' carbon reduction plans even further [133]. CIBSE guide A [134] prescribes thermal comfort temperature ranges for free-running buildings, the upper values of which should not surpass  $25^{\circ}\text{C}+3^{\circ}\text{C}$  (operative) for more than 88h per year (vs. the HTM03-01's 50h dry-bulb). These seem a little vague however, and single sided natural ventilation such as that at Altnagelvin in Figure 2.15 would appear to be more susceptible to requiring a helping hand from mechanical systems.

Modified advanced natural ventilation (ANV) strategies are a particularly energy efficient option in the long run according to feasibility studies conducted by Lomas et al. [9] and Short et al. [135]. These ventilation strategies make use of internal thermal heat mass and in particular indoor and exterior temperature differences, sometimes in combination with wind pressure to drive air-flow. In particular the temperature stratification within a building induces a stack effect and hence promotes air turnover through windows, skylights and dedicated towers. Figure 2.16 depicts four possible designs each their own merits. Air-flow is often mechanically controlled through louvres, which are opened and closed depending on indoor  $\text{CO}_2$  or temperature levels. Exhaust fans may also aid in maintaining consistency of flow direction.

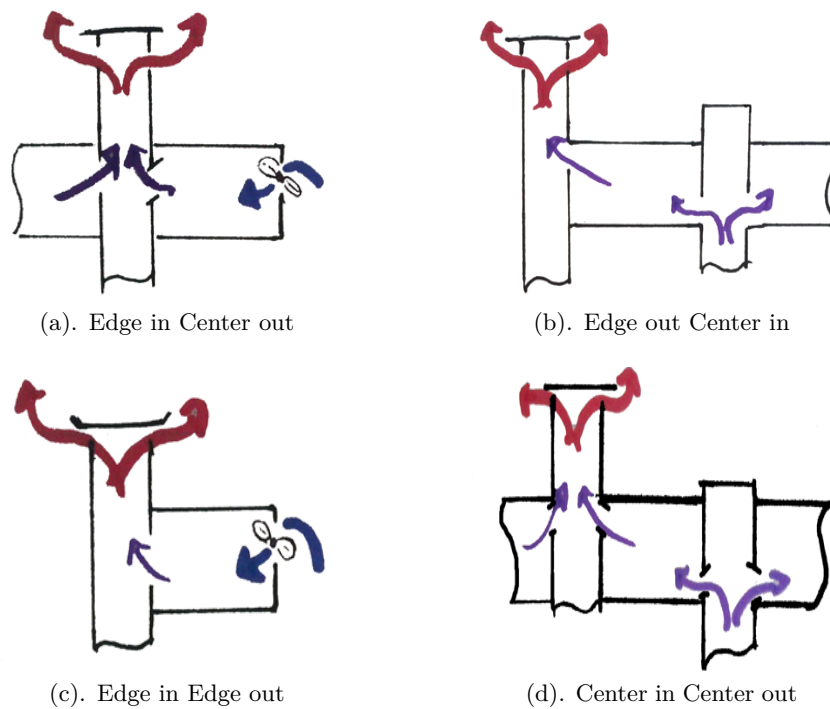


Figure 2.16: Advanced natural ventilation, adapted from Lomas et al. [9].

Figure 2.16b and Figure 2.16d utilise a large central plenum to feed air into the building and require a sealed façade to maintain air-flow regimes. In the context of hospital design this would become somewhat impracticable due to the need for operable windows. This may be achievable for non-clinical areas or relatively open floor plates such as Nightingale wards. Although costs may be low in creating or locating a central air-inlet the trend towards compartmentalised sections and the need for careful air control means that most modern hospitals would not benefit from center-in designs.

Edge-in methods such as Figures 2.16a and 2.16c avoid the need for large central atria but urban noise or pollution may still cause some inconveniences. Locating ventilation stacks on the perimeter of hospitals such as Figures 2.16a and 2.16c allows for uninterrupted floorplate usage, but generally would hinder any truly deep-plan design. Advantages do abound however, both aesthetically from creating a new exterior building skin and functionally allowing for increased shading against solar gains. Windows can be located between ventilation stacks and as such, can be easily controllable by patients or other building occupants. Such an example is shown in the refurbishments suggested for the 1960's Addenbrookes hospital, Cambridge, UK by Short et al. [130] as in Figure 2.17a.

This proved to be particularly energy efficient but still may prove unsuitable in highly polluted metropolitan areas [9].

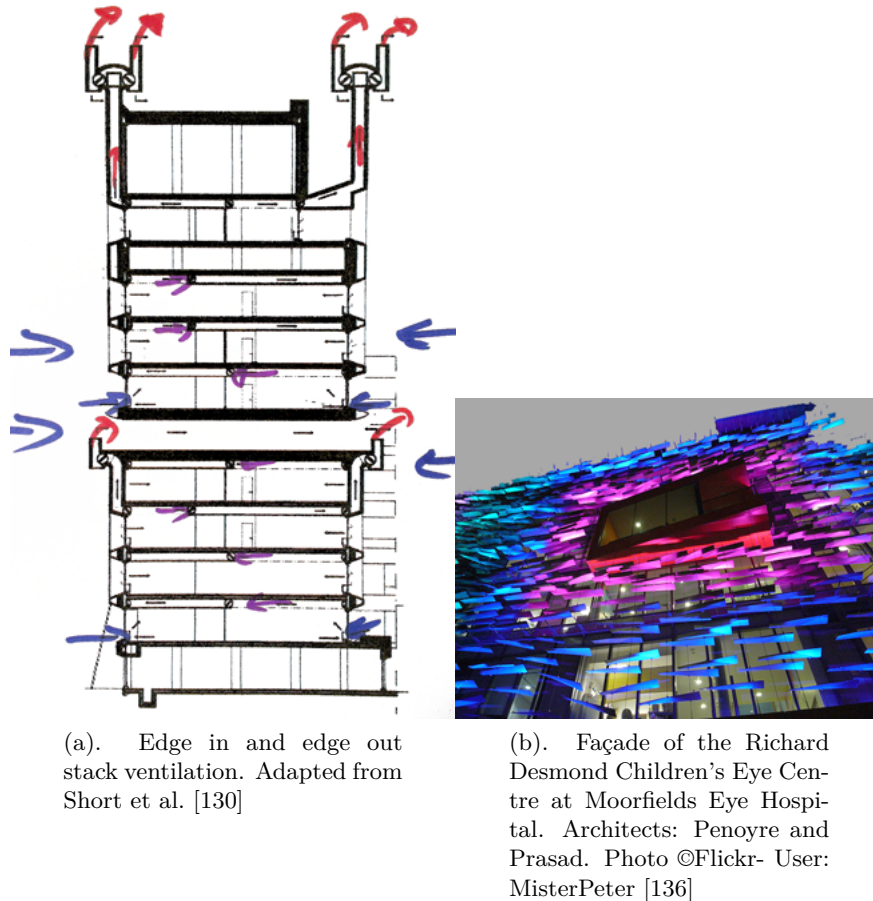


Figure 2.17: Examples of advanced building design for mitigating the effects of climate change.

Indeed, there is a clear CO<sub>2</sub> penalty for some degree of future-proofing, particularly when installing mechanical cooling systems. However some of this can be offset by intelligent solar insulation by means of durable window blinds. The combination of functionality and aesthetics at the Children's Eye clinic in Figure 2.17b is a beautiful example of this.

The design of hospital rooms has changed over the last centuries to follow patient preferences, government policy and understanding of infection/healing. Similarly, the role of ventilation is increasingly well understood, and the need to provide adequate ventilation without compromising energy efficiency is the driving force for research in this area.

## Chapter 3

# Infection transmission pathways and modelling approaches

### Contents

---

<b>3.1</b>	<b>Understanding Infection Transmission Pathways . . . . .</b>	<b>52</b>
<b>3.2</b>	<b>Mathematical Epidemiology and Quantitative Infection Risk Modelling . . . . .</b>	<b>64</b>
<b>3.3</b>	<b>Stochastic Transmission Effects . . . . .</b>	<b>69</b>
<b>3.4</b>	<b>Modelling Individual Patient Risk . . . . .</b>	<b>80</b>
<b>3.5</b>	<b>Computational Fluid Dynamics: Modelling Airborne Parti- cles in Buildings . . . . .</b>	<b>88</b>

---

Hospital patients are at risk of acquiring a secondary infection during their stay. An open wound, a catheter or simply a lowered immune system can leave patients susceptible to a nosocomial infection [137]. This chapter analyses the routes of infection transmission associated with HCAI in the UK and discusses the methodologies that can be applied to quantify infection transmission.

### 3.1 Understanding Infection Transmission Pathways

As discussed in Chapter 1, research has shown that potentially, a significant fraction of HCAs could be prevented. Research has also shown that HCAs may be related in some

measure to the layout and design of the built environment [41, 69, 113, 114]. Infection risk assessment can provide quantitative analysis of disease transmission and the effectiveness of infection control measures. However, what remains unclear is how these infections are transmitted, and much controversy reigns regarding the most appropriate method of tackling them. At least logically, it is known that the transmission of infections (see Figure 1.4) requires at least three elements: A source of infecting pathogenic microorganisms, a susceptible host and a mode of transmission [28]. Understanding modes of infection transmission is of utmost importance but remains poorly defined and even less well understood. Transmission may depend on the microorganism involved [138, 139] and may be complicated by a process involving multiple transfer routes [140]. The Center for Disease Control in the USA [3] outlines the five main modes of infection spread in the developed world some, or all of which, can be involved during transmission. This was shown diagrammatically in Chapter 1 Figure 1.4.

### 3.1.1 Contact Transmission

Dr. Ignaz Semmelweis is considered the pioneer of discovering the causal link between contaminated hands of medical staff and the death rate in an Viennese obstetrics ward during the summer of 1847. Being appointed the house officer at the *Wiener Allgemeine Krankenhaus* during the mid 1800s he noted that the mortality of new mothers was considerably higher in one clinic than another (16% vs. 7%), see Figure 3.1. He observed male medical students and doctors moving directly from the morgue to the delivery room, while the female midwives on the other ward did not. He hypothesised that necrotic material was lingering on their hands. After implementing a strict hand scrubbing regime with lime water the mortality rate dropped to a consistently low 3% across the hospital. Despite this success, he was unable to convince his peers, who ridiculed him. Eventually he was confined to a sanatorium, dying ironically of septicemia, a health care acquired infection. And still, handwashing compliance remained low.

*“Doctors are gentlemen and a gentleman’s hands are clean”* (Dr. Delucena-Meigs, contemporary of Dr Semmelweis, 1848, USA)

The act of contact transfer requires an intermediary object, in most cases fingers or equipment, to pick up pathogens from one location and deposit them elsewhere. Transfer may

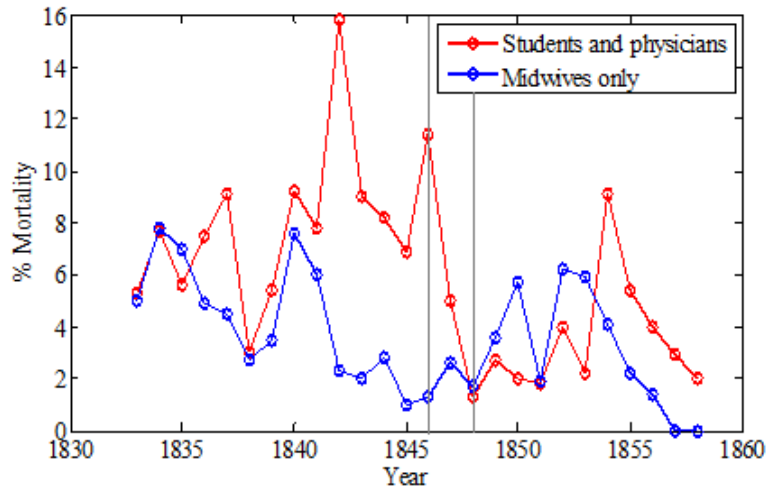


Figure 3.1: Mortality rate plotted against year in the obstetrics ward at the *Wiener Allgemeine Krankenhaus* [10].

occur from *endogenous* sources relating to the patient’s own skin micro-flora or *exogenous* pathogens from a foreign ‘reservoir’ [141]. As laid out in Chapter 1 Section 1.5.1 contact transmission refers to the process of either a **direct** placement of pathogenic material into a susceptible host (via touching of mucosa, wounds or the insertion of catheters) or an **indirect contamination** of a host via an intermediary fomite or surface.

Endogenous pathogen transfer often occurs from bowel flora contaminating the urinary tract, particularly in bed-ridden patients [22]. Exogenous transmission, particularly via surfaces in the patient’s environment is of greatest interest to this study. Figure 3.2 shows the most likely contact transmission pathways in diagrammatic fashion, highlighting the necessity of a moving vector such as a nurse or doctor. Very occasionally patient-to-patient contact is possible, mainly occurring in pediatric wards [142].

Pinning down the transfer of pathogens from patient to patient via a HCW is notoriously difficult and studies have often relied on polymerase chain reaction (PCR) and nucleic sequencing [143] or direct culture methods of microorganisms [19] to identify this. This involves locating an infectious patient, subsequent swabbing of HCWs’ hands and finally the swabbing of surfaces in the vicinity of susceptible patients.

Cross-transmission is believed also to be linked to HCW clothing where initiatives such as *bare below the elbows* [144] attempt to mitigate this. Length of hospital stay has also been linked with increased likelihood of finding cross-transmission of same-strain

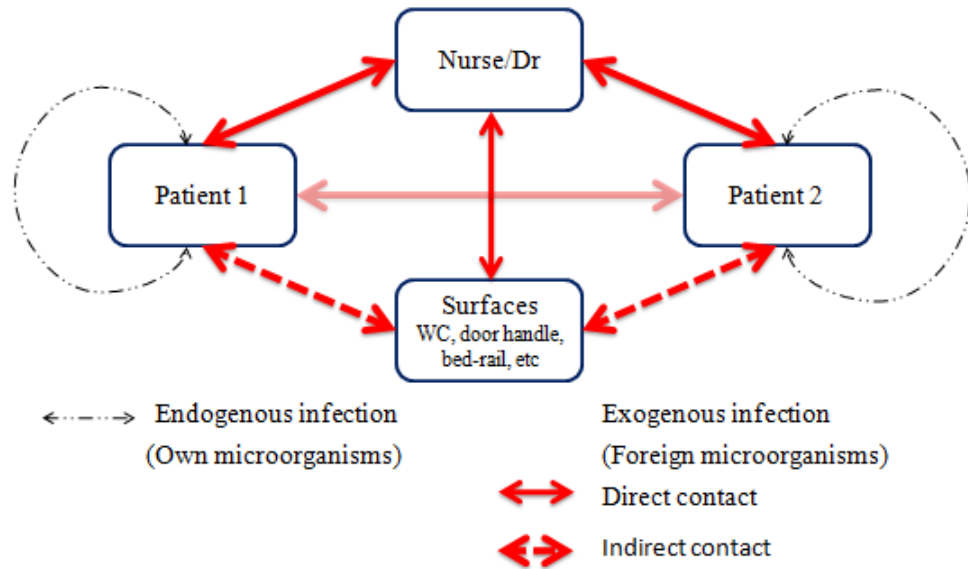


Figure 3.2: Horizontal transmission diagram including endogenous and exogenous transmission routes.

microorganisms in multiple patients' rooms [51]. This still doesn't rule out any other method of cross-contamination however, in particular, the airborne route.

### 3.1.2 Airborne Particles, Droplets and Bioaerosols

An airborne particle of any physiognomy is called an aerosol. The term aerosol refers to a disperse system of liquid or small solid particles suspended in a gas, often air. Eames et al. [145] describes them as also applying to airborne particles of biological origin known as bioaerosols, including pollens, spores, bacteria, fungi and viruses [146]. A representative selection of bioaerosol sizes are shown in Figure 3.3. Critically, microorganisms may be transmitted by droplets: Deposition of infectious droplets directly onto the nasal mucosa or conjunctiva (*droplet transmission*), or by inoculation of these membranes by contaminated hands following droplet deposition on surfaces (as part of *indirect contact transmission*) [54]. Alternatively, and perhaps more fundamentally, bioaerosols may be inhaled directly into the lungs, a process which is termed: *Airborne transmission*. Understanding of airborne transmission stems from the work of William Firth Wells who laid down the physical concepts for aerosols containing microorganisms in his pioneering work in 1934 entitled: *On air-borne infection. II. Droplets and droplet nuclei* [147]. He continued to build on this throughout his career, culminating in his exhaustive volume entitled: *Airborne Contagion and Air Hygiene* [86]. Wells coined the pivotal definition

of a droplet nucleus, stating that it is: “The airborne residue of a potentially infectious microorganism aerosol from which most of the liquid has evaporated” [147]. Highlights of his extensive work investigate airborne droplet size distributions, their evaporation rates and their subsequent settling rates. Figure 3.3 shows example size distributions of some of the most common aerosols, many of which are abundant in the hospital environment [100].

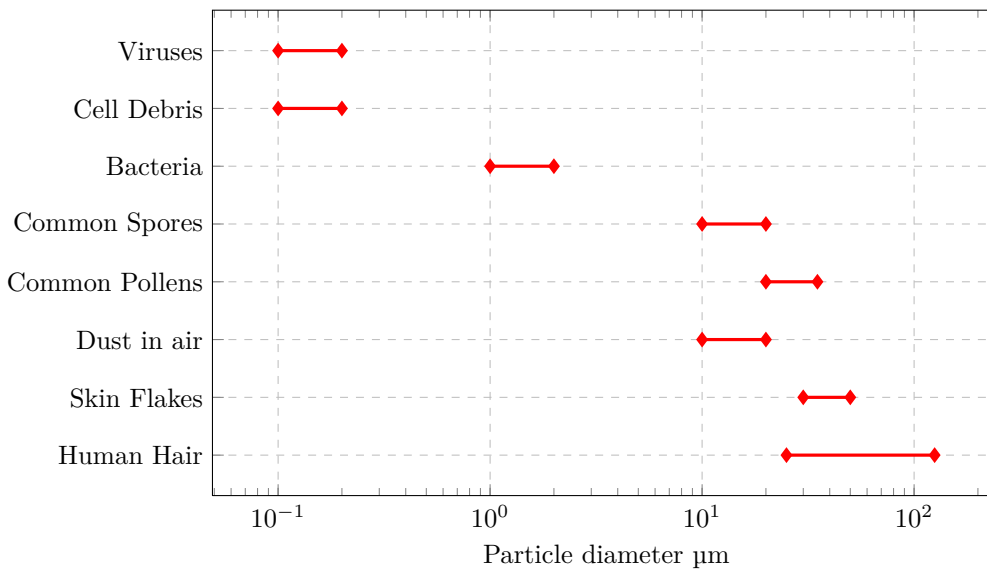


Figure 3.3: Diameter ranges in  $\mu\text{m}$  of some commonly found indoor particles [11].

### 3.1.2.1 Droplet vs. Airborne transmission

Humans are sources or ‘reservoirs’ of potentially infectious material [146]. Droplets containing pathogens can be expelled into the air during ordinary human activities including breathing, coughing, sneezing, singing and talking [138]. Hospital procedures such as cutting, drilling or aspirating have also been found to produce large quantities of airborne droplets [99]. Such microbial nuclei are surrounded by water or a mucus matrix before leaving the host [12, 57, 96, 103, 145, 148]. The fate of such droplets depends on size and evaporation rate:

*“Larger droplets evaporate slowly, settle rapidly and could deposit to the ground before drying, while smaller droplets evaporate very quickly, settle slowly and would totally evaporate in the air before reaching the ground. Droplets larger*

than this critical size would deposit on the ground before total evaporation” Xie et al. [12].

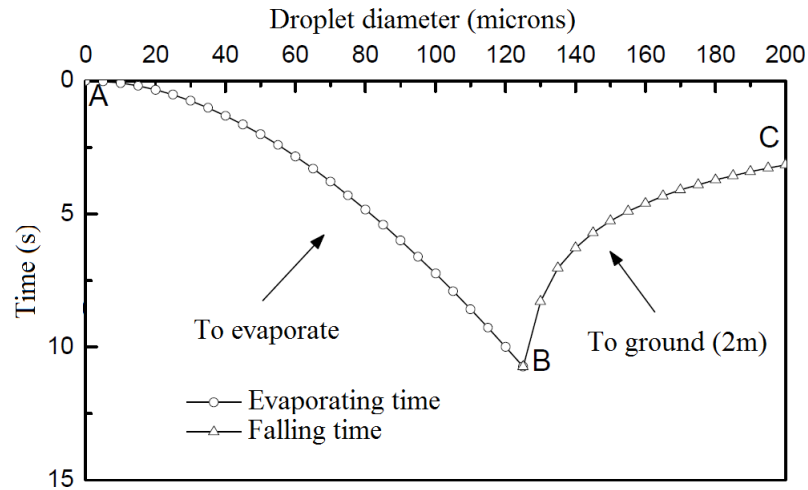


Figure 3.4: Wells’ original evaporation curve representing particles falling 2m in quiescent air. Adapted from Xie et al. [12].

Figure 3.4 represents Wells’ pioneering work in 1934 [147], revisited by Xie [12] in 2008, showing that large expelled respiratory droplets of  $100+\mu\text{m}$  would evaporate within 2m of the host relatively quickly as they fell to the ground. A threshold value of  $120\mu\text{m}$  represents the largest droplet which will not evaporate completely in quiescent air before landing. The lower size boundary between a droplet and its desiccated nucleus is somewhat vague, but a value of about  $1\mu\text{m}$  appears to be generally accepted as this threshold [145]. This is important for judging whether particles will deposit out of the air or be carried around by air currents [93], eventually being extracted via ventilation or being inhaled by susceptible hosts.

How pathogenic particles are ingested into a susceptible host has been categorised depending upon the distance from infectious source to susceptible host.

**Short-range transmission** can be regarded as direct inoculation of the susceptible host’s mucosa or conjunctiva by large infectious particles within close proximity of the infected source. Wells [86], and subsequently Xie et al. [12] coined the definitions in Table 3.1:

Definition	Diameter
Large droplet	$>60 \mu\text{m}$
Small droplet	$\leq 60 \mu\text{m}$
Droplet nuclei	$<10\mu\text{m}$ .

Table 3.1: Droplet sizes and definitions.

**Long-range transmission** refers to the potential for pathogenic material to be carried by air flows to cause infection many meters away from the infectious source. This includes the terms ‘small-droplet’ or ‘droplet nucleus’ and ‘airborne’.

Virtually all infectious agents that can cause infection at long range can also cause infection at short range as well as by direct contact [138]. Therefore, use of the term ‘long range’ refers to the greatest distance from their source at which these agents have the potential to cause infection.

Not only does the quantity of pathogenic material released during these activities vary according to the pathogen itself [57], the procedure and the person involved [143], but the size distribution of these droplets can span the sub-micron to millimeter range [149]. The velocity at which these bioaerosols are expelled can also vary [18]. Qian [99] and Xie [12] estimated through experiment that the largest droplets (60-100 $\mu\text{m}$ ) are expelled at 50 m/s during sneezing and could travel more than 6m away. Although, very recent work suggests this velocity may be much lower [150]. In the case of coughing (10 m/s) and breathing (1 m/s) particles are thought to travel less than 2m and 1m respectively. This assertion has been recently questioned [93], showing that infectious droplets can be carried for many meters by indoor air-currents. Hospitals abound with procedures that expel high quantities of bioaerosols. Tang et al. [138] found that tracheostomies and bronchoscopies, along with the use of oxygen masks or nebulisers generate high numbers of infectious aerosols [138]. Other sources of bioaerosols are highlighted by Chadwick et al. [151] which include vomiting and diarrhoea as particular causes of winter-vomiting type illnesses.

### 3.1.2.2 Aerial transmission of HCAI

The importance of the air we breathe for the transmission of certain pathogenic bioaerosols is accepted [147] but still poorly understood [88]. It has long been known that viruses such as *Varicella*, *Influenza* and *Rhinovirus* can be effectively transported via aerial dissemination [3, 48]. *Mycobacterium tuberculosis* (TB) is another example of an archetypal communicable disease which is well known to be transmitted primarily via the host breathing in the bacteria [59].

However, other potentially pathogenic microorganisms have been found to remain airborne for prolonged periods of time. In fact, laboratory studies show that humans shed approximately 700 million skin squamae [75] per hour. This translates to 208,000 particles per second which may also become aerosolised [94, 152] while walking, hence coining the term: ‘*cloud adult*’ [153]. The particles may contain pathogenic material such as *norovirus*, *C. diff* spores, VRE or MRSA, all which have been found to remain viable for prolonged periods of time [145]. Both Hathway and Roberts highlight that routine cleaning activities also cause aerosolisation of pathogen laden particles, particularly during bed making and sweeping [46, 141].

Levels of particles larger than  $5\mu\text{m}$  were found between  $6 \times 10^4$  and  $1 \times 10^5$  during at least half an hour within the patient space. Results of clinical agar tests showed several species of Gram-negative bacteria in the ward air including *Acinetobacter spp.*, *Haemophilus spp.*, and *Moraxella spp.*, all of which were subsequently found on environmental surfaces.

Hathway et al. [100] find a direct link between total levels of culturable (or viable) microorganism with the presence of Staphylococcal strains and in particular *S. aureus*. This is often a good indicator of pathogenic microorganism presence [46]. Indoor air sampling within hospitals using hand-held Andersen samplers reveals that size distributions and biological physiognomy of bioaerosols can range from sub-micron to tens of microns [100]. Critically all size ranges can carry viable pathogenic material [154].

The microbiome or microorganism footprint of any given hospital represents in some senses, its biological signature [154]. DNA sequencing techniques such as polymerase chain reaction (PCR) [155] have revealed a strong correlation between air temperature, relative humidity, ventilation rate and indoor bioaerosol loadings. In particular, Kembel et al.’s [154] pioneering work reinforces the notion that indoor biological loads, regardless

of room ventilation method, are varied, highlighting the predominance of bacterial taxa commonly associated with humans. This is in contrast to outdoor loadings of predominantly floral-related or soil-related bacteria. They suggest that this may be the resultant relationship between the growth or survival of certain biological species and environmental conditions in patient rooms. They do not find a significant difference in the microbiome of mechanically and naturally ventilated rooms. However, critically, ventilation rate is found to be indirectly proportional to pathogenic loadings.

### **3.1.3 Environmental Factors Influencing Pathogen Viability**

The environment plays an important role in the survival rate or viability of microorganisms. Hence important questions arise regarding the processes that occur during the time that the pathogen must exist outside of a human host. Xie [12] provides evidence supporting that the evaporation process itself does not lead to virus inactivation, however the desiccation of the lipid envelope of certain bacteria might.

In such a case environmental factors other than air velocity affecting shear stress, must be considered [156, 157]. Humidity and temperature of the surrounding air has been shown to greatly impact on the survival rates of nearly all pathogens [34, 146, 158]. Depending on the type of bacteria, fungus or virus, their physiological structure is either benefited or disadvantaged by increasing or decreasing temperature and humidity [108].

The connection between infection risk and hospital ventilation design has long been suspected, particularly with TB. Escombe et al. [159] make the case that nurses working in environments with lower than recommended fresh air supply rates (see Chapter 2) are at a substantially higher risk of contracting the disease. Their in-vivo clinical research made inroads into proving the importance of droplet bioaerosols in the transmission of TB within hospitals, supporting the need for active ventilation.

Indoor air and ventilation systems can affect the dispersion of aerosols and can potentially propagate infectious materials further than expected [93, 103]. The Severe acute respiratory syndrome (SARS) outbreak during 2003 highlighted the importance of this. In particular the Prince of Wales Hospital epidemic emphasised the importance of short and long range travel of aerosolised infectious particles [57, 122, 138]. This particular outbreak along with that in the Amoy Garden Hotel has been revisited repeatedly [57, 89, 122, 138].

The Hospital T1 in Beijing also found SARS infections on multiple floors [57]. In all cases the ventilation effectiveness (or lack thereof) was to blame for the spread of infection. In the latter case a maintenance shaft within the bathrooms acted as a chimney, distributing the coronavirus to many floors, several days apart.

Eventually, airborne particles or droplets settle onto surfaces through the process of deposition [100, 160, 161]. The surface itself can have a strong impact on the levels of viability of microorganism [156]. A study by Thomas et al. [162] shows the importance of surface properties with respect to *Influenza (A and B)*, and *Rhinovirus*. For example most viruses died within 12 hours on a bank note. However Thomas illustrates that when a protective matrix of nasopharyngeal secretions enveloped the pathogen, the average viable period increased drastically. Results here ranged up to 12 days in the case of *Influenza A*. Faeces played an important role in the H5N1 virus spread as large quantities are excreted by fowl, with viruses remaining viable up to 90 days at 277 K [162]. Viability of influenza in air has been found to be strain-dependent but most definitely related to relative humidity (RH) [163]. In particular, at low RH, influenza retains maximal infectivity. Noti et al. [163] shows that inactivation of the virus at higher RH occurs rapidly after release. They suggest that the effects of RH above 40% may mitigate the ability of virus-laden particles  $< 4\mu\text{m}$  to remain airborne for prolonged periods of time.

<b>Pathogen or main disease</b>	<b>Average viability</b>	<b>Ref.</b>
VRE	5 days	[19]
MRSA	average 7 days	[157]
<i>C. diff</i>	Many months	[157, 164]

Table 3.2: Viability of some Department of Health (UK) surveillance microorganisms.

Table 3.3 shows a sample of the Department of Health surveillance pathogens and their attributed most likely route of transmission. The fact that many pathogens can remain viable outside of a human host for several hours, makes pinning an exact or even most likely route of cross-contamination notoriously difficult.

Potential pathogens	Main mode of transmission [165]
<i>Escherichia coli</i> , <i>Shigella</i> , <i>hepatitis A</i> and <i>rotavirus</i>	Contact and common vehicle
<i>Clostridium difficile</i>	Contact
<i>Neisseria meningitidis</i>	Droplet
<i>Varicella</i>	Airborne and Contact
<i>Rubeola</i>	Airborne
<i>Mycobacterium tuberculosis</i> (TB)	Airborne
<i>Staphylococcus aureus</i>	Contact

Table 3.3: Examples of some pathogens and their cited modes of transmission

### 3.1.3.1 Environmental surface contamination

“*The inanimate environment of the hospital is of little importance in the spread of endemic hospital infection*”(Ayliffe et al., 2000, [48]).

Even until recently, environmental surfaces have been dismissed as playing only minor roles in the transmission chain of hospital acquired infections. Pathogens are not only transmitted directly from patient-to-patient or from patient-HCW-patient but also indirectly through an intermediary surface [19]. Droplets or airborne particles which deposit out of the air and onto environmental surfaces may well be the cause. Incomplete cleaning procedures after a patient has left the room have been shown to occur in over 50% of observed cases [51, 166]. Good examples of this are contaminated cubicle curtains or WC door handles, particularly in a multi-bed setting [167]. Surfaces such as bed rails have been consistently linked with the harbouring of hospital infections. Many of these types of frequently used surfaces in hospitals have been found to contain viable pathogens including staphylococci and enterococci strains [13, 19, 49]. Cooper et al. [142] ignore surfaces when considering MRSA transmission, which may lead one to believe that contact with inanimate surfaces to be unimportant. Hayden et al. [19] undertake the first published in-vivo experiment to determine the percentage of surface contacts that result in transfer of a pathogen. Their findings, summarised in Figure 3.5, showed that at the lowest end, one in five contacts with the patient’s table equated to viable material transfer elsewhere.

Bed rails proved to yield a 50/50 chance and a pressure cuff was almost certain to be susceptible to pathogen transfer.

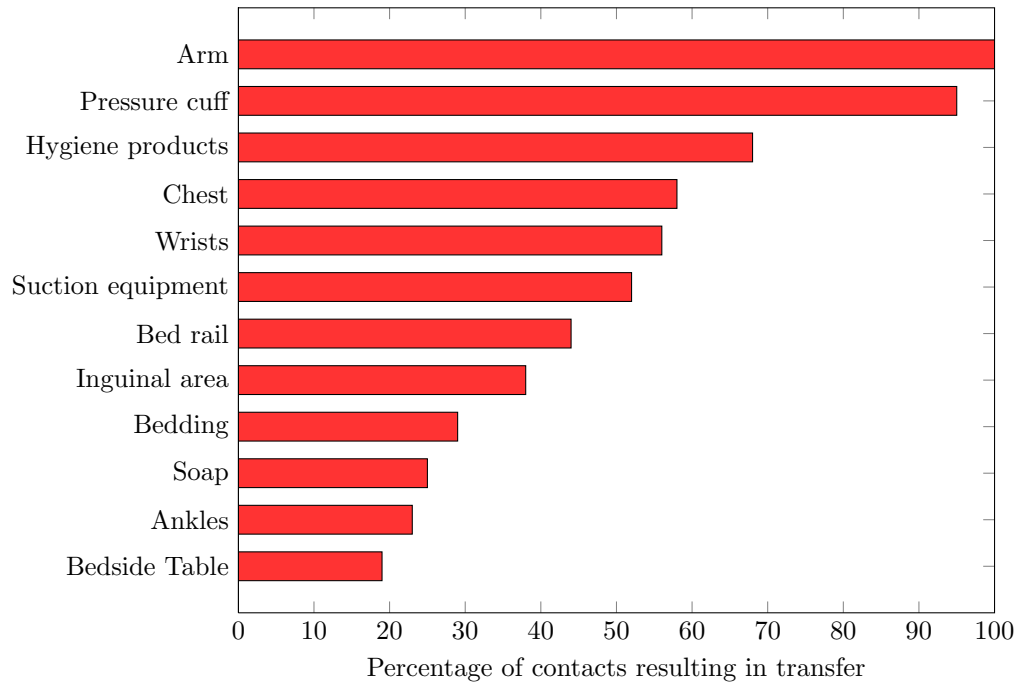


Figure 3.5: Percentage of times transfer from the originating surface was detected through swabbing. Adapted from Duckro et al. [13]

### 3.1.3.2 Cleaning procedures

‘*Visually clean and dry*’ are often heard to be the simple requirements for hospital surface cleanliness levels [168]. However biological sampling and culturing of samples have revealed a much starker reality: Visual inspection isn’t sufficient [50]. Smith et al. [25] show a host of recently cleaned, visibly clean surfaces which ultimately fail a bacterial culture test. Although the role of surfaces within the chain of infection is still unclear and probably highly variable, there is consensus that effective environmental cleaning is important in helping to break this cycle [24].

In an era of austerity, where UK Trusts are increasingly under pressure to balance budgets, cleaning surfaces costs a great deal of money. However the best way of cleaning is still a contentious issue. Chemical bioluminescence tests can represent microorganism presence under UV light, and as such, are an important tool in investigating cleaning methods[169]. In an effort to achieve maximum value NHS trusts recommend the usage of a pure water

with microfibre cloths during cleaning procedures, which Griffith et al. found to be unsuccessful in many cases [169]. Surface wipes are conducted using either non-ionic detergent spray in conjunction with a reusable cloth [166] or disposable detergent-soaked wipes. Not only how but when this happens is vitally important in understanding the life-cycle of pathogens on surfaces. Detergent of surfaces continues to remove bacteria for hours after the cleaner has left [166], but promotes a bacterial bloom before the next cleaning event. Lewis et al. [168] supported these conclusions, and recommend modified procedures which include using disinfectant not detergent, disposable cloths and subsequent drying of surfaces with paper towels. Surface cleanliness results are assessed yearly by the Patient Environment Action Team (PEAT) who suggest a value of 100CFU/cm<sup>2</sup> on patient surfaces to be acceptably clean. This figure has caused controversy within infection control teams, who consider a stricter value of 2.5CFU/cm<sup>2</sup> to be more realistic [24]. Although the role of the health care environment in the spread of some infections is far from universally agreed, circumstantial evidence suggests that contaminated hospital environmental surfaces can be a risk factor for infection [25, 50, 167].

### 3.2 Mathematical Epidemiology and Quantitative Infection Risk Modelling

*Analysis of well-constructed models can provide insight into the course of an epidemic and can be used to test ‘what if’ scenarios to inform the development of policy.* Hollingsworth, Controlling infectious disease outbreaks: Lessons from mathematical modelling, 2009 [170]

The study of mathematical epidemiology has continued to occupy scientists since the beginning of the eighteenth century. Understanding and capturing the parameters associated with real world systems is known as the study of dynamical systems. Disease dynamics are particularly important when influencing mitigation procedures. Conventionally this has included vaccination and management policies [171], but evaluation of building layout and ventilation strategies have also been considered [59, 90, 172]. By quantitatively evaluating infection risks, the influence of different environmental factors on disease transmission and the effectiveness of different infection control measures can be evaluated.

Some of the first forays into the concept of investigating the effects of disease through mathematical modelling was carried out by Bernoulli in 1766 who formulated the study of vaccination against smallpox [173]. However formalised continuous models did not appear until the twentieth century. Measles posed an important threat at the time, which Hamer [174, 175] analysed in 1906, creating a time changing (or transient) model of infection spread based on the frequency of interaction between susceptible and infected patients. However it wasn't until the late nineteen twenties that saw Kermack and McKendrick investigate the tipping point or threshold between infection spreading or dying out of a disease [79, 80, 81].

### 3.2.1 Population Models and the Epidemic Threshold: $R_0$

When modeling any disease transmission it is essential to consider the population and timescales; is the model considering the population as a whole over a long time period, or a distinct group such as hospital patient over days or weeks? In describing disease modelling, Hethcote [175] specifies epidemic models as referring to rapid outbreaks that occur in less than one year, while endemic models are used for studying diseases over longer periods. Consequently in the latter, population size can vary significantly, mainly from the introduction of new susceptibles by births or recovery from temporary immunity.

Determining whether a disease spreads through a population indiscriminately or whether it infects only small clusters of hosts can be represented by an epidemic threshold or basic reproduction number  $R_0$ . This is often denominated also as the basic reproduction ratio or basic reproductive rate [175].  $R_0$  represents the number of secondary infections occurring due to an index infectious case introduced into a susceptible population. Such that it can be defined as follows:

$$\begin{cases} R_0 < 1, & \text{infection will die out (provided infection rates are constant);} \\ R_0 > 1, & \text{infection may spread in a population.} \end{cases}$$

Graham MacDonald's [176] study of a vector borne disease: Malaria, in 1952, developed research by Ross and introduced the concepts of  $\beta$  (the infectious contact rate) and  $\gamma$  (the mean recovery rate). When a population is of size  $N$  the basic reproduction number can be represented by:

$$R_0 = \frac{\beta}{\gamma}N \quad (3.2.1)$$

Their realisation that in order to control the spread of Malaria, the eradication of the causative parasite was not necessary: Instead the ratio of  $\beta/\gamma$  must remain beneath a certain number for epidemics to be unable to spread. However, the basic reproduction number is hence presented as a single value estimate, with no indication of the variability inherent in the estimation of biological parameters [177].

### 3.2.2 Compartmental Models

Compartmentalised models can be very apt when considering a sufficiently large population. Taking as reference many communicable infections, a population (size  $N$ ) can be dissected into three categories: Susceptible hosts ( $S$ ), Infectious ( $I$ ) and Removed ( $R$ ).

Known as the SIR model, the disease dynamics are represented by a system of coupled nonlinear differential equations dependent on time  $t$ . Transmission of infection relies on the contact between the Susceptible host and an Infected subject. Transmission is dependent on  $\beta$ , the probability of infection of the susceptible host, due to contact. Within this model contact is constant. Removal occurs based on  $\gamma$  infectives leaving that class per unit time. Here the population is assumed to be *closed*, *homogeneous* and *homogeneously mixing* [178]. A closed a population is one that does not change demographically. Hence, it is assumed that throughout the course of the epidemic no births, deaths or immigrations occur.

$$\begin{aligned} \frac{dS}{dt} &= -\beta SI \\ \frac{dI}{dt} &= \beta SI - \gamma I \\ \frac{dR}{dt} &= \gamma I \end{aligned}$$

Non-dimensionalisation shows [103] how the system is explicitly dependent on  $R_0$ :  $u = \frac{S}{N}$ ,  $v = \frac{I}{N}$ ,  $w = \frac{R}{N}$ ,  $\tau = t\gamma$  and  $R_0 = \frac{\beta N}{\gamma}$  the system can be rewritten in terms of the

reproductive number  $R_0$ :

$$\frac{du}{d\tau} = -R_0uv, \quad (3.2.2)$$

$$\frac{dv}{d\tau} = (R_0u - 1)v, \quad (3.2.3)$$

$$\frac{dw}{d\tau} = v \quad (3.2.4)$$

This system of differential equations has a continuous, analytical solution  $(u, v, w) \in (\mathbb{R}^+, \mathbb{R}^3)$ , found by dividing Equation (3.2.2) by Equation (3.2.4) and integrating to give:

$$u(t) = u(0) \exp \{R_0(w_0 - w(t))\} \quad (3.2.5)$$

$$v(t) = \frac{1}{R_0}(u(t) - u_0) + v_0 + \ln \left( \frac{u_0}{u} \right) \quad (3.2.6)$$

$$w(t) = N - u(t) - v(t) \quad (3.2.7)$$

Full description can be found in Noakes et al. [103]. The number of susceptibles  $u(t)$  is a non-increasing function on  $[0, \infty)$  and  $w(t)$  is an increasing function on  $[0, \infty)$ . The limits  $u_\infty$ ,  $v_\infty$  and  $w_\infty$  exist, and  $v_\infty = 0$  where  $u(0) = u_0$ ,  $v(0) = v_0$  and  $w(0) = w_0$ , and  $t \in (0, \infty]$ . An example of this model is given in Figure 3.6, where a value of  $R_0=2.133$  is used and is commonly associated with some types of influenza [103].

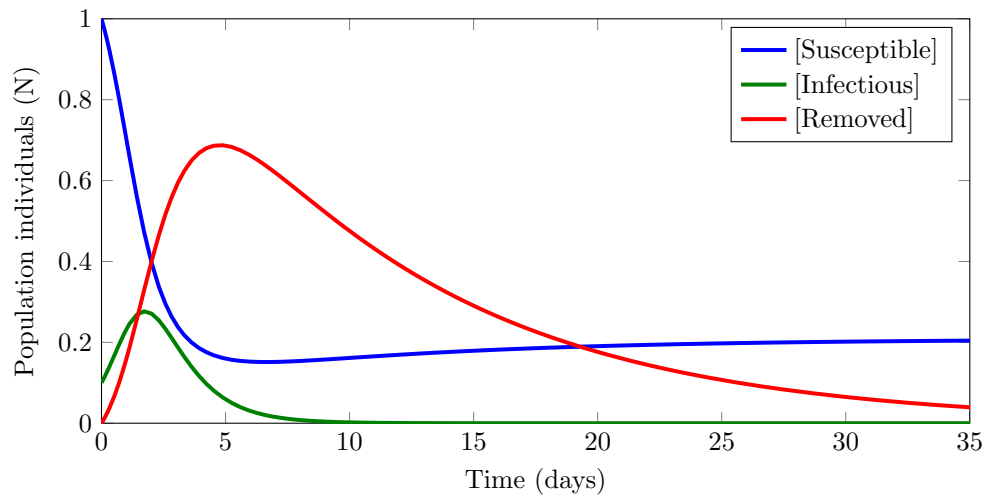


Figure 3.6: Non-dimensionalised SIR model with  $R_0 = 2.133$

The end of an epidemic is caused by the decline in the number of infected individuals rather than an absolute lack of susceptible subjects. This is explained by the concept of herd immunity, where in fact, infection cannot be sustained due to the lack of sufficient infectious members. Each transition between compartments is governed by an exponential distribution over time  $e^{R_0 t}$ . Hence, the disease-free states are absorbing, and all other states are transient. One of the major downfalls of the model resides in the immediate infectiousness of hosts, not accounting for a period of exposure and incubation of the pathogen. This can be included in an SIR model such that there exists an extra category of where individuals are infected but are not yet infectious [179]. As a consequence of this time delay, a fourth category (Exposed) has been added which accounts for the exposed population as in Figure 3.7:

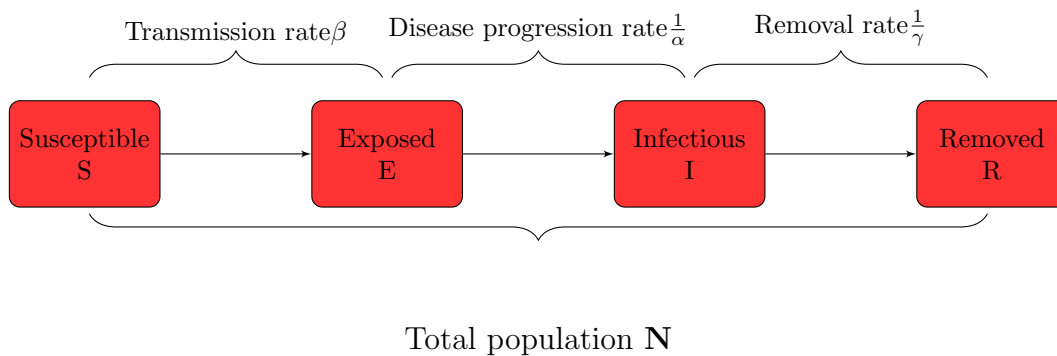


Figure 3.7: Flow diagram of the SEIR model

Non-dimensional equations are then given in Equation (3.2.8)

$$\frac{du}{d\tau} = -R_0 uv, \quad \frac{dx}{d\tau} = R_0 uv - \theta x, \quad \frac{dv}{d\tau} = \theta x - v, \quad \frac{dw}{d\tau} = v \quad (3.2.8)$$

Where  $\theta = \frac{\alpha}{\gamma}$  and  $\alpha$  is the progression rate from exposed to infectious. An example of the same  $R_0 = 2.133$  is given in Figure 3.8.

This relationship assumes that the average number of contacts is sufficient to produce infection per individual in unit time is proportional to the population density [78]. Studies have shown that in fact, only a very weak correlation exists between contact number and population size [79, 175, 180, 181]. Epidemic models are used to describe rapid outbreaks that occur in less than a year, while endemic models are used for studying diseases over

longer periods [175]. Variations on these models exist, particularly for the incorporation of population dynamics such as birth and death rates. Passive immunity is important within such endemic models but also within those that reflect vertical (from mother to child) transmission.

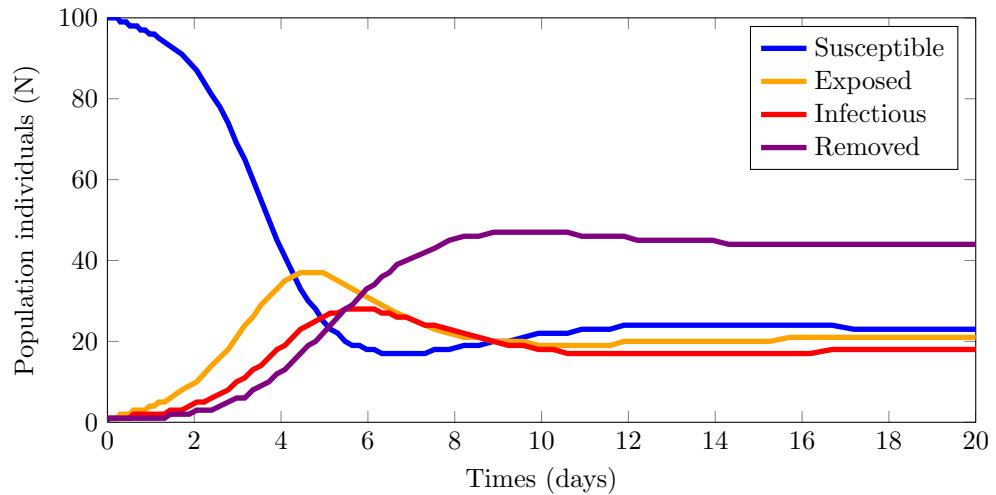


Figure 3.8: Non-dimensionalised SEIR model,  $N=100$ ,  $R_0 = 2.133$

### 3.3 Stochastic Transmission Effects

Renshaw [182] jests that many mathematically minded biologists attempt to apply simplistic differential equations to biological problems with moderate success. By the same juxtaposition he muses that mathematicians with an interest in these systems spend only the minimum time with biologists in order to create large and complex models, equally with minimal biological realism. Such a sweeping statement should be contemplated carefully and to realise that in fact the afore presented deterministic models should be applied with utmost care.

The epidemic models introduced so far rely on a continuous domain in both time and population which implies that fractions of people can become infected over time.

In Section 3.2.2, the hand-waving statement of requiring ‘*a sufficiently large population*’ was made, in reference to compartmentalised SIR models. Here is the time to clarify why this does not apply in the current context, particularly within the hospital ecosystem.

The importance of stochastic modelling for infection modelling has been highlighted frequently [140, 142, 171, 181, 183], particularly when disease incidence is low or population size renders the stochastic nature of the transmission process significant.

**Deterministic models** by their very nature, infer that they are determined *ex-ante* by initial conditions. Consider a population model with incorporated dynamics where  $\gamma =$  births and  $\mu =$  deaths [182]. Population growth is based on these factors ( $\gamma - \mu$ ) but the ultimate fate of the group is determined by the initial condition  $N(0)$  thus:

$$N(t) = N(0)e^{(\gamma - \mu)t}, \quad \gamma, \mu, t \geq 0$$

For short periods of time and where the initial population is large, this represents a satisfactory demographic model, however where  $N$  is small such as where  $N = 1$  problems arise. Renshaw [182] considers the case where deaths are only half as likely as births (i.e.  $\gamma = 2\mu$ ) and hence  $N(t) = \exp(\mu t)$ . Despite the obvious exponential growth expected by this deterministic model, there still exists the real probability that the population will in fact become extinct. This is given by  $\frac{\mu}{\gamma + \mu} = \frac{1}{3}$ . Therefore if a simulation was run three times, at most one of these would result in the population disappearing, which is in direct contradiction to the theory proposed. Simultaneously the exact dynamics of the population appear not to be immediately visible. Wilkinson [184] highlights how the shape of the population curves are defined by  $(\gamma - \mu)$ , not the individual values of  $\gamma$  and  $\mu$ . For example the shape of the curve would be identical whether  $\gamma = 0.5$  and  $\mu = 0.1$  or  $\gamma = 0.4$  and  $\mu = 0$ .

**Stochastic models** are primarily used to show the native variability due to the demographics or environment variability and are particularly important when quantities in the processes are small; small population size or initial number of infectives [14]. Hence it is a collection of random variables:

$$\{X_t(s) \mid t \in T, s \in S\},$$

The sample space, or outcome space  $S$ , represents the number of members in a population  $S \in [0, 1, 2, \dots]$  or  $S \in [0, \infty)$ . The index set often represents time  $T$ ,

which can be discrete or continuous such as:

$$T = \{0, 1, 2, \dots\} \quad \text{or} \quad T = [0, \infty)$$

Different models and methods exist according to whether the index set and the sample set are continuous or discrete. The distinction between the two types of variables determines the techniques used to examine models. In the simple case of discrete sets, a stochastic process amounts to a sequence of random variables known as a time series, where only one event may occur at any one time. At the most simple level, a stochastic system can be thought of as purely random and undetermined by and current or future state [185]. Clearly this is not quite realistic since the wellbeing of a patient is likely to be influenced in some way by their current health. Hospital patients are a countable discrete set which lends itself well to the use of stochastic modelling and in particular Markov chains.

### 3.3.1 Markov Chains

A Markov chain is a random sequence in which the dependency of the successive events goes back only one unit in time. In other words, the future probabilistic behaviour of the process depends only on the present state of the process and is not influenced by its past history. This is called the *Markovian property* [185]. More formally this is given here:

$$Pr(X_{n+1} = x \mid X_1 = x_1, \dots, X_n = x_n) = Pr(X_{n+1} = x \mid X_n = x_n), \quad \sum_j p_{ij} = 1$$

#### 3.3.1.1 Discrete time Markov chains (DTMC)

Suppose  $I$  is finite or countably infinite, hence a discrete set. A stochastic process with state space  $I$  and discrete time parameter set  $T = 0, 1, 2, \dots$  is a collection  $\{X_t : t \in T\}$  of random variables (on the same probability space) with values in  $I$ . The stochastic process  $\{X_t : t \in T\}$  is called a Markov chain with state space  $I$  and discrete time parameter set  $T$  if its law of evolution is specified by the following:

1. An initial distribution on the state space  $I$  given by a probability mass function  $\{p_t : t \in T\}$  with  $p_i \geq 0$  and  $\sum_{i \in I} p_i = 1$ .

2. A one-step transition matrix  $P = (p_{ij} : i, j \in I)$  with  $p_{ij} \geq 0 \quad \forall i, j \in I$  and

$$\sum_{j \in I} p_{ij} = 1 \quad \forall i \in I$$

The SIS compartmental model represents an ecosystem where the population is categorised as either Susceptibles or Infected. This can represent the infection occurring due to influenza [186], given no long lasting immunity has developed. Consequently infected hosts will return to the susceptible category [14]. Within this particular model the population dynamics of both births and deaths are included due to the timescale involved. The deterministic set of ordinary differential equations (ODEs) is given as follows, where the overall population remains constant:

$$\frac{dS}{dt} = -\frac{\beta}{N}SI + (\gamma + b)I \quad (3.3.1)$$

$$\frac{dI}{dt} = \frac{\beta}{N}SI - (\gamma + b)I \quad (3.3.2)$$

Where

$\beta \geq 0$  = transmission rate    $b \geq 0$  = birth rate = death rate    $\gamma \geq 0$  = recovery rate

$N \geq 0$  = population count

In terms of the stochastic counterpart, let  $I(t)$  denote the discrete random variable for the number of infected (and infectious) individuals with associated probability function

$$p_i(t) = Prob\{I(t) = i\}$$

where  $i = 0, 1, 2, \dots, N$  is the total number infected at time  $t$ . The probability distribution is then

$$p(t) = (p_0(t), p_1(t), \dots, p_N(t))^T$$

for  $t = 0, \Delta t, 2\Delta t, \dots$ . Now we relate the random variables  $\{I(t)\}$  indexed by time  $t$  by defining the probability of a transition from state  $i$  to state  $j$ ,  $i \rightarrow j$ , in time  $\Delta t$  as

$$p_{ji}(\Delta t) = Prob\{I(t + \Delta t) = j \mid I(t) = i\} \quad (3.3.3)$$

Assume that  $\Delta t$  is sufficiently small, such that the number of infectives changes by at most one in time  $\Delta t$ . That is,  $i \rightarrow i + 1$ ,  $i \rightarrow i - 1$  or  $i \rightarrow i$ . Either there is a new infection, birth, death, or a recovery. This is a time-homogeneous model whereby the transmission rate does not vary over time. Therefore, the *transition probabilities* are given by:

$$p_{ji}(\Delta t) = \begin{cases} \beta i(N - i)/N\Delta t = b(i)\Delta t, & j = i + 1; \\ (b + \gamma)\Delta t = d(i)\Delta t, & j = i - 1; \\ 1 - (b(i) + d(i))\Delta t & j = i; \\ 0, & j \neq i + 1, i, i - 1. \end{cases}$$

The probability distribution associated with the epidemic process over time is found by repeated multiplication of the transition matrix  $P(\Delta t) = (p_{ji}(\Delta t))$ :

$$p(t + \Delta t) = P(\Delta t)p(t),$$

where  $p(t) = (p_0(t), \dots, p_N(t))^T$  is the probability distribution and  $P(\Delta t)$  is given by:

$$P(\Delta t) = \begin{pmatrix} 1 & d(1)\Delta t & 0 & \dots & 0 \\ 0 & 1 - [d(1) + b(1)]\Delta t & d(2)\Delta t & \dots & 0 \\ 0 & b(1)\Delta t & 1 - [d(2) + b(2)]\Delta t & \dots & 0 \\ 0 & 0 & b(2)\Delta t & \dots & 0 \\ \vdots & \vdots & \vdots & \vdots & \vdots \\ 0 & 0 & 0 & \dots & d(N)\Delta t \\ 0 & 0 & 0 & \dots & 1 - d(N)\Delta t \end{pmatrix}$$

### 3.3.1.2 Calculating $n^{\text{th}}$ step transitions

The matrix  $P(\Delta t)$  is known as stochastic and hence the columns sum to one. Which is to say the vector  $v = (1, \dots, 1)^T$  satisfies  $Pv = Iv$ , where  $I$  refers to the identity matrix. The  $(N + 1, N + 1)^{\text{th}}$  element is the transition probability from state  $N$  to state  $N$ ,  $p_{NN}(\Delta t) = 1 - [b + \gamma]\Delta t = 1 - d(N)\Delta t$ . Denote the transition matrix as  $P(\Delta t)$ . Therefore matrix  $P(\Delta t)$  is  $(N + 1) \times (N + 1)$  tridiagonal. The Markov property shows

that, whatever the initial distribution of the Markov chain is, we have [187]:

$$Pr \{X_{n+1} = j | X_n = i\} = p_{ij}$$

Consider a two-step transition,

$$\begin{aligned} Pr \{X_{n+2} = j | X_n = i\} &= \sum_{k \in I} P \{X_{n+2} = j, X_{n+1} = k | X_n = i\} \\ &= \sum_{k \in I} Pr \{X_{n+1} = k | X_n = i\} Pr \{X_{n+2} = j | X_{n+1} = k, X_n = i\} \\ &= \sum_{k \in I} p_{ik} p_{kj} = (P^2)_{ij} \end{aligned}$$

where  $P^2$  is the product of the matrix  $P$  with itself. More generally,

$$Pr \{X_{n+k} = j | X_n = i\} = (P^n)_{ij}$$

Moreover, if the vector  $(p_i : i \in I)$  is the initial distribution, we get

$$\begin{aligned} Pr \{X_n = j\} &= \sum_{k \in I} Pr \{X_0 = k\} Pr \{X_n = j | X_0 = k\} \\ &= \sum_{k \in I} p_k (P^n)_{kj}. \end{aligned}$$

Hence we arrive at:

$$Pr \{X_n = j\} = (pP^n)_j$$

Three realisations of a Susceptible-Infectious-Susceptible model (SIS) are plotted in Figure 3.9 against the deterministic solution. It is evident that here there exists a non-zero probability of the infection dying out before it gets started.

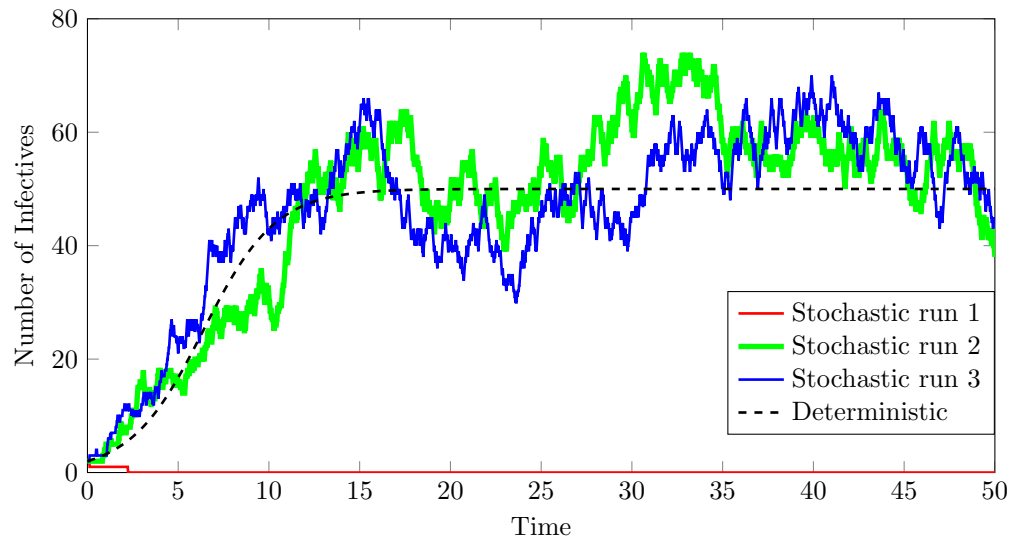


Figure 3.9: SIS model comparing stochastic vs. deterministic solutions, adapted from Allen et al. [14].

### 3.3.2 Airborne Transmission Models

Wells, in his publication entitled *Airborne Contagion and Air Hygiene: an Ecological Study of Droplet Infection* [86], he outlined the concept of a “*quantum of infection*” which has become widely used, though not fully understood. The idea of a quantum ( $q$ ) is the generation rate of pathogenic doses per infectious individual. Although some interpretations may lead one to believe that a quantum refers to a single particle or a single colony forming unit (CFU), it is the average dose required to infect 63% of the population or equivalently an infectious dose:  $ID_{63}$ . It can be assumed to be the source strength if there are no viability losses [188]. In some ways it is a description of the amount of infectious material released combined with the virulence of an organism and susceptibility of an individual [103]. Wells described the probability of becoming exposed to a single quantum through a Poisson distribution [188] hence promoting a threshold quantity theory [189].

$$P = 1 - e^{-1} \simeq 0.63 \quad (3.3.4)$$

Based upon this representation of infectious material within the air, Riley et al. [60] investigated a measles outbreak in a school and postulated that the number of infected children followed an exponential probability distribution. They proposed, the now famous,

Wells-Riley equation, that there exists a relationship between, infection rate, building ventilation rate, breathing rate, and exposure time [190]. The probability of infection is defined by Equation (3.3.5) as follows:

$$P \simeq S \left( 1 - \exp \left\{ -\frac{I p q t}{Q} + \delta \right\} \right) \quad (3.3.5)$$

$$\lim_{Qt/V \rightarrow \infty} \delta \rightarrow 0$$

where

$P$  = Probability of infection     $q$  = quanta/h     $S$  = Susceptible population fraction  
 $I$  = Infectious individuals     $p$  = pulmonary rate m<sup>3</sup>/h     $A$  = air changes per hour ACH  
 $V$  = room volume m<sup>3</sup>     $Q$  = ventilation rate m<sup>3</sup>/h

### 3.3.2.1 General assumptions

Equation (3.3.5) corresponds to the complement probability of a person remaining uninfected ( $1 - e^{-1}$ ). By definition several major assumptions are made within this model and ultimately it can become somewhat unphysical in reality:

1. The room's air is considered to be homogeneously mixed. As a consequence an infectious particle may reside randomly and immediately anywhere within the room.
2. Host ventilation rate and immune response is considered homogeneous [190].
3. Particle size and quantity generation are considered consistent along with the ventilation rate. All parameters are considered to be an average or most likely value.
4. Most often, quanta values must be measured retrospectively from disease data. [103]
5. Particle decay (loss of viability, deposition, etc.) is thought to be negligible versus ventilation extraction.
6. Quanta are released continuously over a period of time [87]

### 3.3.3 Unsteady Quanta Production

Gammaitoni and Nucci [87] sought to combine the Wells-Riley model with the room ventilation rate for non-steady state quanta production [88, 103, 188]. The change of susceptible population fraction is determined by the change in quanta concentration within the space.

$$\frac{dS}{dt} = -\frac{p}{V}CS \quad (3.3.6)$$

$$\frac{dC}{dt} = -CA + qI \quad (3.3.7)$$

where  $dC$  is the change in quanta level within the room, and where  $t$  is the time elapsed from when the room becomes occupied.  $Q$  as well as being the ventilation rate, can also incorporate a decay model of the particles through deposition. Integrating Equation (3.3.7) over the time period 0 to  $t$ :

$$\int_0^C \frac{dC}{Iq - CQ} = \int_0^t dt$$

$$C = \frac{Iq}{Q} (1 - e^{-Qt}) \quad (3.3.8)$$

If the time averaged value of  $C$  is required for steady-state quanta production then integration is made over  $0 - t_\infty$  to give:

$$\bar{C} = \frac{1}{t} \int_0^{t_\infty} C dt = \frac{Iq}{Q} \left\{ 1 - \frac{1}{QC} [1 - \exp(-Qt_\infty)] \right\} \quad (3.3.9)$$

when  $\frac{Qt}{V}$  is small Equation (3.3.5) becomes:

$$P = 1 - \exp \left[ -\frac{Iqpt}{Q} \left\{ 1 - \frac{V}{Qt} \left[ 1 - \exp \left( -\frac{Qt}{V} \right) \right] \right\} \right] \quad (3.3.10)$$

From their investigation of a measles epidemic, Gammaitoni et al. reinforce the belief that there exists a finite probability that infections will occur regardless of the efficacy of environmental control strategies such as air-change rates [87].

Noakes et al.'s work [103] successfully integrated the Wells-Riley steady state quanta production equation into both the standard SIR and SEIR epidemic models. Given the possible invariance of quanta production rates in a particular environment Equation (3.3.7) reduces to

$$C = \frac{Iq}{A} \quad (3.3.11)$$

Substituting this expression into Equation (3.3.6) produces:

$$\frac{dS}{dt} = -\frac{pq}{VA}IS \quad (3.3.12)$$

In fact, on inspection it is apparent  $\frac{pq}{VA} = \beta$ , which expresses the contact transmission rate in terms of quanta generation, pulmonary rate and air flow rate. Given that the SIR compartmental model is based upon the contact rate (per capita), this parameter ( $\beta$ ) was notoriously difficult to specify even after a retrospective study [103]. Through this study, the model was shown to be capable of incorporating contact rate in terms of the room ventilation. By the same token the basic reproduction number is shown to be directly proportional to the quanta production. And hence:

$$R_0 = \frac{pq}{\gamma Q}N$$

where  $\gamma$  is the recovery time for the patients suffering from the given infection. Intrinsically  $R_0$  is therefore coupled to the human immune response and also the pathogens viability or infectivity [103]. Despite this it is usually represented as a single point estimate [190] and hence does not reflect the variability or population heterogeneity. Noakes et al. expand on the possibility of incorporating the effects of personal intervention ventilation devices (PIV) on the patient environment. Their review of TB studies carried out by Gammaitoni and Nucci [87] show how this can be incorporated by varying the pulmonary ventilation rate [103]. By the same token Noakes et al. also relate the basic reproductive number directly to the probability of infection from Equation (3.3.10) when  $I=1$ . This implies that since the population remained constant:  $S - 1 = N$  and hence:

$$R_0 = [N - 1] \left( 1 - \exp \left[ -\frac{Iqpt}{Q} \left( 1 - \frac{V}{Qt} \left[ 1 - \exp \left( -\frac{Qt}{V} \right) \right] \right) \right] \right) \quad (3.3.13)$$

Room overcrowding or population density are highlighted in both Beggs et al. [34] and Noakes et al. [103] as having the strongest influence on infection spread. This is shown to be particularly evident when halving the initial percentage of susceptibles reduces  $R_0 < 1$  for a given infection of influenza [103]. It is doubtful that this alone governs infectivity probability but in particular the proximity of the susceptibles and infectors intuitively will reflect on infection rates. Applicability of the Wells-Riley equation and the modified [87] model to incorporate varying quanta values is shown by Beggs et al. [88] to be useful when studying TB, particularly because it exhibits a lengthy incubation period. The same authors underline the scepticism surrounding the effectiveness of this model which is restricted by many assumptions. Principally, the notion of a perfectly mixed environment contravenes the very nature of mechanically ventilated rooms [96, 191, 192, 193, 194]. This notion is borne out by parametric studies which support the hypothesis that poorly ventilated spaces promote the spread of TB [88]. Following from such a corollary Nardell's [195] fatalist approach also supports the theory of a non-zero possibility of infection occurring regardless the level of ventilation.

While there is a fair amount of literature on modeling airborne transmission, these models cannot natively consider the contribution of particles that deposit onto surfaces. The Wells-Riley equation depends on back-calculating quanta values rather than specific quantities of pathogens, and so has a tendency to under-predict the risk to an individual patient [15]. The next section introduces the more plausible concept of the dose-response model.

### 3.4 Modelling Individual Patient Risk

So far modelling has focused on entire populations, making little differentiation between individuals. In a hospital setting, populations are often very small and individual immunity may well prove an important parameter which may need to be modelled.

Threshold infection risk assessments assume that infection is certain for an entire population if a threshold amount or dose of pathogenic material is ingested. This is also assumed to be independent of when it is accrued [16]. Models such as the deterministic or stochastic SIR [103] described earlier are based on the effective reproductive number  $R_0$ . Which, by definition, takes on only two states (no infection spread or infection spread), hereby losing the very nature of variability of population immunity. Figure 3.10 is a diagrammatic representation of threshold theory.

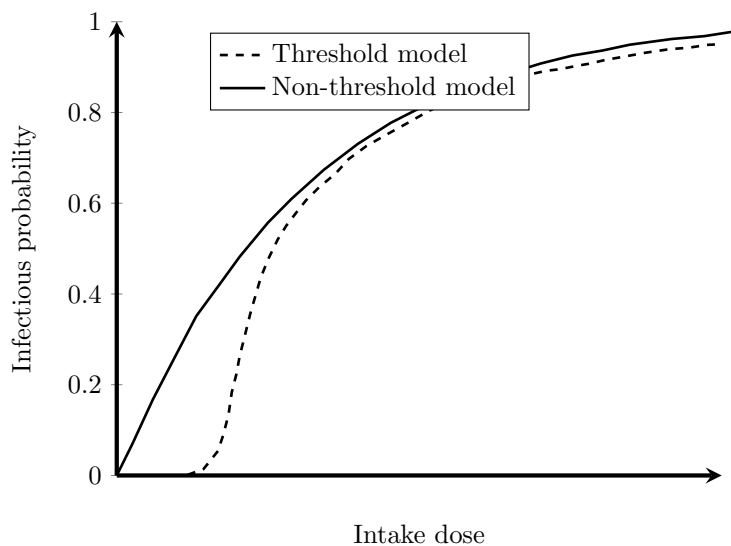


Figure 3.10: Threshold vs non-threshold concept of infection probability. Adapted from Sze et al. [15].

#### 3.4.1 Single-Hit Dose-Response Models

Contrary to the threshold principle where an individual is certain to become infected only after the inoculation of a particular dose, dose-response takes into the consideration that a single pathogen entering the host could initiate an infection. The concept of infectious dose

(ID) relates to the number of pathogens required to cause an infection in an individual. Working within a population it is usually more relevant to refer to the  $ID_{50}$ , which refers to the number of pathogens required per individual to infect 50% of a population [15]. Feeding trials on animals and humans refer to the clinical inoculation of a group of volunteers and their monitored immune response for different IDs. These can then produce probability curves for different pathogens such as in Figure 3.11

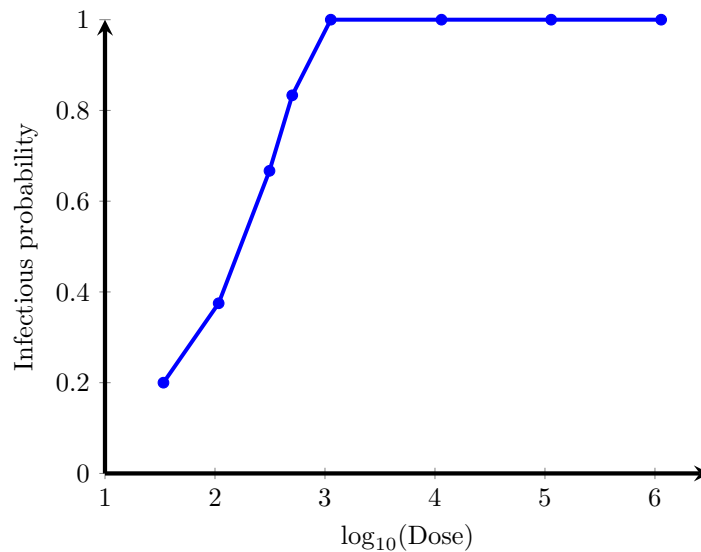


Figure 3.11: A typical dose-response curve for norovirus, adapted from Pujol et al. [16].

However, inoculation in reality may occur over a period of time [16]. Consider a situation where an influenza pandemic epidemic is underway, and a government has to spend a budget on either facemasks, hand antiseptics or a combination of both. An individual in proximity to an infectious person may constantly be breathing in small doses of pathogens, whereas they may only directly inoculate themselves via hand to mucosa a few times per hour, but with a much larger dose. Threshold risk analysis may then favour the acquisition of masks, placing less weight on hand hygiene simply because it occurs less often, hereby ignoring that the human immune system may be capable of fighting off small doses of infection spread out over periods of time. Quantitative microbial risk assessment metrics often make use of four individual infection risk models known as dose-response models [16, 196] outlined subsequently.

### 3.4.1.1 Exponential Model

Assume in the most simplest of cases that the probability of infection is conditionally dependent solely on the expected inoculum dosage  $D$  and that each pathogen exerts equal and independent probability of causing infection  $k$ . This is a reasonable assumption given low inocula which are typical of environmental exposure [197]. Then this system can be considered to be defined by a binomial distribution:

$$\mathbf{P}(\text{infection}|D) = 1 - (1 - k)^D \quad (3.4.1)$$

The main assumption here is that the inoculum  $D$  is given all at once [198].

The binomial assumption of a binary state: Infection or no infection, requires the dose to be an integer value. Typically however, the expected dose is rarely known exactly and hence  $D$  is considered the mean of a Poisson random variable with mean  $\lambda$ , where  $d$  is an integer value representing  $D$ .

$$\begin{aligned} \mathbf{P}(d|\lambda) &= \frac{\lambda^d}{d!} \exp(-\lambda) \\ \mathbf{P}(\text{infection}) &= 1 - (1 - k)^d \end{aligned} \quad (3.4.2)$$

Poisson distributed doses are a reasonable assumption of independent identically distributed pathogens, that share equal probability of reaching a susceptible colonisation site and infecting the host. Therefore the exponential model is given in the form:

$$\mathbf{P}(\text{infection}|\lambda) = 1 - \exp(-k\lambda) \quad (3.4.3)$$

Here  $k$  can be regarded as the probability of a single organism overcoming the host's defences and multiplying. Quantifying  $k$  is not straightforward, and parameters are only available in the published literature for a small number of infections [15]. For faecal-oral pathogens, a value can be obtained from conducting a clinical study of healthy individuals being inoculated with varying infectious doses. Their immune response are measured (termed a feeding trial) and fitted to an exponential curve of the form  $a \exp^b$  [198]. In such studies the inocula are typically high, in the orders of magnitude of  $1 \times 10^6$  CFU [16] which is well represented by the Poisson distribution with mean and standard deviation  $\lambda$ . Little added randomness is added at high values. However, consider a lower inocula of

10 pathogens, in cases where the exact value is not known, the Poisson distribution allows a non-zero probability of 0 particles to be inoculated.

### 3.4.1.2 Beta-Poisson Model

The exponential model assumes a constant survival and infection probability, which implies a steeper curve for low doses. Microorganisms often tend to aggregate in aqueous suspension depending on the ionic strength, pH, and certain physiological properties [46]. Visual electro-micrography of a norwalk virion cluster published by Teunis et al. [199] support the claim that the dose administered to feeding trial subjects may be, in reality, substantially higher than estimated for this reason. As a consequence point estimates of pathogen infectivity, as in the case of the exponential model may not be realistic. Allowing for non-constant pathogen survival, the value of  $k$  can be allowed to vary by the Beta distribution  $k = f(k|\alpha, \beta)$ . Where  $\alpha$  and  $\beta$  are shape fitting functions of the Beta distribution.

$$f(k|\alpha, \beta) = \frac{\Gamma(\alpha + \beta)}{\Gamma(\alpha)\Gamma(\beta)} k^{\alpha-1} (1-k)^{\beta-1}$$

Hence the marginal probability of infection is given by:

$$\begin{aligned} \mathbf{P}(\text{infection}|\lambda; \alpha, \beta) &= \int_{0 < k \leq 1} (1 - \exp(-k\lambda)) f(k|\alpha, \beta) dk \\ &= 1 - \int_{0 < k \leq 1} \exp(-k\lambda) f(k|\alpha, \beta) dk \end{aligned} \quad (3.4.4)$$

However in this preliminary form, the integral does not simplify to an elegant form (in equation Section 3.4.1.2<sup>1</sup> without strict limitations on the shape parameters  $\alpha$  and  $\beta$  insofar that  $\mathbb{R}b > \mathbb{R}a > 0$ . In such a case the Beta-Poisson model is given by [197]:

$$\mathbf{P}(\lambda|\alpha, \beta) \simeq \left(1 - \frac{\lambda}{\beta}\right)^{-\alpha} \quad (3.4.5)$$

$$(3.4.6)$$

---

<sup>1</sup>Kummer's hypergeometric series can be approximated by the limit of its Riemann sum

Quantitative analysis of patient risk is especially susceptible to the variability of inter- and intra-pathogen doses [197], for example quality and viability of the organisms, but also the variability between hosts, for instance depending on patient susceptibility or acquired immunity. The Beta-Poisson model Section 3.4.1.2 creates doubts as to whether these are truly represented by pairing  $k$  with  $\alpha$  and  $\beta$  at each integration. Again,  $\alpha$  and  $\beta$  are shape parameters which are fitted to feeding trial data, which by definition rules out patient variability to a great extent [16, 196, 197]. Only young, healthy specimens are used in the trials as to minimise risk to the individual. On the other hand the pathogen dose that is administered to the candidate is homogenised as much as possible through the culture process. Hence valid extrapolation of these parameters for an entire human population is sceptical at the very least and especially for a hospital sub-set where patients are immuno-compromised, substantial error may be incurred.

### 3.4.1.3 Beta-Binomial Model

In the case where a pathogen dose was unknown, the Poisson approximation is assumed valid, given the properties of the Poisson distribution. However in the case where the inoculum is known, such as the cases where feeding trials are conducted then it is logical to use the un-approximated value  $D$ . The Beta-Binomial model employs the same shape parameters  $\alpha$  and  $\beta$  as previously:

$$\begin{aligned} \mathbf{P}(\text{infection} \mid D) &= 1 - (1 - f(k \mid \alpha, \beta))^D \\ &= 1 - \frac{\Gamma(D + \beta)\Gamma(\alpha + \beta)}{\Gamma(\alpha + \beta + D)\Gamma(\beta)} \end{aligned} \quad (3.4.7)$$

This form is cumbersome to handle due to the difficulty of calculating  $\Gamma(D)$  when  $D$  is very large, and so the logarithmic form is often preferred [196].

### 3.4.1.4 Infection Heterogeneity: Statistical non-identifiability

In the special case where  $\alpha$  and  $\beta$  are less than 1 a bimodal distribution arises. Heterogeneity in host-pathogen interaction, is bimodal, with part of the cases having a very high risk of infection, and others a very low risk. In other words: part of the host-pathogen

encounters are associated with a very high risk, and the remainder has a very low risk, virtually zero. This is an interesting phenomenon, which we may interpret as partial immunity: A fraction of the population appears protected against infection (and unprotected subjects may be at high risk). The corresponding dose response relation looks different: A steep rise at low doses, and saturation at an infection probability below 1.

In the absence of any heterogeneity the shape of the dose response relation depends only on exposure. For a Poisson inoculum this produces an exponential dose response relation. Any heterogeneity added, for instance by assuming variation in infectivity parameter  $k$  or over-dispersed inoculum (e.g. aggregation) produces a less steep dose response relation. The exponential relation is the steepest model in the hit theory family of functions. Variation between the age of pathogens can reflect on their viability and as such not all inocula are identical. Such heterogeneity is adequately modelled by using the Beta-Poisson relation. One comment needs to be made: If action of the infectious particles is not independent (as assumed in the single hit model), for instance if there is cooperation (a dose twice as high leads to a more than twofold increase in infectivity) the dose response relation is steeper. In the absence of heterogeneity an elegant demonstration of cooperative effects (like quorum sensing) might be found in testing whether the observed dose response relation is steeper than the exponential model. Unfortunately, in the real world heterogeneity is always present and we cannot discriminate cooperative interaction from heterogeneity: One tends to make the relation steeper, the other less steep. Any effect of cooperation might be countered by a certain amount of heterogeneity producing a relation with arbitrary slope. In statistics this is called ‘non-identifiability’ [196].

### 3.4.2 Cumulative Dose-Response Models

Feeding trials such as those conducted to elicit immune responses [199] conclude generally that, for a particular inocula, the probability of response can be modelled by a single hit model. Despite the simplicity and elegance of their solutions, the single hit models exclude the effect of a staggered immune system response. Inoculation may not be made in a single dose such as is often the case with contact or airborne transmission. And therefore these models conclude that the cumulative dosage administered can be done so over any time period. Pujol et al. [16] discuss the effects of staggered inocula over a period of time allowing for the immune system to mount a defence. Two classes are defined as

pathogens ( $P$ ) and immune cells ( $I$ ), and similar in construct to a predator-prey model, a coupled system of ODEs are defined:

$$\frac{dI}{dt} = \alpha_I + P \lambda_I - I \gamma_I - P I \delta_I \quad (3.4.8)$$

$$\frac{dP}{dt} = \alpha_P + P \theta_P - P I \delta_P \quad (3.4.9)$$

Given a small enough time step ( $\delta t$ ), it is a reasonable assumption that only one event takes place during each period. Hence from Section 3.4.2 we identify four states which are governed by transition probabilities:

State	Transition	Probability
Increase of I	$I \rightarrow I+1$	$\alpha_I + P \lambda_I$
Loss of I	$I \rightarrow I-1$	$I \gamma_I - P I \delta_I$
Increase of P	$P \rightarrow P+1$	$\alpha_P + P \theta_P$
Loss of P	$P \rightarrow P-1$	$P I \delta_P$

Table 3.4: Transition states for the stochastic model by Pujol et al. [16]

Accretion of immune cells is governed by the natural ebb and flow ( $\alpha_I$ ) in the absence of infection as well due to the activity of increased numbers of pathogens  $P \lambda_I$ . Acquired immunity is not meant to be reflected here, as the time-frame is intended to be substantially smaller than for this to develop. Immune effectors decrease either at a natural death rate  $\gamma_I$  or due to mass-action deactivation in the presence of pathogens  $P I \delta_I$ .

Inoculation of the pathogen dose ( $D$ ) takes place over a designated time-frame  $T$ , which is represented linearly as a constant arrival rate  $\alpha_P$  thus:

$$\alpha_P = \begin{cases} \frac{D}{T} & \text{if } t \leq T \\ 0 & \text{otherwise.} \end{cases}$$

After this inoculation period, pathogens can increase only by net reproduction rate  $\theta_P$ . However interaction with immune effectors produces a mass-action induced deactivation

$PI\delta_P$ . Ultimately the host is able to fight off the infection or the infection takes over. Figure 3.12 is an example of a 1000 simulations, where red runs end up in infections and blue runs represent no infection.

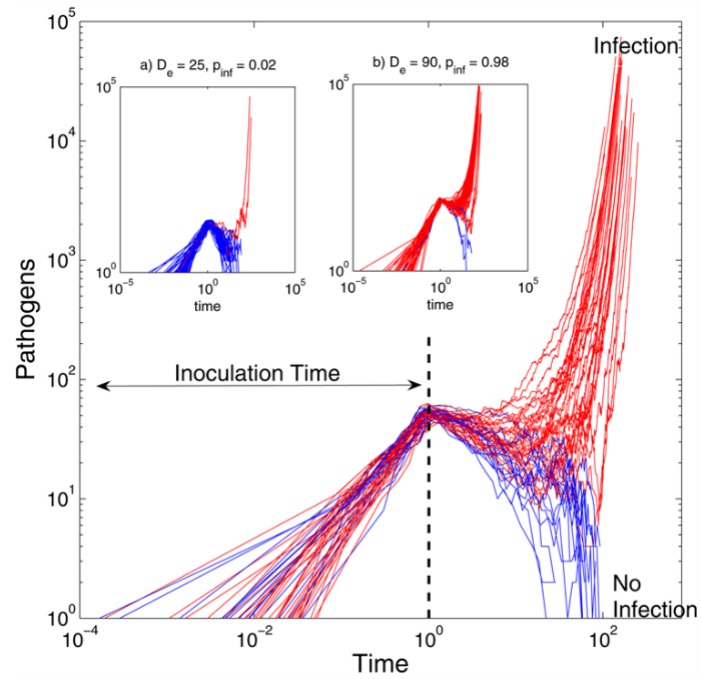


Figure 3.12: Stochastic cumulative dose model by Pujol et al. [16]

### 3.5 Computational Fluid Dynamics: Modelling Airborne Particles in Buildings

Understanding the role that ventilation airflow and ward design plays in the dispersion and deposition of infectious bioaerosols is tantamount to assessing pathogen exposure risk [75, 103]. With the difficulties in aerosolising microorganisms in experimental settings, studies have turned to inert particle tracers [55, 91] or computational fluid dynamics (CFD) models to infer bioaerosol behaviour in air [67].

Spatial distribution of airborne pathogens is unlikely to be homogeneous in nature [90]. This simplification makes modelling infection spread often easier, but the reality is that ventilation systems do not provide fully mixed air and certain locations or proximity to infectious patients will, logically, provide a higher likelihood of spreading infection [122].

Computational fluid dynamics is a numerical modelling approach that deals with the inherent properties and movement of liquids, gases, and the suspension of solid particles. CFD can predict the most likely ventilation airflow pathways in a room or building by splitting up the room into many smaller volumes or elements and solving the continuity Equation (3.5.2) and momentum Equation (3.5.1) through each volume face. By knowing the magnitude and direction of the fluid in each volume the larger picture equates to the sum of the pieces. In general, the smaller the volume the more accurate the picture [172]. However, often a substantial error may accumulate and an iterative approach is applied in an effort to minimise this. Here, a brief overview of the governing equations are given before focusing in more detail on the approaches for modeling microorganism spread. A comprehensive account of CFD including solution methods can be found in many texts such as Tu et al. [200].

$$\overbrace{\frac{\partial \rho \mathbf{U}}{\partial t}}^{\text{time derivative}} + \overbrace{\mathbf{U} \cdot \nabla \rho \mathbf{U}}^{\text{advection}} = \overbrace{-\nabla P}^{\text{pressure gradient}} + \overbrace{\mu \nabla^2 \mathbf{U}}^{\text{diffusion}} + \overbrace{\rho \mathbf{g}}^{\text{body force}}, \quad \text{momentum eq.} \quad (3.5.1)$$

$$\frac{\partial \rho}{\partial t} + \nabla \cdot \rho \mathbf{U} = 0 \quad \text{continuity eq.} \quad (3.5.2)$$

Where  $\mathbf{U} = (u, v, w)$  and  $P$  are the fluid velocity and the pressure respectively and gravity is given by  $g = g(\sin \theta, 0, -\cos \theta)$ .

### 3.5.1 CFD Approaches to Model Bioaerosols

CFD modelling has the potential to investigate the airborne dispersion of infectious microorganisms and the effectiveness of different design measures. It has been found particularly useful to evaluate ventilation design strategies in hospital areas such as single and multi-bed ward accommodation [33, 103, 122] and high risk areas such as operating theatres [55, 94] and isolation rooms [98]. However the validity of such simulations relies on appropriate definition of a pathogen source and an appropriate model for the transport of the pathogen through the air.

CFD is a useful tool for studying the transport of contaminants in fluids as such it is capable of simulating the movement of particles which could be biologically active throughout a room space. As explained in Section 3.1.2, bioaerosols range in size, from a mere tenth of a micron to hundreds of microns in diameter. Pathogen transport is typically approached in one of two ways [191, 201]:

- Passive scalar transport
- Lagrangian particle tracking

#### 3.5.1.1 Passive scalar transport

The most fundamental form of monitoring pollutant spread is via a passive scalar field, which can be thought of as a massless dye. Contaminants move under advection and diffusion only, where any particle dynamics are ignored:

$$\overbrace{\frac{\partial \rho \phi}{\partial t}}^{\text{time derivative}} + \overbrace{\nabla \cdot (\rho \mathbf{U} \phi)}^{\text{advection}} = \overbrace{\nabla \cdot (\Gamma \nabla \phi)}^{\text{diffusion}} + \overbrace{S_\phi}^{\text{source term}}, \quad \text{scalar transport} \quad (3.5.3)$$

The lack of body force interaction on the scalar field may prove an appropriate assumption for respiratory particles which are expelled through coughing and rapidly evaporate to droplet nuclei with a diameter of less than  $1\mu\text{m}$  [202]. As such the model tends to be used for demonstrating ventilation efficacy [201], where it is ideal for modelling steady state behaviour. However, skin squamae have a larger size distribution, often appearing an

average diameter of  $14\mu\text{m}$  and hence may not be well modelled due to the lack of gravity force [46].

Despite limitations, many authors including Li et al., Noakes et al. and Sekhar et al. [102, 103, 203, 204] modelled the concentration of bioaerosols via this procedure demonstrating its ability to determine exposure to airborne pathogenic particles in hospitals. The advantage of this method resides in treating airborne bioaerosols below  $1\mu\text{m}$  [201, 205] as a massless dye. Consequently this method proves popular for modelling contaminant dispersal in room air. Disadvantages to this method arise when buoyancy needs to be taken into account as well as the effects of gravity, implying that the particles would behave differently at different diameters [148], and hence negating the initial assumption that body forces exert no effect on particles.

The 2004 SARS outbreak in south-east Asia prompted a vigorous foray into modelling airborne respiratory droplets. Not for the first time, CFD proved useful in investigating the propagation of contaminants throughout entire buildings, such as the Amoy gardens in Hong Kong [206], whereby revealing previously unsuspected transmission routes [95, 122, 190]. Comparison with experimental tracer gas techniques corroborated the CFD findings, showing that a maintenance shaft formed the principal route of cross-contamination within the building.

Inherently, the concentration field of passive scalar predicted by the CFD simulation is only a representation of pathogen concentration. As it stands this is not an infection risk. This allows for retrospective studies which compare the likely spread of airborne pathogens in hospitals and to combine these with the spatial location of subsequently infected patients and doctors. Li et al. [102] combined a calculated spatial distribution of SARS virus droplets with the residence time of doctors within the Prince of Wales hospital in Hong Kong. Quantity of inhaled droplets and the subsequent risk of infection was evaluated via the Wells-Riley model, dubbing it the inhomogeneous risk model. The virulence of SARS is considered high and the model compared quite well to reported infections. Airflow or pathogen spread in large expanses such as entire buildings are difficult to predict particularly, when ventilation cannot be fully characterised.

More recently, Noakes et al. modelled the spread of archetypal airborne infections such as TB within hospital rooms [59]. Since the route of transmission is certain, this allows for the

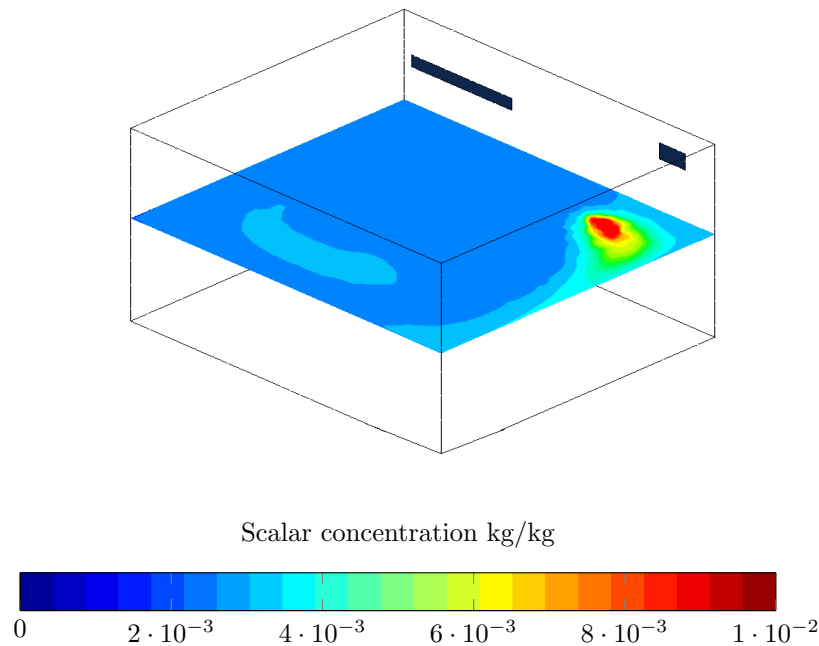


Figure 3.13: Tracer spread within a hospital isolation room. Adapted from work by King [17].

effectiveness of intervention strategies such as room partitions and UV light disinfection devices to be evaluated. Figure 3.13 shows a representative usage of passive scalar transport within a hospital single room as part of investigating ventilation layout [17].

The spread of pathogens in aeroplane cabins [207] has resulted in experimental tracer gas comparisons between CFD passive scalar transport. However passive scalar fields are, by nature, massless and cannot predict the time-dependent gravity-induced sinking of heavier than air  $\text{CO}_2$  or  $\text{SF}_6$  tracer gases [201]. Neither can they approximate the different behaviours of 100 micron sized particles that tend to settle out of the air. Consequently this techniques makes for an approximate first-guess estimate.

Midway through the first decade of the 21st century saw a resurgence in the use of species transport to predict infection transmission within airliner cabins such as by Karthikeyan et al. [208] and Zhang et al.[194]. Nielsen et al. [172] also applies this formula to hospital double patient rooms, by comparing  $\text{NO}_2$  and smoke tracers against multiphase CFD simulations. The conclusions were that comparison was qualitatively quite good. Nevertheless tracer gases do not represent the full range of particle sizes, their evaporation rate and cannot account for their deposition rates.

### 3.5.1.2 Lagrangian particle tracking

In problems where a secondary phase within the fluid domain has a negligible volume, regardless of mass, such as in the case of particles released from a cough, the Lagrangian method tracks particles individually. This approach allows for the discrete phase, where mass and size play an important role in the transport dynamics, to have a variable coordinate in both space and time. The trajectory of a particle is found considering the change in particle velocity over time due to the particle's inertia, gravity, and drag forces. Hence the position and velocity of the position of the particles form a coupled ordinary differential equation: Equation (3.5.4). Consequently the Lagrangian approach is computationally intensive especially when tracking many thousands of particles. Particle trajectories can be calculated by a fifth order Runge-Kutta method by considering the change in particle velocity  $u_i^p$  due to drag force, inertia ( $u_i - u_i^p$ ), gravity  $g_i$ , lift force  $F_i^L$  and Brownian motion  $n_i(t)$ . Equation (3.5.4) considers only the  $x$  direction:

$$\frac{du_i^p}{dt} = \frac{1}{\tau} \frac{C_D Re_P}{24} (u_i - u_i^p) + g_i + F_i^L + n_i(t) \quad (3.5.4)$$

where  $\mathbf{u}_p$  is the velocity of the particle,  $\rho_p$  and  $\rho$  are the particle and fluid density respectively.  $n_i(t)$  represents Brownian forces while,  $g$  is that of gravitational acceleration. Lift force is represented by  $F_i^L$ . The time required from a particle at rest to reach terminal velocity within the surrounding fluid [92] is given by  $\tau$  and is denoted as:

$$\tau = \frac{Sd^2C_c}{18} \quad (3.5.5)$$

Where,  $S$  is the particle-fluid density ratio,  $d$  the particle diameter,  $C_c$  is the Cunningham-Stokes slip correction factor and  $\mu$  the fluid kinematic viscosity.  $C_c = 1 + \frac{2}{d}(1.257 + 0.4e^{-\frac{1.1d}{\lambda}})$ ,  $\lambda$ = gas molecular mean free path.

Validation of particle tracking models has been conducted mainly against experiments conducted in pipes and channels [209, 210]. High quantities of particles are required to produce an averaged pattern [211], while good correlation with particle distribution has been demonstrated up to 10 $\mu\text{m}$  [194, 212].

However, direct comparisons between CFD particle models and bioaerosol experiments are scarce [18]. This is undoubtedly due to the inherent nature of the microorganisms involved. 2006 saw the first published [213] small scale experimental/numerical comparison using airborne biological organisms within a climatically controlled enclosure which Wong et al. [92] describe as “encouraging”. However since then respiratory droplets have been shown to be well characterised by Lagrangian particle tracking as found by Qian et al. [57, 89, 89, 99]. Application of this validated techniques was then applied to compare the effect of hospital room layout on airborne particle distribution [12, 17] to some extent. Lai and Chen [213] predicted deposition of particle sizes ranging from  $0.01\ \mu\text{m}$  to  $10\ \mu\text{m}$  with strong evidence supporting the claim that larger particles drop close to the source and do not remain suspended.

This approach proves popular for investigating respiratory droplets, mainly because each individual particle is tracked throughout the domain separately. Computation can be expensive and has always restricted the quantity of particles being released. Figure 3.14 is an example set of particles as they are tracked through a replica hospital room similar to the published study by myself and colleagues in King et al. [93], and presented in the following chapter.

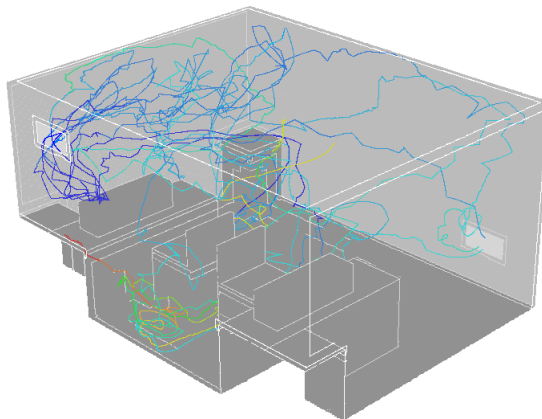


Figure 3.14: Example of multiple particle tracks coloured by residence time within an enclosed environment.

### 3.5.2 Other CFD and Experimental Approaches

Understanding the immediate microclimate around people in indoor environments and how these change is important in getting a handle on airborne infection transmission. With

the inherent difficulties attributed to the use of live subjects such as ethical issues and inter-person variability, breathing mannequins can be a good substitute [138]. Figure 3.15 shows a representative comparison between a breathing mannequin and CFD comparison under test conditions.

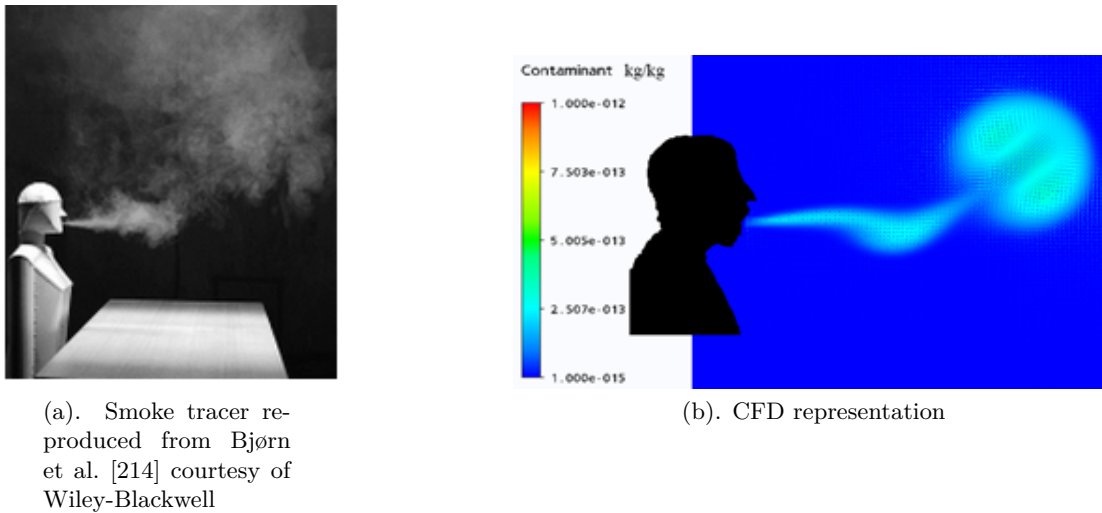


Figure 3.15: Use of mannequins for tracer gas techniques and CFD comparison.

The use of mannequins in airflow visualisation experiments seeks to characterise realistic scenarios in which repeatable analyses can be performed. These include the analysis of flow and particle transport in the immediate microclimate surrounding the mannequin or human volunteer[18]. Heated and breathing mannequins are easy to control within test facilities and have yielded encouraging results. Tang et al. [138] investigate the spread of a tracer gas ( $\text{NO}_2$ ) between two quiescent mannequins in a test chamber hereby comparing the effects of different ventilation strategies. This provided visual qualitative smoke-test data as well as quantitative potential exposure levels.

Techniques involving non-toxic tracer gases such as  $\text{CO}_2$  provide a convenient way of tracking contaminant dispersal within indoor environments such as hospital wards and operating theatres [112, 215]. These can represent the release of infectious particles to some extent and provide validation data for CFD simulations [99, 122, 205], however cannot reflect the behaviour of droplets, evaporating or settling onto surfaces.

### 3.5.2.1 Schlieren or shadowgraph photography

Respiratory droplets produced during coughing and sneezing have been at the center of research attention since the early part of the last decade. Initially SARS and latterly the H1N1 pandemic have been the driving forces behind the search for increased experimental and modelling granularity. Schlieren or shadowgraph photography relies on the thermal differences in the air to refract an incident light beam in order to visualise airflows [18]. Figure 3.16b is a diagrammatic setup of instruments required. Human volunteers stand in front of a concave mirror and cough across the illuminating light beam producing an instantaneous, visible image of their exhaled airflows and thermal plume [18].

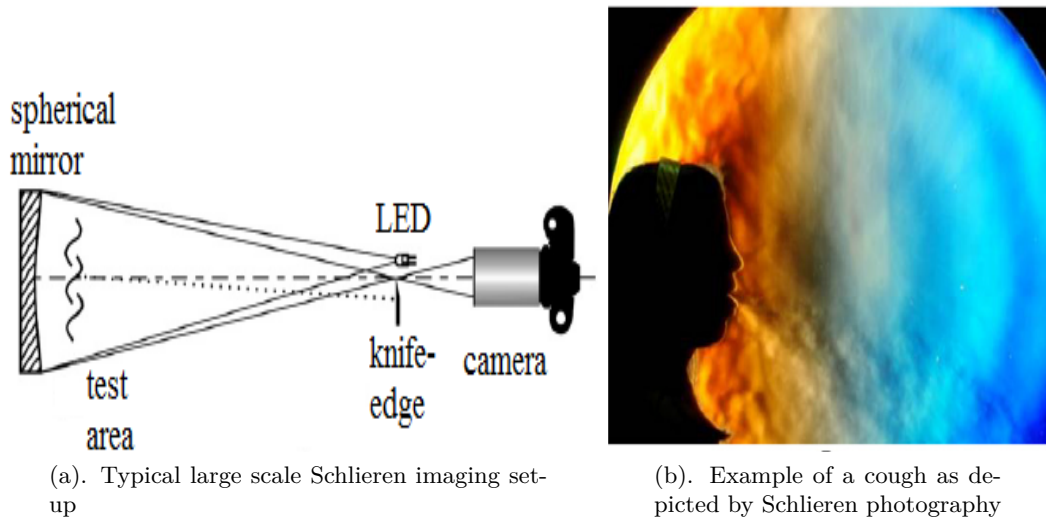


Figure 3.16: Schlieren set-up and photography of a breathing subject reproduced with kind permission from Tang et al. [18].

### 3.5.2.2 Small- and large-scale models

Characterising the movement of contaminants within a working indoor environment such as a hospital is difficult due to their transient nature. Model analogues of hospital rooms can be recreated at a tenth of the size within test facilities. To ensure airflow characteristics are similar between scenarios dynamical similarity of the Reynolds' number must be maintained by changing of length and velocity scales [18]. Eames et al. [96] investigate the transport and dilution of a tracer dye within a transparent acrylic model using photography and computational image tracking techniques. Figure 3.17 shows the spreading of ink from a model isolation room under mechanically ventilated conditions. Optically,

this is a pleasing method, which is quick to resolve. However, currently, it has been found to provide a more qualitative rather quantitative solution due to the Reynolds' number associated difficulties of scaling up the models [96].

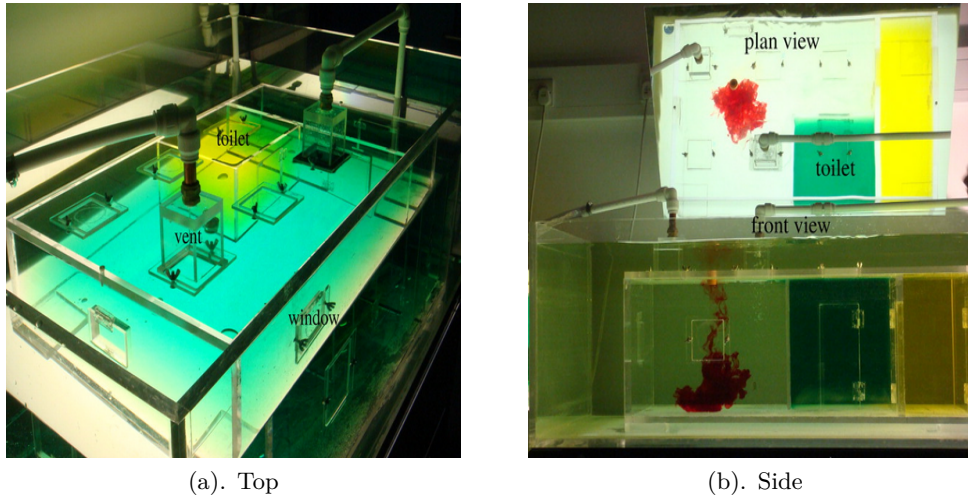


Figure 3.17: Water bath model of tracer escaping from an isolation, reproduced from of Eames et al. [18], courtesy of the Royal Society Publishing.

Large-scale hospital room replicas are hard to find, nevertheless disused wards have been shown to provide excellent test facilities [112, 216]. Despite this, much of the current data on hospital ventilation is derived from investigations of controlled, mechanically ventilated environments such as operating theatres [66, 124], isolation rooms [138, 145] and idealised studies conducted in test-chamber environments [202]. Figure 3.18 shows examples of mechanically ventilated test facilities that replicate hospital isolation rooms. Figure 3.18a shows the aerobiology chamber, which is capable of handling category II microorganisms at the University of Leeds, used later on in this investigation. Figure 3.18b shows the environmental (without capacity to handle biological agents) chamber at BSRIA, Reading.



(a). Aerobiology chamber at the University of Leeds



(b). Environmental chamber at BSRIA

Figure 3.18: Mechanically ventilated experimental facilities of different types.

Table 3.5 shows a summary of the major advantages and disadvantages of modelling techniques described above.

<b>Approach</b>	<b>Advantage</b>	<b>Disadvantage</b>
<b>Human volunteers</b>	Realistic subjects and physiology, particularly with regard to thermal characteristics and thermal boundary layers Safety is important.	Human volunteers cannot be exposed to high intensity (e.g. laser) light or irritant or toxic tracer gases or particles. Hospital monitoring Realistic situations and environments Highly variable results, often obtained using non-standard techniques, making interpretation difficult, and therefore limiting any useful generalisation
<b>Computational fluid dynamics (CFD)</b>	Good spatial/temporal information. It is a standard modelling tool in the industry	Difficult to model moving bodies. Difficult to obtain accurate simulations due to required computing power and/or simulation time.
<b>Physical analogues in scale model or in full scale (models)</b>	Quick and relatively easy to build with reasonable spatial resolution. Able to test different hypotheses related to flow patterns in different geometries using a variety of flow-generating techniques/devices. Easy to work with tracer gas and airborne particles for the simulation of viruses and bacteria in full scale experiments with thermal mannequins	Difficult to combine different contributions to bulk air flows in small scale, and difficult to work with movements of persons in full scale

Table 3.5: Advantages and disadvantages of some airflow visualisation techniques. Adapted from Tang et al. [18].

In order to model infection transmission a considerable amount of information about the transmission route and the interaction of people is required. In addition to the need for adequate characterisation of the air and airborne droplet, it is necessary to employ physical techniques to understand transport mechanisms alongside the epidemic modelling approaches.

## Chapter 4

# Bioaerosol deposition: Experimental and CFD comparison

### Contents

---

4.1	Experimental Methodology . . . . .	101
4.2	CFD Methodology . . . . .	112
4.3	Results and Discussion . . . . .	132
4.4	Conclusions . . . . .	155

---

This chapter examines the spatial deposition of *Staphylococcus aureus* onto environmental surfaces under experimental conditions. Hospital single and double rooms are recreated in an experimental environment within a mechanically ventilated biological chamber (known as the PaCE chamber). A parametric study of room and ventilation layout is undertaken to compare the effects of infectious source location and the mitigation effect of a partition curtain. These scenarios are then compared to numerical CFD models and analysis is made of their accuracy. Turbulence models have been found to significantly affect the predicted deposition patterns [217] so the k- $\epsilon$  RNG model is compared against the more sophisticated Reynolds' Stress Model. The work presented here was partially published as: King et al. *Bioaerosol deposition in single and two-bed hospital rooms: A numerical and experimental study*, Building and Environment, 2013 [93].

## 4.1 Experimental Methodology

Recommended bed spacing in multi-bed environments is often cited as being based on droplet transmission risk [218], and studies have recognised the relevance for pathogens such as *Staphylococcus aureus* as well as respiratory diseases [153]. Tracer gas and numerical simulation studies have shown that ventilation design [59, 99, 112] and the presence of partitions between beds [59] influences airborne cross-infection risk between two patients. There is currently little knowledge as to the importance of bioaerosol deposition in environmental contamination, so quantifying deposition in both single and multi-bed rooms is important for informing nursing practice and design.

This Chapter describes an investigation into the appropriateness of CFD particle tracking techniques for simulating deposited pathogenic bioaerosols in an enclosed environment. With the inherent difficulties of releasing bioaerosols within operational hospital building one must rely on other methods to quantify risk. This work builds on Hathway et al.'s [202] to carry out a direct comparison between the deposition pattern of *Staphylococcus aureus* onto surfaces in a climatically controlled aerobiology test room. The study considers the ability of CFD simulations to predict realistic deposition patterns for small diameter bioaerosol particles and the influence of simulation parameters, in particular, frequently used turbulence models.

Experiments and simulations also consider room layout whereby recreating a single patient and a two-bed hospital room. This then relates the findings to pathogen exposure risks in single and multi-bed hospital rooms. The mitigation effect of a partial divider is subsequently tested under the same conditions.

### 4.1.1 Overview of Experimental Scenarios

Experiments were conducted in the environmentally controlled, negatively pressurised, aerobiology chamber at the University of Leeds (PaCE chamber). Dimensions are close to a hospital single room: 4.26m (L) x 3.36m (W) x 2.26m (H). All walls are well insulated and considered adiabatic. External air was HEPA filtered before being conditioned by a humidifier and heater. This air was supplied to the chamber through a high level wall mounted diffuser as shown in Figure 4.1. Extraction of air was at a low-level, diagonally

opposite; through a grille of the same design (Outlet). Inlet air temperature ( $21.8^{\circ}\text{C} \pm 1^{\circ}\text{C}$ ) and humidity ( $60\% \pm 7\%$ ) were controlled throughout the experiments.

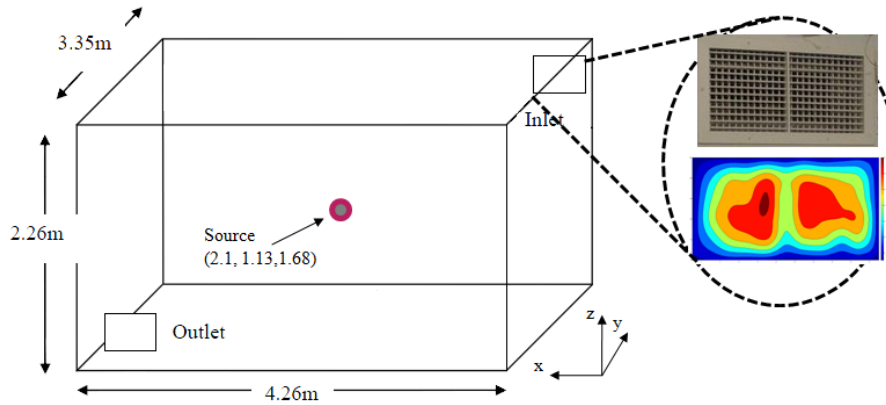


Figure 4.1: PaCE chamber geometry

This experimental arrangement was used to investigate four separate scenarios including an empty room, a hospital single room and a hospital double-patient room. The effect of infectious patient location and a partial partition between beds was also examined. In total four main experimental scenarios were investigated and are summarised in Table 4.1:

Case N°	1	2	3a and 3b	4a and 4b
<b>Scenario</b>	Empty room	Single room	Double room no partition	Double room with partition
<b>Experimental Description</b>	No furniture or mannequin	Hospital single room & heated mannequin	Hospital double room & 2 heated mannequins	Hospital double room & 2 heated mannequins & partition between beds
<b>Aerosol release</b>	Room centre	Patient head	Patient 1 Patient 2	Patient 1 Patient 2

Table 4.1: Experimental case scenarios, single and double-room particle deposition

**Empty room:** Is similar to Hathway et al. [202], quantifying the spatial distribution of deposition in a similar manner to Wong et al. [92] but at a room-scale. Bioaerosol injection occurred at the geometric centre point in the room and no furniture or heat sources were present.

**Single room:** Replicates the situation within a single-bed, hospital room, where an infectious patient lays resting (Figure 4.2). A heated mannequin is used to represent the heat source of the human. Particle collection is made on surfaces which mimic hospital furniture.

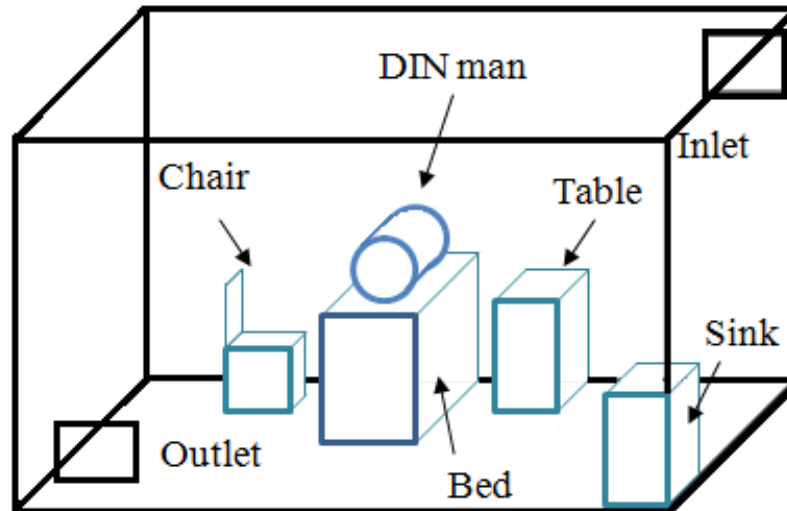
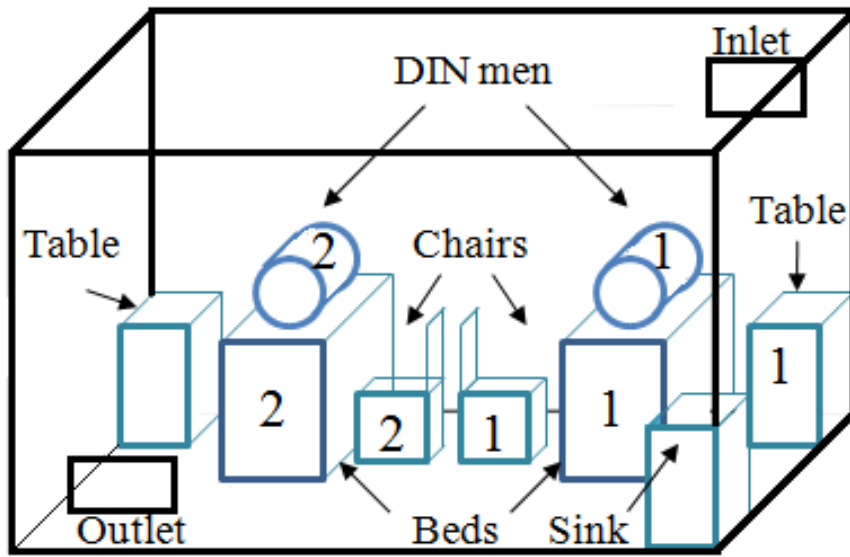


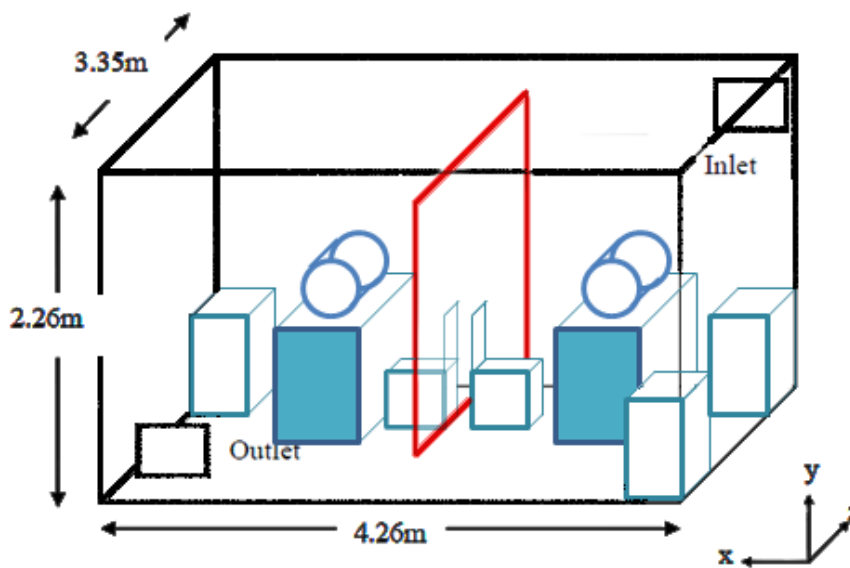
Figure 4.2: Single room set-up

**Double room:** Scenarios 3 (Figure 4.3a) and 4 (Figure 4.3b) both present two heated mannequins, employed in a similar manner to Qian et al. [89]. Cross contamination of surfaces surrounding an infectious and a susceptible patient is examined by the collection of bioaerosols on adjacent surfaces. The effect of ventilation is investigated by reversing the location of susceptible and infectious source. The effect of a partition (Figure 4.3b) between the two beds is also examined. Table 4.2 shows the dimensions of the items present in experimental scenarios 2-4.

As is the case in many developing countries or during times of pandemics the shortage of beds forces hospitals to overcrowd rooms. Noakes et al. demonstrated that low-cost room partition solutions can significantly reduce risk of airborne exposure [59]. It was therefore of significant interest to investigate the effectiveness of one of the cheapest options available: Polythene sheeting, as to whether this could provide significant mitigation effects.



(a). No partition: for scenarios 3a and 3b



(b). Curtain partition in for scenarios 4a and 4b

Figure 4.3: Double patient room

Originally, hospital curtains were employed to create an environment of privacy for the patient and to aid cleaning procedures. These hang approximately 20cm from the ground and similarly from the ceiling. This gap may possibly allow pathogen cross-transmission.

Item		Quantity	
Name	Dimension (m)	Scenario 2	Scenarios 3-4
Bed	1.75 x 0.60 x 0.8	1	2
DIN man	1 x 0.35	1	2
Bedside table	0.50 x 0.50 x 0.80	1	2
Chair	0.60 x 0.60 x 0.55	1	2
Sink	0.40 x 0.40 x 0.20	1	0

Table 4.2: Dimensions of surfaces and items in the double room

#### 4.1.1.1 Heated mannequin

In scenarios 2-4, a quiescent patient was simulated by a DIN man (*Deutsche Institut für Normung*), a hollow aluminium cylinder (length 1m by diameter 0.35m) with an interior heat source. The heat source was created by a 100W light bulb to represent the thermal emission of a resting adult human. Convective heat output from the skin is considered to be approximately 50% [172]. Dimensions of the cylinder are however smaller than the average person but emit a similar heat flux. Infra-red thermal imaging of the DIN man shows the surface temperature in Figure 4.4, which represents approximate body equivalents.

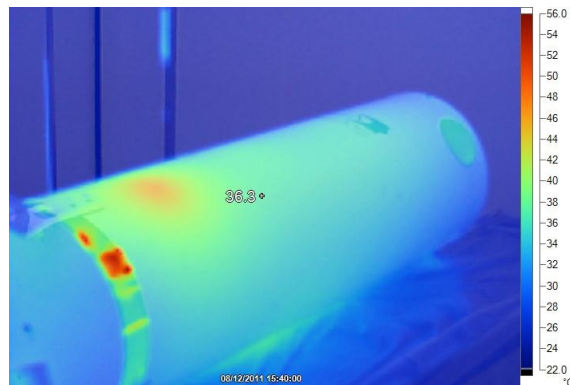


Figure 4.4: Heated mannequin thermal image

### 4.1.2 Characterising the Airflow Patterns

To maintain an accurate air change rate within the chamber, the ventilation system was calibrated using a hand-held balometer as in Figure 4.5 (Digital Balometer TSI, Model PH721, TSI Incorporated, Shoreview, MN). The blue canvas hood is placed over the diffuser inlet thus converging all the flow through a known aperture size. The flow velocity is measured as it passes through the aperture by an array of nine anemometers and so the volumetric flow can be deduced. Both the flow-rates at the inlet and the outlet were measured, observing a negative pressure within the chamber. Air patterns were characterised using a comfort probe (hot-wire anemometer from Testo Ltd, Germany) at five poles (locations) within the room as per Figure 4.5a, and measurements were taken at five positions up each pole.

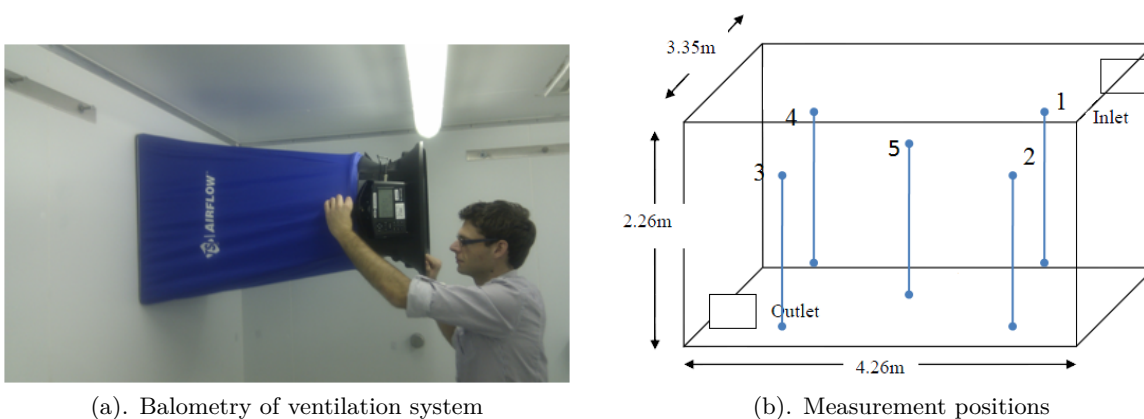


Figure 4.5: Airflow measurements within the PaCE chamber

### 4.1.3 Bioaerosol Generation

Staphylococci are approximately spherical gram positive bacteria existing endogenously on most human skin squamae. With shedding of some  $10^6$  skin flakes per day, they are consequently abundant in many health-care settings [92, 202]. *Staphylococcus aureus*, a surrogate representative of MRSA, was chosen as the bacteriological agent given its ability to grow on general purpose media and its relevance to HCAI. The *S. aureus* culture was incubated in nutrient broth (Oxoid, UK) for 24 hours at  $37^\circ\text{C}$ . Subsequent dilution tests showed the concentration to be circa  $10^{11}$  organisms per millilitre. A 10ml aliquot of the pure culture was aseptically removed and suspended in 100ml of sterile distilled water in

a pre-autoclaved nebuliser. Sterile distilled water was the preferred suspension medium since it did not produce foaming of the suspension during nebulisation.

Aerosols were injected into the room via a six jet Collison Nebuliser (CN 25, BGI Inc, USA) attached to the inlet port of the chamber. The nebuliser utilises a separate pump, pressure regulator and meter operating at a flow rate of 8l/min at 25Pa to deliver HEPA filtered air. Manufacturer's data from BGI indicate the size distribution of particles ejected during the process to have a mean mass diameter of 2.5  $\mu\text{m}$  and a standard deviation of 1.8  $\mu\text{m}$ . Eventual size distribution may vary through evaporation. Method of injection varied based on the requirements for each experimental scenario. In the case of the empty chamber (scenario 1), bioaerosols were released from the centre of the room isotropically at the centre (2.13m, 1.15m, 1.675m) as per Figure 4.6. In subsequent cases, (scenarios 2-4) a plastic tube of 2.5cm  $\text{\O}$  was clamped at the head of the infectious DIN-man and droplets were released into the thermal plume (see Figure 4.6).



Figure 4.6: Scenario 1: Isotropic release from inside red diffuser ball in centre of room

#### 4.1.4 Bioaerosol Collection

All biological samples were taken on Tryptone soya agar (Oxoid, UK) as the controlled chamber conditions meant that no other species were present. Deposition was measured using 90mm Petri dishes located on the floor or on surfaces in the room as per Figure 4.7. Given the inherent variability of biological particle collection, it was found that experiments carried out with fewer than five settle plates at each point yielded inconsistent results (Kruskal-Wallis test:  $p \sim 0.1$ ). Electrostatic effects of aerosolisation were deemed to be negligible because of isotropic distribution of settle plates. A possible remedy in

other situations where this may be a factor would be to use Rodac plates (Petri dishes without sides) or glass Petri dishes.

**Scenario 1:** Five 90mm Petri dishes containing the growth media were placed at each enumerated position as shown in Figure 4.7 with a total of 125 plates.

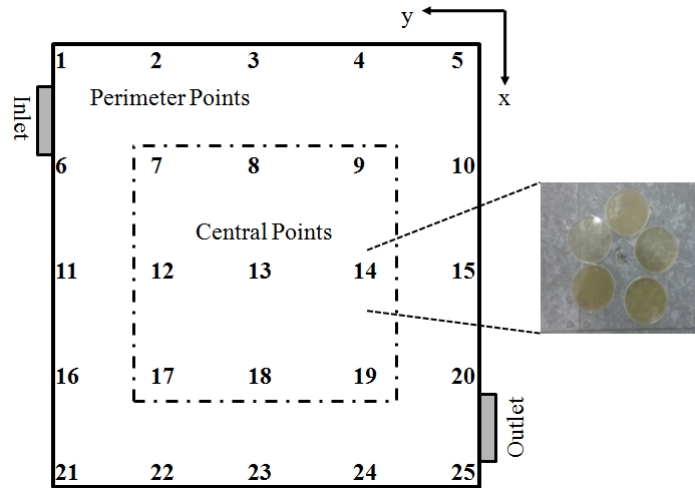
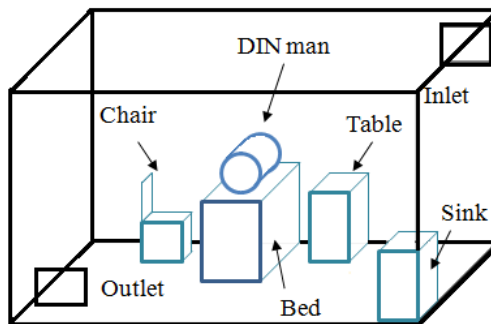


Figure 4.7: Location of settle plates in the empty chamber scenario with photograph showing a sampling point with a typical group of 5 plates (scenario 1)

**Scenarios 2:** Petri-dishes were placed on furniture surfaces in the single rooms as indicated in Figure 4.30. A minimum of seven plates were located at each position. Generally all available horizontal surface area of the furniture was covered with settle plates. Floor deposition was not measured in these cases.



(a). Single room sketch



(b). One DIN man

Figure 4.8: Single-bed room experimental set up. Petri dishes were located on surfaces representing the Bed, Chair, Table and Sink

**Scenarios 3-4:** Petri-dishes were placed on furniture surfaces as indicated in Figure 4.9. A minimum of seven plates, often nine were located at each position. Floor or curtain deposition was not measured in these cases.

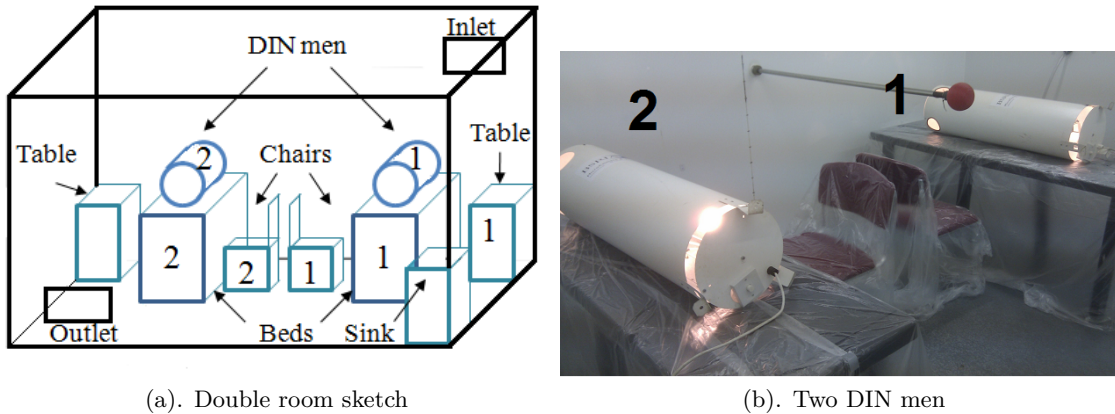


Figure 4.9: Double-bed room experimental set up Petri dishes were located on surfaces representing the Bed, Chair and Table for each patient and the Sink.

Throughout all experiments particle concentrations (particle sizes  $0.5\text{-}1\mu\text{m}$ ,  $1\text{-}3\mu\text{m}$ ,  $3\text{-}5\mu\text{m}$ ) were monitored at the outlet via a laser particle counter (at  $2.83\text{ l min}^{-1}$ , Kanomax 3886 Optical Sciences Ltd, UK) to ensure steady state conditions were reached. Following experiments, the covered Petri-dishes were incubated for 24hrs at  $37\text{ }^{\circ}\text{C}$ . Individual colony forming units (CFU) were then counted and recorded. All samples were subjected to minimal viable count threshold and those with less than 25 CFU per plate were discarded ( $n=3$ ).

#### 4.1.5 Data Analysis

Variation is known to be due to, at least in part, by unsteady airflow patterns and sampling techniques [100]. Sample sizes used here are reasonable for investigating biological microorganisms. However since parametric statistics are notoriously sensitive to outliers, non-parametric statistical inference was used. Variation between sample distributions within each experiment were evaluated via a Kruskal-Wallis test at the 5% level. Subsequently the post-hoc Wilcoxon rank-sum test was used to compare experimental samples against CFD predictions. Comparison was made based on the null hypothesis of both samples stemming from distributions with equal variances, or more strictly that two independent samples emanate from the same distribution.

In all four study scenarios the environmental conditions remain reasonably constant, but variation can be encountered within the biological organisms in use. In particular it is difficult to ensure that the injected concentration remains the same in different experiments.

A uniform normalisation metric is therefore used to ensure comparability of results between experiments. The fractional bacteria counts  $C_i$  represent the normalised deposition distributions at each location given by Equation (4.1.1):

$$C_i = \frac{\frac{1}{m} \sum_{j=1}^m c_{ij}}{\frac{1}{mn} \sum_i \sum_j c_{ij}}, \quad (4.1.1)$$

where  $n$  is the number of zones and  $m$  is the total number of Petri dishes in each zone. Values from colony counting were averaged out based on the number of Petri dishes at each point giving raw spatial counts. Each positional value was then divided by the global mean of the experiment. Although scenario experiments were conducted on different days and using different microorganism cultures it was found that the mean deposition count within each experiment scenario remained constant ( $p=0.3$  from t-test comparing means). In addition dilution cultures were carried out for each new culture to ensure microorganism levels were maintained. This therefore allows for quantitative as well as qualitative comparison between scenarios.

## 4.2 CFD Methodology

With the inherent difficulty of aerosolising bacteria into a working environment such as a hospital, studies have turned to computational fluid dynamics to test the validity of ‘what if’ scenarios without the need to move away from the computer screen [12, 55, 55, 57, 103, 172, 219].

Steady-state computational fluid dynamics models of the four experimental scenarios were developed using Fluent (ANSYS, version 12.0). Flow was simulated using Reynolds Average Navier-Stokes (RANS) approach computed via the finite volume method, the most widely used method for indoor airflow [89, 90, 172, 194, 214]. In all cases the double precision solver was utilised as default along with the SIMPLE pressure-velocity coupling algorithm and 2<sup>nd</sup> order upwind discretisation for all variables.

### 4.2.1 Turbulence Modelling

The choice of turbulence model depends on the context of the problem at hand and how much detail is needed. *Are you modelling a flow through a capillary tube or flow over a jumbo jet?* Broadly speaking the choice is between empirically or semi-empirically derived methods or direct numerical simulation of turbulent eddies. With the computational power available today (2013), only being able to calculate a mili-second over a postage stamp is not of much use when studying indoor airflow. And so, for the time being, semi-empirical models will be used. These can be split into five categories:

- Mixing length models (algebraic models).
- Spalart-Allmaras model [Spalart and Allmaras, 1992] (one transport equation).
- k- $\epsilon$  model [Launder and Spalding, 1974] (two transport equations)
- k- $\omega$  model [Wilcox, 1994] (two transport equations)
- Reynolds stress model [Wilcox, 1998] (seven transport equations).

This chapter will examine only the k- $\epsilon$  and the Reynolds’ Stress Model because they are optimised and heavily validated for indoor airflows. The others are mainly for outside

airflow. Firstly a brief overview is given: The highly chaotic and complex form of turbulent airflow renders it inherently very unpredictable. However, over the past century, increasingly more complex models have appeared [220].

The concept of Reynolds averaging

$$u_i = \bar{u}_i + u'_i$$

of the Navier-Stokes' equation is given by:

$$\frac{\partial \rho u_i}{\partial t} + \frac{\partial \rho u_i u_j}{\partial x_j} = -\frac{\partial p}{\partial x_i} + \frac{\partial}{\partial x_j} \left[ \mu \left( \frac{\partial u_i}{\partial x_j} + \frac{\partial u_j}{\partial x_i} - \frac{2}{3} \delta_{ij} \frac{\partial u_k}{\partial x_k} \right) \right] + \frac{\partial}{\partial x_j} \overbrace{\left( -\rho \overline{u'_i u'_j} \right)}^{\text{Reynolds' Stresses}} \quad (4.2.1)$$

Reynolds published pioneering groundwork in 1895 which laid the foundation for the time averaging approach seen today. However, much about viscosity remained a mystery until Prandtl opened the door to future investigation into boundary layer theory in 1904. Around the mid-1940s Prandtl again hypothesised that eddy viscosity was proportional to turbulent kinetic energy  $k$ , which inherently takes into consideration flow history. However, specification of a turbulent eddy length scale still remained; and hence prior knowledge of the flow must be known before a solution can be calculated. Progress was marred up until the mid-1960s due to the lack of computing power. An implicit and incomplete problem still remained.

#### 4.2.1.1 Two equation Eddy Viscosity Model $k$ - $\epsilon$

Raynolds' Averaged Navier-Stokes' (RANS) turbulence models are divided into two categories. How the Reynolds' stresses  $(\overline{u'_i u'_j})$  are treated in Equation (4.2.1) dictates this. Launder and Spalding [221] are considered to be pioneers in developing a generalised turbulence model based on the creation of turbulent kinetic energy and it's subsequent dissipation. The so-called  $k$ - $\epsilon$  model, first introduced in 1974, is empirically based on two extra transport equations representing the turbulent properties of the flow:

$$\frac{\partial \rho k}{\partial t} + \nabla \cdot (\rho k \mathbf{U}) = \nabla \cdot \left( \frac{\mu_t}{\sigma_k} \nabla k \right) + 2\mu_t S_{ij} \cdot S_{ij} - \rho \epsilon \quad (4.2.2)$$

$$\frac{\partial \rho \epsilon}{\partial t} + \nabla \cdot (\rho \epsilon \mathbf{U}) = \nabla \cdot \left( \frac{\mu_t}{\sigma_k} \nabla \epsilon \right) + C_{1\epsilon} \frac{\epsilon}{k} 2\mu_t S_{ij} \cdot S_{ij} - C_{2\epsilon} \rho \frac{\epsilon^2}{k} \quad (4.2.3)$$

where adjustable empirical constants have been most commonly set to:

$$C_\mu = 0.09 \quad \sigma_k = 1.30 \quad C_{1\epsilon} = 1.44 \quad C_{2\epsilon} = 1.92$$

$S_{ij}$  is the fluid strain rate and the turbulent eddy viscosity is given by

$$\mu_t = \rho C_\mu \frac{k^2}{\epsilon} \quad (4.2.4)$$

Boussinesq [222] in 1877 introduced the assumption that the Reynolds' stresses are proportional to the velocity gradients or strain:

$$-\overline{\rho u'_i u'_j} = \mu_t \left( \frac{\partial \overline{u}_i}{\partial x_j} + \frac{\partial \overline{u}_j}{\partial x_i} \right) - \frac{2}{3} \delta_{ij} \left( \rho k + \mu_t \frac{\partial \overline{u}_k}{\partial x_k} \right) \quad (4.2.5)$$

Where the turbulent kinetic energy is postulated by Prandtl to be the basis of the velocity scale:

$$k = \frac{1}{2} \overline{u'_i u'_i} = \frac{1}{2} \sqrt{u'^2 + v'^2 + w'^2} \quad (4.2.6)$$

The Re-Normalisation Group (**RNG**)  $k$ - $\epsilon$  model attempts to account for these smaller turbulent eddies by adding an extra term to the turbulent dissipation in Equation (4.2.3):

$$\frac{\partial \rho \epsilon}{\partial t} + \nabla \cdot (\rho \epsilon \mathbf{U}) = \nabla \cdot \left( \frac{\mu_t}{\sigma_k} \nabla \epsilon \right) + C_{1\epsilon} \frac{\epsilon}{k} (G_k + C_{3\epsilon} G_b) - C_{2\epsilon} \rho \frac{\epsilon^2}{k} - R_\epsilon + S_\epsilon \quad (4.2.7)$$

where  $G_k$  is the generation of turbulence kinetic energy and  $G_b$  is the generation of turbulence kinetic energy due to buoyancy. Moreover renormalisation group techniques are used to develop a theory for the large scales in which the effects of the small scales are

represented by modified transport coefficients. These constants used in the formulation of the RNG model are derived mathematically as opposed to empirically in the standard k- $\epsilon$  model. Comprehensive descriptions can be found in Fluent's theory manual [223] or Tu et al. [224].

However, this assumption ensures that turbulence is isotropic in all directions, which in the case of swirling flow is unlikely [225]. Cases of high velocity gradients and shear flow pose significant problems for the k- $\epsilon$  model, most famously where the re-attachment length of a backward facing step needs to be calculated [200]. In the standard k-epsilon model the eddy viscosity is determined from a single turbulence length scale, so the calculated turbulent diffusion is that which occurs only at the specified scale, which is unphysical in real domains.

#### 4.2.1.2 Seven equation Reynolds' Stress Model

One of the inherent disadvantages of the k- $\epsilon$  model was its isotropic treatment of eddy viscosity. The Reynolds Stress Model (RSM) closes the RANS equations by solving an extra six transport equations for the individual Reynolds stress components  $\delta_{ij}\overline{u'_i u'_j}$ . A separate equation is then required for the dissipation rate  $\epsilon$ . Hence a total of 7 extra transport equations are solved in 3D. By taking the moment of the stress term in Equation (4.2.1) we obtain the transport equations thus:

$$\begin{aligned}
 & \overbrace{\frac{\partial}{\partial t} (\rho \overline{u'_i u'_j})}^{\text{Time derivative}} + \overbrace{\frac{\partial}{\partial x_k} (\rho u_k \overline{u'_i u'_j})}^{C_{ij}=\text{Convection}} = - \overbrace{\frac{\partial}{\partial x_k} \left[ \rho \overline{u'_i u'_j u'_k} + p (\delta_{kj} \overline{u'_i} + \delta_{ik} \overline{u'_j}) \right]}^{D_{T,ij}=\text{Turbulent diffusion}} \\
 & + \overbrace{\frac{\partial}{\partial x_k} \left[ \mu \left( \frac{\partial \overline{u'_i u'_j}}{\partial x_k} \right) \right]}^{D_{L,ij}=\text{Molecular diffusion}} - \overbrace{\rho \left( \overline{u'_i u'_j} \frac{\partial u_j}{\partial x_k} + \overline{u'_i u'_k} \frac{\partial u_i}{\partial x_k} \right)}^{P_{ij}=\text{Stress production}} - \overbrace{\rho \beta \left( \overline{g_i u'_j \theta} + \overline{g_j u'_i \theta} \right)}^{G_{ij}=\text{Buoyancy}} \\
 & + p \overbrace{\left( \frac{\partial \overline{u'_i}}{\partial x_j} + \frac{\partial \overline{u'_j}}{\partial x_i} \right)}^{\phi_{ij}=\text{Pressure strain}} - 2\mu \overbrace{\left( \frac{\partial \overline{u'_i}}{\partial x_k} \frac{\partial \overline{u'_j}}{\partial x_k} \right)}^{\epsilon_{ij}=\text{Dissipation}} \tag{4.2.8}
 \end{aligned}$$

By this method, a more computationally demanding model turbulence model is defined, but for that, inhomogeneous turbulence components are calculated at each point.

### 4.2.1.3 Large eddy simulation

Large Eddy Simulation (LES), is an amalgamation of methods which melds a direct simulation approach for the largest eddies and entrusts a RANS approach for the eddies below a certain size. This method is quite appealing but makes very strict requisits about meshing, particularly with respect to  $y^+ < 20$  values. Realising that modelling a simple small room would require some 16 million grid cells, is not particularly intractable but has proven excessive [67], and so will be left to future endeavours.

### 4.2.1.4 Choosing a turbulence model

Previous studies centered on particle deposition have focused on small scale channel flow such as in the case described in Lai and Nazaroff [217]. Over-prediction of deposition quantities have been found when using the standard  $k-\epsilon$  due to its Boussinesq modelling of isotropic Reynolds' stresses, worsening predictions close to the wall. Ideally, all Reynolds' stresses are calculated individually as in the case of the RSM model. Although Wong et al. [92] found good comparison using the RNG  $k-\epsilon$  model, other studies have found that improvement achieved over standard  $k-\epsilon$  models, still show significant differences compared to empirically measured DNS data [226]. In order to further explore the influence of turbulence models to particle deposition in indoor air, both the RNG  $k-\epsilon$  and the Reynolds' Stresses Model are applied in this study.

As the focus of the simulations was on prediction of particle deposition, the resolution of turbulence, particularly close to the wall is important. RANS solutions of bulk-flow do not calculate turbulent fluctuations up to the wall, hence high Reynolds flows employ wall-functions, and therefore an amalgamation of approaches is made. Enhanced wall functions rely on splitting the boundary region into two layers forcing unrealistic mesh sizes in some situations. Therefore Fluent's standard wall function was employed, requiring the  $y^+$  value to be within 30 and 300 in the first cell.

## 4.2.2 Artificial Viscosity

The term artificial or numerical viscosity [223, 224] refers to the excessive diffusion produced by any upwind discretisation scheme. As an analogy, the reader must imagine a

structured, square, grid with fluid flow moving across it diagonally. Since the fluid can only move either vertically or horizontally as in a Manhattan metric, the grid quickly becomes filled showing some excessive diffusion, not present in the original flow. This is particularly visible when discontinuities as in Figure 4.10b must be approximated such as hot and cold fluid mixing or in flows with pockets of high velocity gradients such as swirling flow:

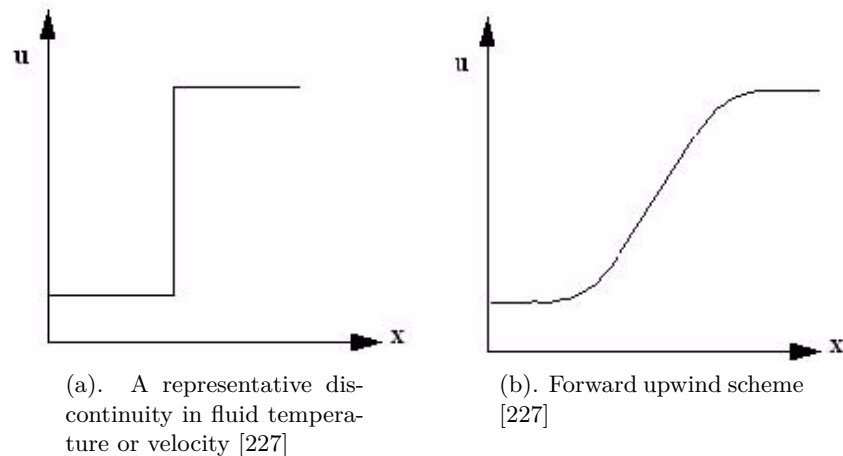


Figure 4.10: Representation of a discontinuity via an upwind scheme

Despite the initial poor performance of this low order scheme, it does offer some comfort for establishing a platform upon which to base initial solutions for a higher order scheme to solve [228].

### 4.2.3 High Resolution Schemes

There exist several ways to improve on this approximation, most notably either to refine the mesh involved to physically reduce diffusion or to employ a higher order scheme. Second order schemes tend to give spurious oscillations close to the discontinuity but approximate the discontinuity more accurately; this is called Gibb's phenomenon [229] shown in Figure 4.11. One way of rectifying this is to incorporate both low and higher order schemes depending on the situation, in a mixed mode.

Essentially, the main point of this discussion is that the diffusive effects of lower order discretisation methods can be reduced with higher order schemes. However, striking a

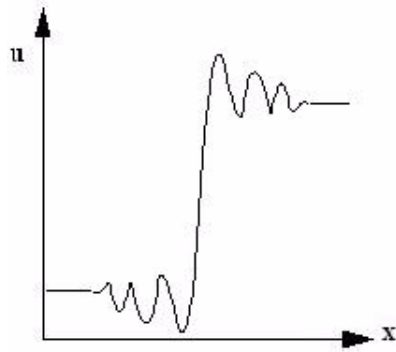


Figure 4.11: Second order upwind scheme

balance between accuracy and stability is absolutely vital for attaining solutions to complex flow problems, and this can only be achieved with experience. Simulations throughout this chapter use the second order upwind scheme available in Fluent for all variables.

#### 4.2.4 Defining Ventilation Diffusers

Mechanical ventilation described in Chapter 2 has been found to provide improved indoor air quality according to several studies, most notably in that of Bauman et al. [230]. Since the 1970s this type of ventilation has been tested extensively experimentally [68] and also computationally [231]. Standard airflow modelling within indoor spaces by computational fluid dynamics (CFD) differs significantly from techniques required for incorporating the complexities of ventilation diffusers [232]. Consequently this has been regarded as a cornerstone in being a major limiting factor in applying CFD to room airflow [231]. Particularly given the actual complexities of some of the diffuser geometries the application of boundary conditions is not made easy. In the vast majority of cases obstacles such as louvres or vanes prevent the implementation directly into CFD geometry. However correct airflow prescription is vital to achieving successful CFD representations [172, 231, 233].

Such methods of simplification can be categorised into four areas:

1. Simplified geometrical models
2. Prescribed velocity models
3. Momentum models
4. Box models

Some ventilation diffusers can be quite complicated, made up of many fine geometrical details. The most common found in the office and hospital is that of the four-way diffuser pictured (Figure 4.12), which typically uses shaped aerofoils to direct the flow. These are sometimes called baffles or deflectors. Given their intricate shape, careful consideration must be given to either their simplification or full inclusion.

##### 4.2.4.1 Velocity prescription

The simplest method for defining an inlet involves direct velocity prescription at the diffuser face. In reality this may at best represent the geometry in Figure 4.14. In the case of most diffusers, a significant part of their inlet face is obstructed by louvres which reduce the actual inlet area ( $A$ ). Therefore, although the mass flow rate ( $\dot{m}$ ) may be maintained



Figure 4.12: Typical four-way diffuser (0.5m x 0.5m)

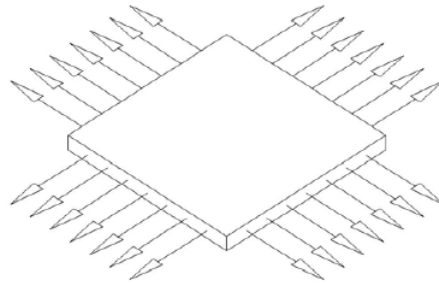


Figure 4.13: Simplified diffuser geometry

by this method, the velocity  $U = \frac{\dot{m}}{A\rho}$ , where  $A$ = cross-sectional area and  $\rho$ = density, will have altered as consequence. Therefore as a correction based on the CIBSE guide B [127] can be used:

$$A = \frac{Q}{0.84\sqrt{\Delta P}}$$

where  $\Delta P$  is the pressure gradient across the diffuser face. The lack of a resulting Coanda effect is really the main drawback to this method, mainly due to the lack of knowledge regarding turbulent intensities at the inlet [127].



Figure 4.14: Diffuser opening

#### 4.2.4.2 Momentum Method

A diffuser is designed to deliver a prescribed mass of air per second, however due to geometry design and posterior simplification in CFD, substantial compensation for flow speed would be unrealistic. This unphysical increase in air velocity can alter flow patterns further afield hence creating features which are not actually present. To avoid this Srebric et al. [231] propose defining a known momentum to a volume in front of the diffuser, thus both

mass and velocity are correctly defined. In many cases the energy and turbulent kinetic energy must also be calculated and these are often unknown a priori. A disadvantage to this process lies in not being able to prescribe a velocity profile, relying on homogeneity across the inlet.

#### 4.2.4.3 Box Method

Measurement of either velocity magnitude or direction of a diffuser jet may be difficult due to several factors. Despite deflectors being useful for directing flow, they often pose a hinderance for flow measurement instruments. Such instruments are either too bulky to fit between the vanes, such as in the case of comfort probes or in fact disturb the flow field itself. In the latter case the anemometer often carries a protective hood which prevents close measurement and hence a substitute method was presented [172]. The *box method* consists of measuring flow variable data on an imaginary bounding volume such as in Figure 4.15 and Figure 4.16. The challenge arises in compromising between the accuracy of the measurements within the fully developed region of the jet without altering the flow further afield.



Figure 4.15: Measurement surfaces away from the grille

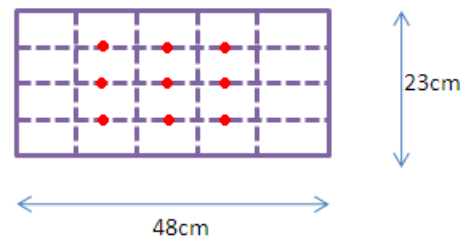


Figure 4.16: A single surface showing 9 measurement points

#### 4.2.4.4 Turbulence intensity

Turbulence plays a role in the generation of fluid friction losses and fluid induced noise [221]. Turbulence intensity is the ratio between mean and fluctuating velocity magnitude, characterising turbulence expressed as a percentage. An idea of this intensity can be deduced from measuring the time-averaged velocity and the fluctuating velocity at a point. A single time-series measured like the one in Figure 4.17 contains a mean velocity ( $U_{mean}$ ) and

a fluctuating component ( $U_{rms}$ ).

$$U = U_{mean} + U_{rms}$$

$$Tu = \frac{U_{rms}}{U_{mean}} \quad (4.2.9)$$

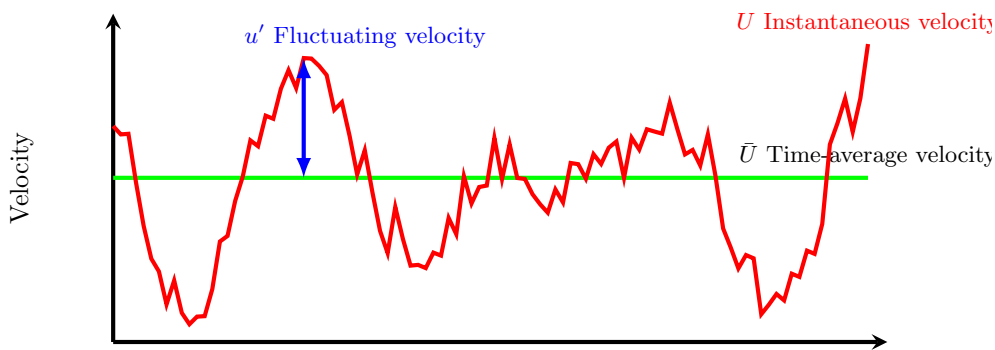


Figure 4.17: Hypothetical plot of fluctuating velocity along time-averaged velocity

From the single time series, two quantities can be deduced: the mean velocity and the root mean squared velocity value:

$$U_{mean} = \frac{1}{N} \sum_i^N U_i \quad (4.2.10)$$

$$U_{rms} = \frac{1}{N-1} \sqrt{\left( \sum_i^N (U_i - U_{mean})^2 \right)} \quad (4.2.11)$$

An idealised flow of air with absolutely no fluctuations in air speed or direction would have a turbulence intensity value of 0%. In practice this does not occur indoors [234], and duct-flow generally ranges between 4 and 10%. The measurement and estimation of this quantity will be used for setting up the boundary conditions of the numerical simulation.

#### 4.2.5 Instruments and Instrumentation Error

The instrumentation within this investigation is calibrated professionally by the manufacturer.

Air velocity magnitudes are measured by means of a Testo low velocity anemometer with an error ( $\delta v_e$ ) of  $\pm 0.03 \text{ms}^{-1}$ . Fluctuations occur at the same point within a certain range depending on the type of flow measured. In the case of fluctuations within the room space, differences of up to 5% either side of the mean were recorded <sup>1</sup>. Temperature was measured via a Testo temperature sensor at the same time as the velocity magnitudes. Error treatment is in accordance to that set out by Taylor [235] such that two categories exist:

- Uncertainty of flow magnitude ( $\delta v_e$ )
- Uncertainty due to fluctuations ( $\delta v_f$ )

Taylor's description of error is via a metric given here:

$$\delta v_s = \sqrt{(\delta v_e)^2 + (\delta v_f)^2}$$

Hence in the case of the anemometer used and the rooms measured, the error  $\delta v_s$  is  $\sqrt{(0.05\bar{x})^2 + 0.03^2} \text{ms}^{-1}$ . Where  $\bar{x}$  represents the mean.

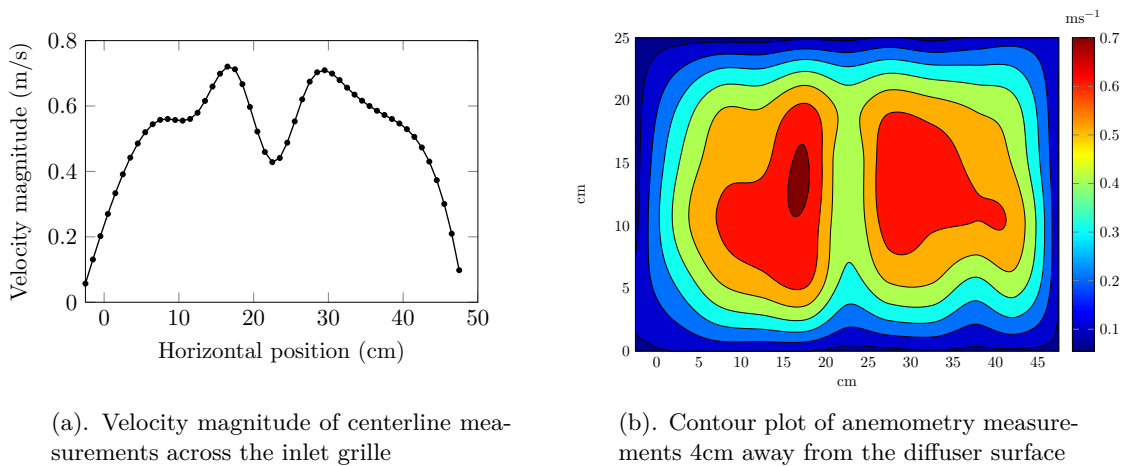
Accuracy of the positioning of the magnitude sensors can only be determined realistically to the nearest 1cm. The proximity to the nearest surface was restricted by the protector casing attached to the anemometer itself. Hence in the case of diffuser louvresm fluctuations caused by high turbulence would be reduced due to entrainment of the jet further away from the source. Despite the best efforts to capture data, misalignments and configurations of the ventilation duct-work may compound certain errors. In order to consider this type of asymmetry, careful thought was given when choosing how to represent the boundary conditions in CFD.

#### 4.2.6 Boundary Conditions

A velocity profile shown in Figure 4.18b was defined at the supply air diffuser based on the *box method* described in Section 4.2.4.3. This was due to the complexity of the diffusers involved and secondly the substantially high Reynolds' number ( $\simeq 1.6 \times 10^5$ ) flow involved.

<sup>1</sup>the standard deviation will be used ( $\sigma^2$ ) in handling errorbars within plots

A series of sixty six airspeed measurements using an hot wire anemometer (Testo Ltd, Germany. Accuracy:  $\pm 0.03$  m/s +5% of mean, resolution: 0.01 m/s), was used throughout. Measurements at equally spaced intervals as per Figure 4.16), were taken across the inlet surface to create a lattice of air speeds (Figure 4.18b). Flow speeds exiting the diffusers were captured at a 4cm distance from the inlet surface. Closer measurement was not possible due to the protective casing surrounding the wire filament. The averaging time at each point was 5 minutes and the sampling frequency for both temperature and velocity magnitude was 1 Hz. The supply airflow rate and the temperature were monitored and remained constant during the measurements and all subsequent experiments. Figure 4.18a shows the velocity magnitude distribution across the centreline of the inlet diffuser. The extract was modelled as a negative pressure outlet (-25Pa) on the boundary.



(a). Velocity magnitude of centerline measurements across the inlet grille

(b). Contour plot of anemometry measurements 4cm away from the diffuser surface

Figure 4.18: Anemometry measurements of inlet diffuser air velocity

An isothermal assumption was applied to the empty room simulation (scenario 1), while a heat load of  $35 \text{ W/m}^2$  was applied to the DIN man in the hospital room scenarios (scenarios 2-4). The Grashof/Reynolds's ratio indicates convective secondary flows and hence the energy equation was solved using the Boussinesq approximation in the latter cases. A momentum source of 1 N s is applied to the DIN man to help stabilise the thermal plume. Fluent's standard air material  $\rho=1.225 \text{ kg/m}^3$ ,  $\mu=1.84 \times 10^{-5} \text{ ns/m}^2$  was used for the continuous phase.

### 4.2.7 Modelling Particle Deposition

Although CFD has been shown to well represent the bulk flow within indoor spaces, modelling of particles has been the study of much contention. Although the tracking of a log down a river can be done either by sitting on it (Lagrangian) or viewing it from the bank (Eulerian), the actual mechanics of micron-sized particles makes these techniques somewhat harder to implement correctly.

Lagrangian particle tracking with stochastic discrete random walk (DRW) was used to represent the eddy interactions of the discrete phase. Bioaerosols were simulated as spherical water droplets, 2.5 $\mu\text{m}$  in diameter and released from source points comparable to the experimental study. Particle trajectories are calculated by a fifth order Runge-Kutta method by considering the change in particle velocity  $u_i^p$  due to drag force, inertia ( $u_i - u_i^p$ ), gravity  $g_i$ , lift force  $F_i^L$  and Brownian motion  $n_i(t)$  thus:

$$\frac{d u_i^p}{d t} = \frac{1}{\tau} \frac{C_D Re_P}{24} (u_i - u_i^p) + g_i + F_i^L + n_i(t) \quad (4.2.12)$$

Where  $\tau$  is the particle relaxation time given by:

$$\tau = \frac{S d^2 C_c}{18} \nu \quad (4.2.13)$$

Where,  $S$  is the particle-fluid density ratio,  $d$  the particle diameter,  $C_c$  is the Cunningham-Stokes slip correction factor and  $\nu$  the fluid kinematic viscosity.

$$C_c = 1 + \frac{2\lambda}{d} (1.257 + 0.4 \exp(-\frac{1.1d}{2\lambda})), \quad \lambda = \text{gas molecular mean free path.}$$

Compared to the bulk-flow in the chamber, particle contribution to density was considered sufficiently low and therefore only one-way turbulence interaction was employed.

#### 4.2.7.1 Discrete random walk: DRW

Laminar flow allows for reasonable deposition accuracy as it is predicted in a deterministic manner, especially in the case where the fluid is in steady state equilibrium. However in the case where diffusional deposition is predominant, which in the context of indoor air flows is a reasonable assumption, particles require a sort of final push to become

deposited [236]. The eddy interaction model by Gosman and Ioannides [67] is a discrete random walk treatment. This was shown to be the turbulent fluctuating velocity  $u'$  which is the instantaneous fluctuating fluid velocity along the particle path line.

$$u' = G\sqrt{u'^2} = G\sqrt{\frac{2k}{3}} \quad (4.2.14)$$

Where  $G$  is Gaussian white noise generated by a random number between (0,1] and constant during one eddy interaction.  $K$  is the kinetic energy. This also shows that turbulent kinetic energy is isotropic i.e.  $\sqrt{u'^2} = \sqrt{v'^2} = \sqrt{w'^2} = \sqrt{2k/3}$ . Figure 4.19 shows the comparison of particles modelled with and without applying the DRW. Deposition percentages (with= 68% and without=12%) compared similarly to Wong et al. [92] and Hathway [46]. In the case without using DRW, particles do not deposit readily which is unphysical, somewhat akin to a light aircraft gliding over a runway at 4 miles an hour on a blisteringly hot day, unable to land.

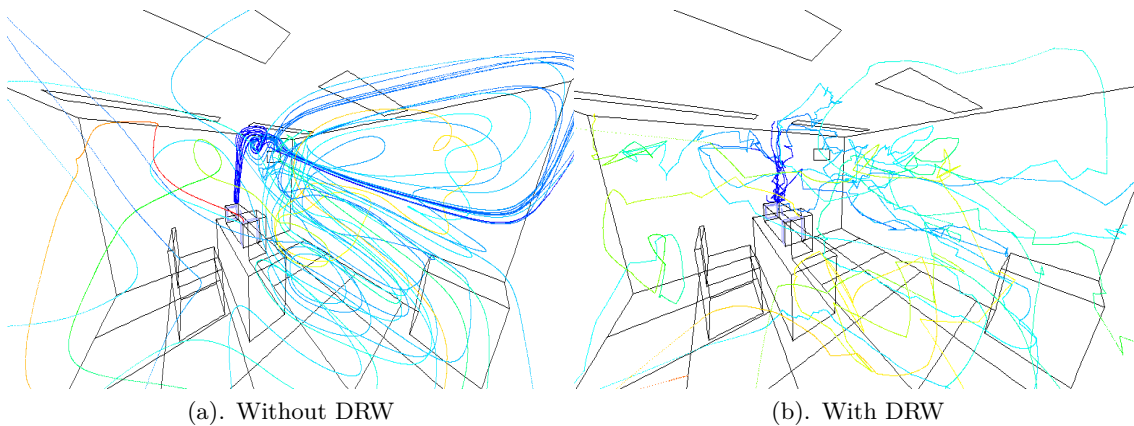


Figure 4.19: Particle tracking within a room showing the effects of modelling the dispersion with and without DRW

### 4.2.8 Mesh Generation

Grid choice is important and often geometry dependent. Structured grids of cells with equal sizes are often computationally the most inexpensive due to their cartesian layout. However, geometry often dictates the need for unstructured cells which closely fit the underlying contours [228]. To mesh a ventilation duct  $5\text{m} \times 1\text{m} \times 1\text{m}$  three possibilities are available: hexahedral (Figure 4.20a), tetrahedral (Figure 4.20b) or polyhedral (Figure 4.20c) dominant meshes.

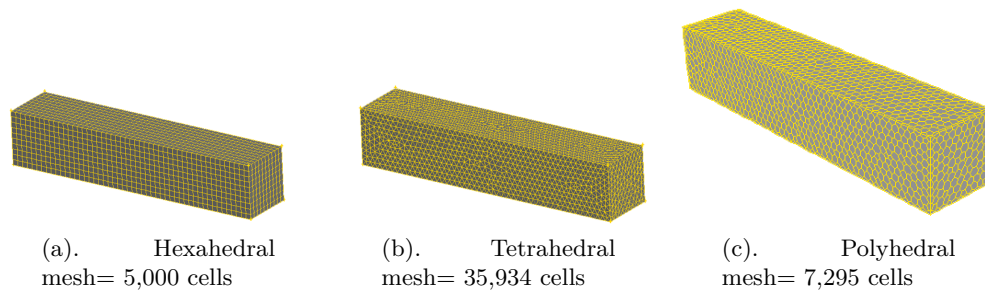


Figure 4.20: Hexahedral meshing within the single room

The application of unstructured cells has the distinct advantage of being able to cope with sudden geometrical changes [228] such as edges and gaps. Meshing this volume with a constant cell size of  $0.1\text{m} \times 0.1\text{m} \times 0.1$  requires 5,000 hexahedral cells, 35,934 tetrahedral cells and 7,295 polyhedral cells respectively. For memory allocation alone the hexahedral mesh is most advantageous. Overall crass conclusions about meshing domains are summarised below:

- Solutions on **hexahedral** meshes develop quickest using the least memory for the given problem
- **Hexahedral** cells can be aligned to the flow and hence reduce accumulation of errors or *numerical diffusion*
- **Polyhedral** cells reduce the cell-node count by amalgamating contiguous tetrahedra so approximating hexahedral cell counts, but are still marginally higher
- **Tetrahedral** cell counts are substantially larger and therefore more memory intensive and solutions are slowest to converge

- Numerical diffusion is heavily dominant in **tetrahedral** meshes due to the comparatively high number of cell nodes compared to the other mesh types [223].

The geometry of the rooms in scenarios 1-4 are dominated by varying sizes of shapes therefore unstructured meshing is required. Additionally, given the cuboidal natures of the bed, table chair, DIN man etc, hexahedral meshing is chosen. This also reduces the number of cells used in comparison to all other choices. Meshing is fully hexahedral with a maximum cell volume of  $1.5625 \times 10^{-5} \text{ m}^{-3}$  within the bulk domain Figure 4.21

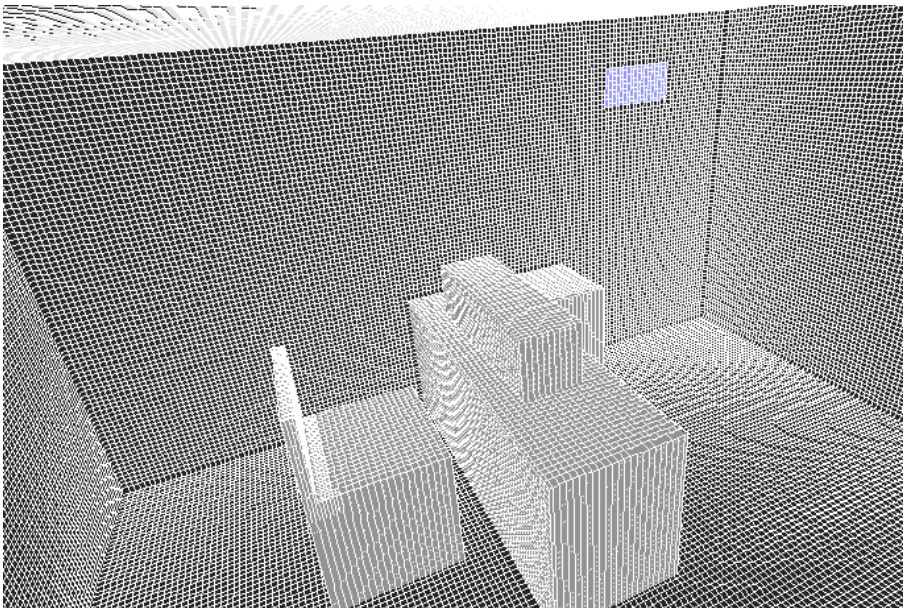


Figure 4.21: Hexahedral meshing within the single room

#### 4.2.8.1 Mesh refinement

Careful and high quality boundary meshing is essential to accurately capture particle deposition velocity [67]. Cells  $1 \times 10^{-6} \text{ m}^{-3}$ , 10cm away from all horizontal surfaces are used throughout. An example of this can be seen in Figure 4.22, corresponding to scenario 1. This type of refinement is called hanging-node.

Reducing the cell size any further at the boundary would cause  $y^+$  values to drop below 1 under these conditions causing the standard boundary layer resolution techniques to become unreliable. Hence no further mesh size reduction should be carried out. Final cell count is in the region of 4 million volumes.

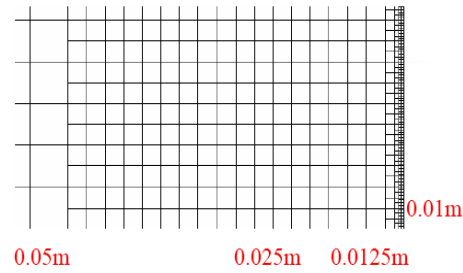


Figure 4.22: Hexahedral mesh refinement from bulk flow area to boundary wall highlighting the cell size reductions in red

#### 4.2.9 Preliminary Mesh-Independence

Grid density and construction have been shown to influence flow results heavily [172, 231, 237]. A misnomer is that it is worth continuously refining the computational mesh ad-infinitum whereby gaining increased accuracy of the solution. Nielsen highlights that although this may be true for “*a millisecond over a postage stamp*”, a rule of thumb suggests that if by halving the grid sizing produces less than a 5% difference in solution then stop and use the coarser grid [172].

Roache [237] proposes an error metric which compares the ratio between solutions of coarse and fine grid solutions:

$$\epsilon = \sqrt{\frac{\sum_i^{100} |u_{\text{coarse}} - u_{\text{fine}}/u_{\text{fine}}|}{100}} \quad (4.2.15)$$

where  $u_{\text{fine}}$   $u_{\text{coarse}}$  are velocity magnitudes at the same point on the fine and coarse grids respectively, for a hundred points. Thus,  $\epsilon$  is simply a measure of the difference in solution variables and how that relates to the coarse or fine grid solution. Roache [237] proposes that this ratio is not sufficiently descriptive of the variables present in CFD simulations. In fact a more rigorous approach is to consider the formal order of accuracy,  $p$ , and the grid refinement ratio,  $r$ , namely:

$$r = \frac{h_c}{h_f} \quad (4.2.16)$$

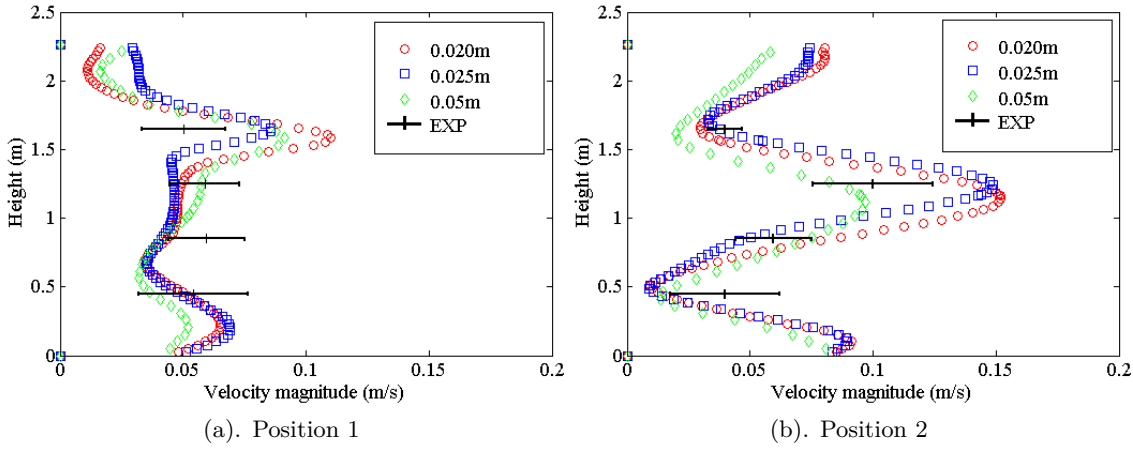


Figure 4.23: Anemometry comparison against three hexahedral mesh sizes for the empty chamber (Scenario 1). Errorbars represent one standard deviation either side of the mean.

where  $h_f$  and  $h_c$  are the fine and coarse grid element edge lengths respectively. Thus a more appropriate measure of the discretisation error, (based on Richardson Extrapolation) is given by:

$$E = \frac{\epsilon}{r^p - 1} \quad (4.2.17)$$

where  $p$  represents the truncation error order of the discretisation scheme used in both simulations. For example a  $p$  value of 1 would represent the 1<sup>st</sup> order accuracy of Euler's Forward Upwinding Scheme, or  $p=2$  for a 2<sup>nd</sup> order scheme.

Therefore a three-mesh solution independence study was first undertaken in the empty room. All meshes contained structured hexahedral elements with  $8 \times 10^{-6}$  m,  $1.5625 \times 10^{-5}$  m and  $1.25 \times 10^{-4}$  m cell volumes respectively. Figure 4.23 shows the visual comparison of the results at two positions within the empty chamber against experimental measurements.

Computational restrictions on memory meant that meshes of  $1 \times 10^{-6}$  cm and below across the whole volume could not be visualised as the cell count reached over 32 million. This would also impose a restriction on the  $y^+$  value. Therefore a compromise was reached where 0.1m from relevant surfaces, cell volumes were  $8 \times 10^{-5}$  m and in the remaining volume,  $1.5625 \times 10^{-5}$  m<sup>3</sup>.

#### 4.2.9.1 Particle-mesh independence

Roache [237] suggests that often velocity grid independence may be reached prematurely with respect to particle tracking, since large disparity must exist between cell size and particle diameter. Therefore, particle tracking length scale was increased to reflect at least five calculations per cell. Particle count independence was achieved at particle numbers above 50,000 and little significant improvement was gained thereafter. Figure 4.24 shows the convergence on particle deposition percentages plotted against particle injection count. Mesh independence based on particle deposition distribution was also achieved at this particle count.

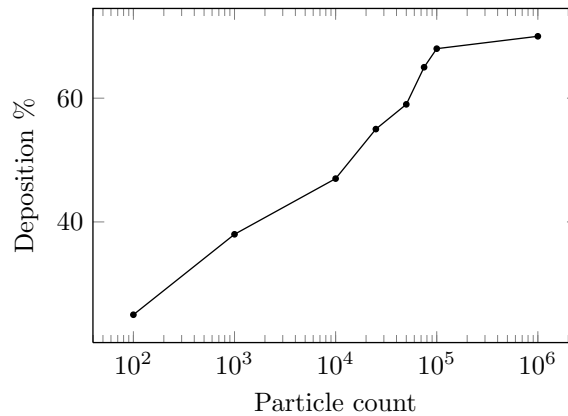


Figure 4.24: Particle deposition percentage on all surfaces within Scenario 1: The empty room

#### 4.2.9.2 Convergence criteria

Simulations were considered converged when Fluent's residuals for continuity and all other variables dropped below  $1 \times 10^{-4}$ , and remained below this for at least 100 iterations. All variables are scaled with respect to the sum of the errors in all cells. In addition continuity is scaled with respect to the largest absolute value within the first five iterations and so can be considered normalised [223].

## 4.3 Results and Discussion

The (0,0,0) origin in all simulations can be found at the bottom corner facing the inlet diffuser.

### 4.3.1 Scenario 1: Empty Room

The first scenario represents a controlled condition to ensure that experimental scenarios are directly comparable to idealised numerical scenarios. Due to the physical dimensions of the anemometer's protective cage there were some restrictions to the distance from the wall at which the flow could be measured.

#### 4.3.1.1 Airflow patterns

Figure 4.25a shows the representative velocity vectors plotted on the vertical plane perpendicular to the inlet diffuser. The inlet jet clearly forces its way into the room where slower moving air prevents quick turbulent diffusion of the eddies. Both lower left and upper right quadrants depict recirculation zones, but no visible Coanda effect is present. Figure 4.25b shows vectors plotted on the horizontal plane, with the highspeed jet impinging on the opposite wall. This creates a large recirculation zone in the upper-left quadrant

Simulated velocity magnitudes at five vertical locations are presented in Figure 4.26 and compared against experimental data from anemometry readings at four points at each location. These measurements were recorded during a prolonged period of steady airflow and in each case show the mean and standard deviation over a 20 minute measurement period. Despite some variability in the measured data, both the  $k-\epsilon$  RNG and RSM turbulence model simulations capture the main features of the flow well. The data clearly indicates the spatial variability in the chamber airflow. In the breathing zone ( $y=1.6\text{m}$ ), the velocity profiles at poles 1 and 2 are generally higher due to the impinging jet from the inlet diffuser, while there appears to be recirculation in the region of pole-4, characterised by low velocities. These results also concur with smoke tracer tests conducted by Hathway [46] and appropriate mesh density and boundary conditions have been chosen confidently.

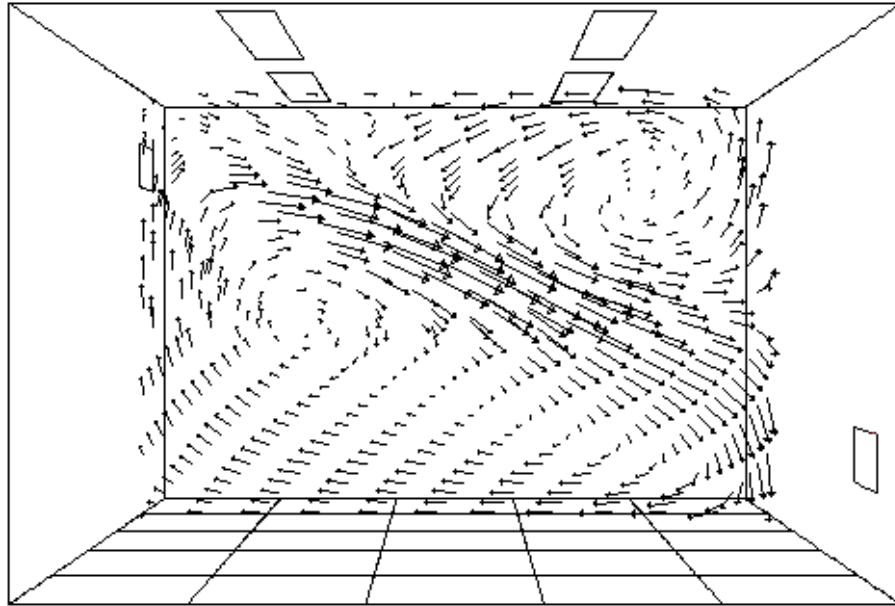
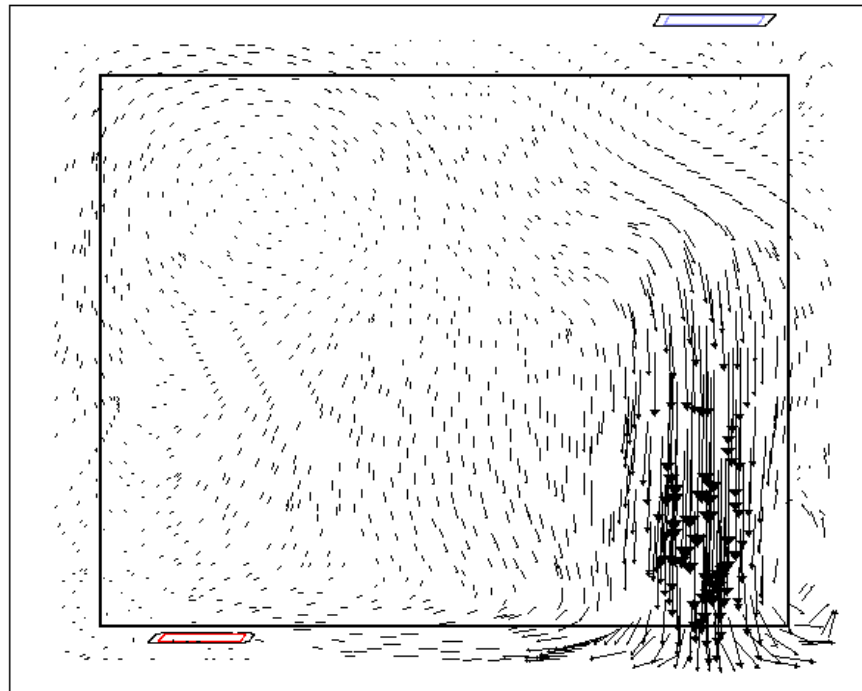
(a). Vertical plane,  $x=0.8\text{m}$ (b). Horizontal plane,  $y=1.2\text{m}$ 

Figure 4.25: Velocity vectors 0.001-0.07(m/s) plotted on planes within the empty room

It is clear that CFD is capable of representing the bulk flow field within the chamber to a high degree. Indoor air patterns are inherently variable but the CFD models using

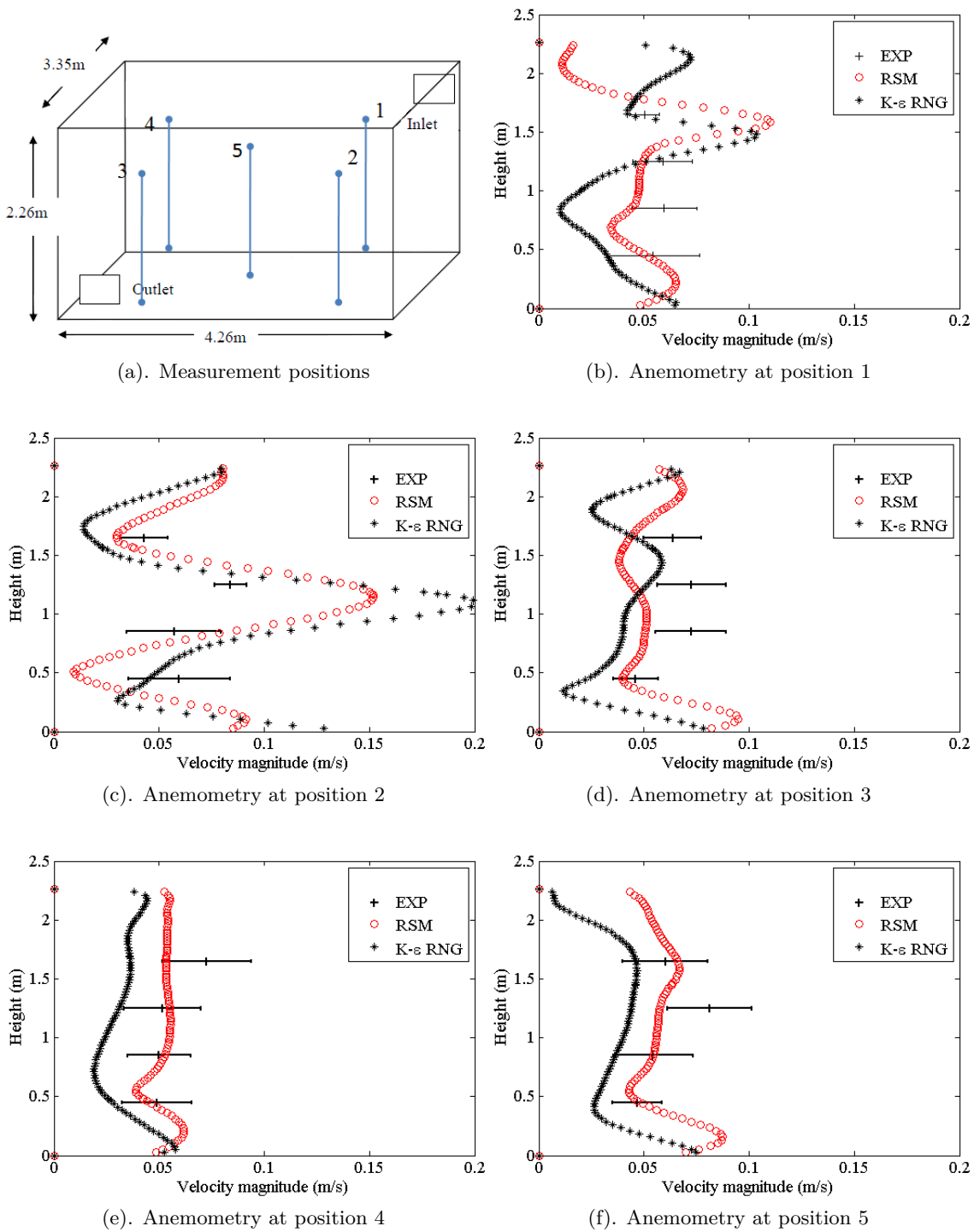


Figure 4.26: Anemometry comparison against  $k-\epsilon$  RNG and RSM turbulence models for the empty chamber (Scenario 1). Errorbars represent one standard deviation either side of the mean.

both RSM and  $k-\epsilon$  RNG turbulence models predict reasonable characterisations. Nevertheless the anisotropic turbulence model generally provides an improvement over the eddy viscosity assumption model, particularly in the regions of higher shear and velocity gradients.

## 4.3.1.2 Bioaerosol deposition

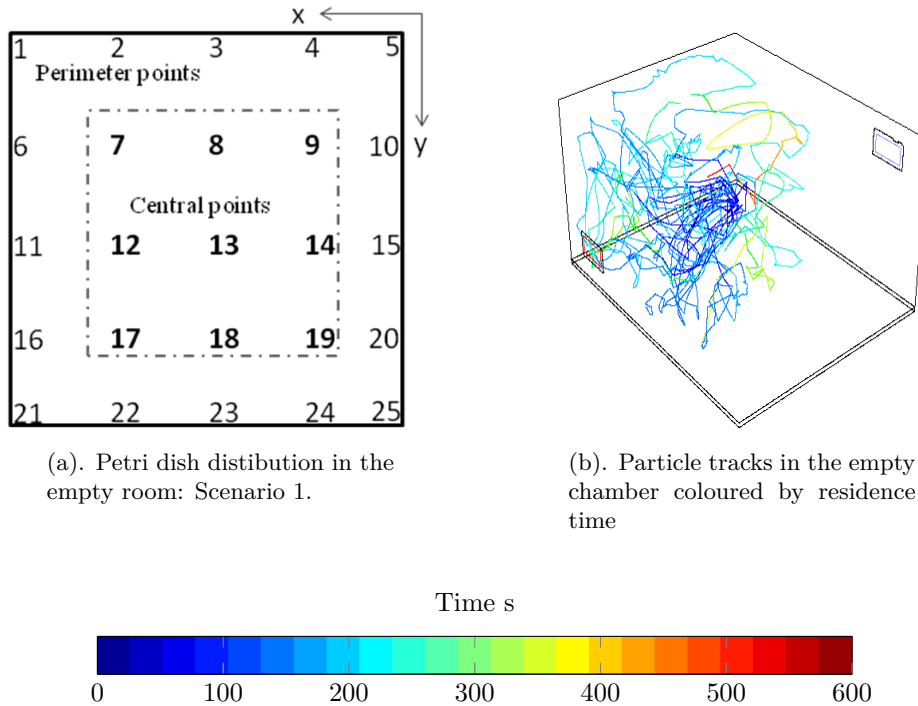
Figure 4.27: Representative images from *scenario 1*.

Figure 4.27a indicates the positions of Petri dishes within the empty room. Nine central and the remaining sixteen periphery points are shown pictorially here. Normalised experimental deposition  $C_i$  values (from Equation (4.1.1) on page 111) are presented together with numerical predictions from the RSM and k- $\epsilon$  RNG turbulence models at all floor collection points within the empty room in Figure 4.28. Figure 4.27b shows a representative number of particles tracked throughout the domain for 10 minutes.

As explained in Section 4.1.5 comparison is made between numerical and experimental data sets by means of the correlation coefficient ( $r$ ) obtained from linear regression. Ideal fit would be a direct 1:1 relationship between the data (i.e. a line  $y = x$ ), showing that either higher or lower experimental values were also captured in the numerical counterpart. To investigate the statistical significance of the relationship between them, a Wilcoxon-Ranksum test was performed between the two data sets. Briefly recapping, this ranks the data in each set, thus preserving spatial differences but remaining unbiased to underlying extrema if any exist. The null-hypothesis tested is whether the population median ranks differ (i.e. it is a paired difference test such that  $H_0$ : median difference between the pairs is

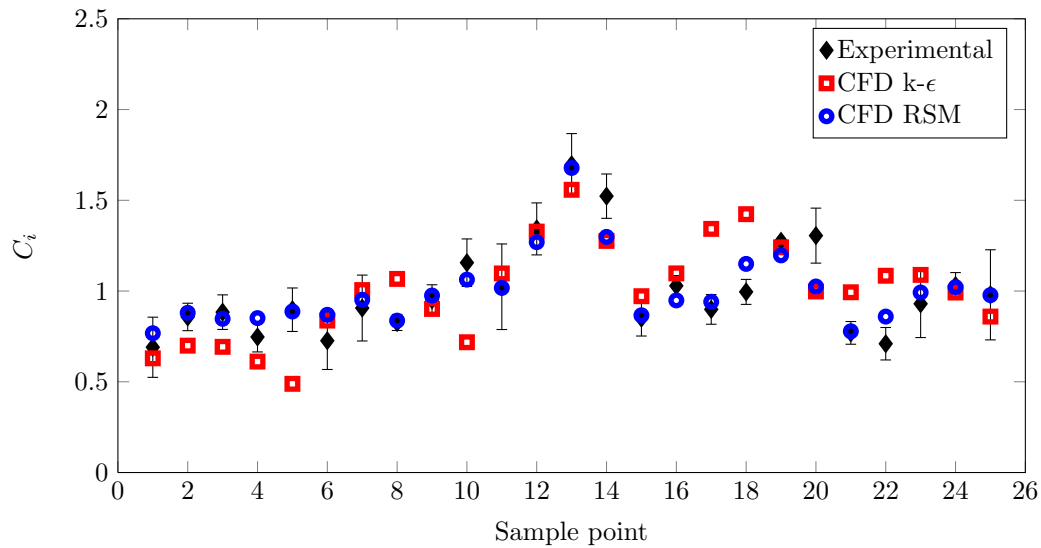
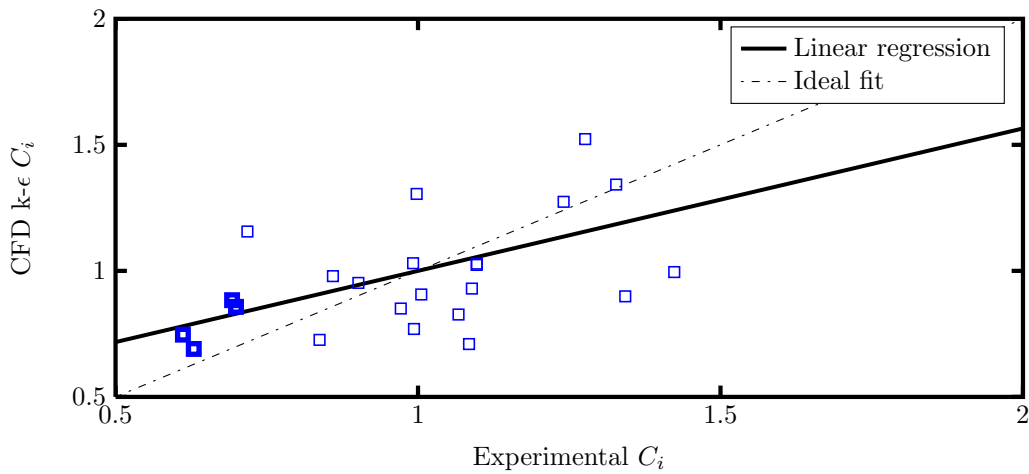
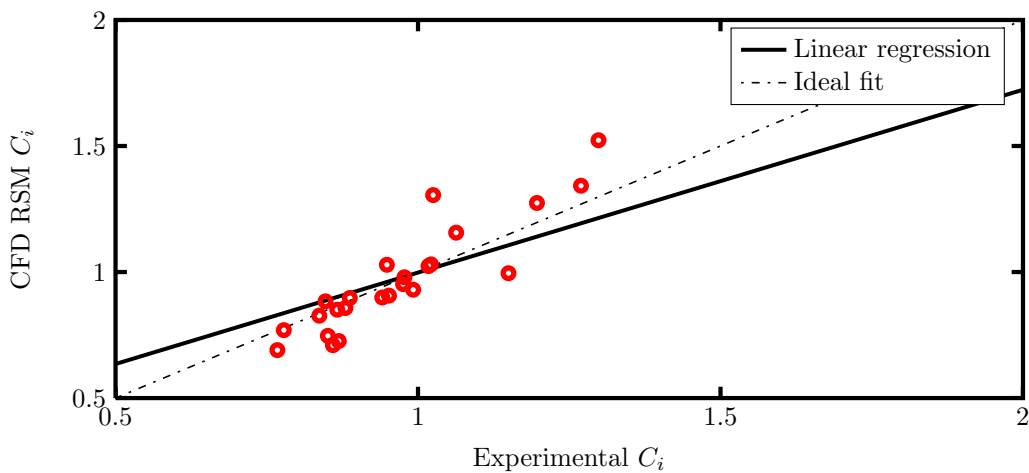


Figure 4.28: Comparison between experimental data and numerical deposition predicted by the two turbulence models. Errorbars represent one standard deviation either side of the mean.

zero and  $H_1$ : median difference is not zero). This is the non-parametric alternative to the paired Student's t-test, t-test for matched pairs, or the t-test for dependent samples when the population cannot be assumed to be normally distributed. Assumptions for this test require that the data be paired, be measured on an ordinal scale, need not be normal but the differences should be symmetric about the median. These experiments and simulations comply with all of the above. In addition each pair should ideally be randomly chosen and independent. By the nature of the experiment this assumption must be relaxed somewhat as the entire population must be tested, hence these cannot be truly random even if they are independent. Based on these assumptions if data sets do not differ significantly at the 5% level, the null-hypothesis cannot be rejected. This value is displayed subsequently alongside the correlation coefficient as the accompanying p-value.

Scatter plots comparing the numerical results with experimental averages at all 25 points are presented for both turbulence models in Figure 4.29. Table 4.3 presents linear correlation coefficients for all data points and then the central and perimeter points separately. The measured deposition in the nine zones directly below the source is fairly uniform with normalised reported values between 0.82 and 1.62. Relatively little variance was found here. Accompanying p-values do not reject the null-hypothesis of 0 median differences between ranks.

(a). k- $\epsilon$  RNG

(b). RSM

Figure 4.29: Scatter plots showing correlation between experimental data and numerical deposition predicted by the two turbulence models

Figure 4.28 shows a comparison between the experimental ( $C_i$ ) and the numerical prediction, depicting the spatial deposition. Comparison with the simulation results shows the RSM model more accurately corresponds to experimental data ( $r=0.93$ ), however k- $\epsilon$  RNG does not perform poorly ( $r=0.63$ ) in this region. Zones around the perimeter of the room showed more sizable scatter (not pictured) with normalised deposition down to 0.69 and compared less well with the CFD models, with correlation coefficients of  $r=0.27$  and  $r=0.86$  for the RSM and k- $\epsilon$  RNG, respectively. The k- $\epsilon$  model simulation tends to predict a more uniform spatial deposition, with higher  $C_i$  around the mean (Figure 4.29a).

Location	Correlation, p-value	Correlation, p-value
	k- $\epsilon$ RNG	RSM
Overall	r=0.60, p=0.72	r=0.92, p=0.59
Central	r=0.63, p=0.29	r=0.95, p=0.92
Perimeter	r=0.27, p=0.61	r=0.86, p=0.46

Table 4.3: Correlation between CFD and experimental results for both turbulence models. The p-value corresponds to the Wilcoxon-Ranksum test comparing median differences between ranks.

However, the calculations of anisotropic Reynolds stresses under the RSM model produces a tighter relationship (Figure 4.29b) and hence makes an improved comparison ( $r=0.95$ ). Both models tend to over-predict low deposition and under-predict high deposition, but this is found to a greater extent with the k- $\epsilon$  model. This is indicated in the lines of best fit and also in both data sets displaying a weak right skew. Overall the p-values associated the Wilcoxon-Ranksum test suggest that the null-hypothesis cannot be rejected at the 5% level, showing there is no significant difference evident in the test for either turbulence model which again is in line with the conclusion that both turbulence models appear to predict well. Moreover the correlation coefficients in all cases show that the RSM model outperforms the k- $\epsilon$ .

Experience from the current study shows that a minimum of five settle plates are needed at each collection point to achieve statistically reliable and replicable results. Bioaerosol deposition comparisons tended to be well predicted by both turbulence models in the central regions, but accuracy deteriorated towards the outer edges of the room, particularly in the case of k- $\epsilon$  RNG. The prevalence of homogeneity in turbulence appears to translate to particle depositions, particularly for size ranges where body forces dominate [202]. The Reynolds' Stress turbulence model allowed anisotropic flow patterns to be adequately captured, leading to a very strong comparison between spatial depositions. In addition only minor variations were observed in the CFD prediction, given particle number independence, which is reflected in the high r value of the linear polynomial fit. Lai et al. [217] suggest that the inclusion of the effect of turbophoresis may enhance particle deposition, particularly where the vertical turbulence gradient is high close to the wall.

Overall the results suggest slightly higher deposition close to the source (sample points 12-14), possibly due to the largest particles dropping out of the air before evaporating. However deposition is apparent across the room indicating the combined influence of air movement and gravitational settling on the small diameter particles.

### 4.3.2 Scenario 2: Single Patient Room

The second scenario considered adds both complexity and realism by including key items of furniture plus a DIN-man to take into account the heat plume generated by a quiescent, resting patient in a hospital single-bed room.

#### 4.3.2.1 Airflow patterns

Figure 4.30 shows simulated temperature contours and velocity vectors for the single patient room, plotted on horizontal and vertical surface through the bed. Complex flow structures can be observed, with the cold inlet air impinging on the opposite wall and multiple recirculation zones at the foot of the bed. A vertical heat plume emanates from the supine mannequin and is depicted in the vertical plane.

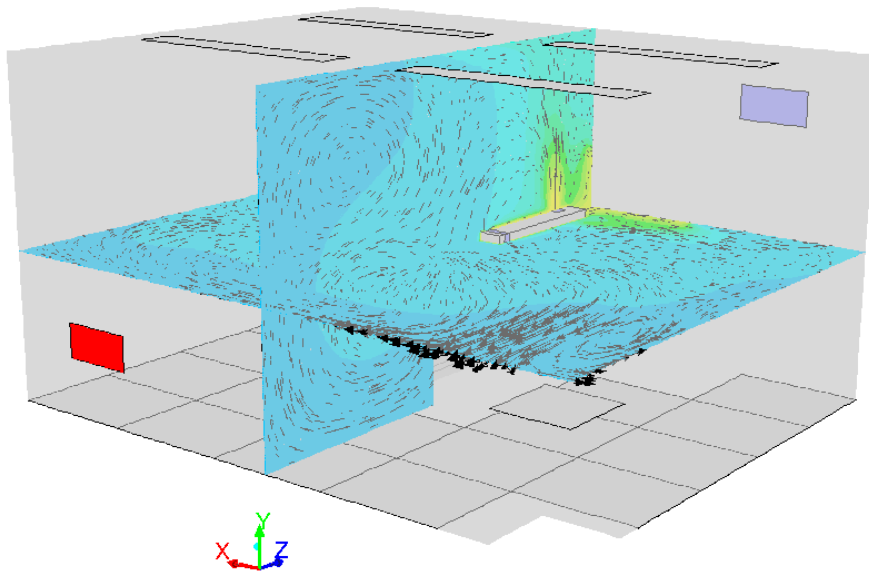
These depict three main different flow features within the chamber, all of which are typical of indoor air patterns:

**A convective plume** appears due to density differences created by the heat flux generated by the DIN man and mainly appears above the head area.

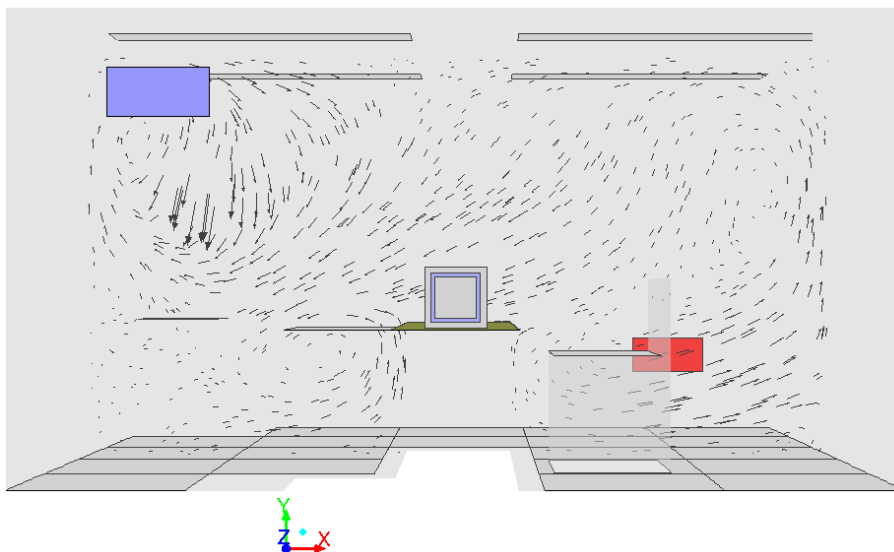
**Recirculation zone(s)** in the upper left quadrant vortices can be seen rotating in opposite directions as shown in Figure 4.30b. These occur as a result from the convective plume mentioned earlier rolling off the end of the bed and mixing with the colder air from the ventilation inlet.

**An impinging jet** feature is visible and grows as colder, faster moving air is vented into the room, falling due to density and hitting the opposite wall. This is often a common feature with slot diffuser grilles when density differences occur.

As such, short circuiting is suspected due to the impinging jet effect. Since the air change rate chosen is approximate of a real hospital scenario it is reasonable to believe that this may occur in a room of similar dimensions and make-up.



(a). Temperature contours and superimposed velocity vectors on vertical (x=2.5m) and horizontal (y=1.2m) planes



(b). Velocity vectors plotted on vertical plane only.

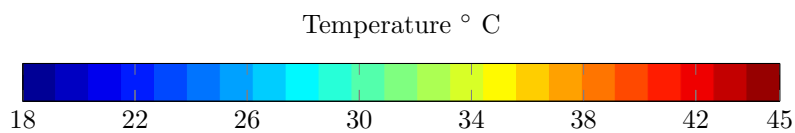


Figure 4.30: Velocity vectors (0.001-0.07m/s) superimposed onto temperature contours in single room.

### 4.3.2.2 Bioaerosol deposition

Normalised experimental deposition on the four horizontal furniture surfaces is compared to simulation results with two turbulence models in Figure 4.31. While Figure 4.30 shows the flow in this situation is less homogeneous than the empty room, the experimentally measured deposition still remains relatively uniform with mean normalised values between 0.64 and 1.16 on the four surfaces. Although the bioaerosol source was located at the patient head, deposition on the bed is lower than other surfaces which may be due to the convective plumes above the DIN-man promoting transport away from the source. The highest measured deposition is on the surface representing a sink, despite this being the furthest location from the source. While both turbulence models predict the same spatial trends as the experiments, the  $k-\epsilon$  model has a greater tendency to over- or under-predict in this case, with only one of the four locations showing a good comparison with the experimental result. However the RSM model shows very good comparison with the experimental results, with similar magnitude deposition as well as spatial distribution with a small but consistent tendency to over-predict.

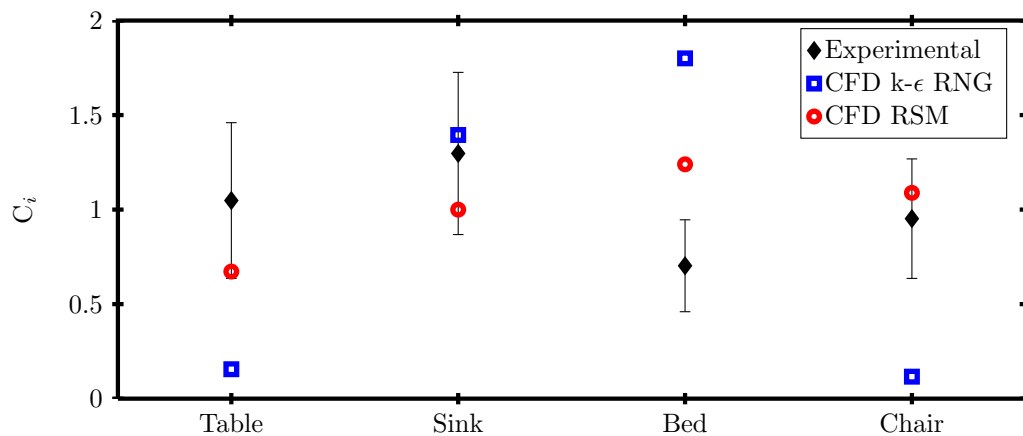


Figure 4.31: Comparison between numerical and experimental deposition on furniture surfaces in the single patient room. Errorbars show one standard deviation either side of the mean.

A stronger heterogeneity was observed here in comparison to the empty chamber, mainly due to the modified flow gradients, e.g. Figure 4.30a, imposed by furniture and the convective heat plume. Due most probably to the latter, the patient's bed showed lower deposition quantities in comparison to neighbouring surfaces. While this gives some insight into the potential influence of the thermal plume in transporting bioaerosol particles away

from the source, the results must be interpreted with caution. In reality the patient may not be permanently facing upwards and would likely move during their sleep. Additionally, bed clothes are usually present on hospital beds, producing a larger surface area on which particles may be trapped. While the assumption of a quasi-steady state simulation and experimental set-up is considered suitable for evaluating the constant release of pathogens from a breathing patient, this is unlikely to be appropriate for situations where doctors and nurses are disturbing the airflow patterns by opening doors or shaking bed clothes, creating inherently transient airflow patterns. Despite the simplifications, it is worth noting that, as in the empty room scenario, the experiments and simulations both show measurable deposition across the room space clearly indicating the ability for a bioaerosol source to result in environmental contamination at some distance from the source.

In terms of numerical comparison, the  $k-\epsilon$  turbulence model simulation at best predicts normalised particle deposition values within one standard deviation of experimental findings. In particular both the bed side table and the chair have almost zero predicted deposition values. RSM on the other hand appears to slightly over-predict deposition in all cases, but remains within one standard deviation of the experimental results. The latter is supported by previous numerical conclusions of particle depositions in pipes [238]. While comparison for both turbulence models shows a lower agreement than the empty room scenario, this is not unexpected. The addition of a significant heat source and furniture adds complexity and hence uncertainty to the CFD model. It is necessary to simplify the geometries of furniture and the DIN man in the model, which will have some effect on the solution accuracy.

### 4.3.3 Scenarios 3 and 4: Double Patient Room

The double-bed room experimental setup was designed to test two main scenarios: The influence of a partition and influence of the airflow on deposition patterns. The influence of the airflow is considered by switching the location of the infectious source from *patient 1* to *patient 2*. Comparison between *scenario 3* and 4 therefore allows for observation of the effect of a partial partition and also the extent to which the fresh supply air above *patient 1* influences deposition in that and the neighbouring bed bay. In scenario 4, where a partial partition is required, a plastic sheet was hung between the patients such that it provided a physical barrier between beds. Gaps of 20cm were left at the top and the bottom of the sheet as well as 80cm at the end of the beds to allow for health care worker passage.

In experiments investigating scenarios 3 and 4 bioaerosol deposition was measured through 9 Petri dishes located on surfaces representing the chair, sink and bedside table for each patient respectively. Due to the large area of the bed, this was covered by 15 dishes over 3 zones to avoid the effect of spatial variation.

The results from the final stage of this study give some insight into the potential for cross-transmission of infection between patients due to deposition of pathogenic aerosol particles on key surfaces. As with the two previous scenarios, both experiments and simulations demonstrated that a bioaerosol release in both an open (*scenario 3*) and partitioned (*scenario 4*) room can result in measurable surface contamination across the whole of the room space. Of particular interest was the effect of both the location of the infectious source with respect to the inlet diffuser and the level of protection that a partition provides in terms of surface deposition in the neighbouring cubicle. When the source patient is located directly under the inlet vent (cubicle 1) the partition proved effective at limiting the deposition in the neighbouring cubicle (Figure 4.37a). However the partition's influence appears to be quite sensitive to reversing the source location (see Figure 4.37b). In the latter case particle deposition proved more homogeneous and hence the partition played a secondary role to the effect of ventilation inlet position.

As noted during the CFD and anemometry measurements, cubicle 2 provides areas of very slow moving air and consequently probable recirculation pockets. Therefore these allow particles to be dispersed towards cubicle 1 as well as being extracted. As a corollary,

positioning the susceptible patient upwind of the infectious source (in our case in cubicle 1) also results in a significant reduction in risk. The effectiveness of the partition is also likely related to its particular deployment in the form of a curtain with gaps above and below. However during a common diurnal hospital scene most curtains are usually only half drawn or fully retracted. In addition to this, and mainly to aid in cleaning, they often hang approximately 20cm from the ground and a similar distance from the ceiling. Consequently this space poses a gap for potential passage of pathogens, increasing cross-transfer susceptibility. Previous numerical simulations have shown that full height partitions may reduce airborne transmission risk [41] and that curtaining the length of patient beds are more effective than partially extended ones at preventing infection [239]. Physical barriers clearly point to effective intervention measures however further evaluation is needed to explore the most appropriate design and the limitations of such an approach.

CFD comparison concurred with the findings from the two previous scenarios. The further increase in complexity in the two-bed case again led to further variation in the CFD solutions. As previously shown, the RSM model generally led to better predicted deposition than the  $k-\epsilon$  RNG model, although both models produced realistic deposition patterns. Simulations suggested that particles released from *patient 2* were drawn towards the inlet jet, probably due to the regions of low pressure created by the faster moving air. This effect dominated the simulations where a partial partition was absent and to a lesser effect when one was present.

#### 4.3.3.1 Airflow patterns

Firstly CFD airflow visualisation results are shown depicting the double room set-up with and without a partition. Subsequently, experimental colony forming unit values are compared with predicted results from the same CFD simulations with the use of the Lagrangian tracking formulation.

Figure 4.32 shows simulated temperatures for *scenarios 3* and *4*. In the case with no partition the temperature distribution indicates a tendency for air movement from *patient 1* to *patient 2* on the way to the outlet, aided by a convective plume. The partition, however creates a physical barrier whereby streamlining the flow towards the extract (Figure 4.33). The most striking feature is the influence which the partition has in altering

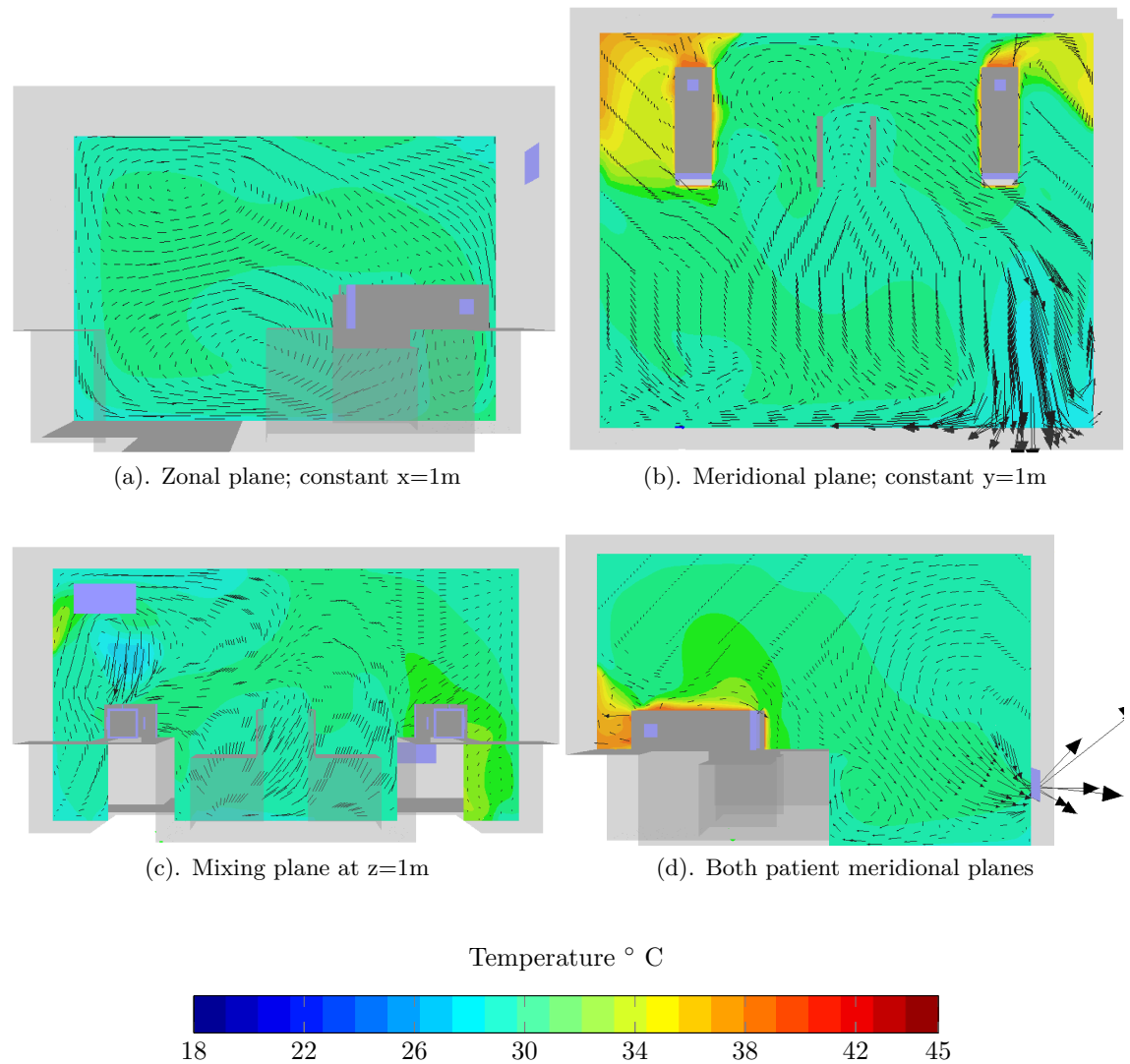
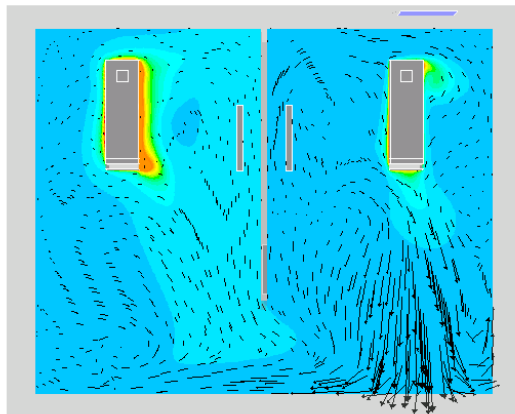
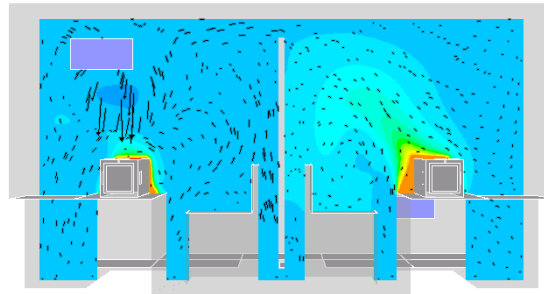


Figure 4.32: Velocity contours (0.001-0.07m/s) superimposed onto temperature contours. No intervention scenarios 3a 3b.

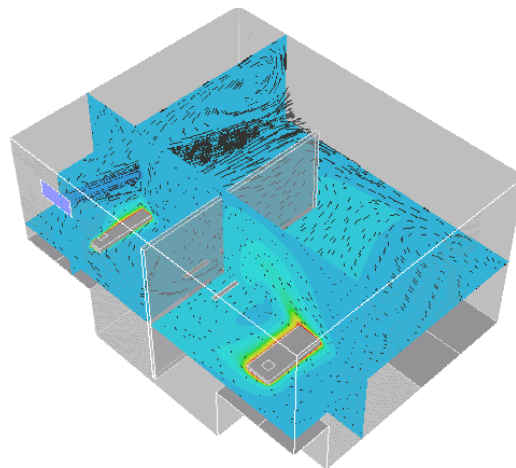
the temperature distribution at breathing level (Figure 4.32). In the absence of a physical partition, hot and cold air is able to mix freely, increasing the average temperature in both zones (Figure 4.33b). Installation of a curtain blocks off hot and cold air by streamlining the airflow pattern from inlet to outlet. The temperature contours in *patient 2*'s cubicle also appear to reduce as a possible corollary.



(a). Meridional plane; constant  $y=1\text{m}$



(b). Mixing plane at  $z=1\text{m}$



(c). Patient 2 zonal plane

Temperature ° C

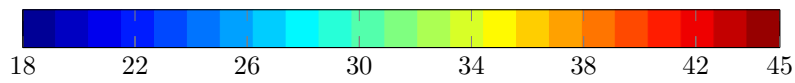


Figure 4.33: Velocity contours (0.001-0.07m/s) superimposed onto temperature contours. Partial partition scenarios 4a and 4b

#### 4.3.4 The Effect of a Curtain Partition

Figure 4.34 depicts the normalised experimental deposition results at each patient surface group for scenarios 3 and 4 based on the source of bioaerosols. Scenarios 4a and 4b investigated the effect of a partial partition. A plastic sheet was hung between the patients (as explained in Section 4.3.3) such that it provided a physical barrier between beds. Gaps were left at the top and the bottom as well as at the end of the beds to allow for HCW and equipment movement (see Figure 4.3b).

When *patient 1*, lying directly beneath the supply air vent is made to be the infectious source (Figure 4.34a) the partition has a negligible effect on the deposition onto the infectious patient surface group (table 1, bed 1 and chair 1). However, the partition does influence the deposition on the surface group for patient two. In the absence of a partition, bed 2 becomes the main destination surface for particles released at *patient 1*, surpassing that of the own infectious patient. A significant decrease is apparent at this point and other surfaces around *patient 2* when the curtain is installed, although the deposition is still a similar magnitude to that around *patient 1*. It is also noticeable that in both cases with *patient 1* as the source, there is greater spatial variation in the deposition pattern than for any other scenarios under scrutiny.

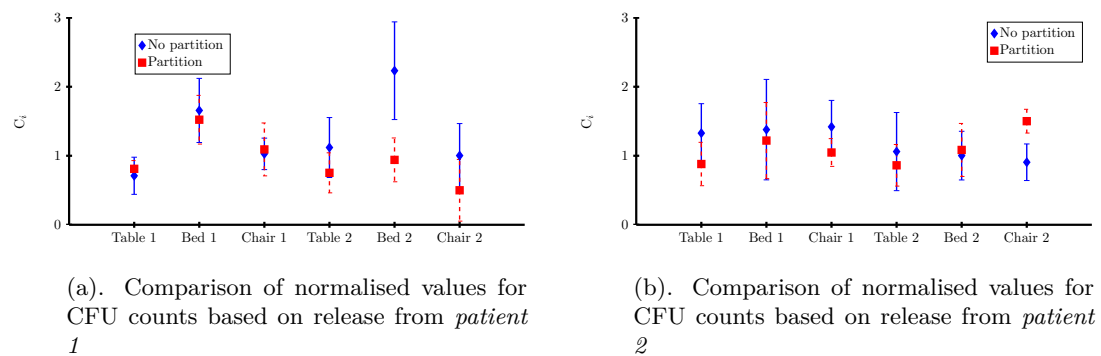


Figure 4.34: Influence of curtain and source location on experimentally measured deposition. Errorbars represent one standard deviation either side of the mean.

Figure 4.34b reverses the source position, where now the infectious point becomes *patient 2*. Statistically there appears to be no significant difference between the distributions, where the null hypothesis of equal medians cannot be rejected at the 5% level. However a tendency of higher deposition on bed and chair 2, which are closer to the partition, can be observed. This could be in part explained by the thermal plume from the *patient 2*

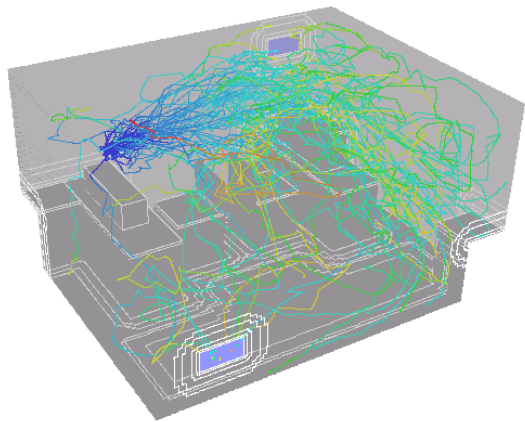
tending to drift towards the partition and hence towards chair 2 (see Figure 4.33). In contrast *patient 1*'s thermal plume is quickly dispersed and overwhelmed by the incoming faster, cooler air.

#### 4.3.4.1 Bioaerosol deposition

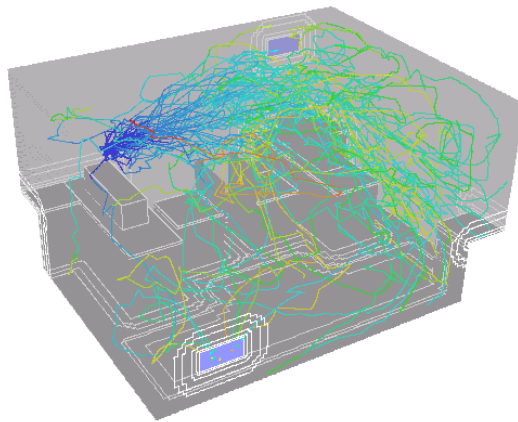
Figure 4.35 shows the particle tracking of 1,000 bioaerosols released from the infectious source within sub-scenarios 3 and 4. Particles are coloured by residence time, with a maximum turnover of 10 minutes. Most particles are extracted by the ventilation during this period, but others become attached to surfaces, while a small fraction remain trapped within the domain. Within Figure 4.35a and Figure 4.35b no partition exists and particles can be seen to readily spread between patients. In particular, when patient 1 is infectious a large percentage of particles can be seen to be entrained by the inlet jet above patient 2. This phenomenon is not reversed, with the majority of patient 2's bioaerosols being evacuated directly, bypassing patient 1. Figure 4.35c and Figure 4.35d show the scenario 4 with a partial partition between patients and highlights qualitatively the effectiveness of this simple measure.

Comparison of the experimental deposition patterns with CFD simulations are presented in Figure 4.36 for scenarios 3 and 4 with both patients alternating as the source. In all cases, both models give a reasonable prediction with only a small number of locations, notably the values at bed 2 in Figure 4.36a and table 1 in Figure 4.36b, where the CFD simulations compare poorly with the experimental results. There is noticeably more variation in these scenarios, with less clear differentiation between the results produced by the two turbulence models. Generally the predictions are closer to the experimental data nearer to the source with the RSM model giving slightly better results. This is also evident in the correlation coefficients presented in Table 4.4.

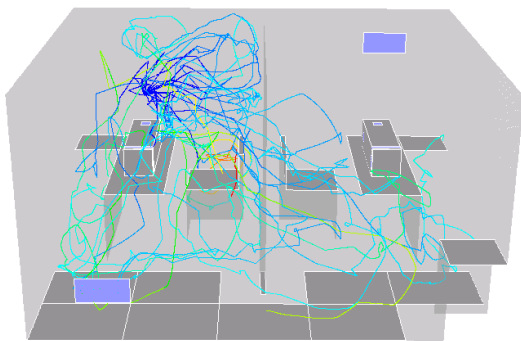
To further explore the influence of the partition (Figure 4.37) univariate linear regression was carried out between the data sets, where the only dependent variable was the normalised deposition count. In the case where *patient 1* is the source (Figure 4.37a yields: No partition CFU=-2.016\*Partitioned CFU+3.8) a two-fold reduction in pathogen deposition per surface can be predicted ( $r=0.32$ ,  $p=0.0254$ ). The p-value is calculated for Spearman's rho, testing the hypothesis of no correlation against the alternative that there is a nonzero correlation. Since the null-hypothesis cannot be rejected at the 5% level, a significant underlying correlation is present. Reduction in the second case (Figure 4.37b yields: No partition CFU=-0.235\*Partitioned CFU+1.63), when the pathogen source is situated directly opposite the extract vent, is however negligible.



(a). No partition infectious source= Patient 1



(b). No partition infectious source= Patient 2



(c). Partition infectious source= Patient 1



(d). Partition infectious source= Patient 2

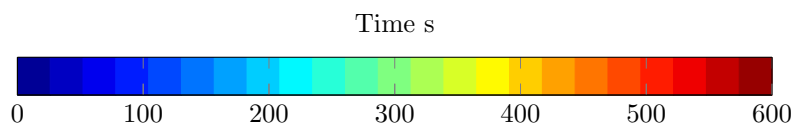
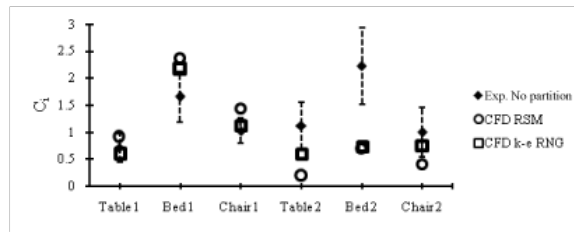
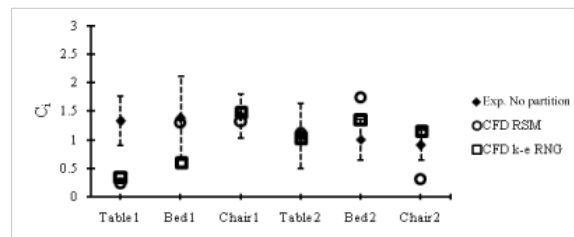


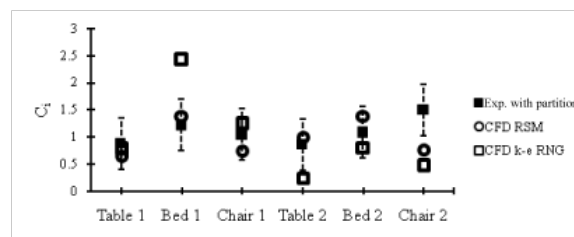
Figure 4.35: Particle tracking for scenarios 3a,b,4a and b. Coloured by residence time (s).



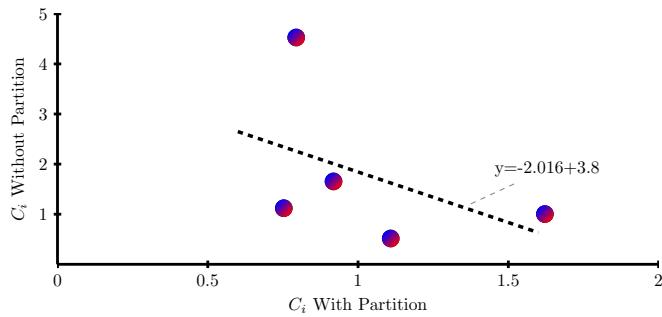
(a). Scenario 3: Infectious patient=1, Susceptible patient=2



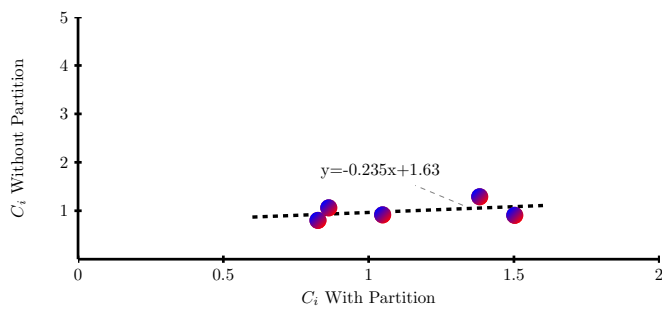
(b). Scenario 3: Infectious patient=2, Susceptible patient=1



(c). Scenario 4: Infectious patient=1, Susceptible patient=2



(a). Source= Patient 1



(b). Source= Patient 2

Figure 4.37: Comparison between scenarios 3 and 4. Spatial comparison of particle deposition with and without a permanent partial partition

		Scenario 3		Scenario 4	
Infectious patient		1	2	1	2
<b>k-ε RNG model</b>	p-value	0.46	0.67	0.13	0.81
	correlation coefficient (r)	0.23	0.2	0.35	0.94
<b>RSM model</b>	p-value	0.48	0.7	0.93	0.59
	correlation coefficient (r)	0.8	0.2	0.55	0.43

Table 4.4: Statistical analysis of correlation between experimental deposition and CFD for scenarios 3 and 4. p-values do not reject null-hypothesis of 0 median differences between ranks.

## 4.4 Conclusions

Although limitations are often acknowledged regarding the accuracy of predicting indoor particle deposition models, the paucity of literature regarding large scale validation, particularly for bioaerosol dispersion is clear. This study addresses this issue by providing a direct room-scale comparison between CFD simulations and experimental bioaerosol deposition under idealised and realistic single- and two-bed room scenarios. The results have demonstrated the following:

- Small diameter ( $<5\ \mu\text{m}$ ) bioaerosols are likely to be deposited across a space, regardless of the layout of the room with surface concentration not related to distance from the source. This suggests that such small pathogen carrying particles may play a role in the environmental contamination of hospital rooms and hence the risk of indirect contact transmission. Hospital studies have shown that bed side tables are both high contact nodes for health care workers [35] and are also proven to exhibit contact transmission probabilities of at least 1 in 5 [19].
- Deposition onto such surfaces may therefore be important in some situations and may have implications for nursing practices or frequency of cleaning procedures.
- A good comparison is possible between the spatial deposition patterns predicted through CFD simulation and experimentation. Comparison is improved by using an RSM turbulence model which correctly resolves the anisotropic nature of the flow compared to the  $k-\epsilon$  turbulence model that is applied in the majority of indoor air studies. It is recommended that when CFD is applied as a design tool, careful consideration should be given to which turbulence model is used particularly where particle deposition is considered.
- The spatial deposition of particles is influenced by the layout of the room and the location of the ventilation supply inlet. Locating a susceptible patient closer to the supply air and introducing a partition between beds are both likely to reduce the risk of environmental contamination due to bioaerosol release from a neighbouring patient. This finding concurs with tracer gas and simulation based studies evaluating airborne infection risk [41, 99]. An added effect of the partition is the separation

of cool and warm air, reducing horizontal mixing and therefore reducing the overall temperature of the room.

#### 4.4.1 Implications of Results

Across all scenarios it is noted that both experiments and simulations predict measurable deposition across the room space. While spatial variation depends on layout, the results suggest there is clear potential for small diameter ( $\sim 2.5 \mu\text{m}$ ) particles to play a role in transmission of infection through indirect contact routes. This is an important consideration; such particles are routinely regarded as airborne and hence controlled through ventilation rather than cleaning. Moreover, these small particles are usually only considered of concern where the pathogen is classed as possibly capable of direct airborne transmission, for example tuberculosis, measles or influenza. The deposition of culturable bioaerosols in this study adds support to the hypothesis that airborne dispersion may play a role in non-respiratory infections such as MRSA and *C. difficile* [59, 240], with surface contamination and subsequent contact by susceptible people resulting in transmission.

The study conducted here demonstrates the potential for CFD simulations to accurately predict the relative spatial distribution of bioaerosol deposition, but it has not been possible to confirm whether simulations can predict the actual level of contamination based on a particular amount released into the space. The reason for this lies in the limitations of the experimental methods. To relate the deposition to the bioaerosol concentration in the air requires taking air samples. While this is straightforward [202], it is well documented that sampler efficiencies are far from 100%, with some estimated to sample well below 50% of the viable concentration in the air [238]. The settle plate approach used to measure deposition is unlikely to experience microbial losses due to physical damage from impaction that is present in an air sampler, but may still underestimate total counts as it is based on colony formation after incubation. As the surface deposition and air samples must be measured using different techniques, neither of which has a well characterised sampling efficiency, it is not feasible to quantitatively relate the results from the two approaches. It is for this reason that biological air sampling was not conducted in this study.

The CFD solutions may benefit in future from the use of a low-Reynolds' turbulence model instead of the logarithmic law utilised with both turbulence models tested. Given the exclusion of the effect of turbophoresis, the DRW model provides extra impetus to deposition velocities. In some cases this may be unphysically large, which probably accounts for some of the over-deposition observed. However computational costs would still be unreasonable due to the level of grid resolution required.

The Reynolds' Stress model used in this study requires greater care during pre-processing and initially defining the geometry and mesh than the empirically based  $k-\epsilon$  RNG model. It was found that small fascia such as a patient's mouth proved a source of instability when utilising the second order spatial discretisation scheme and hence these should be replaced by appropriate energy and momentum sources. Implications for convergence and computational resources are also considerable however substantially lower than those required for a transient LES simulation. Ultimately a physically realistic solution can nevertheless be obtained.

# Chapter 5

## HCW behavioural and observational study

### Contents

---

<b>5.1</b>	<b>Background . . . . .</b>	<b>159</b>
<b>5.2</b>	<b>Observational Study: Ysbyty Aneurin Bevan (YAB) . . . . .</b>	<b>166</b>
<b>5.3</b>	<b>Methodology . . . . .</b>	<b>167</b>
<b>5.4</b>	<b>Results &amp; Discussion . . . . .</b>	<b>172</b>
<b>5.5</b>	<b>Summary . . . . .</b>	<b>190</b>
<b>5.6</b>	<b>Implementation of the Results . . . . .</b>	<b>190</b>

---

Conservative estimates by Harbarth et al. [40] show that potentially 20% of HCAI contracted through contact transmission may be preventable. Chapters 3 and 4 highlight the importance played by environmental surface contamination in this process. However, there is currently little robust understanding as to how HCW activities in the health care environment result in patient exposure to such pathogens. This chapter is an exposé on obtaining real data on hand-to-surface contact frequencies in a community hospital during different health care activities. This data is used in Chapter 6 to show how behaviour can be modelled realistically in different environments by probabilistic methods.

## 5.1 Background

*“Human behaviour has been established as playing a vital and largely unpredictable link in the infection transmission chain.”* Hayden et al. [19]

Health care settings are known to be reservoirs for pathogenic material [48]. Patients and staff are likely to supply most of this, but if allowed, environmental surfaces can harbour them for prolonged periods [20, 48, 49, 50]. Therefore the process of decontamination and sanitation has been the subject of much contention. ‘*Mopping up hospital infection*’ by Dancer [24] highlights the struggle to implement efficient cleaning procedures despite their accepted importance in infection control. Particular difficulties are apparent when terminal cleaning after a patient is discharged is incomplete as shown by over 50% of rooms in a study by Bhalla et al. [51]. Pittet et al. describe in their 2006 [20] infection dissemination review for the World Health Organisation the five vital conditions that are necessary for successful indirect pathogen transmission:

1. Microorganisms must be present on either the patient’s skin or surrounding inanimate intermediary surface (fomites)
2. Transfer of pathogens must occur during contact between the inoculated surface and the HCW’s hand
3. The transferred organisms must be able to remain viable during this process and for some time after
4. The hygiene procedure following the patient contact must be inadequate at removing all the pathogenic material
5. Lastly the HCW’s hands must re-transfer the microorganisms in a timely manner to another surface or patient

While environmental contamination is recognised as a potential source of infection, there is surprisingly little data to establish the relationship between surface contamination and risk of transmission. Hayden et al. [13, 19] undertook an observational study to quantify the effects of surface contacts by HCWs during patient care by testing surfaces touched during a procedure for vancomycin resistant enterococci. Careful recordings were made of

the order in which surfaces and patient skin were touched, meaning that a probabilistic route of pathogen transmission could be established. Their technique to evaluate cross-transmission risk relied on microbial swabbing of surfaces, which potentially could mask occasions in which transmission may have occurred but was not recorded. In other words if a surface was swabbed and a large proportion of microbial colonies removed then logically, the probability of the transmission occurring may be altered. Nevertheless, microbial transfer was established to occur in at least 10% of surface contacts. However this was not restricted to patient-to-environment contact, but also vice-versa, thus highlighting the potential for cross-infection. Importantly, patient and environmental surface contact counts are reported; Figure 5.1 shows that on average 8.5 contacts were made while the HCW was in the room, 5.1 of which were environmental (any surface but the patient). However the environmental contacts are not separated into individual surfaces, and as such this data cannot be used to identify relative risks for different surface contacts.

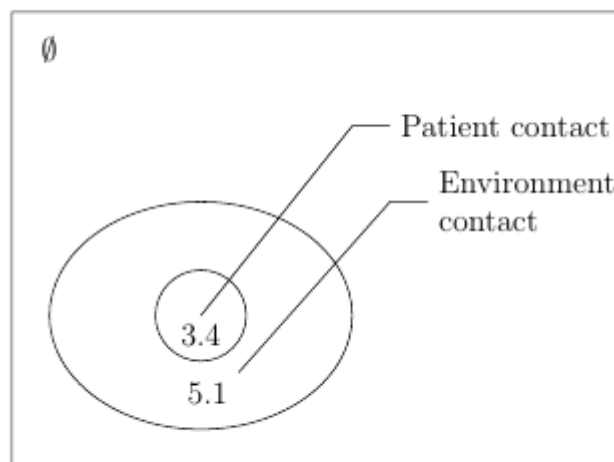


Figure 5.1: Venn diagram showing the distribution of average contact counts per episode of care as observed by Hayden et al. [19].

### 5.1.1 Hand Hygiene

The hand hygiene guidelines elaborated by the CDC [3] and the WHO [39] both place hand hygiene and compliance as the gold-standard in preventing infection transmission. Indeed, there is still some scepticism over the full adoption of alcohol based antiseptics. Epidemics

of gram positive spore forming bacteria such as *Clostridium difficile* have been linked to the usage of alcohol-based hand rubs. However since no hand hygiene agents have been proven reliably sporicidal [241] (eliminates spores), this may not be unfounded. Placing alcohol-rub as the most effective weapon in the control arsenal has proven controversial given the desire for a magic bullet solution. The WHO clearly states that 30 second hand washing procedures with soap, are and remain, the most basic intervention measure. Allegranzi and Pittet [241] highlight the factors influencing hand hygiene compliance amongst HCWs: Primarily job status, under-staffing and the misguided belief that generic latex gloves and gowns are impenetrable to pathogens appear to be the most influential factors. Religious beliefs in some cases provide barriers to full hand hygiene compliance [241]. Transmission of pathogens in non-surgical gloves is bi-directional meaning that microorganisms can traverse the barrier both onto the hand from the patient and out onto the glove surface from the HCW's skin [242].

#### 5.1.1.1 Guidelines

Hand hygiene or antiseptics guidelines are set out globally by the WHO [39] and reviewed periodically; the latest guidelines were published in 2008. Within the UK, further guidance to health-care professionals is given by the National Patient Safety Agency (NPSA), and is based on *Epic2*: National Evidence-Based Guidelines for Preventing Healthcare-Associated Infections in NHS Hospitals in England [28] (henceforth: *Epic2*), commissioned under the Department of Health. Every HCW is trained using the “5 Moments for hand hygiene” approach as shown in Figure 5.2, which corresponds to the Table 5.2.

The Fulkerson scale [27] outlined in Table 5.1 outlines a fifteen point scale of clinical objects/procedures ranking them in order of dirtiness [sic]. The “5 Moments for hand hygiene”, is broken down into three hygiene opportunities: Social, hygienic and surgical. The usage of gloves is a separate agenda, which also includes personal protection equipment.



Figure 5.2: *5 moments of hand hygiene* in the NHS, reproduced with kind permission from the WHO.

Rank	Contact with
1	Sterile or autoclaved materials
2	Thoroughly cleaned or washed materials
3	Materials not necessarily cleaned but free from patient contact
4	Objects contacted by patients either infrequently or not expected to be contaminated (e.g. Furniture)
5	Objects intimately associated with patients but not known to be contaminated (e.g. Patient gowns, linens, dishes, bedside rail)
6	Patients but minimal and limited (e.g. Shaking hands and taking pulses)
7	Objects in contact with patient secretions
8	Patient secretions or mouth, nose, genito-anal area
9	Material contaminated by patient urine
10	Patient urine
11	Material contaminated with faeces
12	Faeces
13	Materials contaminated with secretions or excretions from infected sites
14	Secretions or excretions from infected sites
15	Infected patient sites (e.g. Wounds or tracheotomy)

Table 5.1: Fulkerson scale ranking hand hygiene [27].

### 5.1.1.2 Types of hand hygiene opportunities

Epic2 categorises care types and procedures into categories of hand hygiene: Social, hygienic and surgical. Differing antiseptis guidelines are prescribed for each one of these, thus reducing the scope and margin of error for each hand hygiene opportunity.

**Social hand washing** is carried out before and after the following which corresponds to (3-7 on the Fulkerson scale): Liquid soap (antimicrobial or otherwise) under

When	Procedure type
<b>Before</b>	<ul style="list-style-type: none"> <li>the beginning of the shift</li> <li>preparing, handling and eating food</li> <li>donning gloves</li> <li>any patient contact</li> <li>clean/aseptic procedures</li> <li>entering/leaving clinical areas</li> <li>entering/leaving isolation cubicles</li> <li>preparing/giving medications</li> <li>using a computer keyboard in a clinical area</li> </ul>
<b>After</b>	<ul style="list-style-type: none"> <li>the end of a shift</li> <li><i>any</i> patient contact</li> <li>bed making</li> <li>contact with patient surroundings</li> <li>visiting the toilet</li> <li>the removal of gloves</li> <li>hands become visibly soiled</li> <li>handling laundry/waste</li> <li>using a computer keyboard in a clinical area</li> <li>the administration of medications</li> <li>blood and/or body fluid exposure risk</li> </ul>

Table 5.2: Hand-washing opportunities from Epic2: 5 moments [28]

warm water for 30 seconds. Bar soap *must* be avoided. Drying should be with a disposable paper towel and using a blow-drying in non-clinical areas due to aerosol productions [28]. Alternatively an Alcohol gel may be used during social hand hygiene but not under these circumstances:

1. Prior to handling gas cylinders
2. When a patient is known to be infected with *C. diff* or *norovirus*

**Hygienic hand wash** should be carried out before any aseptic procedures (6 on Fulkerson scale). An approved antiseptic detergent should be used such as: 4% Chlorhexidine gluconate or 7.5% Povidone iodine.

**Surgical hand wash** must be performed before all invasive procedures such as 7-15 on Fulkerson scale.

### 5.1.1.3 Personal protection equipment (PPE) usage

According to Epic2 gloves must be worn once only. They are donned immediately before an episode of patient contact or treatment and removed immediately following the completed procedure. No mention of contact with surfaces is made however. Gloves are changed between caring for different patients, or between different care/treatment activities for the same patient [28]. Non-sterile gloves are used in preference to sterile gloves while carrying out all but surgical procedures where bodily secretions are involved (e.g. *Personal care*).

## 5.1.2 Hand Hygiene Compliance

Measurement of hand hygiene compliance of any sort is notoriously difficult in part because of the so-called Hawthorne effect [243], where staff being observed either consciously or subconsciously alter their behaviour. Research has shown that this influence incurs a generally improved performance, i.e. suggesting a best case scenario, but is not necessarily fully realistic [25]. The methodology of quantifying compliance therefore has often been modified from direct observation to covert observation. The latter has generally been conducted by health care personnel [25] with more reliable results. Indirect methods include the measurement of hand-sanitiser depletion over a fixed period of time [244].

Adherence to hand hygiene, as prescribed by the Fulkerson scale, appears clearly regional and deep-rooted [27]. Despite the WHO's prescription of hand-hygiene procedure, standards vary internationally, particularly with regards to the method of pathogen removal. Cultural, ethical and religious beliefs [241] have all been found to influence the HCW's

posture towards cleanliness despite strict guidelines. Even good hand hygiene compliance is rendered obsolete if staff touch contaminated surfaces after hand-antiseptics.

Compliance appears to be highly varied and studies have shown that over a year period compliance can be as low as 25% [245] in some American hospitals, somewhat higher in the UK [25] at 25-40% and Germany ranking in the upper 5 percentiles [27]. Overt observation of HCWs appears to subject any study to bias as compliance appears to be affected positively. Smith et al. [25] showed that covert observation returned more realistic compliance values in a Scottish hospital ranging from 7% to 25%, which consistently fell below requirements. As a corollary, hand-hygiene informative campaigns are shown to have a temporary positive effect, what the long-term affect is is still unclear.

Pittet et al. [22] noticed a clear trend indicating that HCWs who wore gloves were less likely to disinfect their hands post-care. This lead the researchers to think that the HCW erroneously believe the gloves to be sterile and impermeable to pathogens.

## 5.2 Observational Study: Ysbyty Aneurin Bevan (YAB)

The use of observational research methodology in the field of hospital care is important to constructing a resilient evidence base and understanding disparities between care. Studies of human behaviour in the health care environment have largely acknowledged the lack of a comprehensive study which collects the minutiae of hand-to-surface contacts.

### 5.2.1 Objectives

An observational study was conducted during two separate visits in the first quarter of 2012 to Ysbyty Aneurin Bevan, a National Health Service (NHS) community hospital. This is a 107 single-bed facility in Ebbw Vale, Gwent, South Wales, UK. This is not an acute hospital, catering mainly for bed-ridden patients, amputees and other postoperative patients. Outbreaks of MRSA infections are minor and rare here due to the size of the wards, however since this is entirely single bedded accommodation, it often served as a quarantine location for neighbouring larger hospitals. During the study one patient was under quarantine for MRSA, which imposed strict hygiene regimes within that room, however the patient often wandered freely down the corridor. Ethical approval (Ref: 11/WA/0200, in Appendix A) was granted by the South East Wales Research Ethics Committee as well as the Aneurin Bevan Local Health Board Scrutiny Committee (Ref:RD964/11). The aims and objectives of this study are to:

1. Establish the different health care activities that are carried out in a typical hospital single room accommodation ward, including:
  - (a) The distribution of surface contacts corresponding to the categories in Table 5.4 and creating a probability density plot of touching each one.
  - (b) The probability frequency density of surface contact counts.
  - (c) The duration in time of typical care types and investigating a relationship between length of time and surface contact count.
2. Observe hand hygiene frequency during patient care, through:
  - (a) Hand washing, usage of gloves and usage of alcohol gel.

- (b) Investigating the three types of hand hygiene suggested by *Epic2* [28] and identifying their differences.
- (c) Identifying whether patient contact influences hand hygiene.
- (d) Identifying whether patient contact influences choice of hand antisepsis.

It is important to bear in mind that this study was developed to identify how care type influenced hand hygiene choice not to pass judgement on compliance.

## 5.3 Methodology

Before describing the main study methodology this section first defines the activities that were observed during the studies.

### 5.3.1 Definition of Activities

Since 2012, health care workers at YAB began implementing a structured process known as “intentional rounding” where they carry out regular checks with individual patients at set intervals, typically hourly. Each hourly check corresponds to a set itinerary or checklist. Care has been previously less regimented and responsive rather than proactive. Rounding helps front-line teams to organise ward workloads to ensure all patients receive attention on a regular basis. This is intended to further personalise care to the patient but could potentially lead to more surface contact risk [246].

Health care workers within this study carried out episodes of care within the framework of intentional rounding categorised into six areas described in Table 5.3. Care types were divided in this manner following standardised procedures as set out in both Pittet et al.[22] and Dancer et al. [50]:

Care Type					
Direct care	House-keeping	Mealtimes	Medication rounds	Miscellaneous	Personal care
Blood pressure measurement	Equipment cleaning	Dispensing meals	Distributing medication	Call requests	Toileting
Weighing patients	Cleaning high touch surfaces		Injections	Bed making	Changing
SATs <sup>1</sup>					

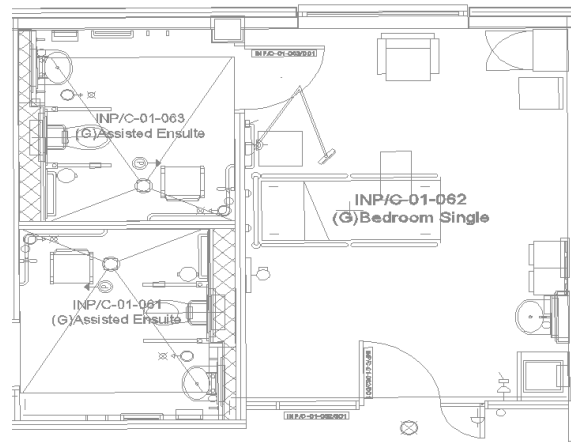
Table 5.3: Care type and examples of each.

### 5.3.2 Definition of Surface Categories

As the HCW performs a care activity, constant observation of their hand-to-surface contact activity is monitored and recorded based on Table 5.3. Surfaces are categorised in five main areas and summarised in Table 5.4. These are in-keeping with standard HBN04-01 room inventory and current available literature [50]. Figure 5.3 shows the positioning of surfaces within the single room at Ysbyty Aneurin Bevan:

Surface Category					
Equipment	Patient	Near-patient	Far-patient	Hygiene products	
IV stand	Clothing	Bedrail	Window	Alcohol gel	
Hoist	Skin	Bedding	Curtain	Soap dispenser	
BP cuff/stand		Tray	Light switch	Taps	
Notes trolley		TV	Chart/workstation	Sink	
Medication trolley		Chair	Door/handles	Paper towel dispenser	

Table 5.4: Room surface categorisation



(a). Room layout



(b). Single room surfaces 1 of 2



(c). Single room surfaces 2 of 2

Figure 5.3: Room surface layout of YAB single room.

### 5.3.3 Observational Strategy

Observations were made within a 32 room single-bed ward, primarily for elderly bed-ridden patients. The ward was split into two interconnecting ‘pods’ of 16 rooms each. These were staffed at all times by 7 or 8 nurses divided between the two, where at least two members were registered nurses (RN). These are rotated in shifts of 8 hours. The complement of staff is then completed by 5 or 6 estate nurses (EN) and physiotherapists depending on the shift. One doctor made daily rounds, while a second consultant made bi-weekly rounds. Nurse practitioners were on call during weekends and after 5pm during the week. Meals were dispensed from a trolley in the corridor and only nurses were permitted to enter

patient rooms to deliver them. Any housekeeping observed was performed by nurses as these must clean high touch surfaces as of 2012 [35].

An initial scoping study was carried out to pre-assess typical patient rooms in conjunction with the nursing staff and identify the list of surfaces of interest and their location in the room Table 5.3.

Over the course of the study a total of 431 care episodes were observed. All patients and staff who were observed were required by the research ethics committee to give written consent for the observation. Details of the ethics approval are given in Appendix A. Data was accrued in the following manner during the period of 8am to 6pm daily for a total of 7 days. Observation actually occurred during two visits due to observer illness. The visits were interspaced by 3 weeks and the staff remained the same.

During a typical ‘non-invasive’ nursing procedure the surfaces touched by the health care worker and the order in which this occurred was recorded. The observation took place from outside of the patient room so as to avoid disrupting the care procedure or influencing the HCW. Glass windows allowed a full view into the room and therefore all surfaces were visible. Each observation period began when a HCW entered a patient room and concluded once they performed a form of hand hygiene, left the room terminally or indicated that they had finished. In the case where hand hygiene was performed during an episode of care prematurely because the HCW had not anticipated need for further care, then any subsequent surface contacts were recorded as a separate observation. Interruptions in the procedure by leaving the room were recorded as an integral part. In other studies such as Hayden et al. [19] interruptions in care were also observed but hand hygiene status at that point was not. The vast majority of observed care activities involved only one HCW, however if more were present their surface contacts were considered as a separate episode.

The majority of invasive or personal procedures such as bathing and toileting could not be observed due to patient privacy and dignity. Therefore during these episodes of care the investigator was informed and room door closed and observations were not recorded.

### 5.3.4 Statistical Analysis

Each objective described above aims to investigate statistical differences (if any) between HCW behaviour over observable care types. Sample sizes are important to bear in mind when choosing a statistical test of any kind, as the influence of outliers may induce unrealistic bias. Objective 1a deals with discrete data and aims to create probability density distributions which consider the relationship between surface contacts and care type. The surface contact order is not taken into consideration at this point and so pooled data is unnecessary.

Objective 1b is to compare surface category contact frequencies between care types. The Lilliefors test [247] (based on Kolmogorov-Smirnov tables) is a robust test for normality appropriate for small sample sizes, where the population mean ( $\mu$ ) and variance ( $\sigma$ ) are unknown. Therefore it tests against the null hypothesis that the data stems from a normal distribution but not which normal distribution and here is applied to all samples. In addition since contacts are grouped into 5 surface categories, this renders standard parametric statistical tests inappropriate, particularly with groups of unequal sample sizes. The Kruskal-Wallis test is the non-parametric equivalent of the one-way ANOVA and is used to infer statistical differences between care type by way of investigating individual surface contact averages. This test performs a post-hoc Mann-Whitney paired test between care types, assuming inter-group independent observation, but not normality [247]. This compares the medians of the samples and tests against the null hypothesis that all samples are drawn from the same population (or equivalently, from different populations with the same distribution) [247].

Objective 1c investigates the correlation between time and surface contacts by the use of linear regression. This will measure the covariance between both variables by investigating their correlation coefficient to linear fit. Pearson's correlation is the standard choice of metric and is a measure of the linear relationship between two continuous random variables. It does not assume normality although it does assume finite variances and finite covariance, a reasonable assumption given current sample sizes. However it is sensitive to outliers and other artifacts, which makes Spearman's Rho represent a better choice [46]. This ranks data pairs instead of using the raw values and so provides a measure of a monotonic relationship between two continuous random variables. It is particularly useful

with ordinal data and unlike Pearson's correlation is robust to outliers. The distribution of either correlation coefficient will depend on the underlying distribution, although both are asymptotically normal because of the central limit theorem. Tied ranks are accounted for by assigning averaged ranks in their place. Spearman's Rho ranges from -1 where negative correlation is observed to +1 where strong positive correlation is apparent. P-values for testing the hypothesis of no correlation against the alternative that there is a nonzero correlation. The p-value is the probability that one would find the value or more extreme if the correlation was in fact 0. Low p-values (less than 10%) associated herewith infer that correlation is unlikely to be by chance alone. As a corollary type I and II errors are avoided where a falsely positive correlation is shown by excluding the biased effect of outliers. P-values for Spearman's rho are calculated in Matlab using exact permutation distributions. Correlation between variables can have high and low p-values. For example a high correlation coefficient ( $r$ ) but equally a high p-value could indicate high variance or noise. A low correlation coefficient but equally low p-value means that the correlation is statistically significantly poor.

Objective 2 aims to investigate the hand hygiene levels within the observed care types. Throughout this part of the investigation, the results of the observational study are binary (yes/no) and therefore can be considered as independent Bernoulli trials. Sub-objectives 2a and 2b aim to investigate the usage of the different hand antisepsis methods by subcategorising them by care type.

Under objective 2c the conditional probability of whether patient contact affects hygiene compliance or indeed hygiene type is scrutinised by a hypothesis test that compares the chance of hand washing being an independent Bernoulli trial with 50% probability of success. Sub-objective 2d tests the difference between hand hygiene methods and compares the HCW's choices against the probability that they select a method by chance.

## 5.4 Results & Discussion

Here the results and discussion are presented in three sections corresponding to the three main top-level objectives outlined above. Each objective outlined at the beginning of this chapter was investigated by the use of statistical tests to deduce possible relationships between variables. Objective 1 requires sufficient observations of all the health-care activities

to be able to differentiate emerging patterns between them. Objective 2 requires meticulous observation of human behaviour particularly with regards surface contacts. Dozens of surface contacts are possible during each episode of care and multiple HCWs must be tracked.

Since results were accrued over two separate observation periods, pooling of data was only possible after comparison of sequence length using the two-sided Kolmogorov-Smirnov test. This rejected the alternative hypothesis of results stemming from different distributions ( $p=0.001$ ) and hence data from both periods could be considered jointly.

#### 5.4.1 Surface Contact Distributions

Throughout the observational period the mornings tended to be the busiest periods, when patients were bathed, fed, medicated and the ward round took place. General house-keeping commenced at 8am after which patient doors remained open throughout the day. Housekeeping conducted by nurses was performed during the afternoon before dinner.

##### 5.4.1.1 Activity profile

Table 5.5 shows the breakdown of all observations by care type. The table shows the quantity of each type of care presented. Observation of care types was not systematic of one single HCW as to avoid bias instead seeking a balance of care types. The reader must bear in mind that the proportion of different care types observed does not necessarily reflect the full breakdown of a whole day, since observation began at 8:30am and ended at 6pm. This did also include weekends. However as many care episodes were observed as possible.

Care Type						
Direct care	House-keeping	Meal-times	Medication rounds	Miscellaneous	Personal-care	TOT.
197	17	21	111	72	13	<b>431</b>

Table 5.5: Observed activities or care types at YAB.

Table 5.5 shows the breakdown of observed care types over the 7 day period. Direct care predominates with just under half of the total observations as this forms the backbone of intentional rounding. Cases of miscellaneous care and mealtimes are also abundant. Personal care might be considered an extension of *direct care* under some circumstances. For example a patient may be taken to the toilet during *direct care*. Total surface contact count were used to compare both care types through the use of the non-parametric Wilcoxon rank test. Comparison was made based on the null hypothesis of both samples stemming from distributions with equal variances, or more strictly that two independent samples emanate from the same distribution. The decision not to merge these two sets of observations came through rejecting the null-hypothesis of equal medians at the 5% level ( $p=0.01$ ).

#### 5.4.1.2 High contact surfaces

Cleaning of the entire patient room occurs daily by housekeeping staff, however “high touch” surfaces are to be cleaned during the afternoon shift by nursing staff. However the definition of a “high touch” surface seems somewhat vague. Huslage et al. [35] define a high contact surface as any exhibiting 1 or more contacts per procedure. The ordering of average contacts at YAB by surface type in descending order of contacts shown in Figure 5.4. According to their cleaning criteria all surfaces fall into this category. By their definition *housekeeping* should be performed on only high risk surfaces, implying that all be cleaned multiple times per day. However YAB defines this cleaning as near-bed surfaces including equipment.

Contacts can also be categorised into those on the patient or their clothing and contacts with everything else: Environmental contacts. Figure 5.5 shows the break-down of contacts divided between patient and environmental surfaces. In the case of Hayden et al. [19], the patient was never touched without also incurring environmental contacts. During the study period at YAB, this was not quite so dichotomous and a number of combinations were observed. The probability of patient contact alone is approximately 2% (see Figure 5.6). Epic2 suggests hygiene after patient contact whereas the Fulkerson scale further differentials between clean and dirty [sic] patient contacts.

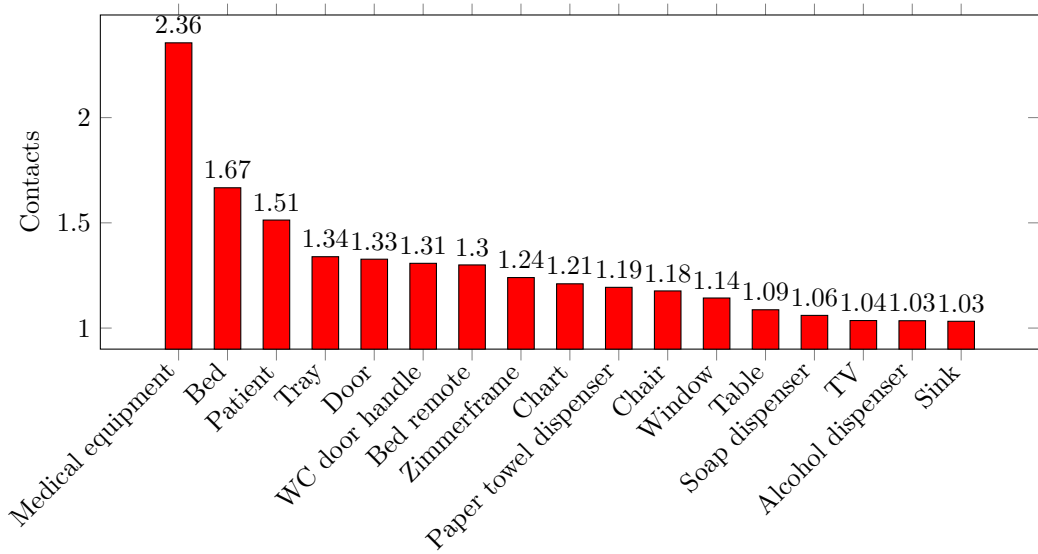


Figure 5.4: Ordered surface contacts for any care type.

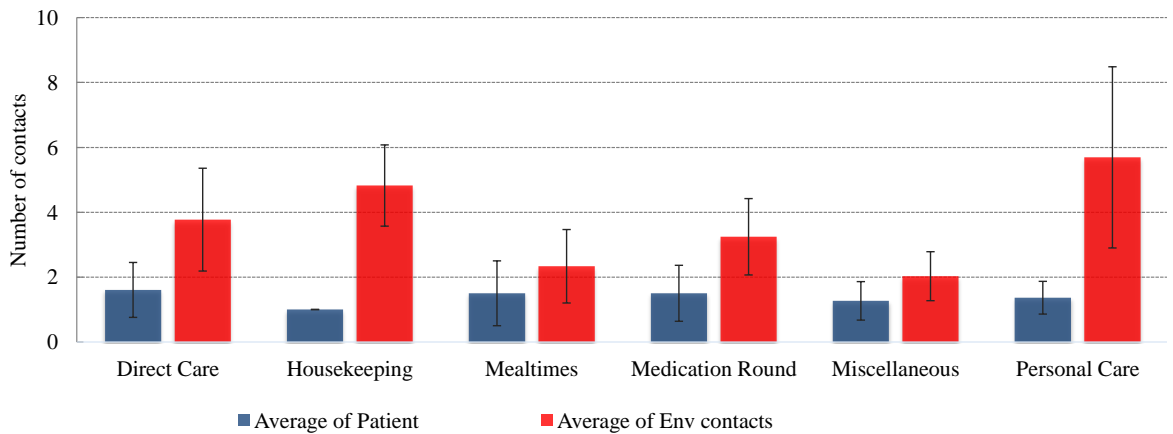


Figure 5.5: Average surface contacts for both patient and other environmental surfaces, categorised for care type. Errorbars represent one standard deviation either side of the mean.

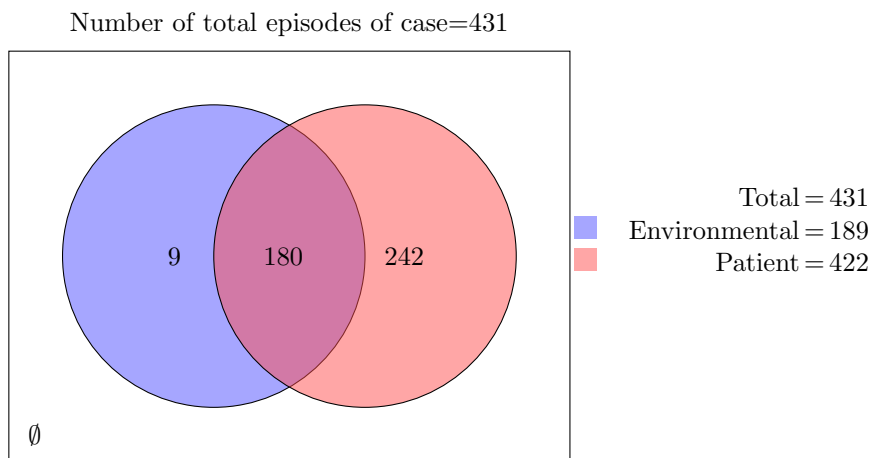


Figure 5.6: Episodes of care containing patient and/or environmental contacts.

#### 5.4.1.3 Surface contact distribution by surface category

Care episodes are subdivided as outlined above in Table 5.3. Principally, the aim of the study is to quantify hand-to-surface contact events. Breaking down care type enables in-depth analysis. Figure 5.7 shows the percentage of surface contacts on five surface categories for each of the six care types observed. Care types can be differentiated by considering the distribution of surface contacts. *a)* As promoted by intentional rounding, HCWs performing *direct care* exhibit a higher tendency to check equipment and patient notes (within Far-bed surfaces). *b)* This is particularly in contrast to *housekeeping* where nurses perform the duties of wiping near-patient surfaces and equipment twice daily and consequently Far-bed surfaces are touched less. *c)* Nurses at *mealtimes* exhibit the opposite behaviour tending to touch surfaces near the patient most often, though surprisingly not the patient themselves. This can be attributed to the fact that not all patients required assistance with feeding, but all needed space making on the bed tray for the food plates. *d)* *Medication rounds* exhibit a peak for near-bed surfaces, with lower tendencies for HCW to come in contact with the equipment. Far-bed surfaces account for a high percentage particularly due to nurses always touching patient notes. *e)* *Miscellaneous care* is much less regimented given that the HCW is responding to a patient pressing the call-bell. This may range from needing a drink to being in pain. Consequently, variedness of surface contacts is observed, highlighting particularly the lack of contact with equipment. *f)*

Near-bed surface contacts dominate within *Personal care* mainly due to the necessity to help a patient in and out of bed.

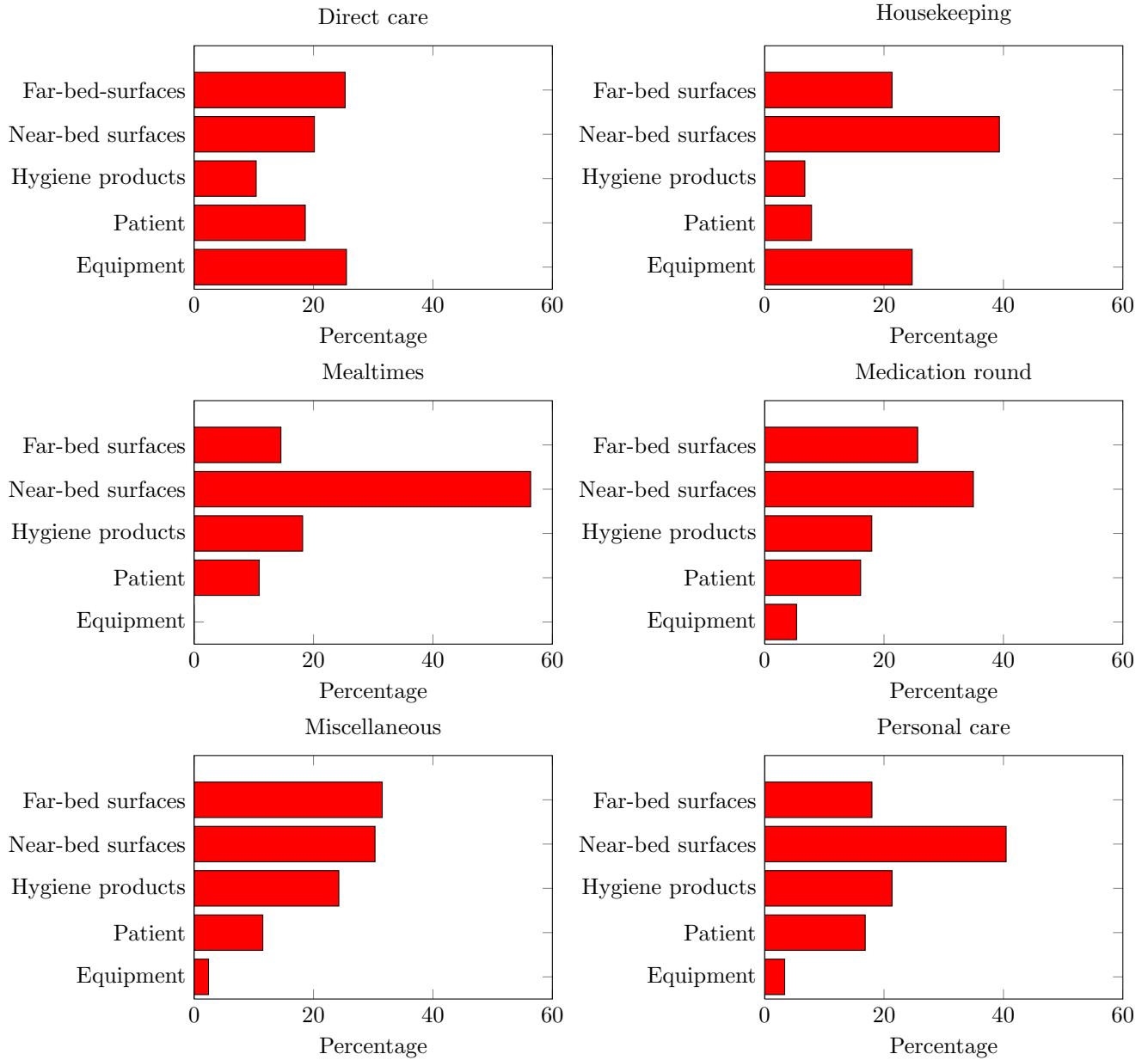


Figure 5.7: Surface contact distribution subdivided by care type.

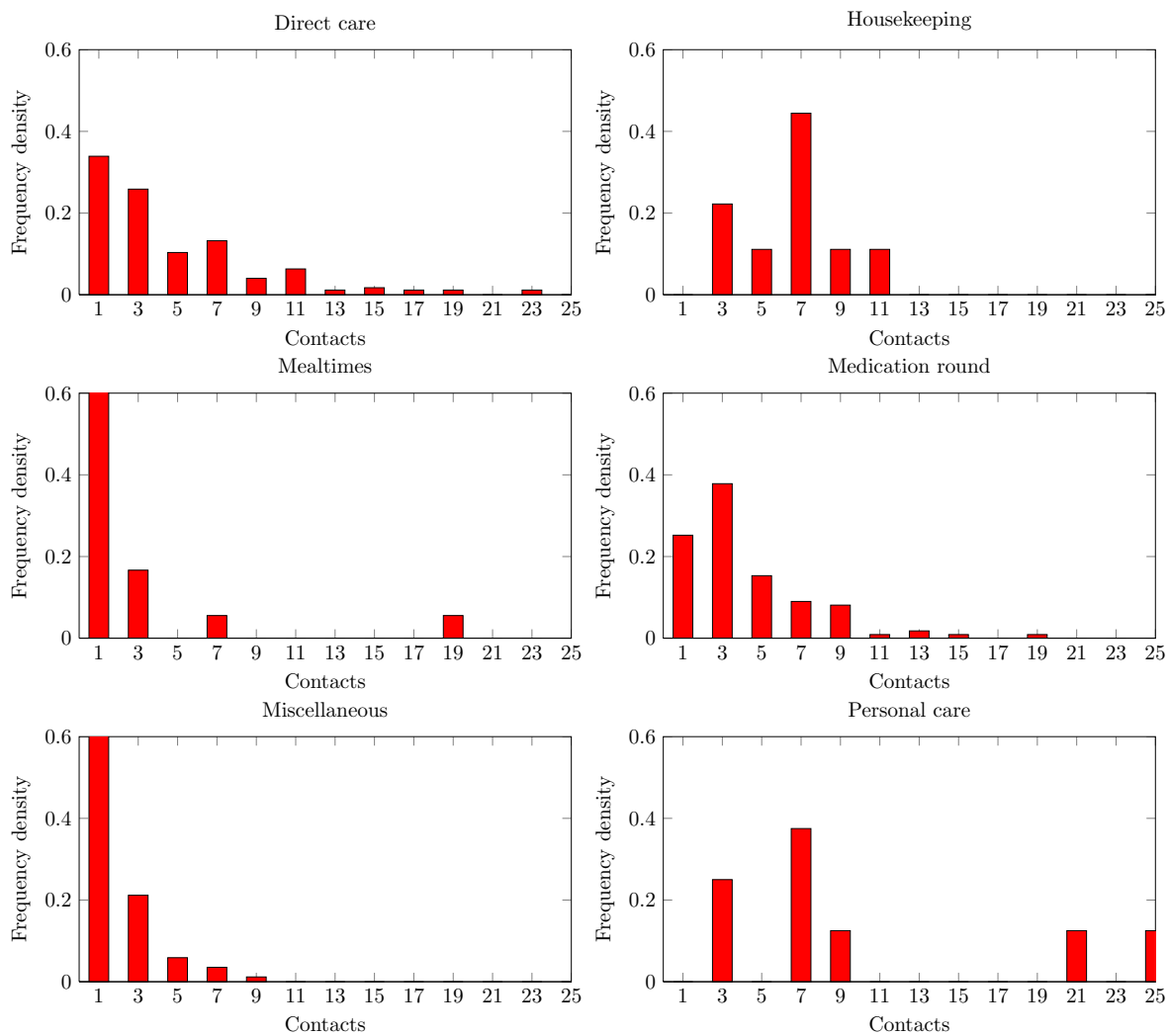


Figure 5.8: Probability density histograms of surface contact counts broken down by care type.

#### 5.4.1.4 Contact frequency distribution

Care types can also be differentiated by the total number of contacts as shown in Table 5.6. Fluctuations are present in all care types representing the variation of human behaviour and of patient needs. Figure 5.8 displays heavy right skew in all care types except *personal care*, where procedures tended to incur higher numbers of total contacts. However this does alter within *housekeeping* where a tendency towards normality (as suggested by the central limit theorem) should be investigated with increased observations. Lilliefors's test for normality showed that none of the observed total surface contacts in any of the care types exhibited a normal distribution ( $p < 1 \times 10^{-9}$ ) and hence the non-parametric Kruskal-Wallis test was chosen to compare medians. This makes a comparison between groups against the null-hypothesis that they all stem from identically shaped and scaled distributions. Surface contact probabilities vary statistically between types of care shown by a p-value of  $\leq 0.001$  thus rejecting the null hypothesis at the 1% level. More importantly it rejects the idea that care is homogenous.

	Care Type					
	Directcare	House-keeping	Mealtimes	Medication rounds	Miscellaneous	Personal-care
$\bar{x}$	4.6	5.2	2.6	3.9	2.3	6.9
$s$	3.8	2.6	3.0	2.8	1.8	6.0

Table 5.6: Breakdown of the number of surface contacts sample mean  $\bar{x}$  and deviation  $s$  for care types observed at YAB.

Splitting contacts into patient contacts and contacts with all other surfaces (environmental contacts) in Figure 5.7 reveals clearly that all care types tended to exhibit higher environmental contact counts than patient contacts. In particular Hayden et al. [19] (shown in Figure 5.1) also found this. A statistically higher environmental surface contact frequency than that of patient contact is visible with 1.5 vs. 3.7 contacts respectively. The patient contact counts on average are not statistically different between care types based on the null hypothesis that they come from the same distribution. Using a Kruskal-Wallis test shows a p-value of 0.38 upholding this, whereas the Wilcoxon signed-rank test rejects the null hypothesis at the 5% level for inter-care environmental contact count averages ( $p=0.001$ ). In this case the null-hypothesis tested is that of 0 median differences between ranks. Hence this may be an important factor which could potentially differentiate risk levels.

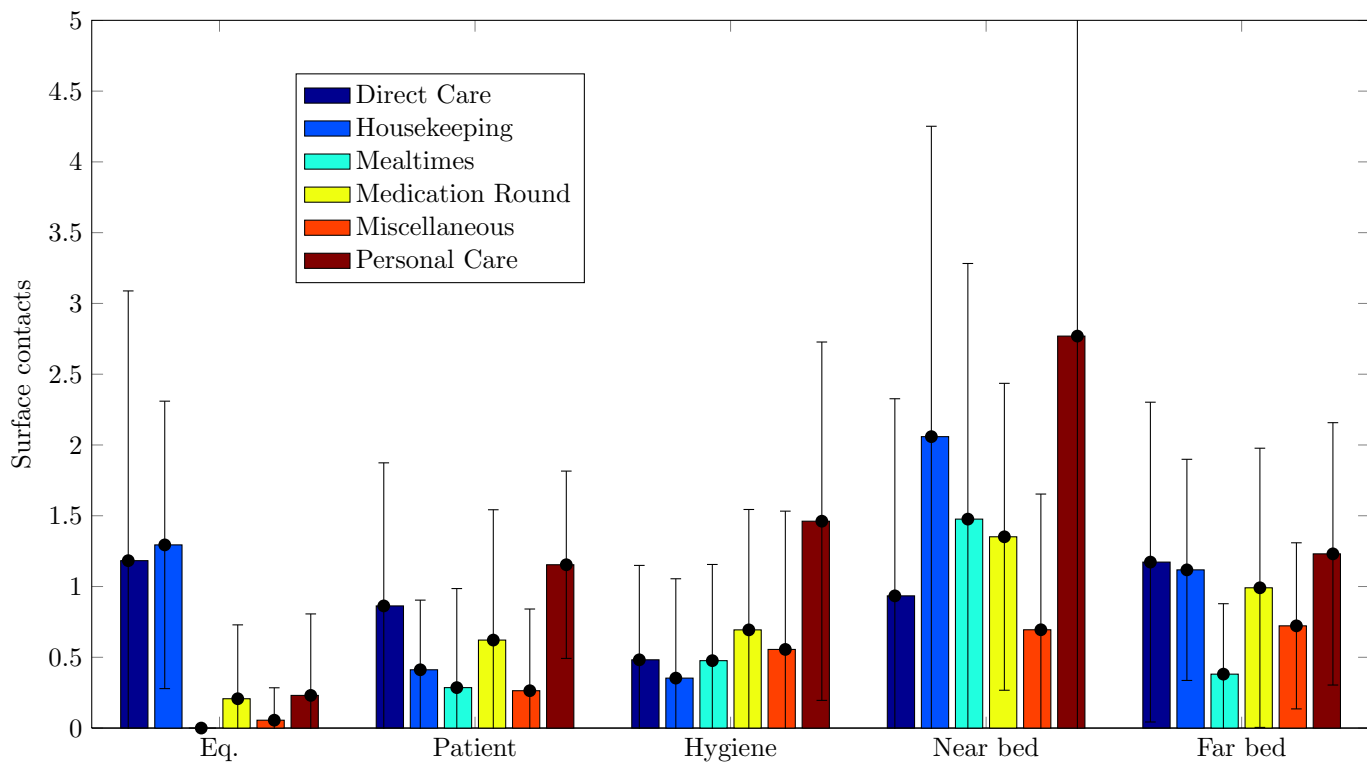


Figure 5.9: Surface contact frequency categorised by care-type. Where Eq. stands for equipment.

Figure 5.9 further divides the environmental surfaces into the categories in Table 5.4. The Kruskal-Wallis test ( $p=0.01$ ) casts further doubt on the hypothesis that the care

types exhibit no statistical differences in surface contact counts. Therefore although there appears no strong difference between patient contact counts, the variation is particularly evident within environmental surfaces amongst all care types.

#### 5.4.1.5 Duration of care

Figure 5.10 displays the average duration of patient care along with error bars representing one standard deviation. On average care length was just under 2 minutes 30seconds with a standard deviation of 2 minutes 40seconds. Personal care exhibited the lengthiest procedures (up to 9 minutes) which reflects the high variety of patient needs. On the other hand miscellaneous care was considerably shorter on average at less than 1 minute.

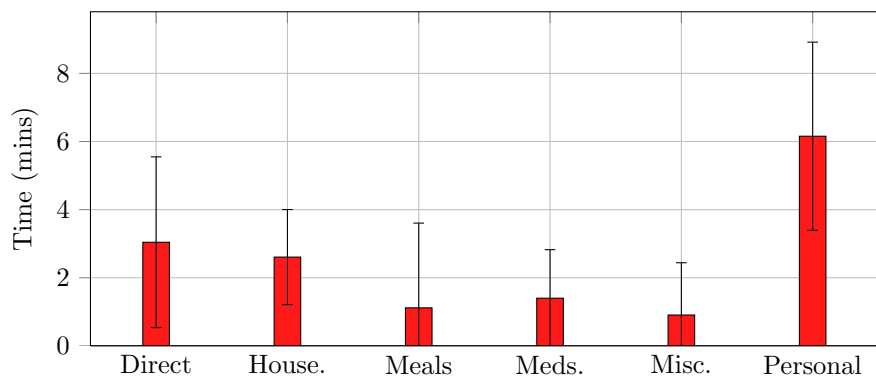


Figure 5.10: Contact duration categorised by care-type. Errorbars represent one standard deviation either side of the mean.

Figure 5.11 shows scatter graphs of total care length plotted against total surface contacts. Surface contacts have not appeared explicitly in published literature, preferring to show care duration instead [22]. Therefore it is important to be able to make viable comparisons to the current study. Spearman Rho rank correlation is used to test for linear correlation and the corresponding correlation coefficients are given in Table 5.7. A low p-value ( $\sim 0.01$ ) casts doubt on the null hypothesis that no correlation exists between variable, however a relatively high ( $p \sim 0.1$ ) p-value may be seen as indicating noisy data if the correlation coefficient is also high. Comparison between data sets shows that correlation, for cases with low p-values, such as *direct care*, *housekeeping* and *miscellaneous* care is often only mildly positive ( $0.33 < r < 0.566$ ). This indicates that high variation was observed. Both *mealtimes* and *medication rounds* reported the highest positive correlation, probably relating to the particularly rigid structure of the procedure. *Medication rounds* preceded

or overlapped *mealtimes* and both care types were conducted by staff who often were subsequently also required to bring food to patients. Thus the confounding factor relating to the variation of the duration of care perhaps lies with the variety of patient motility and speed of movement e.g. during toileting in *personal care*. Other explanations may well be related to time spent chatting to patients. Interestingly *miscellaneous care* showed the poorest correlation of all, perhaps due to the variation of the nature of unplanned procedures within it.

	Care Type					
	Direct care	House-keeping	Meal-times	Medication rounds	Miscellaneous	Personal-care
<i>r</i>	0.525	0.580	0.914	0.678	0.333	0.103
<b>p-value</b>	<0.001 <sup>†</sup>	0.015 <sup>†</sup>	<0.001 <sup>†</sup>	<0.001 <sup>†</sup>	0.004 <sup>†</sup>	0.738

Table 5.7: Correlation coefficients and p-values for time versus surface contacts. Where <sup>†</sup> represents a statistically significant value.

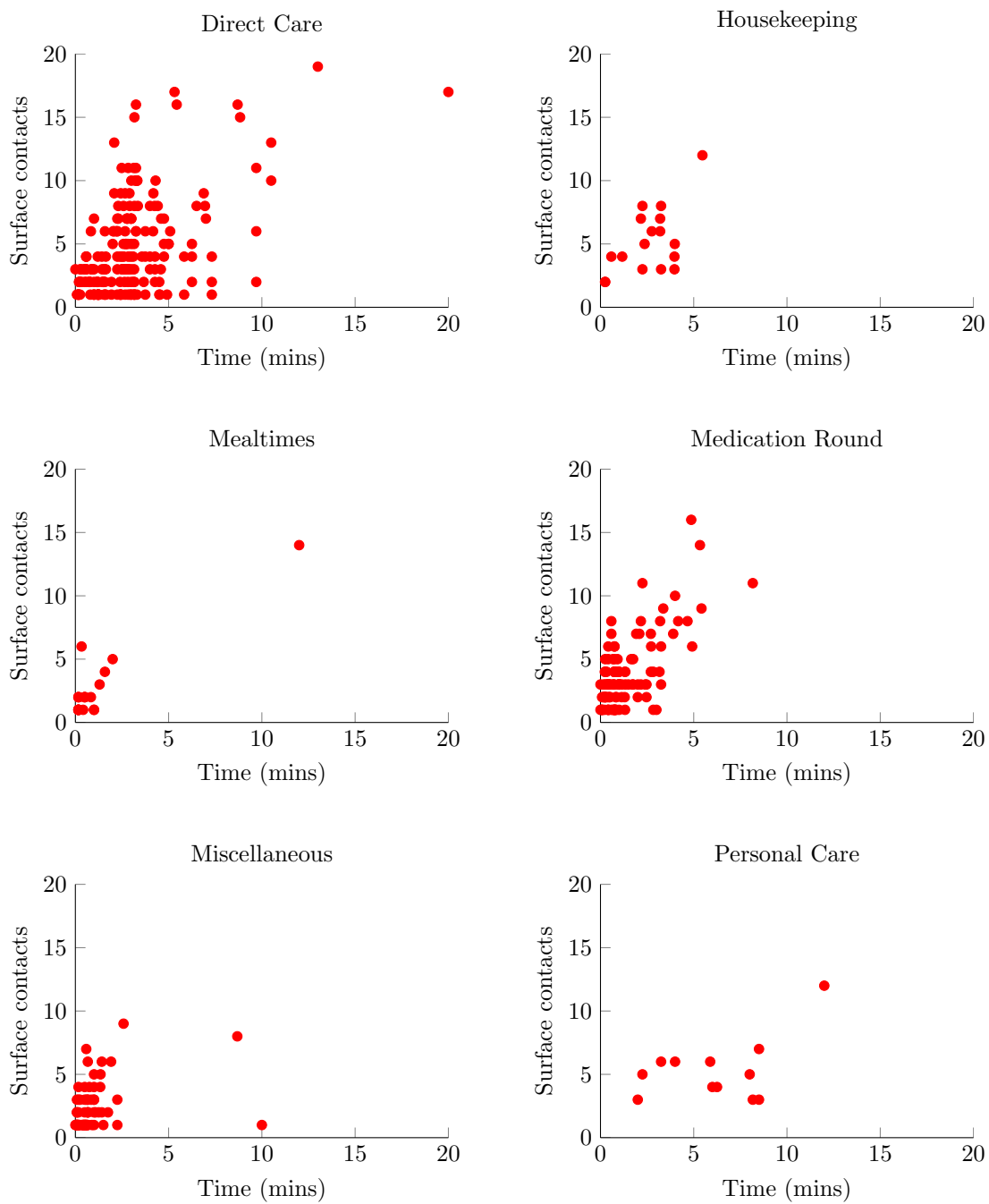


Figure 5.11: Total surface contacts for each type of care plotted over time.

## 5.4.2 Quantitative Analysis of Hand Hygiene

It is important to remind the reader that the objective of this study was purely informative and in no way judgemental insofar that it aims to take a snapshot of the working environment of a typical HCW. Compliance (or non-compliance) with the preset guidelines in *Epic2* is not relevant here and results on frequencies of hand hygiene are to be interpreted as either realistic or potentially slight over-predictions of reality due to the Hawthorne effect [245]. Therefore results will be presented purely as observed with an emphasis to investigate the cause and effect of surface contacts. This then will create a data set which can be used to predict human behaviour in Chapter 6.

### 5.4.2.1 Probability of hand hygiene

*Epic2* suggests that the HCW has a choice of hand antisepsis method from alcohol rub or soap and water when conducting social hand washing. It does not suggest that gloves are to be worn when conducting social or clean care (Fulkerson scale 1-7). Figure 5.12 shows hand hygiene subdivided into hand washing, donning gloves and alcohol rub usage and categorised by care type. The Kruskal-Wallis non-parametric test rejects the null-hypothesis of samples stemming from the same distribution at the 5% level and hence confirms that statistically significant different hand washing probabilities can be seen between care types. The results are reported by investigating the differences between care type and then subsequently by discriminating between hand antisepsis method. Personal care accounts for the highest probability of hand hygiene with over 85% compliance, followed by the *medication round* with over 60%. The possible reason for this is their regimented pattern and staff training [25].

Differences are statistically significant between hand antisepsis choice ( $p < 0.001$ ), where some variation can be seen in Figure 5.12 within each care type. Alcohol rub was used abundantly throughout all but *personal care* in adherence to *Epic2* guidelines. Glove usage accounted for only 2% of observed episodes of care, half of which were during *housekeeping*. It was noticed that on many occasions gloves were not changed between episodes of *housekeeping*. Multiple antisepsis procedures are a requirement within *Epic2* both before donning gloves and after their removal. This however was observed only 50% of the time. Handwashing and the use of alcohol rub was observed during 21% of procedures,

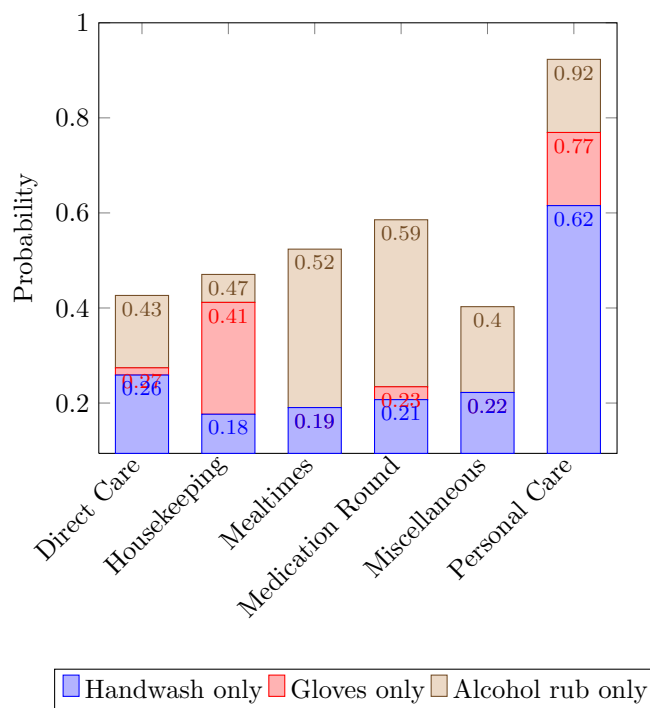


Figure 5.12: Cumulative probability of hand hygiene category subdivided by care type.

most of which were during *direct care*. Interestingly *direct care* exhibited joint lowest probability of hand hygiene along with *miscellaneous* care at 40%. This is statistically significant because these two care types account for 62% of the total observations made.

Figure 5.13 shows the probability of hand hygiene of any type categorised by care type and subdivided into surface contact count. The reader should note that patient contact is included as a separate surface, which will be discussed in the following section. The tendency to perform hand antisepsis of any kind is assumed to increase proportionally as the surface count increases. Pearson's correlation coefficient was calculated for each care type based on the surface contact counts and displayed in Table 5.8. They show strong positive correlation coefficients in all cases but that of *miscellaneous care*, which is only weakly positive. Corresponding p-values are also given to strengthen the statistical inference of the correlation coefficient. As a rough guide, p-values below 0.1 represent a statistically significant or robust correlation. The correlation coefficient may appear to be strongly positive (close to +1) or strongly negative (close to -1) but incurring a high p-value indicates significant noise within the data set. Caution should be exercised when

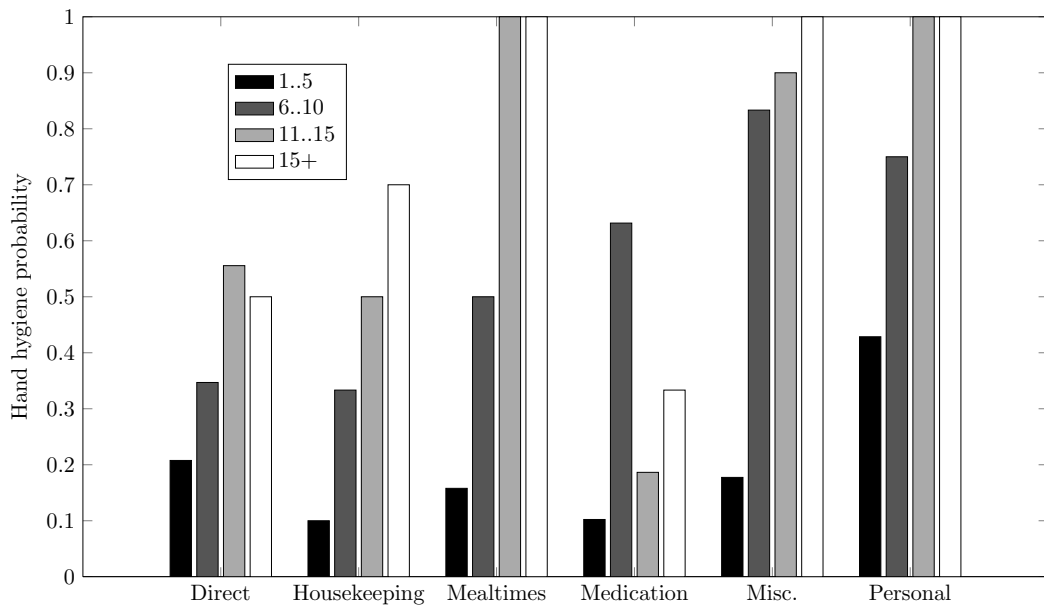


Figure 5.13: Probability of hand hygiene by surface contact count subdivided by care type.

drawing inference in these cases.

	Care Type					
	Directcare	House-keeping	Mealtimes	Medi-cation rounds	Misc-ellaneous	Personal-care
<i>r</i>	0.667	0.869	0.913	0.333	1.000	0.913
<b>p-value</b>	0.333	0.083 <sup>†</sup>	0.167	0.750	0.083 <sup>†</sup>	0.083 <sup>†</sup>

Table 5.8: Correlation coefficients and p-values for hand washing probability versus surface contacts. Where <sup>†</sup> represents a statistically significant value at the 10% level.

#### 5.4.2.2 Preference for hand antiseptis type

As categorised by *Epic2*, the care types observed contain mainly *social* and *hygienic* hand hygiene opportunities as indicated in Table 5.9. Only *personal care* may present reason for minor surgical classed procedures (e.g. catheter insertion). Gloves are a requirement throughout bathing and toileting but since this occurred privately, the quantity of glove

use within this category may be proportionally higher. Care type influenced the choice of hand antiseptis ( $p=0.0003$ ). Figure 5.12 can be used to distinguish antiseptis preference, where care formed mainly of hygienic procedures such as *personal care* was predominated by hand washing with soap and water. *Miscellaneous care* which is a mixture of possible social and hygienic procedures splits the choice of antiseptis method almost 50-50 between alcohol gel and hand washing. *Mealtimes* are classed solely as a social hand hygiene opportunity, which is reflected in the preference for alcohol rub between HCW ( $p=1 \times 10^{-3}$ ). Food on trays was assembled in the corridor and doled out by the HCW present. Given that hand washing with soap and water, according to the “5 moments” guidelines requires a minimum of 30s, alcohol rub is the obvious choice.

Hand antiseptis	Care Type					
	Direct-care	House-keeping	Meal-times	Medication rounds	Miscellaneous	Personal-care
Social	X	X	X	X	X	
Hygienic	X	X		X	X	X
Surgical						X

Table 5.9: Care type categorised by hand hygiene opportunity.

#### 5.4.2.3 Influence of patient contact on hand hygiene

*Epic2* suggests that antiseptis should follow contact with the patient or their near surrounding, see Section 5.1.1.1. This section of results investigates this claim and compares against observed cases. Figure 5.6 shows a breakdown of all hand antiseptis and compares this with patient contact in the form of a Venn diagram. The probability of hand hygiene  $P(H)$  being influenced by patient contact  $P(C)$  is called the conditional probability  $P(H|C)$ , denoted Probability of H given C. This corresponds to the proportion of HCWs

touching patients who subsequently wash their hands and is given by:

$$P(H|C) = \frac{\sum \# \text{care with hand sanitising}}{\sum \# (\text{care with hand sanitising} + \text{care with patient contact})} \quad (5.4.1)$$

Consider each hand antisepsis event as an independent Bernoulli trial with probability of success of  $\lambda=50\%$ . The variance of this binary trial type is given by:

$$\lambda(1 - \lambda) = \frac{1}{4}$$

Table 5.10 displays the probability of any hand hygiene given patient contact  $P(H|C)$  and the standard deviation for each type of care. The normal approximation  $\sqrt{\lambda(1 - \lambda)a}$ , where  $a$  is the number of events has been used to calculate these based on substantial sample sizes. The effect on hygiene of patient contact is calculated by comparing the actual number of episodes of care concluding with hand hygiene (of any kind) against the standard deviation of the Bernoulli trial. Only in the case of *personal care* is there a statistically significant association between patient contact and hand antisepsis. In all other care types, the performance of hand hygiene is close to a 50-50 chance, suggesting that patient contact does not affect it extensively. Based on the Fulkerson scale [27], touching a patient is not considered a dirty contact (scale 1-5). However *Epic2* guidelines allow the HCW to assess the care type as either: *social*, *hygienic* or *surgical*, without providing strict guidelines, thus creating a ‘grey area’.

	Care Type						
	<b>D.C.</b>	<b>H</b>	<b>M.T.</b>	<b>M.R</b>	<b>M.</b>	<b>P.C.</b>	<b>Overall</b>
$P(H C)$	42%	50%	33%	54%	42%	89% <sup>†</sup>	46%*
$a$	197	17	21	111	72	13	431
$\sqrt{\lambda(1 - \lambda)a}$	7.02	2.06	2.29	5.27	4.24	1.8	10.4

Table 5.10: Probabilities of patient contact influencing hand hygiene for each care type given with the standard deviation. Where <sup>†</sup> represents a statistically significant value. D.C.=Direct care, H=housekeeping, M.T.=Mealtimes, M.R.=Medication rounds, M=Miscellaneous, P.C.=Personal care.

## 5.5 Summary

The randomised controlled trial, the gold standard within research design, is not always possible within this framework. The difficulties in conducting these types of trials within palliative care include patient recruitment and physicians gate-keeping [248], hence rendering sample sizes small. Patients changed from study period 1 to study period 2 and also between days hence allowing for a realistic dynamic environment.

Care type influenced the HCWs' surface contact distribution to a large extent. However, length of care was less influential and showed only weakly positive correlation with surface contact counts. Care types could not be distinguished with respect to patient contacts, however environmental surface contacts exhibited a statistically significant variation.

Hand hygiene choice at YAB shows a snapshot of a dynamic modern Welsh hospital. Type of care influenced the choice of hand antiseptics, where HCWs performing short (<30s) episodes of *social care* showed a predilection for alcohol rub. *Direct care* and *miscellaneous care* split the usage of alcohol gel and hand washing almost 50-50. Over 90% of the observed episodes of *personal care* concluded with some form of hand hygiene. These are considered mostly either *hygienic* or *social care* and hence exhibited a 62% preference for hand washing.

## 5.6 Implementation of the Results

The completed observational study enabled realistic first-hand data to be collected which is utilised in the formulation of stochastic models of human behaviour and subsequent infection risk models in Chapter 6 and Chapter 7.

## Chapter 6

# Pathogen accretion model: PAM

### Contents

---

<b>6.1</b>	<b>Introduction to Dermal Models . . . . .</b>	<b>192</b>
<b>6.2</b>	<b>Overview and Objectives of the Dermal Model . . . . .</b>	<b>197</b>
<b>6.3</b>	<b>Model Structure and Approach . . . . .</b>	<b>197</b>
<b>6.4</b>	<b>Model Development: PAM . . . . .</b>	<b>205</b>
<b>6.5</b>	<b>Preliminary Results and Validation . . . . .</b>	<b>220</b>
<b>6.6</b>	<b>Model Sensitivity Analysis . . . . .</b>	<b>222</b>
<b>6.7</b>	<b>Uncertainty Analysis and Parametric Study . . . . .</b>	<b>234</b>
<b>6.8</b>	<b>Summary . . . . .</b>	<b>238</b>

---

This chapter describes the methodology behind the development of a probabilistic pathogen accretion model PAM on HCWs' hands. The aim of this model is to provide a framework which will allow for the quantitative comparison of hospital room design viz. single vs. multi-bed accommodation by means of an indirect metric. Here, the results obtained from the observation study at YAB and presented in Chapter 5 form the basis for the behaviour of the personnel tending to patients. Chapter 4 provides the validation for using CFD analysis to predict spatial distribution of indoor bioaerosol deposition within different scenarios, comparing the effects of design variations. This chapter begins with a background description of why an indirect metric is necessary to compare room design, followed by the model development. The model is then expanded to more realistically represent the HCWs' surface contact patterns by the use of Markov chain modelling, along

with a sophisticated accretion mechanism involving bi-directional transfer from hands-to-surface. A sensitivity analysis evaluates and validates the parameters chosen, and finally, a parametric study is carried out, comparing the effects of parameter modification within a test case scenario. It is important to bear in mind when reading this chapter that many of the model inputs are necessarily uncertain, which allows for examining different parameter spaces referring to relative risk of different care and room types. Subsequently Chapter 7 applies this new methodology to the single room at YAB and a HBN04-01 standard multi-bed [5] room, to demonstrate the application and scope of the model.

## 6.1 Introduction to Dermal Models

Through the literature review in Chapter 3 and the observational study carried out at YAB, HCW hand pathogen loading is known to pose a significant risk for cross-contamination or eventually cross-infection events. In addition, indirect infection transmission shows a distinct possibility of being exacerbated by incomplete or non-existent hand hygiene as found in Chapter 5. Hand hygiene is considered the most important tool in the HCW's armamentarium for preventing HCAI and the spread of antimicrobial resistant pathogens [20]. Much of the transient microflora accrued by HCWs tends to lie on the uppermost level of the skin called the stratum corneum, whereas the resident or endogenous microorganisms are found somewhat deeper [249]. Modelling of microorganism transmission arises from the the interaction between risk assessment and ultimately the study of epidemiology. However, the underlying mechanisms are still poorly understood. Therefore a clearer comprehension of the process of surface-to-hand pathogen transmission is critical for designing prevention strategies. This chapter reviews the available evidence for modelling surface-to-hand pathogen accretion during patient care and proposes a flexible model and subsequent framework for future validation.

Pittet et al. [20] describe the likelihood of accruing pathogens on a HCW's hands during different types of patient care and following subsequent hand-antiseptics as being a critical factor within indirect pathogen transfer. The essential steps for cross-transmission, shown pictorially in Figure 6.1, are given by the WHO [39] as being:

1. Microorganisms must be present on either the patient's skin or surrounding fomites

2. Transfer of pathogens must occur during contact between the inoculated surface and the HCW's hand
3. The transferred organisms must be able to remain viable during this process and for some time after
4. The hygiene procedure following the patient contact must be inadequate at removing all the pathogenic material
5. Lastly the HCW's hands must re-transfer the microorganisms in a timely manner to another surface or patient

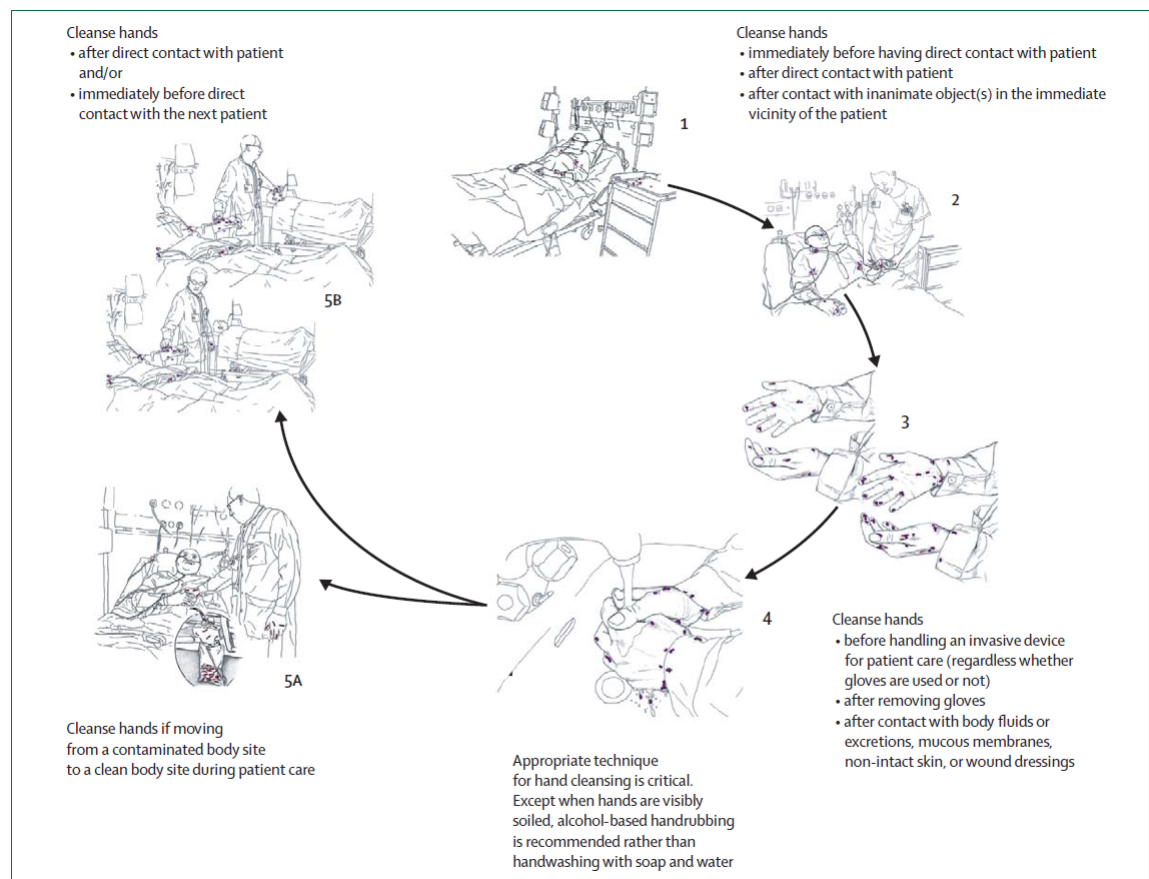


Figure 6.1: Stages involved in pathogen transfer reproduced from Pittet et al. [20].

Attempts to associate types of patient care with pathogen loading have never fully materialised [250]. In earlier research, Pittet et al. [22] performed an observational study of some 417 HCWs during patient visits and conducted subsequent pathogen quantification techniques, known as glove-juice [39] testing, in a teaching hospital to measure hand contamination. Particular activities were statistically associated with increases in colony

forming unit (CFU) counts. CFU values per minute were seen to be highest after direct patient contact, particularly when tracheostomy care or endotracheal tubes were fitted. Particular emphasis shows that medical rehabilitation units tended to harbour higher CFU quantities vs. typical ICUs or step-down units [22]. Possible explanation of this may lie in the use of complex rehabilitation apparatus and the underestimation of cleaning requirements herewith [24]. A significant difference between the transfer efficiency of pathogens to gloved vs. ungloved hands was also found. A positive linear link was established between the bacterial colony count on the hands and the length of the duration of the care. This indicated that the length of care either by surface contact count or time spent in the room, indirectly increases the risk of pathogen transfer between surface and hands. CFU values were found to be between 0 and 300 [250], most of which were Gram-negative *bacilli*, *enterococci* and *S. aureus*. By contrast, in a study [249] carried out prior to glove use being common amongst health-care workers, it was found that nurses carried  $10^4$  CFU of *S. aureus* on their hands ranging up to  $14.3 \times 10^6$  CFU after patient contact. Hands and gloves of HCW were also found to be contaminated during contact with environmental objects and surfaces [13, 51, 250, 251, 252] showing that they may form an integral link in the chain of infection transmission.

Nurse cohorting whereby nurses are restricting to a particular set of patients was considered to be an effective intervention measure by Beggs et al. [32]. However, they suggest that despite a high level of cohorting amongst nurses, doctors move freely between patients, which may compromise the intervention. Cooper et al. [142] uphold this conclusion by directly linking infection to handwashing. Indeed, in their transmission model, pathogen transfer cannot be completely eradicated due to this. Potentially, full hand hygiene compliance to the highest standard can ultimately reduce indirect transfer. However given all the factors involved in hand anti-sepsis this could prove utopian. Whether or not this is truly necessary as in the case of herd immunity [171], remains to be seen.

Comparing the layout of a hospital single room against that of multi-bed accommodation by investigating infection transmission requires a means to measure their parametric design effects on pathogen transfer. To be able to quantify the risk of indirect infection transmission one first must design a method to estimate the level of contamination on HCWs' hands following patient care. But first a little background.

### 6.1.1 Background

Skin exposure from contact with a contaminated surfaces is considered to be a dynamic process in which multiple factors may vary [253]. Considered by the US Environmental Protection Agency (EPA) for chemical exposures, they highlight that contact frequency and hand movement during contact can be individual and job specific, while contact pressure may be more universal. In their published guidelines [83], the EPA proposed evaluation of dermal accretion of hazardous materials through hand-to-surface contact to be deterministic and linear in nature:

$$D = A \times Q \times WF \quad (6.1.1)$$

where  $D$ = dermal potential dose rate (mg per day),  $A$ = surface area of contact ( $\text{cm}^2$ ),  $Q$ =amount retained on skin ( $\text{mg}/\text{cm}^2$ ),  $WF$ = weight fraction of chemical mixture. The EPA also provides default values for  $WF$  and  $Q$  for given chemical compounds. However throughout the last two decades of the twentieth century the EPA Office of Research and Development developed a probabilistic model for estimating exposure to toxic chemicals in the residential setting called Stochastic Human Exposure and Dose Simulation or SHEDS [254]. This estimates the aggregate exposure to specific chemicals over time through multiple pathways including via inhaling contaminated air, touching contaminated surfaces, and ingesting residues from hand/object-to-mouth activities. It then calculates the cumulative exposure and dosage. Since parameters within the model are rates, events or concentrations per time, SHEDS cannot quantify the risk posed by, or to, a specific individual nor represents any one specific real person, therefore the output must be seen as a time-integrated or time-averaged exposure. However, SHEDS makes use of a subscription based activity database called Consolidated Human Activity Database (or CHAD) to simulate human behaviour throughout the day. As a consequence a model which considers micro-activity or individual surface contacts over a shorter timescale is necessary.

Foundations for a conceptual dermal exposure model were published by Schneider et al. [255] being one of the first inclusive models for multiple exposure pathways and dermal *absorption* of contaminants (not to be confused with dermal *adherence* or *adsorption* which is what is of interest here). This compartmental model describes the transport of contaminant mass from exposure sources to the surface of the skin through three main exposure

routes: Ingestion, aerial deposition and skin absorption. No validation was presented however, and subsequently a semi-quantitative dermal model (DREAM) was published by van Wendel-de-Joode et al. [256] developing the concept further. Nevertheless this still tackles the problem of ingestion of toxic chemicals into the hosts own body (absorption) rather than the current problem of temporary hand colonisation by microorganisms (adsorption).

Schaffner [257] highlights the importance of modelling infection transmission pathways as a logical next step, however so far this has not been fully accomplished. In general models (such as [85, 142, 198, 254, 258]) tend to include the wide scope of an entire hospital ward, making generalisations, on the actual mechanics of transmission itself. Within the sphere of food microbiology, simple pathogen transfer models are abundant. These are generally additive in nature and dependent only on surface-to-hand transmission efficiency [259]. Den Aantrekker et al. [260] recognise the importance of the role that hands play during infection transmission, however they develop a deterministic quantitative microbial risk assessment model which mainly focusses on air-to-surface transfer. Zartarian et al. [85] developed a dermal exposure reduction model (DERM) which characterised the different pathways of contaminant exposure, again recognising the importance of contact transmission but appear to gloss over the actual mechanics involved. Their model explores exposure to toxic substances simulated by considering the day-time activities, the concentration of chemical and the skin surface exposed. Although this is stochastically simulated, the specific mechanisms required for analysing pathogen transfer are absent. Canales et al. [36] adapted and refined this model further to simulate the exposure of young children to lead paint, calling their model CASE or (Cumulative Aggregate Simulation of Exposure). Perez-Rodriguez et al. [259] acknowledge the paucity of exhaustive experimental studies within the food-chain preparation environment and liken it to health-care settings. They present a critical analysis of the mathematical transfer models published in current literature by means of a quantitative microbiological risk assessment (QMRA) framework where, at best, pathogen accretion is calculated additively by means of Monte-carlo sampling from sparsely populated transfer efficiency distributions. Subsequent efforts by Zartarian et al. [261, 262] demonstrate that the need for further research into the exposure and transfer of pathogens in the health-care setting is ever more prominent.

## 6.2 Overview and Objectives of the Dermal Model

The aim of creating a probabilistic model of pathogen transfer from surfaces to HCWs' hands is based on the need for:

1. Utilising realistic behavioural data accrued in Chapter 5 as a basis for predicting HCW surface contacts.
2. Creating a flexible model of pathogen accretion onto dermal surfaces through Monte-Carlo sampling of parameters from empirical distributions.
3. Validating the use of the most important parameters through sensitivity analysis.
4. Establishing a parametric study to compare single room patient care against care extrapolated into a four-bed scenario.
5. Refining model variables to improve prediction of pathogen loading, through:
  - (a) Bi-directional transfer from surface-to-hand and vice versa.
  - (b) Markov chain modelling of HCW surface contacts.
6. Laying the foundation for further validation.

It is important for any model to provide quality assurance. This ensures that the model corresponds to the established objectives accurately or within a margin of accuracy (validation) and answers the correct questions (verification) [263].

## 6.3 Model Structure and Approach

The fundamental modelling unit within the pathogen accretion process is the individual HCW. At first glance deterministic modelling following previous research [260] and using single-point estimates or ranges might yield interesting results. Each uncertain variable within a model is assigned a “best guess” estimate and hence yields scenarios such as best, worst, or most likely case [198]. In comparison, Monte-Carlo techniques sample probability distributions for each variable to compute thousands of possible combinations. These results are then statistically analysed to obtain the probabilities of different outcomes occurring.

### 6.3.1 Simulating an Individual HCW

The HCW touching surfaces during an episode of patient care forms the driving force within this model. As the HCW undertakes their duties, they touch surfaces within the patient room and these sequences of surface contacts were recorded meticulously in Chapter 5. This is called the longitudinal activity. 431 care episodes were observed and form the basis for determining surface contact sequences. Six types of patient care were observed, each with their own properties and lengths, namely: *Direct care*, *housekeeping*, *mealtimes*, *medication rounds*, *miscellaneous care* and *personal care*. Each of these is described in detail in Chapter 5 Section 5.3.1.

Within these next sub-sections two methods are described which demonstrate how the behavioural pattern of HCWs are modelled, first by moving randomly between surfaces with weighted probabilities, and secondly by directed probabilities forming ordered sequences in a Markov chain. The flowchart of determining this longitudinal activity is described as follows:

1. Decide which care type the HCW will perform
2. Based on care type predict activity length in number of surface contacts (from observations in Chapter 5)
3. Generate HCW surface contact sequences based on YAB observations for care type chosen based on:

**Method 1** Empirical probability density functions, with no directed probabilities

**Method 2** Markov chains with directed probabilities

#### 6.3.1.1 Method 1: Empirical marginal frequency density ( $\hat{P}$ )

Consider the sequence of surface contacts made by the HCW is independent of the current surface which they are touching and hence is memoryless. The initial state of the HCW denotes the first surface which (s)he touches, which is chosen from the observations at YAB (Figure 5.7). A Monte-Carlo simulation was run to predict the surface contact patterns for 10,000 HCWs by means of the Gillespie Algorithm in Matlab (2012a MathWorks, MA,

USA). This method of sampling is denoted ‘quasi-random’ in the sense that the sequence of chosen points is not completely unpredictable [264]. The random number generator used was Matlab’s own pseudo-random algorithm. Since the maximum number of random numbers generated before duplication exceeds the replicate numbers of this Monte-Carlo simulation it was deemed sufficient.

The probability of contact with a given surface in the patient’s room is created from the results in the previous study explored in Chapter 5 and shown in Table 6.1:

Care type	Surface category				
	Equipment	Patient	Hygiene products	Near-bed objects	Far-bed objects
Direct Care	0.255	0.186	0.104	0.202	0.253
Housekeeping	0.247	0.079	0.067	0.393	0.213
Mealtimes	0.000	0.109	0.182	0.564	0.145
Medication round	0.054	0.161	0.179	0.350	0.256
Misc.	0.024	0.115	0.242	0.303	0.315
Personal Care	0.034	0.169	0.213	0.404	0.180

Table 6.1: Probabilities for surface contacts based on care type and surface category.

Let us assume that the probabilities of moving to any other state (or surface) do not depend on the HCW’s current surface location. At each “step” the health care worker will either remain at the same surface with the probabilities in Table 6.1 or move to another surface. The sequence of surface contacts is produced by the following algorithm:

1. Create the cumulative sum of probabilities for each care type, thus defining the interval width
2. `for jj=1:m %` where `m` is the number of nurses
3. Choose care type
4. Randomly select care length ( $n$ ) based on care type
- 5.
6. `for ii=1:n %` where `n` is the sequence length

7. Generate a random number  $w$
8. Check into which cumulative probability interval  $w$  falls and choose the corresponding surface category
9. update  $ii=ii+1$
10. update  $jj=jj+1$
11. *end*
12. *end*

### 6.3.1.2 Method 2: The Markov Chain

Method 1 assumed no directed probability between surface moves, that is to say that it did not matter which surface the HCW was currently touching to predict the following contact. This is not particularly realistic, insofar that touching a surface category in the next move may be more likely than any other depending where they are currently touching. For example, consider a nurse who is taking the patient's blood oxygen saturation level and ignoring the fact that (s)he is carrying out an episode of *direct care*, they are more likely to touch the patient after opening the oximetry meter than open the window. However, this is not considered in Method 1, and a surface based solely on weighted probabilities is chosen instead.

To test the hypothesis of non-randomness, the Kolmogorov complexity test [265] compares values within a sequence against the assumption that they are placed in random order against the alternative hypothesis that they are not. The test is based on the quantity of sequences of contiguous values either side of the mean. Too few occurrences indicates a tendency for extreme values to cluster, and too many indicate a tendency for high and low values to alternate [265]. Sequences accrued from the YAB observations and presented in Chapter 5, on average reject the null hypothesis of randomness at the 5% level ( $p=0.04$ ). Therefore it is not unreasonable to assume that the HCW touches surfaces in a sequential or directed manner, insofar that jumping from one surface category to another has a higher probability than a transition somewhere else. Let us assume that the surface categories are assigned a numerical value from 1-5: such that *Equipment*=1, *Patient*=2, *Hygiene products*=3, *Near-bed objects*=4 and *Far-bed objects*=5. By means of

directed probabilities between surface categories the HCW can be made to move between them based on the property that, given the present state, the future and past states are independent. This is termed the Markov Property:

$$P(X_i = x_i | X_j = x_j) \quad (6.3.1)$$

The empirical sequences observed contain not only probability frequency densities for each surface contact but also directed probabilities between them. Given the large sample size  $n = 431$ , including 1824 transitions, for the number of states  $d$ , it is reasonable to assume independence by splitting them into two halves. One-step or first order transitions between states are defined from empirical sequence data by a maximum likelihood estimator  $\hat{P}$  for  $n$  observations is given thus:

$$\hat{P}_{ij} = \frac{x_{ij}}{\sum^m x_{ik}} \quad \text{where } m=1..5 \text{ states} \quad (6.3.2)$$

As  $n \rightarrow \infty$ ,  $\hat{P}_{ij} \rightarrow P$ , this is known as asymptotic normality.

By this method all sequences of surface contacts observed at YAB are distilled into creating a general transition matrix of maximum likelihood estimators, based on all care types, given by  $\hat{P}_{ij}$  in Table 6.2.

	Surface category ( $j$ )				
	Equipment	Patient	Hygiene products	Near-bed objects	Far-bed objects
Surface category ( $i$ ) Equipment	0.183	0.308	0.077	0.148	0.284
Patient	0.480	0.114	0.008	0.250	0.159
Hygiene	0.183	0.240	0.221	0.192	0.164
Near-bed	0.238	0.182	0.063	0.336	0.182
Far-bed	0.246	0.179	0.117	0.179	0.279

Table 6.2: Directed probabilities of moving from surface  $i$  to surface  $j$

This matrix  $\hat{P}$  is a general transition matrix and can be used to compute a possible HCW trajectory during a typical episode of care. Figure 6.2 shows the movement between surfaces of a HCW during an episode of typical care. Transitions are chosen based on the above method:

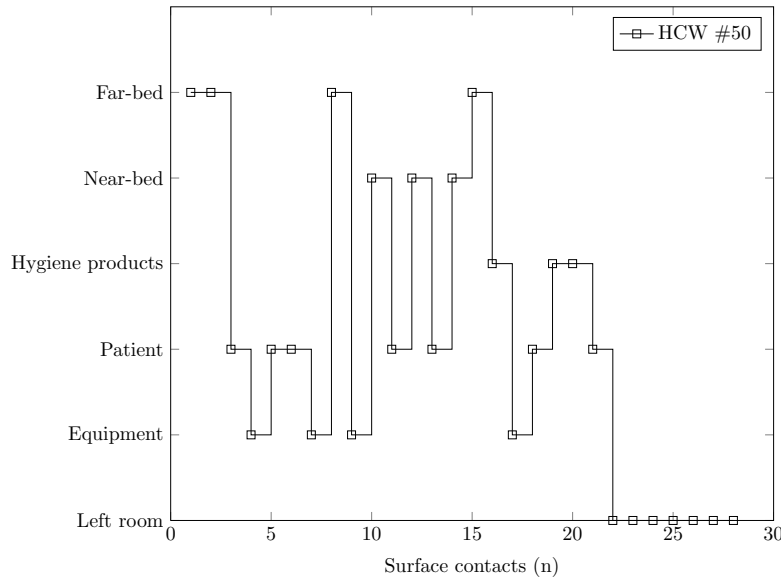


Figure 6.2: Example of surface contacts of HCW #50 performing a standard episode of care.

### 6.3.1.3 Bootstrapping, Laplace smoothing and confidence intervals of $\hat{P}_{ij}$

Transition matrices  $\hat{P}_{\text{care type}}$  can also be computed for each care type: *Direct care*, *House-keeping*, *Mealtimes*, *Medication rounds*, *Miscellaneous care* and *Personal care* by collecting the observed sequences of transitions for each episode of care. For example *personal care* is given by:

$$\hat{P}_{\text{personal care}} = \begin{pmatrix} 0 & 0 & 0 & 1.00 & 0 \\ 0 & 0 & 0.22 & 0.44 & 0.33 \\ 0 & 0.19 & 0.57 & 0.10 & 0.14 \\ 0.03 & 0.19 & 0.09 & 0.50 & 0.19 \\ 0 & 0.06 & 0.13 & 0.56 & 0.25 \end{pmatrix} \quad (6.3.3)$$

However, this results in a sparse matrix, with some 0 entries suggesting that the corresponding transition  $i \rightarrow j$  is impossible. Since the physical movement between these states *is* possible, one must attempt to account for this in some fashion, given the data observed. Furthermore, the non-sparse transition matrix  $\tilde{P}_{\text{personal care}}$  can be calculated by the method of bootstrapping and Laplace smoothing [266].

A bootstrap is a statistical technique whereby observed values  $\mathbf{X} = (x_1, \dots, x_n)$  are re-sampled, with replacement, on the basis that the best available estimate of a distribution,  $F$ , is the empirical distribution,  $\hat{F}$ . This allows some idea of the sampling uncertainty associated with a distribution's property  $F(\hat{\theta})$  to be investigated [266]. Here, a 1000 bootstrap samples are used throughout. Coupled with this, Laplace smoothing accounts for unobserved transitions by introducing a small probability  $\alpha$  of observing a particular transition [267]:

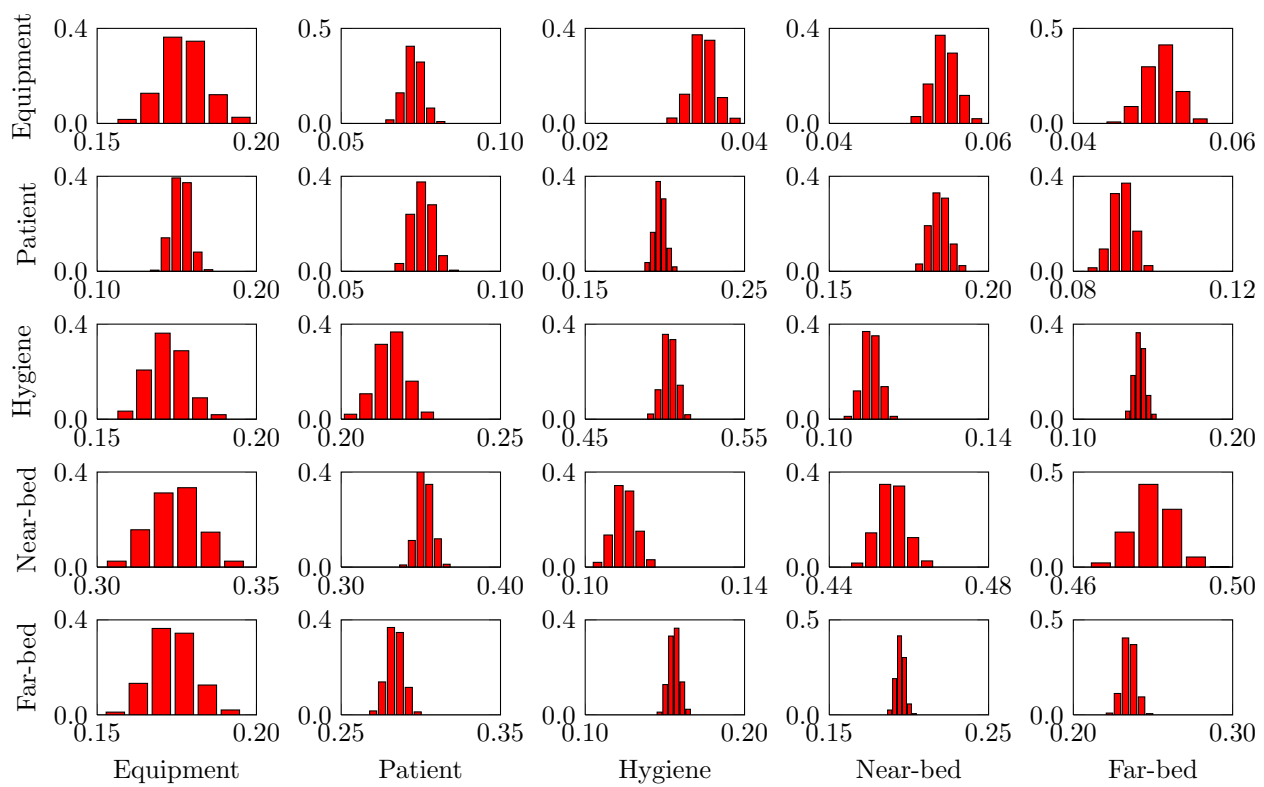
$$\tilde{P}_{ij} = \frac{x_{ij} + \alpha}{\sum^m x_{ik} + \alpha x_{ij}} \quad \text{where } m=1..5 \text{ states and } 0 \leq \alpha, \quad (6.3.4)$$

An optimum value of  $\alpha$  appears to be somewhat subjective, however to ensure boundedness and hence maintain asymptotic normality, Teodorescu [268] concludes that  $|\hat{P}_{ij} - P_{ij}|$  is minimised with an  $\alpha$  value of 1. 95% confidence intervals on  $\tilde{P}_{ij}$  are then calculated through this method for each care type. For reasons of succinctness an example of *personal care* is given below, all other transition matrices can be found in Appendix B. To what extent this variation is important, is investigated by sensitivity analysis in Section 6.6. Figure 6.3 represents the confidence intervals calculated for transition probabilities of *personal care*  $\hat{P}_{\text{personal care}}$ , where  $\tilde{P}_{\text{lower}2.5\%}$  represents the lower confidence interval and  $\tilde{P}_{\text{upper}2.5\%}$  the upper. A wider distribution suggests more uncertainty.

$$\tilde{P}_{\text{p. care}} = \begin{pmatrix} 0.167 & 0.167 & 0.167 & 0.331 & 0.167 \\ 0.073 & 0.073 & 0.215 & 0.352 & 0.284 \\ 0.041 & 0.198 & 0.479 & 0.121 & 0.159 \\ 0.059 & 0.196 & 0.114 & 0.435 & 0.195 \\ 0.050 & 0.099 & 0.147 & 0.461 & 0.241 \end{pmatrix}$$

$$\tilde{P}_{\text{lower CI}2.5\%} = \begin{pmatrix} 0.159 & 0.158 & 0.148 & 0.310 & 0.165 \\ 0.064 & 0.067 & 0.206 & 0.346 & 0.275 \\ 0.035 & 0.192 & 0.471 & 0.117 & 0.151 \\ 0.057 & 0.190 & 0.112 & 0.425 & 0.189 \\ 0.048 & 0.097 & 0.138 & 0.448 & 0.235 \end{pmatrix}$$

$$\tilde{P}_{\text{upper CI}2.5\%} = \begin{pmatrix} 0.183 & 0.181 & 0.175 & 0.338 & 0.187 \\ 0.074 & 0.078 & 0.225 & 0.366 & 0.294 \\ 0.043 & 0.205 & 0.490 & 0.127 & 0.165 \\ 0.064 & 0.201 & 0.123 & 0.437 & 0.200 \\ 0.055 & 0.107 & 0.149 & 0.468 & 0.249 \end{pmatrix}$$

Figure 6.3: Bootstrap confidence intervals for  $\tilde{P}_{\text{personal care}}$ .

## 6.4 Model Development: PAM

Given that existing dermal exposure models to date are additive in nature it is reasonable to assume that over the time scales of interest, pathogen loading will also be so too. To what extent is still debatable. However a very compelling argument is put forward by Montville et al. [269] which shows a negative linear correlation between the increase of inoculum on a surface and the percentage transfer to hands. Therefore the corollary would suggest that there is no upper limit of pathogen loading on hands. They examined up to  $8 \log_{10}$  CFU which is well above any in-situ testing results. That is to say, inocula levels on HCW hands have not been detected above this quantity in-vivo. Therefore let us also make a similar assumption.

Let us simplify notation by allowing the number of colony forming units accrued on the HCW hands to be called  $Y$ . The amount of pathogens accrued currently on hands depends on the surface contamination levels ( $V$ ) and the surface area of skin in contact with the surface ( $A$ ). However, it is reasonable to assume that not all of the pathogens in contact with the surface area of skin touching the surface are transferred. Therefore a transfer efficiency ( $\lambda$ ) is defined to represent the proportion of pathogens that are transferred in the upward direction. During hand-to-surface contact it is equally reasonable to assume that some quantity of pathogens already acquired ( $\beta Y$ ) are deposited from the hand onto the surface during a contact. However this quantity deposited will depend on the current hand inoculum level ( $Y_{i-1}$ ). Therefore this model will consider transfer in both directions or bi-directional transfer. Consequently pathogen accretion ( $Y$ ) can be modelled by means of a recurrence relationship given in Equation (6.4.1):

$$Y_i = \lambda_i V_i A_i + \beta_i Y_{i-1} \quad (6.4.1)$$

where  $i = 1..n$ , is the surface contact count. Hand sanitation (with probability  $P$  and efficacy  $1 - h$ ) is performed only once on the final  $Y$  value.

For purposes of remaining succinct let  $\sigma = \lambda AV$  then assuming that the transfer of pathogens to the surface from the HCW occurs sequentially and is independent of the

surface loading then  $Y$  can be described as follows:

$$\begin{aligned}
 Y_i &= \sigma_i + \beta_i(\sigma_{i-1} + \beta_{i-1}(\sigma_{i-2} + \dots)) \\
 &= \sigma_i + \beta_i\sigma_{i-1} + \beta_i\beta_{i-1}\sigma_{i-2} + \dots \\
 &= \sum_{j=0}^i \left( \prod_{k=j+1}^i \beta_k \sigma_j \right)
 \end{aligned} \tag{6.4.2}$$

### 6.4.1 Model Input: Contact Surface Area ( $A$ )

Canales et al. [270] consider hand contact to be qualitatively categorised into: Side hand contacts, pinch grips, full front fingers, closed handgrips, and full hand immersions. They conduct a study to investigate absorption of a chemical over varying hand surface areas. Results were for children and described in terms of hand surface %. Interestingly however, their results did show a bimodal distribution for smooth surface contacts, the lower peak appearing between 4-8% and the higher peak at 23-35%. Brouwer et al. [271] performed an extensive hand-to-surface contact experiment to estimate the surface contact area. Results showed that this exhibits a mean of  $7 \text{ cm}^2$  and standard deviation of  $1.9 \text{ cm}^2$ . However during in-vivo experiments hand surface area contacts with objects or surfaces may well be somewhat lower [140]. Given the paucity of experimental data a continuous log-normal distribution  $\ln N(1.91, 0.266)$ , corroborated by the Kolmogorov-Smirnov goodness of fit test ( $p=0.04$ ) will be used based on the empirical data by Brouwer et al.

During episodes of care both hands are often used in conjunction, therefore a second random value is drawn from Figure 6.4 to reflect this. No evidence supports the necessity to make distinction for the dominant hand. CFU values are then cumulative for each HCW over both hands.

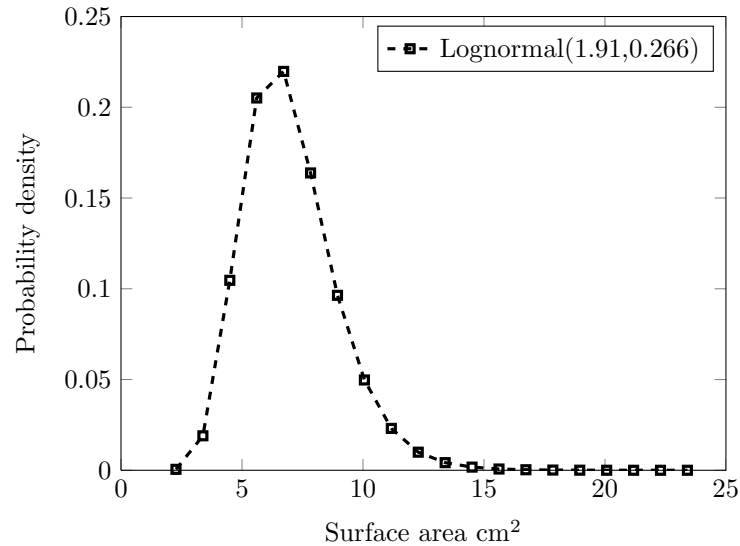


Figure 6.4: Probability density function of hand surface area contact parameter  $A$ .

#### 6.4.2 Model Input: Surface Pathogen Load ( $V$ )

During routine activities, the human body has been found to shed nearly  $10^6$  skin squamae that may contain viable pathogens [272] daily. Chapter 4 outlines the spread of respiratory droplets within the hospital setting, showing how particles can be dispersed throughout the entire room. Therefore it is without surprise that patient gowns, bed linen, bedside furniture, and other objects in the immediate environment of the patient become contaminated with pathogenic material [20]. Many such pathogens tend to be *staphylococcus* or *enterococcus* strains which are hardy and resistant to environmental desiccation [273]. Noskin et al. [274] show experimentally that *enterococci* strains can survive for a minimum of 1 hour on gloved and ungloved fingertips equally effectively. Moreover, viable colonies were recovered from bed-rails, stethoscopes and telephone handpieces up to a day later and *E. faecalis* was recovered from counter tops five days after inoculation. The importance of hospital surfaces harbouring pathogenic material for extended periods of time cannot be underestimated. Since it was found that a single *C. difficile* colony /cm<sup>2</sup> is capable

of eliciting a 100% immune system response in mice and a single milligram of faeces containing VRE could equally infect a human [272]. Surfaces have been found to harbour VRE colonies even after extensive terminal cleaning hence allowing viable organisms to be transmitted between HCW and patient [19, 51, 53]. Similarly Weber and colleagues review the importance of hospital surfaces harbouring pathogenic material of extended periods of time, hence allowing viable organisms to be transmitted between HCW and patient.

There appears however to be a lack of recent information and experimental studies regarding surface contamination levels, perhaps because of the inherent biological variability. Ayliffe et al. [48] conducted a combination of swabbing and settle plate collection techniques for both floor and walls within a hospital ward and operating theatre. Colony forming unit counts oscillated between  $10^3/\text{m}^2$ , putting this within the WHO cleanliness guideline [167] of  $2.5\text{CFU}/\text{cm}^2$ . White et al. [50] conducted a yearlong study of surface swabbing within a Scottish hospital ward and discovered that more than half the surfaces failed the WHO minimum standard. Otter reviews surface CFU counts and errs on the side of caution, reporting values in the region of  $1\text{-}100\text{CFU}/\text{cm}^2$ . However reports of CFU values higher than  $200+\text{CFU}/\text{cm}^2$  exist even after cleaning procedures [272]. Friberg et al. [66] concluded through empirical evidence based on air sampling that a ten-fold linear correlation exists between airborne  $\text{CFU}/\text{m}^3$  and surface values of  $\text{CFU}/\text{cm}^2$ . Given the uncertainties surrounding the efficacy of Andersen sampling, this comparison may be untractable.

Surface CFU values will depend on the scenario being modelled insofar that for the testing and calibration purposes of PAM, Chapter 4 will provide the experimental spatial distributions from aerial deposition. In the first instance a mock single room within the PaCE chamber will be used as a test scenario to provide calibration, raw CFU values for which are shown in Section 6.4.2. Subsequent settings such as the single room at YAB and the HBN04-01 standard hospital four-bed accommodation will be modelled using computational fluid dynamics and investigated in Chapter 7. There is no evidence to suggest the existence of extremely high CFU values or clumping sometimes represented by a Poisson distribution [198] and hence will not be assumed within this model. Instead a log-normal distribution will be used based on CFD data produced for each scenario including the respective standard deviation.

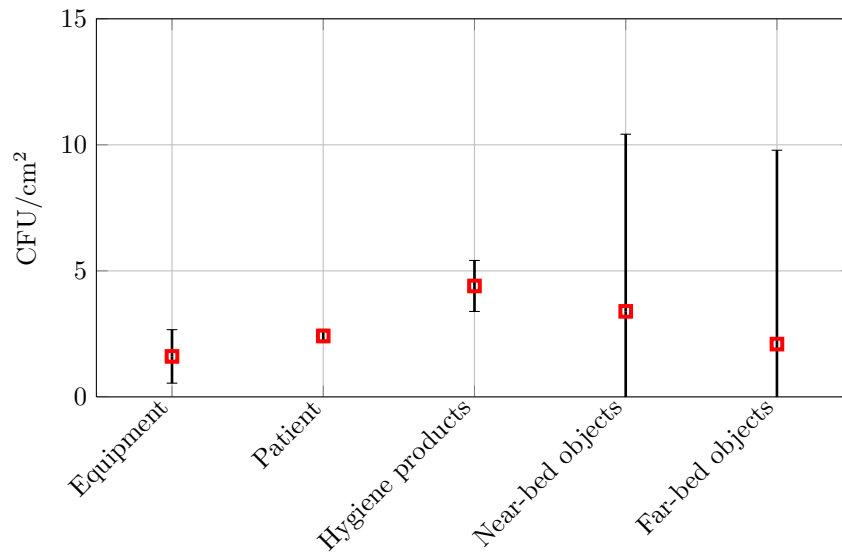


Figure 6.5: Empirical CFU values for test case PaCE chamber single room parameter  $V$ .

### 6.4.3 Model Input: Surface-To-Hand Transfer Efficiency ( $\lambda$ )

Transfer efficiency, which represents the percentage of surface contaminant transferred to the hand during a contact event has been shown to be one of the most important parameters when modelling dermal exposure [83], yet it is one of the most troublesome to accurately measure [84]. However transfer efficiency could possibly be a function of multiple ambient parameters such as surface physiology, contact frequency, duration and pressure; concentration of transferrable material on surface; temperature and or humidity. Parameters that are not taken into account during pathogen transfer are often denoted: The physiological state. Bacterial environmental stress such as extreme temperature, starvation, exposure to detergent or UV rays and biofilm formation can significantly affect transfer efficiency [259]. Hand-to-surface contacts may also result in no transfer or a *failed transfer*. Beamer et al. [84] highlights the paucity of thorough experimental studies for estimating surface-to-skin pathogen transfer and raises the question whether chemicals tracers can act as acceptable surrogates.

Probability distributions for  $\lambda$  have been published by the EPA for chemicals, mainly relating to pesticides or other toxic household compounds. Beamer et al. [84] collate the most extensive database of chemical transfer experiments known to date. Results show

measurements from surfaces in the domestic environment such as carpet, vinyl or foil, and no such database exists for pathogen transfer.

Rusin et al. [275] conclude from experimental studies, that the transfer efficiency from surfaces to hands varies between pathogens. In three separate experiments, the transfer of Gram-positive bacteria, Gram-negative bacteria and bacteriophage is reported to be 38.5%, 65.8% and 27.6-40% respectively from non-porous surfaces. However, the transfer rate reduces to below 0.01% when porous fomites are evaluated. In other studies conducted on transfer to hands from a wider range of surfaces [21, 253], Rusin's findings are corroborated with regards the high discrepancy between porous and non-porous materials. Furthermore ambient humidity appeared to play an important factor by increasing transfer rates, where Brouwer et al. support this with powder transfer experiments from glass plates to hands [271].

Lopez [21] detected significant differences of pathogen transfer under controlled conditions where in particular: Drying time, contact time, pressure, friction, type of material, and porosity of the fomite significantly altered transfer. However transfer efficiency was found to be greatest under high relative humidity (40-65%) for both porous and nonporous surfaces. Widmer et al. [276] allude to the repellent effect of natural fats on hands against pathogen accretion, however they did not note that this may be down to the individual microorganism type. In particular hydrophobic bacteria such as *enterococcus* adhere better to hydrophobic surfaces such as unwashed oily hands, PVC or rubber and therefore do not transfer to non-hydrophobic surfaces readily [259, 277]. On the other hand, bacteria exhibiting hydrophilic characteristics (e.g. *S. aureus*) attach better to hydrophilic surfaces such as stainless steel. Therefore these may be transferred less readily to oily skin. Widmer et al. [276] do highlight the detrimental effect of hand washing on the skin's natural properties. Nevertheless, humidity may be the overriding factor against the natural preference for attachment of the microorganism. Cracks and unevenness in rough surfaces tend to transfer microorganism less readily due to the adhesion properties within the microscopic level undulations. However biofilm may also grow here, creating large inocula but consequently prevent high transfer efficiency [277].

Combinations of wet and dry transfer in experiments conducted by Satter et al. [253] show that six species of bacteria are more efficiently transferred from moist donor fabrics than from dry ones. Percentage transfer efficiencies ranged from 0.1% to 2% which compare

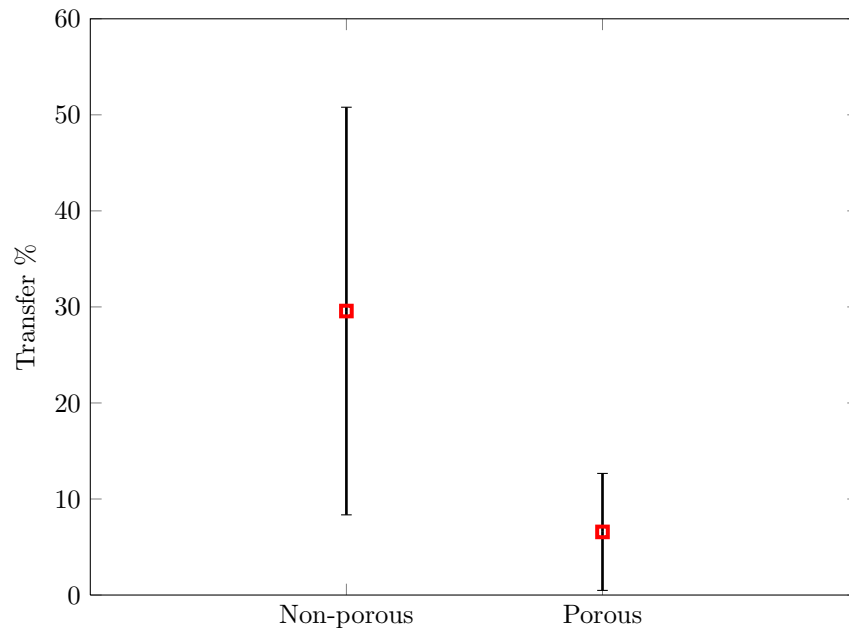


Figure 6.6: Empirical comparison between transfer of bacteria to porous and non-porous surfaces  $\lambda$ . Data reproduced from Lopez et al. [21].

well to those by Rusin et al. [275] for non-porous surface to finger pad transfers. Surface categories within the hospital room are categorised into porous or hard and non-porous. All except the patient and bed are considered non-porous. Friction was also found to yield a fivefold increase in the level of transfer from fabrics to finger pads. Differences also existed between materials tested where *S. aureus* transferred more readily from hydrophobic polymer based materials in comparison to cotton, a hydrophilic material. Furthermore McDonagh et al. [278] reveal that the effect of pressure may be of more importance than previously thought, where a clear step transition in transfer of fluorescein between surfaces is observed as pressure increases. However to what extent synthetic tracers can be compared to pathogens remains unclear. Inconsistencies within experimental techniques, in particular including methodology and data collection render transfer efficiency particularly hard to capture. It is important to note that pressure recovery methods such as agar stamping or swabbing can alter the recovery rates due to the unequal pressure exerted during experimentation. Biofilms or variations in bacterial adherence can also confound these results [259]. The glove-juice method [39] for sampling CFU counts on hands eliminates much of this variation where a glove is filled with 20ml of agar broth fitted onto hands and massaged for 1 min.

The food and drug administration (FDA) in the USA produce research often parallel to that within the health-care setting, investigating the same mechanisms of transmission. Montville et al. [279] conducted an in-vitro experiment (n=30) to examine the transfer of *Bacillus* spores from artificially inoculated chicken to food handlers' gloved and ungloved hands. To an ungloved hand bacillus spores were transmitted more readily based on a normal distribution with sample mean  $0.71 \log_{10}$  reductions and a standard deviation of  $0.42 \log_{10}$ . Conversely, transfer to a gloved hand was found to exhibit a Gamma distribution with shape parameter 5.91 and scale parameter 0.40. This is equivalent to a minimum of  $0.583 \log_{10}$  and a maximum of  $6 \log_{10}$  reductions.

Perhaps counterintuitively, a negative linear correlation was found by Montville et al. [269] for the acquisition of bacteria with respect to inoculum size on the source surface. This may well pose important implications for research seeking to determine bacterial accretion rates, since the variation in transfer efficiencies previously reported to be associated with particular activities may in fact be the result of differing initial surface pathogen loadings. The initial inoculum size on the source and the amount of bacteria transferred must both be considered to accurately determine bacterial transfer rates. Pèrez-Rodriguez et al. [259] suggest that either the attachment strength to a surface alters depending on inoculum size or alternatively that biofilm matrix strength increases exponentially as clump size increases as possible explanations. It has been also reported that non-grouped or clumped cells present poor adherence properties and hence lower pressures are required for transfer. Therefore the length of time since disinfection is an important factor to be considered [166]. This investigation works on the premise however, that the microorganism under consideration present relatively low resistance to transfer due to frequent cleaning. Therefore Table 6.3 will be used as the basis for an empirical distribution for  $\lambda$ .

Lead author	Ref.	% transfer or distribution	Surface type	Organism
Lopez	[21]	12 - 54	Non-Porous	Gram -ve bacteria
Lopez	[21]	1.9 - 15	Porous	Gram -ve bacteria
Montville	[279]	$\Gamma(5.91, 0.4, -5)$	Porous	Bacillus spores
Rusin	[275]	40 - 41	Non-porous	Micrococcus: Gram +ve bacteria
Rusin	[275]	0.1	Porous	Micrococcus: Gram +ve bacteria
Rusin	[275]	27.6 - 38.47	Non-porous	Serratia: Gram -ve bacteria
Rusin	[275]	<0.01	Porous	Serratia: Gram -ve bacteria
Rusin	[275]	33.47 - 65.8	Non-porous	PRD-1: bacteriophage
Rusin	[275]	0.01 - 0.04	Porous	PRD-1: bacteriophage
Schaffner	[257]	$\ln N \sim (-0.93, 0.27)$	Porous	Gram -ve bacteria
Satter	[253]	0.1 - 2	Porous	Gram -ve bacteria

Table 6.3: Published data on percentage transfers ( $\lambda$ ) from surfaces onto hands

#### 6.4.4 Model Input: Hand-To-Surface Transfer Efficiency ( $\beta$ )

Experimental investigations show that in some special cases pathogens are only accrued and not deposited, in general however a significant quantity of material residing on hands will be transmitted reversely to the surface during contact [272, 275]. It has previously been acknowledged in Section 6.4.3 that the transfer efficiency  $\lambda$  may depend heavily on surface contact time and also frequency due to skin saturation [271] such that the same may be true for its counterpart  $\beta$ :

$$\beta = \beta(\text{inoculum size, contact time, pressure, skin/surface humidity, surface type, friction})$$

More generally however, Brouwer et al. [271] explored this relationship and discovered that at a relatively low surface contact count of 6, saturation appears to affect accretion and deposition is visible. Again however, the chemical tracer used in the aforementioned experiment altered the hand's natural humidity through its hydrophilic properties. Therefore to include a possible deposition parameter ( $\beta$ ) into the accretion model, the extent to which this affects CFU counts can be evaluated through sensitivity analysis described in Section 6.6. Rusin et al. [275] conduct an experiment to examine the transfer efficiency

from subjects' fingertips to their lips. And although this appears to be an uncontrolled set-up their results showed transfer rates up to 35%. Montville et al. [269] demonstrate that a difference exists between the direction of CFU transfer. Statistically significantly lower transmission is shown during transfer from hands to fomites than vice-versa. They also highlight the influence of inoculum size on the efficiency of transfer, showing that when high levels are used transfer rates are more accurately characterised [23]. Surface-to-hand transfer efficiencies ( $\beta$ ) will be sampled from the empirical data Figure 6.7.

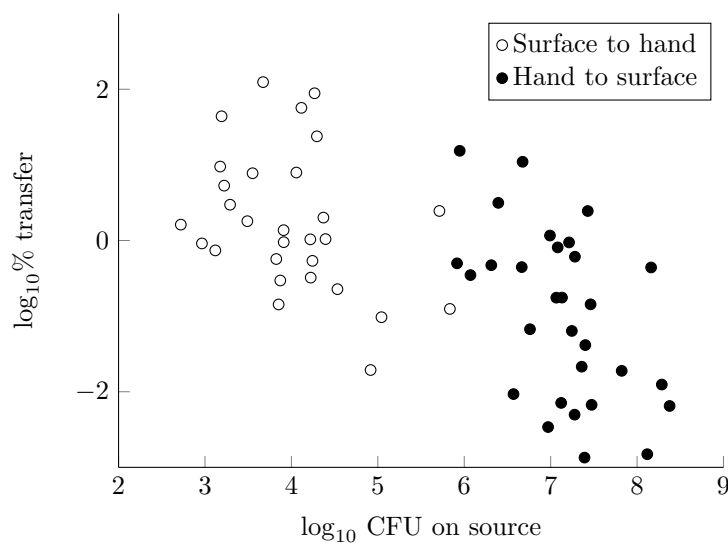


Figure 6.7: Comparison between a non-porous surface-to-hand and hand-to-surface transfers

#### 6.4.5 Model Input: Antisepsis Efficacy ( $h$ )

Antisepsis efficacy refers to the efficiency of reducing the CFU count on HCWs' hands after performing one of the three type of hand hygiene: Hand washing with either bland or medicated/antibacterial soap, removal of non-surgical gloves or dry rubbing with a waterless alcohol agent (minimum 61 or 62% ethanol by volume).

##### 6.4.5.1 Gloves

Pittet et al. [22] performed an observational study of some 417 HCW during 281 rounds and subsequent glove juice testing in a tertiary teaching hospital finding a significant

increase between the transfer efficiency of pathogens to gloved vs. ungloved hands (see Figure 6.8). This translated to 3 CFU/min on average with gloves vs 16 CFU/min in the ungloved case. Interestingly they noticed a clear trend indicating that HCW who wore gloves were less likely to disinfect their hands post-event. A linear link had then been established between the bacterial colony count on the hands and the length of the duration of the care. This led the researchers to interpret that the HCW erroneously believe the gloves to be impermeable to pathogens. Gloves made from latex or nitrile compounds are hydrophobic in nature, naturally repelling hydrophilic microorganism [276]. Their data is presented in Figure 6.8 and may appear bimodal in nature, however truncation of results are noted due to measuring techniques particularly with respect to maximum colony counts on Petri dishes.

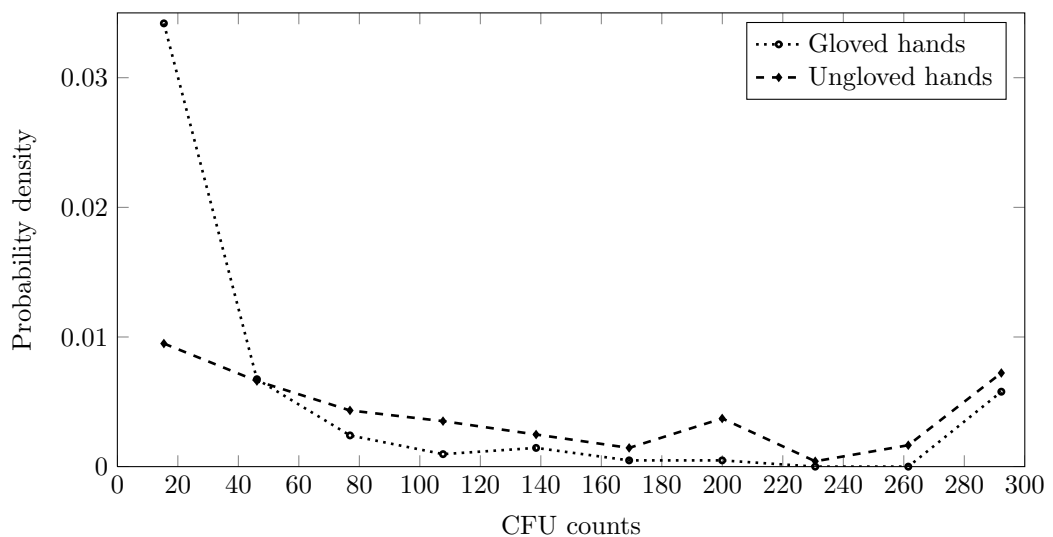


Figure 6.8: Distribution of CFU adhering to nurses' hands after care, comparing gloved vs. ungloved hands. Data reproduced from Pittet et al. [22].

Montville et al. [279] demonstrate the partial effectiveness of the glove as a physical barrier, in particular highlighting the higher adherence % of Gram-positive bacteria to skin through latex gloves during cutting and moving chicken pieces. These results are also supported by investigating the transfer from a fomite such as a water tap to hands. However “*A dirty hand in a clean glove*” [242] highlights the permeability of latex gloves to pathogens both resident and transient. Research also suggests that permeability of gloves increases over time, such as when handling food. However this current study considers only relatively

short care activities and hence will assume constant transfer [280]. Epic2 [28] stipulates that hand-washing should take place after de-gloving, however this was only observed in 8% of the cases at YAB and the effects of hand-antiseptics on very low inocula has not been experimentally characterised. Therefore this research will focus on sole hand antiseptics after each episode of care (see Table 6.4).

Lead author	Ref.	Distribution	In-vivo (i) /-vitro (t)	Organism
Montville	[279]	$\Gamma \sim (5.91, 0.40)$	t	Bacillus spores

Table 6.4: Literature for % transfer through clinical permeable gloves onto hands.

#### 6.4.5.2 Hand washing

Hospitals in the UK are at liberty to choose and use a variety of handwashing products, including both plain and antimicrobial soaps. The latter, as outlined in Chapter 5 includes 4% minimum Chlorhexidine gluconate (CHG), triclosan and iodophor products [28], the former being the most common. Blood and bodily fluids however have been shown to inactivate the active ingredient in CHG and thus is not used universally [249]. Montville et al. [23] highlight the difference between standard plain soap and antimicrobial soap, where the latter performs statistically better when sufficiently high inocula are used during testing. Differences between results and cohorts of participants appear to be somewhat vague below inocula levels of  $10^5$  CFU per surface. Montville et al. [23] suggest through meta-analysis that the most important factors in hand hygiene efficacy are the soap type followed closely by hand drying method along with the use of a sanitiser. Inoculum size was shown to be highly significant when reporting  $\log_{10}$  CFU reductions, with realistic values of 5-7  $\log_{10}$  demonstrating the full effect of the antimicrobial soaps tested. A test of the same anti-sepsis agent should be conducted against incremental inocula sizes to verify this claim and hence avoid confounding factors such as variation in experimental method or compound preparation. Nevertheless a significant positive linear correlation was found between inocula size and log reduction. A minimum level of inocula was shown to be particularly important when evaluating hand-antiseptics efficacy, where statistically anomalous  $\log_{10}$  increases were noticed at inocula values below adequate detection levels

( $2 \log_{10}$  CFU). Resident microflora also proved to be statistically harder to remove compared to exogenous organisms in all experiments conducted, the rationale for which was thought to be one of two reasons: Firstly the inocula levels were insufficient to produce accurate experiments or secondly the physical attachment characteristics of endogenous microflora may be actually different. No significant differences were found between Gram-positive and Gram-negative bacteria however (see Figure 6.9). This raises the question of whether certain hospital pathogens can actually be considered endogenous to HCWs's hands [22].

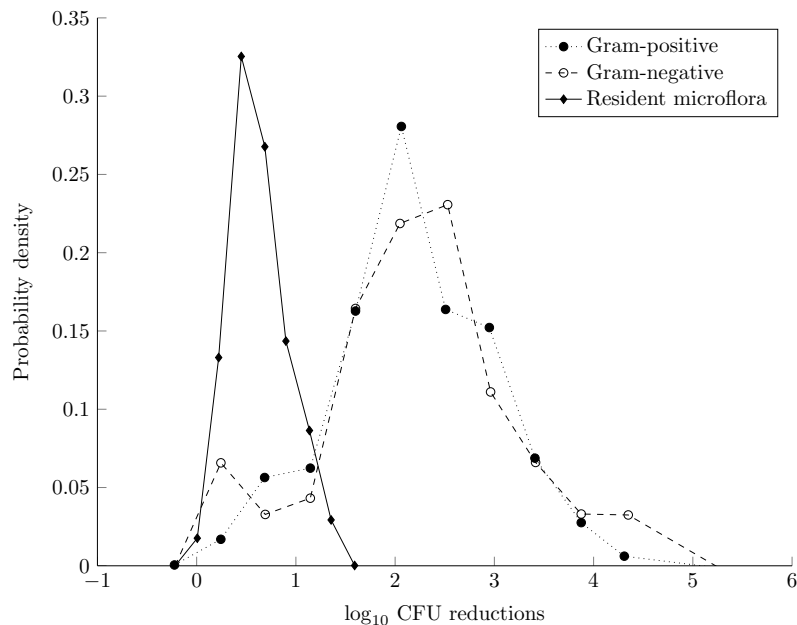


Figure 6.9: Hand hygiene efficacy of antibacterial soap comparing resident vs. exogenous microflora reduction (data from Montville et al. [23]).

Sickbert-Bennet et al. [281] conducted an extensive laboratory study of typical handwashing agents used on hospital premises, two of which were in use at YAB: A waterless foam 62% alcohol rub and antibacterial soap and water. They used *Serratia marcescens*, a Gram-negative bacteria, along with MS2 bacteriophage both of which pose a low risk to humans but that serve as surrogate organisms. The inherent variability in hand washing seen in the published literature [23], particularly within the food protection industry, underscores the importance in efficacy differences between removal of Gram-positive and Gram-negative bacteria as well as viruses. Emphasis is also made on discrepancies between ease of elimination of exogenous (or foreign) rather than endogenous microflora.

Therefore, the data is not amalgamated and forms a normal distribution curve of  $\log_{10}$  reductions.

Girou et al. [282] conducted in-vivo testing of the efficacy of alcohol rub and antimicrobial soap against CFU counts. Their methodology used hand imprints on Petri dishes and subsequent dilution and culturing techniques rather than glove-juice analysis. Marked differences were noted over results obtained by Sickbert-Bennet [281]. It appears that in-situ (in-vivo) testing, under less stringent conditions results in efficacy substantially lower than previously suspected during in-vitro testing. This may be related to the theory proposed by Montville et al. [269], that inocula sizes under a certain level cannot accurately predict the efficacy of the hand-antiseptics, where detection and variation errors dominate.

According to published experimental data by the CDC hand washing with plain soap for 15s achieves a microbial reduction of of 0.6-1.1  $\log_{10}$  which increases to 1.8-2.8 $\log_{10}$  after 30 seconds [283]. However, hand washing within hospital scenarios of typically <10 seconds [20]. Therefore, hand washing with bland or plain soap may fail to remove the stated amount of exogenous microflora under heavy burdens. Minimal decreases or indeed minimal increases in resident microflora have been associated with the daily use of soap and water [284].

Lead author	Ref.	$\log_{10}$ reduction	i/t	Antiseptis agent	Organism
Girou	[282]	(1.40 - 1.97)	i	4% CHG	Gram +ve bacteria
Larson	[249]	(1.2 - 2.1)	i	4% CHG	Gram -ve bacteria
Montville	[23]	(2.42 $\pm$ 0.88)	t	Plain soap	Gram -ve bacteria
Montville	[23]	(1.91 $\pm$ 0.75)	t	4% CHG	Gram -ve bacteria
Sickbert-Bennet	[281]	$N \sim (1.89, 0.1)$	t	4% CHG	Gram -ve bacteria
Sickbert-Bennet	[281]	(0.70 - 2.01)	t	4% CHG	MS2 bacteriophage
Weber	[284]	(2.1 - 2.4)	t	Plain soap	Bacillus spores
Weber	[284]	(1.1 - 2.2)	t	2% CHG	Bacillus spores

Table 6.5: Literature for  $\log_{10}$  reductions of CFU for hand-washing. Where i=in-vivo and t=in-vitro, and CHG denotes chlorhexidine gluconate.  $N \sim (\mu, \sigma)$  represent the normal distribution with parameters  $\mu$  and  $\sigma$ .

### 6.4.5.3 Alcohol rub

Results obtained by Girou et al. [282] consistently showed that alcohol rub under-performed significantly in comparison to antimicrobial soap when experiments were carried out in-vivo on HCWs' hands. In fact, results showed that either a neutral or negative effect was shown on resident flora. Hand rubbing length only showed minor increases in reduction from 10-120 seconds. Discrepancies with these results were found by Weber et al. [284] however, where the alcohol rubs (61 and 62% ethanol by volume) often outperformed antibacterial soap under laboratory conditions. Sickbert-Bennet et al. [281] conduct an extensive investigation comparing alcohol rubs against antimicrobial soaps but cannot substantiate Weber's claim for Gram-negative bacteria. Further in-vitro tests against MS2 bacteriophage further negated this claim, where significant increases of organism counts were found after alcohol usage.

Widmer et al. [276] conclude that in general waterless hand-rub is an ideal replacement for hand-washing both for time-saving purposes and level of antiseptis. Table 6.6 shows the typical ranges of  $\log_{10}$  reductions used to formulate the hand-hygiene input parameter ( $h$ ) in PAM.

Lead author	Ref.	$\log_{10}$ reduction	i/t	Antiseptis agent	Organism
Girou	[282]	(1.85- 1.98)	i	62% alcohol	Gram +ve bacteria
Sickbert-Bennet	[281]	(-0.66 - 0.15)	t	62% ethanol	MS2 Phage
Sickbert-Bennet	[281]	(1.19 - 1.83)	t	62% ethanol	Gram -ve bacteria
Sickbert-Bennet	[281]	$N \sim(1.10,0.81)$	t	62% ethanol	Gram +ve bacteria
Weber	[284]	(-0.2 - 0.2)	t	61% ethanol	Bacillus spores

Table 6.6: Literature for  $\log_{10}$  reductions of CFU for waterless alcohol rub, displayed as a continuous distribution or as a range. Where i=in-vivo and t=in-vitro testing.

#### 6.4.5.4 Summary

Based on the literature findings it is important to differentiate between clinical settings where inocula are often small and laboratory results, where inocula levels are generally higher whereby avoiding erroneous or biased results. Inocula levels on HCWs' hands tended to be often quite low  $0.75 \log_{10} \sim 2.5 \log_{10}$  CFU [285], but never exceeding  $3 \log_{10}$  CFU in the case of Pittet et al. [22]. This was often due to the detection technique such as glove-juice methods [39]. Soap volume (in millilitres) or hand-wash time appeared to exert no strong distinguishable effect on  $\log_{10}$  reductions, nor was there any sizeable discrepancy between bland soap and antimicrobial soap when analysing these variables [23]. Hence this study will judiciously err on the side of caution, sampling hand hygiene efficaciousness from published literatures only where significant sample sizes are available [23] such as the data in Figure 6.9. Microorganism type also appears to exert a difference on transfer efficiency or hand hygiene efficacy, which is likely to be due to their individual adherence properties. Particular difference is noticed between bacteria and viruses (or bacteriophage), where removal of the latter is often an order of magnitude lower. Nevertheless bacteria is the primary concern of many infection control teams, where *MRSA* or *C.Diff* rank highest on the prevention list. Consequently a broad view is taken, taking into consideration a wider distribution in order to be less organism specific.

## 6.5 Preliminary Results and Validation

Based on each type of care laid out in Section 5.3.1 PAM was calculated via Monte-Carlo sampling in Matlab (R2012a). Values were drawn from the above distributions for 1,000 HCWs to produce CFU ( $Y$ ) for each type of care based on:

$$Y \sim Y(\lambda, h, A, V, \beta, n)$$

Figure 6.11 shows a scatter plot of CFU values against the total number of surface each HCW touched while performing an episode of *direct care*. At first glance the data appears to positively correlated. That is to say, that as the number of surface contacts increases so does the final CFU value; which is a logical trend given the construction of PAM.

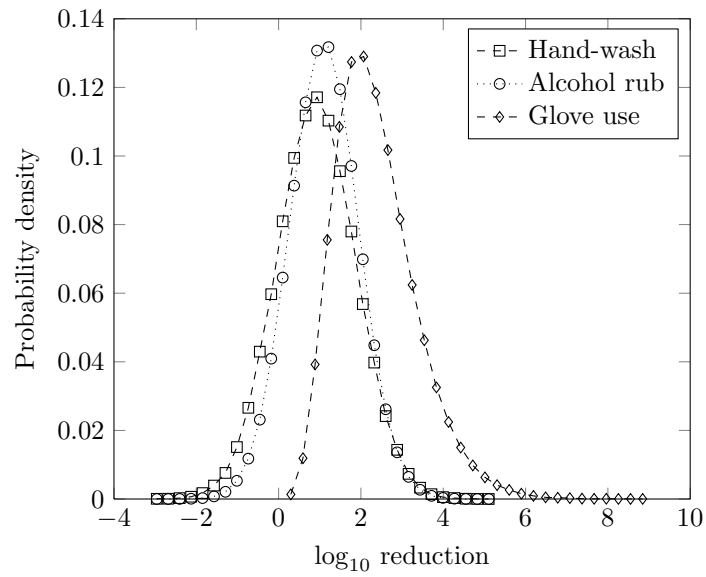


Figure 6.10: Hand hygiene efficacy of three different types of hand-antiseptics. Data from Montville et al. [23].

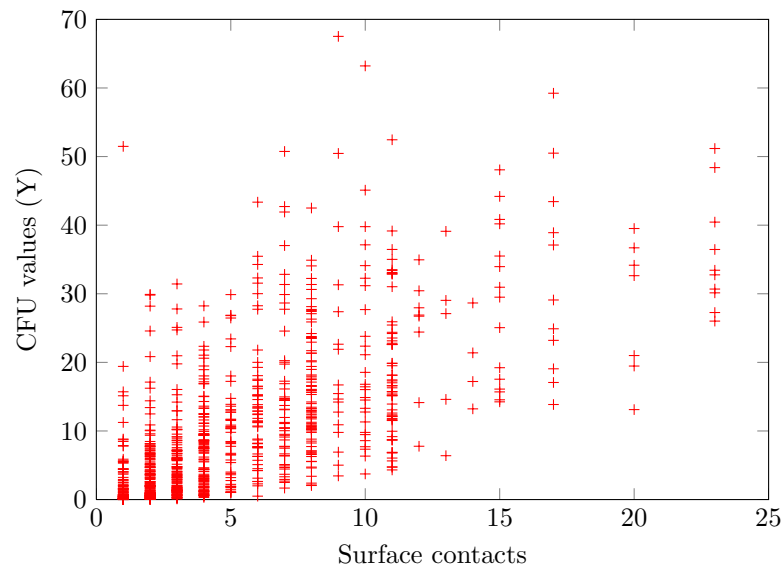


Figure 6.11: Scatter plot of CFU (Y) against patient contact for *direct care*.

The important question now is: “To what extent is this model realistic?” Making good estimates of the input parameters is only half way there. Published validation data which measures contamination levels of HCWs’ hands is very scarce. In particular, Pittet et al.’s [22] is the only known published study to exist that quantifies both CFU values along with the time spent in the room by the HCW. However their methodology does not include surface swabbing and hence a specific value for  $V$  cannot be estimated. Nevertheless let us assume that other variables such as HCW hand surface area, surface types and nursing behaviour are comparable between scenarios. Therefore it is reasonable to compare the distribution parameters such as the shape of the resultant plots of CFU counts. Data produced by PAM is hence compared against the empirical data published by Pittet et al. (and reproduced in Figure 6.8).

Rather than attempting to convert surface contacts to time spent in the room and perform ANOVA on the two data samples, a visual quantile-quantile plot (or QQ-plot) is shown in Figure 6.12. Since every hospital has its own microbial burden absolute values are not of interest here, but the closeness to linearity of the data comparison. This is a robust linear fit of the two samples. The solid red line joins the first and third data quartiles, where the dashed portion extrapolates the solid line. Good comparison is shown particularly at lower (first quartile) values ( $p=1 \times 10^{-3}$ ), where a higher concentration of data exists. Higher values on both sides become scarcer and the fit performs less aptly ( $p=0.12$ ). The reader must note that detection levels by glove-juice and subsequent Petri-dish techniques carried out by Pittet et al. have lead to truncated data, where colony counts over 300 were rounded down to 300 CFU. If this data were extrapolated, potentially a tighter fit may be produced ( $p \simeq 0.02$ ). However, pending greater sources of data, it is not unreasonable to conclude that at least through the first two quartiles or the first 50% of CFU colonisation levels, PAM is a capable and realistic model.

## 6.6 Model Sensitivity Analysis

Quantitative sensitivity analysis (SA) of a mathematical model addresses two of the fundamental questions surrounding the effect that input parameters have on the overall output uncertainty [286]:

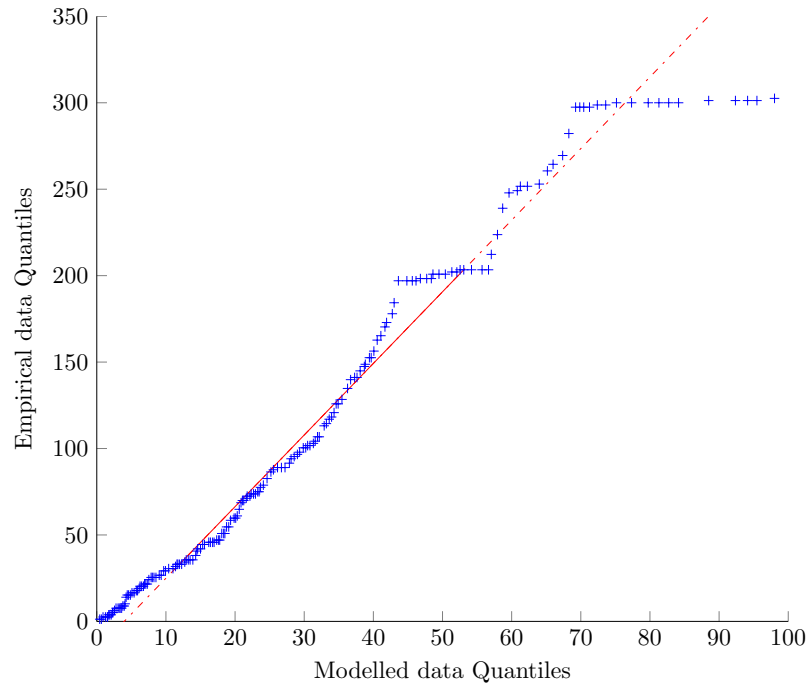


Figure 6.12: Q-Q plot of published empirical data from Pittet et al. [22] against modelled data by PAM.

1. “Which of the input variables’ variance influences the model output variance the most?”
2. “Which of the input variables have to be known more accurately to reduce output variance?”

Existing literature concentrates on two categories of sensitivity analysis: local and global SA. Local SA studies show some small variations of inputs around a given value change in the value of the output. Typically this is done by partial derivatives of the model output  $Y$  with respect to a given input factor  $X_i$  evaluated at its baseline  $x_0$ . Consider the model:

$$Y = f(X_1, X_2, X_3, \dots, X_n) \quad (6.6.1)$$

Where  $X$  is a set of  $n$  non-zero input parameters drawn from some distributions. Then:

$$\left. \frac{\partial Y}{\partial X_i} \right|_{x_0}$$

However we cannot use this method on the current model due to it being defined as a recurrence relationship, i.e.  $Y_i = A_i V_i \lambda_i - \beta Y_{i-1}$ . This does not yield a easily definably analytical derivative and instead we should seek other numerical methods as follows. Global SA takes into account all the variation ranges of the inputs, and apportions the output's uncertainty to the uncertainty in the input factors. For the subsequent chapter we will make use of global SA. It is worth mentioning that in SA type I errors are those that are made by incorrectly suggesting that a non-influential factor is important. Type II errors are defined as finding important factors uninfluential. It is also worth including errors of type III which refer to analysis of input factors which are completely off the mark. [264].

### 6.6.1 Methodology

Common methods of sensitivity analysis amongst modellers leads to the application of what is known as a perfunctory 'One-factor-at-a-Time' analysis [287]. This technique fixes all-but-one input variables and allows this to vary over some 'best guess' threshold. The resulting output variance is then deemed to be solely due to the variation of the one input factor which was allowed to vary. However what is not accounted for here is the interaction between input factors, which may be exacerbated by the extent of uncertainty of all factors. Hence, once this method is judiciously excluded, the choice of SA techniques will depend mainly on the following factors:

- The computational cost of the model
- The number of input factors
- Model features such as additivity

#### 6.6.1.1 Effect of unobserved Markov chain transitions

The implicit variable of Markov transition probabilities needs to be treated separately to all other explicit parameters of the model. As discussed in Section 6.3.1.3, sparse transition matrices  $\hat{P}$  may cause certain transitions  $i \rightarrow j$  to appear impossible. However, through the use of bootstrapping and smoothing techniques, some variation can be accounted for

in  $\tilde{P}$ . Confidence intervals at the 5% level show where the bulk of the bootstrapped transition probabilities reside. Consequently, this has an effect on the HCWs'  $Y$  value. The CFU count on a 1000 HCWs was calculated based on the lower and upper confidence interval transition matrices  $\tilde{P}_{\text{lower CI}}$  and  $\tilde{P}_{\text{upper CI}}$  respectively. These individual values were compared against the values for  $Y$  computed based on the maximum likelihood estimate  $\hat{P}$  for each care type:

$$\frac{|Y(\hat{P}) - Y(\tilde{P}_{\text{lower CI}})|}{Y(\hat{P})} \times 100, \quad \frac{|Y(\hat{P}) - Y(\tilde{P}_{\text{upper CI}})|}{Y(\hat{P})} \times 100,$$

Percentage differences are quantified in Figure 6.13. *Mealtimes* shows the lowest discrepancy, largely because the care is so regimented. The opposite is reflected well in *personal care*.

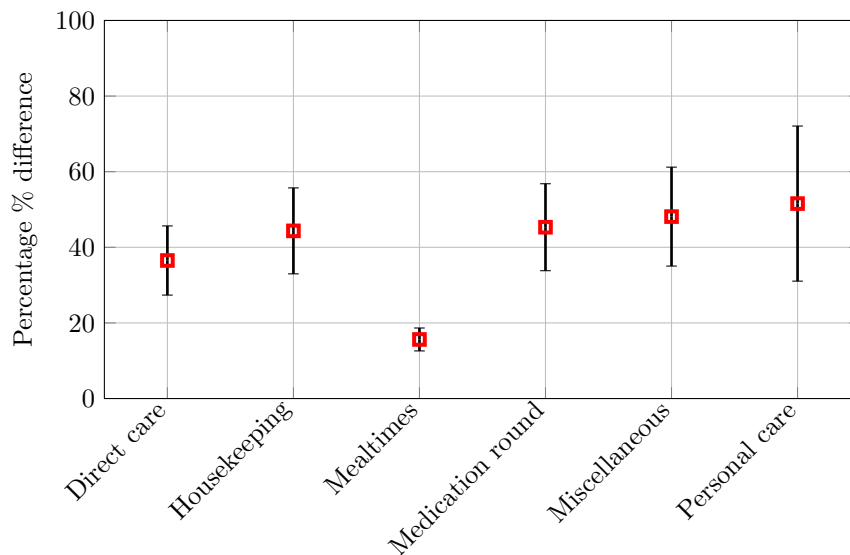


Figure 6.13: Confidence intervals representing the percentage difference between mean  $Y$  values calculated by the maximum likelihood estimates  $\hat{P}$ , and those calculated by  $\tilde{P}_{\text{lower}}$  and  $\tilde{P}_{\text{upper}}$ . Errorbars represent one standard deviation either side of the mean.

## 6.6.2 Pearson Correlation Analysis

Graphical methods play an important role in all sensitivity analysis by means of of visualising the relationships between the input parameters and output factors. Initial investigation

of the effect of parameters on the output  $Y$  can be done via visual scatter plots of input factors (see Figure 6.14). One way of interpreting each figure is that they maintain the value along the x-axis fixed while all other parameters vary. Alternatively they can be seen as allowing all parameters to vary and choosing to plot only one variable against the output in each instance.

Correlation between variables is investigated initially by the use of the Pearson's product-moment introduced in Chapter 5. Briefly, this parametric technique provide a measure of the strength of the linear relationship between two variables where covariance of the two variables is divided by the product of their standard deviations.

Pearson's correlation coefficient ( $r$ ) is given for two samples by:

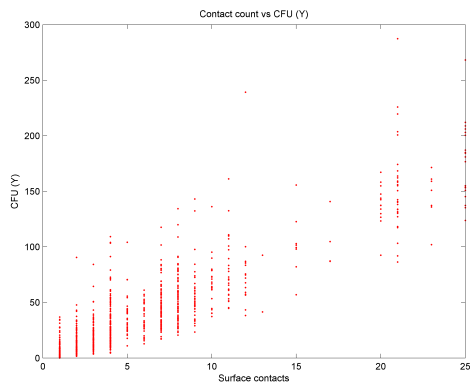
$$r = \frac{\sum_{i=1}^n (X_i - \bar{X})(Y_i - \bar{Y})}{\sqrt{\sum_{i=1}^n (X_i - \bar{X})^2} \sqrt{\sum_{i=1}^n (Y_i - \bar{Y})^2}}$$

where  $\bar{Y}$  is the sample mean and  $Y_i$  are the original values. The geometric interpretation of this value is the cosine angle between the linear regression lines of both samples given by: A linear regression model of an  $N \times k$  input sample  $X$  against the output  $Y$  takes the form:

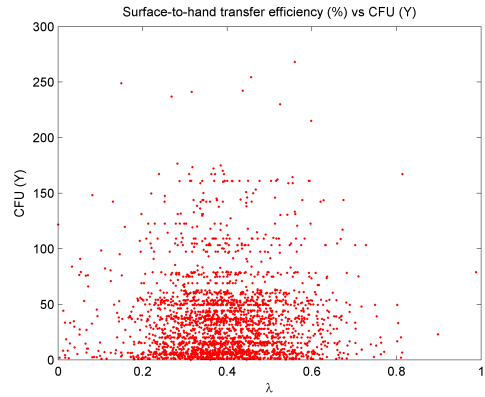
$$Y_i = \beta_0 + \sum_{j=1}^k \beta_j X_{ij} + \epsilon_i$$

where  $\beta_i$  are regression coefficients to be determined and  $\epsilon_i = Y_i - \hat{Y}_i$  is the approximation error. And were  $\hat{Y}_i$  is the approximated output obtained from the regression model and  $Y_i$  are the original values and hence  $\bar{Y}$  is their mean.

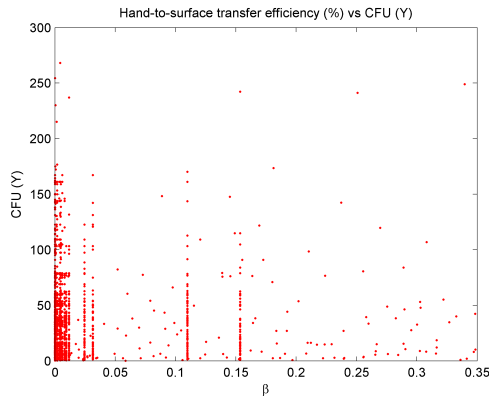
Table 6.7 displays the Pearson correlation coefficients  $r$  and the corresponding p-value for input factor plotted against the output CFU value ( $Y$ ). The p-value is the probability that a correlation is found if in reality there is none, whereby a significance test is performed on the gradient of the resulting linear regression line. That is to say the null-hypothesis is that the correlation is zero. Surface contacts ( $n$ ) appears to be the most important factor in determining the cumulative CFU count, with a strong linear correlation. This is also verifiable through Figure 6.14a where a linear trend is observed, not exempt of noise however. The interactions or influences of the other variables are not quite so visibly quantifiable. Pearson's test reports the influence of each parameter on the output value



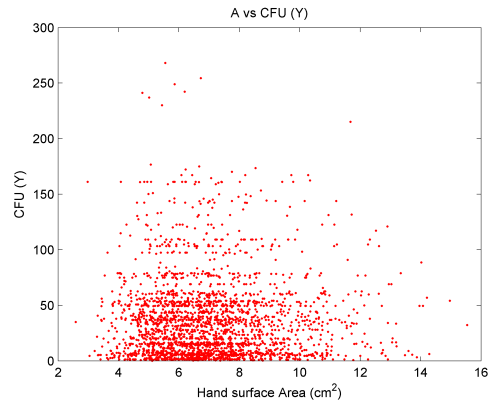
(a). Surface contacts ( $n$ ) vs.  $Y$



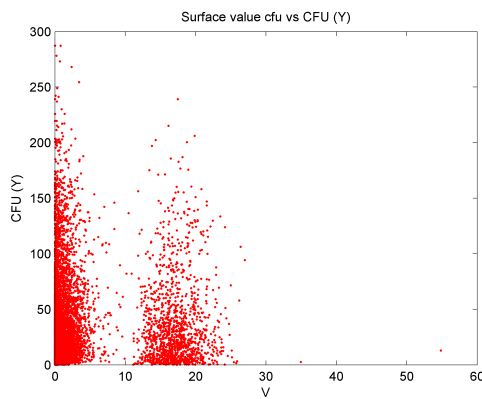
(b). Transfer efficiency  $\lambda$  vs.  $Y$



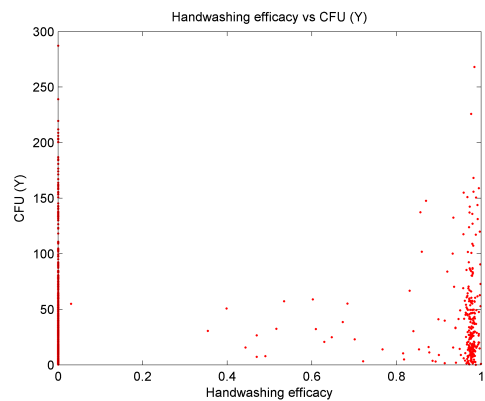
(c). Transfer efficiency  $\beta$  vs.  $Y$



(d). Hand surface area ( $\text{cm}^2$ )  $A$  vs.  $Y$



(e). Surface  $\text{CFU}/\text{cm}^2$  count  $V$  vs.  $Y$



(f). Hand hygiene efficacy  $h$  vs.  $Y$

Figure 6.14: Visual inspection of input parameters plotted against output  $Y$ .

by considering linear correlation. Ranking of correlation coefficient values according to their  $r$ -value implicitly implies importance of a parameter on the variation of the output variable.

	Variable					
	<b>n</b>	<b>A</b>	<b>V</b>	$\lambda$	<b>h*</b>	$\beta$
<b>Corr. coefficient. <math>r</math></b>	0.775	0.085	0.251	0.0182	0.0259	-0.0179
<b>p-value</b>	0.001	0.0891	0.0982	0.0671	0.4	0.0716
<b>Rank by r-value</b>	1	3	2	5	4	6

Table 6.7: Pearson correlation coefficient comparing  $Y$  against the different variables. \* indicates inclusion of probability of hand-antiseptics not just efficacy.

A lower p-value means a more trustworthy correlation, however in the case of hand-washing efficacy Pearson's correlation indicates that the strength of the correlation is poor. However it is important to review this in the visual relationship shown in Figure 6.14f. It can be seen hand-hygiene efficacy appears to exhibit bimodal properties, which is a reasonable assumption given that hand hygiene compliance varies between care type. Clearly this is a binary function with either hygiene taking place and being somewhat efficacious or not taking place at all. Removing those episodes where hand hygiene is not performed yields an  $r$  value of 0.68 with a p-value of 0.04. Surface CFU/cm<sup>2</sup> ( $V$ ) can be seen to be ranked in second position, some way behind the effect of  $n$ , with only a weakly linear influence. Although experimental results tentatively suggest a dependence of transfer efficiency ( $\lambda$ ) on inoculum size, effectively rendering it a function of  $V$  thus:  $\lambda = \lambda(V)$ . There is insufficient data to substantiate this and this particular model does not consider it. Instead scenarios with lower inoculum sizes are contemplated here as representing realistic hospitals. Ranking of parameters by influence can only be achieved qualitatively through Pearson's correlation, where their actual quantitative influence of the individual parameter cannot be measured directly. Therefore a more sophisticated method of sensitivity analysis is required and described subsequently.

### 6.6.3 Sobol Indices $S_i$

Calculating a Sobol index offers another approach to exploring sensitivity. Variance based techniques are best suited to this type of sensitivity analysis because they are model-independent or model-free and have the ability to capture interactions between input factors that are not limited to a small range of values in the factors. The latter often is the case when looking only at scatter plot variations. Each simulation run used here requires less than a second of CPU time which allows scope for the variance-based Sobol techniques.

Different input factors can be denoted in general by  $X_i$ , where  $i = 1 \dots d$  and in our case  $X = (A, V, \lambda, \beta, n, h)$ . Without loss of generality any function  $Y = f(X)$  can be decomposed into the unconditional expectation  $E(Y)$  and the conditional expectation on  $X_i$   $E(Y|X_i)$ :

$$f(X) = f_0 + \sum_{i=1}^d f_i(X_i) + \sum_{i<j}^d f_{ij}(X_i, X_j) + \dots + f_{12\dots d}, \quad (6.6.2)$$

where  $f_0$  is a constant and  $f_i$  is a function of  $X_i$ , and  $f_{ij}$  is a function of  $X_i$  and  $X_j$ , etc. In particular:

$$f_0 = E(Y) \quad (6.6.3)$$

$$f_i(X_i) = E(Y|X_i) - f_0 \quad (6.6.4)$$

$$f_{ij}(X_i, X_j) = E(Y|X_i, X_j) - f_0 - f_i - f_j \quad (6.6.5)$$

$$(6.6.6)$$

It can be noted that  $f_i$  is the effect of varying  $X_i$  alone, and is known as the main effect. The conditional expectation  $E(Y|X_i)$  can be calculated by splitting up the scatter plot in Figure 6.15 into arbitrarily thin slices (e.g. red box in Figure 6.15) along the  $X$  axis and averaging the values of  $(Y|X_i)$  within the same slice  $X_i$ . If this conditional expectation is found to vary strongly across the range of  $X_i$  then this would indicate that  $X_i$  was an important factor.

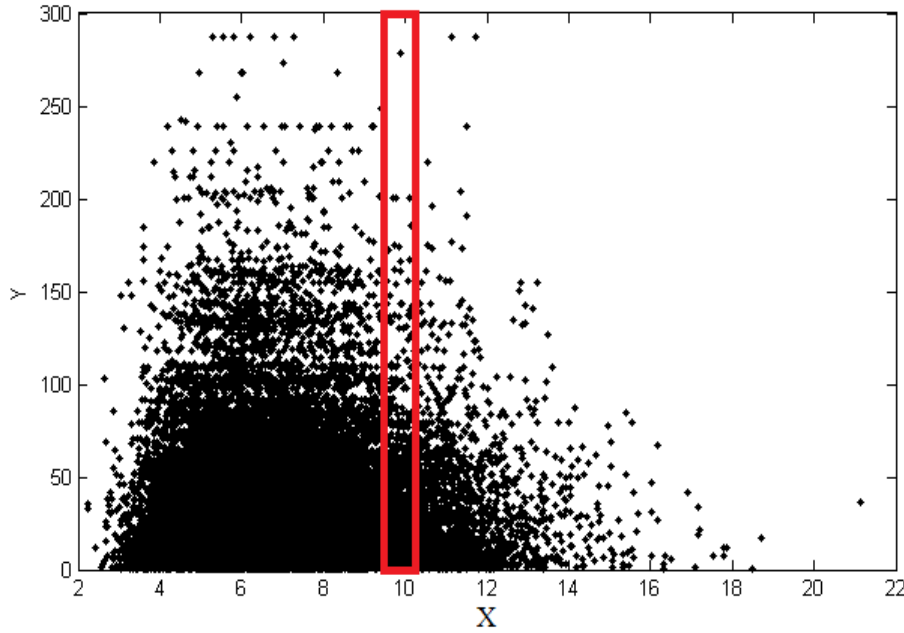


Figure 6.15: Conditional variance of  $Y$  within the red box representing a specific value  $X_i = x_i^*$

Unconditional variance  $V(Y)$  is the variance calculated by allowing all input factors to vary. Fixing a parameter  $X_i$  at a baseline value  $x_i^*$  yields a corresponding output  $Y$  (within the red box in Figure 6.15). The variance due to this factor fixing taken over all factors apart from  $X_i$  (i.e.  $X_{\sim i}$ ) is called the conditional variance and is given by:

$$V_{X_{\sim i}}(Y|X_i = x_i^*) \quad (6.6.7)$$

To avoid the variance due to fixing of a factor  $X_i$  becoming larger than the unconditional variance we take the expectation of Equation (6.6.7):

$$E_{X_i}(V_{X_{\sim i}}(Y|X_i = x_i^*)) \quad (6.6.8)$$

and in particular by the law of total variance:

$$E_{X_i}(V_{X_{\sim i}}(Y|X_i = x_i^*)) + V_{X_{\sim i}}(E_{X_i}(Y|X_i = x_i^*)) = V(Y) \quad (6.6.9)$$

Hence the influence of a particular factor can be seen directly on the unconditional variance when either  $E_{X_i}(V_{X_{\sim i}}(Y|X_i = x_i^*))$  is small or  $V_{X_{\sim i}}(E_{X_i}(Y|X_i = x_i^*))$  is large. A

sensitivity measure is given by:

$$S_i = \frac{V_{X_{\sim i}}(E_{X_i}(Y|X_i = x_i^*))}{V(Y)}, \quad 0 \leq S_i \leq 1 \quad (6.6.10)$$

A high value of  $S_i$  indicates an important factor. However a low value does not necessarily mean the opposite. Properties which will help with interpreting  $S_i$ :

- $S_i$  is the measure of how much the variance of  $Y$  could be reduced if  $X_i$  was fixed.
- By Equation (6.6.9)  $0 \leq S_i \leq 1$ .
- $\sum^i S_i = 1$  for additive models and less than 1 for non-additive models. Then  $1 - \sum^i S_i$  is an indication of factor interaction.

#### 6.6.4 The Total Effect $S_{Ti}$

A measure of non-linear or in particular the effect of factor interaction can be obtained from the Total-effect index  $S_{Ti}$ . This is the contribution of the output variance of  $X_i$ , including all variance caused by its interactions with any other input variable thus:

$$S_{Ti} = \frac{E_{X_{\sim i}}(V_{X_i}(Y|X_{\sim i}))}{V(Y)} = 1 - V_{X_{\sim i}}(E_{X_i}(Y|X_{\sim i}))V(Y) \quad (6.6.11)$$

Properties which will help with interpreting  $S_{Ti}$ :

- $S_{Ti} \geq S_i \Leftrightarrow X_i$  does interact with other factors.

Calculation of Sobol indices of both kinds are achieved numerically as follows: Quasi Monte-Carlo sampling of the distributions in a  $2 \times d$ -dimensional hyperspace were performed in Matlab (2012a MathWorks, MA, USA) and the Sobol indices were calculated using the software package SimLab 2.2.1 [Joint Research Centre of the European Commission]. Table 6.8 shows the Sobol first order indices  $S_i$  and Total order indices  $S_{Ti}$ . PAM is a non-linear recurrence model, which is highlighted by  $\sum^i S_i = 0.827$ , being an indicator of mild non-linearity. However it is also important to note that notable interaction between input factors is shown since  $S_{Ti} \geq S_i \forall X_i$ .

Input factor	First order indices $S_i$	Total order indices $S_{T_i}$
V	0.460152	0.562448
h	0.254362	0.269509
A	0.081124	0.120292
$\lambda$	0.037128	0.093935
$\beta$	9.05e-6	1.94e-5
TOTAL	0.827	1.045

Table 6.8: First order and total sensitivity factors for each input factor for PAM

### 6.6.5 Linear Loading of CFU (Y) Without Deposition

According to SA methods  $\beta$  has been shown to exert the smallest influence on the final CFU count (see Table 6.7 and Table 6.8). It may be considered reasonable to discard this term entirely and simplify the model to a purely linear form. Then since this would assume no deposition, the function of accretion could be described simplistically by the four parameters discussed above:

$$Y = f(V, \lambda, A, h) \quad (6.6.12)$$

In general surface-hand pathogen loading can then be described as the sum of independent contact events. Figure 6.19 shows the comparison between the resulting CFU values generated by Equation (6.6.13) and Equation (6.4.1).

$$Y = \sum_i^n \lambda_i V_i A_i (1 - h) \quad (6.6.13)$$

Comparison between bi-directional and unidirectional transfer by means of ANOVA show that no statistically significant difference exists at the 5% level ( $p=0.042$ ). Brouwer et al. support this conclusion suggesting that pathogen loading on the skin is far from saturation point and therefore non-porous surface contact will lead to negligible deposition. Despite this, Lopez [21] highlighted through in-vitro experimentation that deposition on non-porous hydrophilic surfaces such as glass and stainless steel is statistically non-negligible.

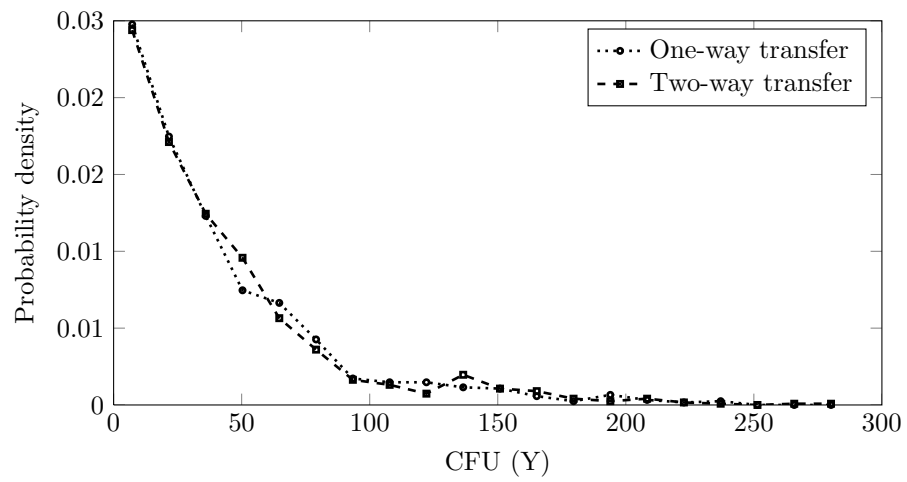


Figure 6.16: Comparison between unidirectional and bi-directional transfer of CFU

Therefore the statistical analysis should be treated with caution and henceforth the bi-directional model will be maintained in this study.

## 6.7 Uncertainty Analysis and Parametric Study

Uncertainty analysis which is also known as error propagation is the process of investigating the intrinsic error of a value that has been calculated from several measured quantities [264]. For example in this case hand-hygiene efficacy. An uncertainty cloud is the set of all possible data points within the parameter's range [254]. If one were 100% certain that the distributions of the input parameters were accurate, then an uncertainty cloud would essentially be multiple copies of the same input parameter distribution. In the more usual case, each point in the uncertainty cloud represents a potentially correct parametrization of the variability distribution for that input. The uncertainty cloud amounts to a set of variability distributions, each of which is given an equal chance of being representative for this target population. The cloud should span the range that could reasonably be assigned to this population, with a greater density of points in the more likely regions of the parameter space.

### 6.7.1 Care Type

The differences between types of patient care are discussed at length in Chapter 5. First a brief recap: 2011 saw the wide-spread introduction of a new nursing paradigm into UK hospitals which emphasised short but frequent periods of care: *Intentional rounding*. This brought the focus towards preventative rather reactive care. Consequently this also reduced paperwork and as a corollary was designed to reassure patients who felt isolated in single rooms, letting them know that a nurse wasn't far away. Care performed by the HCW is now categorised into: *Direct care, housekeeping, mealtimes, medication rounds, miscellaneous care* and *personal care*. Chapter 5 highlighted that the major differences between care types lies in the number of surfaces touched and the hand hygiene regimes/frequencies. However it did not tell us anything about the contamination level of HCWs' hands.

It is assumed that the underlying mechanisms of PAM do not change based on care type therefore by analysing the contamination levels we can indirectly distinguish between care types. Figure 6.17 displays boxplots of before and after hand-hygiene for each type of patient care. Rankings shown in Table 6.9 in order of CFU decontamination was found to remain the same both before and after, implying that hand-hygiene probabilities are

not significantly different between care types. Potential for contamination during *Personal care* was shown to be significantly higher than any other care type. Interestingly, however, *housekeeping* ranked second in both occasions.

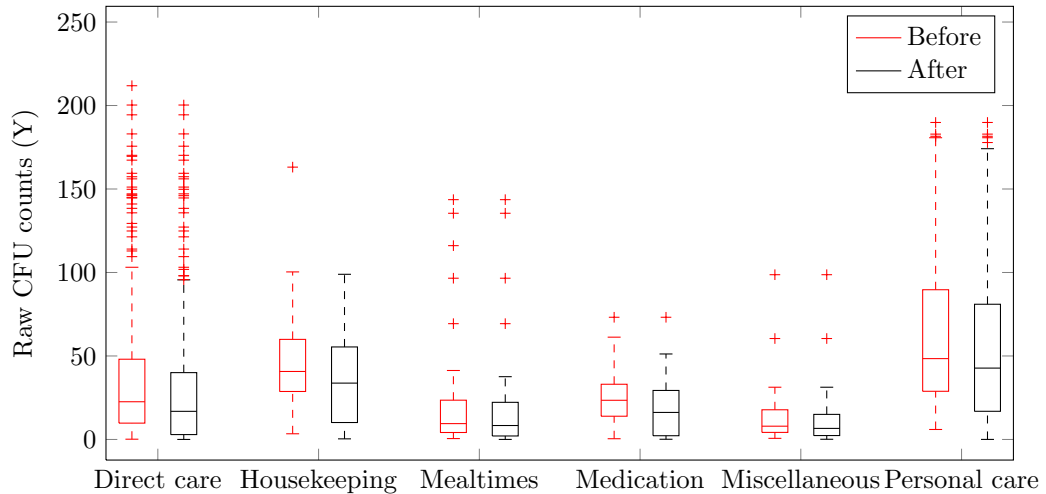


Figure 6.17: CFU count by care type before and after hand-hygiene

Table 6.9 shows the difference in handwashing between care types. The difference between mean before ( $\bar{Y}_b$ ) and the mean after ( $\bar{Y}_a$ ) show that on average *personal care* exhibits the largest reduction of hand contamination followed only closely by *housekeeping*. This is likely to be due to the possible use of gloves during these procedures.

	Care Type					
	Direct care	House-keeping	Meal-times	Medi-cation rounds	Misc-ellaneous	Personal care
$\bar{Y}_b - \bar{Y}_a$	6.8	10.9	10.7	4.5	2.4	16.9
$\log_{10}$ reduction	0.83	1.03	1.03	0.65	0.38	1.23
Ranking <sup>†</sup>	4	2	3	5	6	1

Table 6.9: Average decontamination of hands for all care types and rankings from best to worst performers. <sup>†</sup> lower ranking is better. Higher  $\log_{10}$  reduction is better. All hygiene types are included.

### 6.7.2 Increasing Hand-Hygiene Probability

The hand hygiene guidelines elaborated by the CDC [3] and the WHO [39] both place hand hygiene and compliance as the gold-standard in preventing infection transmission. Epidemics of gram positive spore forming bacteria such as *Clostridium difficile* has been linked with the use of alcohol-based hand rubs, despite no hand hygiene agents being reliably sporicidal [241]. Placing alcohol-rub as the most effective weapon in the control arsenal has proven controversial given the reliance on a ‘magic bullet’ solution. The WHO clearly states that 30 second handwashing procedures with soap are and remain the most basic intervention measure. Given time restrictions to all HCWs this appears almost unrealistic. However Allegranzi and Pittet highlight the factors influencing hand hygiene compliance amongst HCW: Primarily job status, under-staffing and the misguided belief that generic latex gloves and gowns are impenetrable to pathogens appear to be the most influencing factors. McGuckin et al. and Dancer et al. [25] highlight the effects of hand hygiene compliance programmes are often temporary, however do demonstrate that they are effective. In particular Sebille et al. [258] found that increasing hand hygiene compliance rates had only a modest effect on the prevalence of *MRSA* colonisation.

Consider the effects of a compulsory increase of hand hygiene compliance. That is to say, assume an hand-hygiene educational program could be implemented that on average increased the hand-antiseptic probability by 10% each time it was implemented, then what is the effect it has on the final CFU count?

Figure 6.18 shows how a linear regression model was fitted to the mean reduction CFU count showing on average a 10% increase in hand hygiene compliance is likely to result in a just over a 5% reduction in CFU count. In-vitro testing by Montville et al. [23] casts doubt on the linearity of hand antiseptic effectiveness however, suggesting an exponential relationship between inoculum size and  $\log_{10}$  reduction % during antiseptic. It may also be worth considering the realistic scenario where if the compliance increased, length of hand sanitising may decrease to compensate for the interpreted time loss to the HCW.

The percentage of nurse cohorting was considered to be the most effective intervention measure by Beggs et al. [32], however they reveal that despite a high level of cohorting amongst nurses, doctors move freely between patients. Indeed in their transmission model, pathogen transfer cannot be completely eradicated due to this. Dancer et al. again

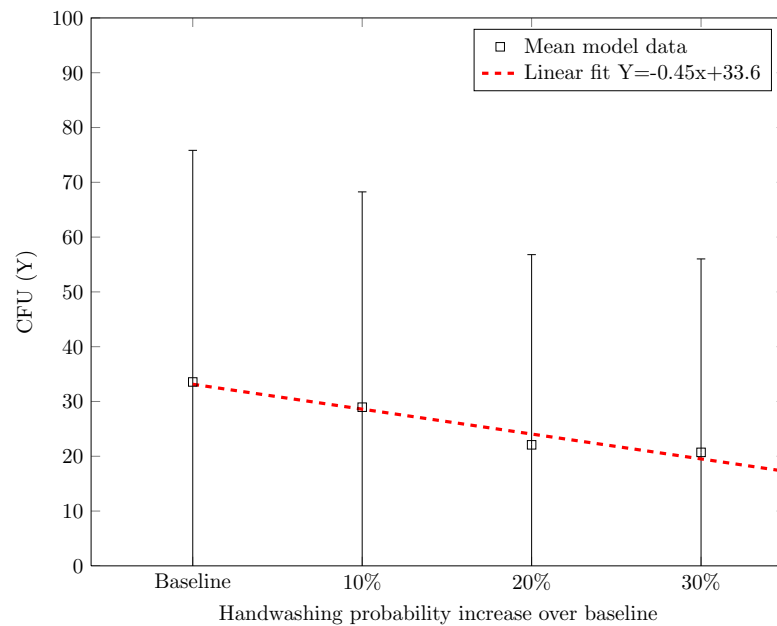


Figure 6.18: Comparison of CFU values due to improved hand hygiene. Errorbars represent one standard deviation either side of the mean.

suggests that doctors in white coats mistakenly believe that their hands and gown are exempt of full disinfection [24].

### 6.7.3 Increasing Surface Cleanliness ( $V$ )

Dancer et al. [24, 50, 167], Ayliffe et al. [48] and Lewis et al. [168] highlight the importance of surface cleanliness, in particular the frequency of cleaning high-touch surfaces. Huslage et al. [35] suggest that high-contact surfaces should undergo decontamination ‘frequently’ but do not assess the relationship between cleaning and surface CFU/cm<sup>2</sup> counts. ‘Frequent’ contact are those surfaces which are touched on average once or more during an episode of care. In the case of the reported data in Chapter 5 this is all the room surfaces observed. Dancer et al. [25] suggest a baseline cleanliness value of 2.5CFU/cm<sup>2</sup> for all surfaces.

Figure 6.19 shows a comparison between the WHO baseline 2.5CFU/cm<sup>2</sup> value for  $V$  and the empirically deduced values from the PaCE chamber experimental scenario. One-way analysis of variance suggests that the null-hypothesis of samples stemming from similar distributions should be rejected at the 5% level ( $p=0.034$ ). Recent research [166] suggests

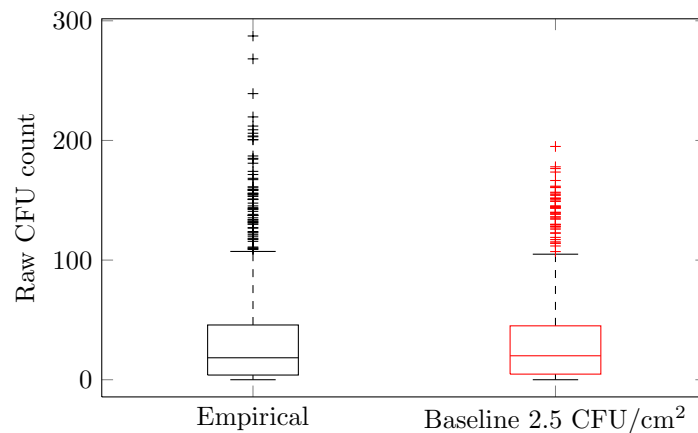


Figure 6.19: Comparison between model or empirical derived CFU counts and the baseline quantity proposed by Dancer et al. [24]

that a latent effect of detergent may in fact cause exponential re-growth after the 8 hour mark post cleaning of the hardest bacteria.

## 6.8 Summary

This chapter represents the creation and development of a flexible, but robust, mathematical model which calculates the CFU contamination level on a HCW's hands. Within the initial sections of the chapter, the relevant model parameters were explored and, where appropriate, continuous distributions fitted to empirical data. Output values compared well in distribution against available literature, thus providing a sensible framework for further data accretion. A sensitivity analysis by quasi-random Monte-Carlo sampling quantified the influence of the input factors described earlier and allows the user to judiciously discard those that create least variance in the output. Or more importantly, focus more effort in reducing the range of uncertainty of the most important factors. Subsequently an uncertainty analysis alongside a parametric study highlighted the differences between care type and colonisation loads. Surprisingly, *housekeeping* posed higher contamination levels than *direct patient care*. As a result the effectiveness of this cleaning procedure carried out by nurses may need to be rethought. The model also showed that an education program which induces a linear increase in hand hygiene compliance may not be as effective as previously considered.

Models that require empirically derived parameters are as a result, at best by definition restricted by the quality of available input data [171]. As a corollary variability of scenario investigation is also restricted by the extent to which the experimental data was tested. Pérez-Rodríguez et al. [259] consider that models that do not include terms which deal with pathogen decay will over predict transfer. However not only is *housekeeping* within UK hospitals carried out every 6 hours but the hardiest pathogens have been found to survive on surfaces days post terminal cleaning [51]. Physical pathogen brush-off or decay via natural causes or via delayed alcohol gel decontamination is not considered in this model. Both surface type (porous vs non-porous, hydrophobic vs. hydrophilic) and inoculum level have been shown tentatively to exhibit an important effect on the transfer of pathogens. To what extent remains unclear and hence this model does not distinguish between surface finishing or inoculum level. In such a case  $\lambda = \lambda(V)$  or potentially  $\lambda = \lambda(n, V)$ :

$$\lambda = \begin{cases} \alpha_1, & \text{hydrophobic surface;} \\ \alpha_2, & \text{hydrophilic surface.} \end{cases}$$

This model will be subsequently applied in Chapter 7 to different hospital room layouts, in particular to the standard single room at YAB and the HBN04-01 four-bed accommodation. This will facilitate comparison between scenarios through the use of a pre-established and validated indirect metric.

# Chapter 7

## Application of PAM and Quantification of Risk

### Contents

---

7.1	Scenario Description and CFD Case Set-Up . . . . .	241
7.2	CFD Results and Discussion . . . . .	247
7.3	Application of PAM to YAB Single Room and HBN04-01 Multi-Bed Accommodation . . . . .	257
7.4	Quantifying Patient Risk and Application of an Exponential Dose-Response Model . . . . .	263
7.5	Summary . . . . .	271

---

This chapter focuses on comparing single and multi-bed ward environments in terms of contamination through pathogens released from an aerosol source and subsequent accretion on the hands of health care workers. This draws on the CFD methodology of particle deposition presented in Chapter 4 to predict the spatial deposition pattern of a bioaerosols released from a quiescent patient in a single or multi-bed room. By combining this with the behavioural patterns of the HCW established in Chapter 5 and the validation of PAM in Chapter 6, the current chapter aims to compare the effect of room layout on the total contamination levels on the HCWs' hands during six different types of patient care. This will be used to compare the standard single room at Ysbyty Aneurin Bevan against the HBN04-01 guideline four-bed room. Subsequently, the infection risk to the patient will be

quantified by a dose-response model based on the observed patient contact frequency at YAB.

## 7.1 Scenario Description and CFD Case Set-Up

Two scenarios are considered in this chapter to compare single and multi-bed room environments. Initially, a typical hospital single room layout based on YAB is investigated and then compared against a standard four-bedded room, similar to wards at Bradford Royal Infirmary (BRI). Both rooms are assumed to be fully occupied, however only one patient is considered to be infectious in both scenarios. Initially the effect of ventilation on the HCW's dermal pathogen load is assessed at HTM03-01 [73] standard 6 air changes per hour ( $\text{ac.h}^{-1}$ ) against 4  $\text{ac.h}^{-1}$  within both the single room (cases 1-2) and then within the multi-bed ward (cases 3-6). All cases and description are shown in Table 7.1.

Case #	Room type	$\text{ac.h}^{-1}$	Bioaerosol release location
1	YAB Single	4	Patient head
2	YAB Single	6	Patient head
3	HBN04-01- 4 beds	4	Patient 1
4	HBN04-01- 4 beds	4	Patient 2
5	HBN04-01- 4 beds	4	Patient 3
6	HBN04-01- 4 beds	4	Patient 4
7	HBN04-01- 4 beds	6	Patient 1
8	HBN04-01- 4 beds	6	Patient 2
9	HBN04-01- 4 beds	6	Patient 3
10	HBN04-01- 4 beds	6	Patient 4

Table 7.1: CFD case names and layout.

Airflow patterns and subsequent particle deposition patterns are investigated using CFD. The CFD settings are as set out in Chapter 4. Simulation of turbulence follows the prescription of the RANS Reynolds' Stress Model with standard boundary wall resolution. Problem specific details are described in the following sections.

### 7.1.1 Single Patient Room: YAB

The room design at the recently built Ysbyty Aneurin Bevan hospital (YAB) at Ebbw Vale is based on standard HBN04-01 single room guideline. The layout of this has been previously described in Chapter 5: dimensions of the main room are  $4.7\text{m} \times 3.8\text{m}$  excluding the en-suite bathroom. Mechanical ventilation is provided by a four-way ceiling diffuser and extracted via a ceiling mounted grille in the en-suite bathroom (see Figure 7.1).



Figure 7.1: Photo of inside a single room at YAB.

#### 7.1.1.1 Model set-up

As this model is designed to represent an occupied room, a quiescent patient is characterised by means of a heated cuboid volume located on the bed. A sink along with a paper towel dispenser are located above the workstation opposite the bed, to the right of the entrance. A bed-side table, chair and windowsill are also modelled. The en-suite itself is not modelled as mainly the door remains shut and hence the air extraction is modelled as a transfer grille within the door itself. This is represented by a void as capturing fine detail in which the air exits the domain is not the primary concern [94]. Heat fluxes are applied to the patient as described in Chapter 4, which is also recapped in Table 7.2.

<b>Boundary name</b>	<b>Dimensions</b>	<b>Boundary value</b>
Bed(s)	$1 \times (1.9\text{m} \times 1.1\text{m})$	Stationary
Inlet diffuser	$0.5\text{m} \times 0.5\text{m}$	4 or $6\text{ac.h}^{-1}$
Outlet transfer grille	$0.3\text{m} \times 0.5\text{m}$	4 or $6\text{ac.h}^{-1}$
Patient	$1\text{m} \times 0.4\text{m}$	$56\text{W/m}^2$
Lighting	None	None
Window $\times 2$	$1.3\text{m} \times 0.8\text{m}$	Closed

Table 7.2: Boundary conditions for YAB single room.

### 7.1.1.2 Mesh generation

The model is similar in dimensions and characteristics to the control environment described and modelled in Chapter 4. Therefore the reader will be referred to page 129 Section 4.2.9 for full details on both validation strategy and results. Meshing is fully hexahedral with a maximum cell volume of  $1.5625 \times 10^{-5} \text{ m}^{-3}$  within the bulk domain and  $1 \times 10^{-6} \text{ m}^{-3}$ , 10cm away from all horizontal surfaces. Careful and high quality boundary meshing is essential to accurately capture particle deposition velocity [67]. Final cell count is in the region of 4 million volumes. Mesh dependency was evaluated at double the cell count as described in Section 4.2.8.1 showing only minor differences, less than 5% in the worst case. Reducing the cell size any further at the boundary would cause  $y^+$  values to drop below 1 under these conditions causing the standard boundary layer resolution techniques to become unreliable. Hence no further mesh size reduction should be carried out.

### 7.1.1.3 Bioaerosol injection

Release was replicated as per Chapter 4, where  $2.5\mu\text{m}$  sized inert particles were released via a volume source 10cm above the patient's head and given an inlet velocity of 1 m/s in the positive vertical direction. Sensitivity studies presented in Chapter 4 showed that 100,000 particles were sufficient to eliminate statistically significant variation. Bioaerosols are characterised within Fluent 13 (ANSYS, Canonsburg, PA, USA) as spherical water droplets with density  $1000 \text{ kg/m}^3$ . Wong et al. showed that minor fluctuations in droplet density did not significantly alter results [92].

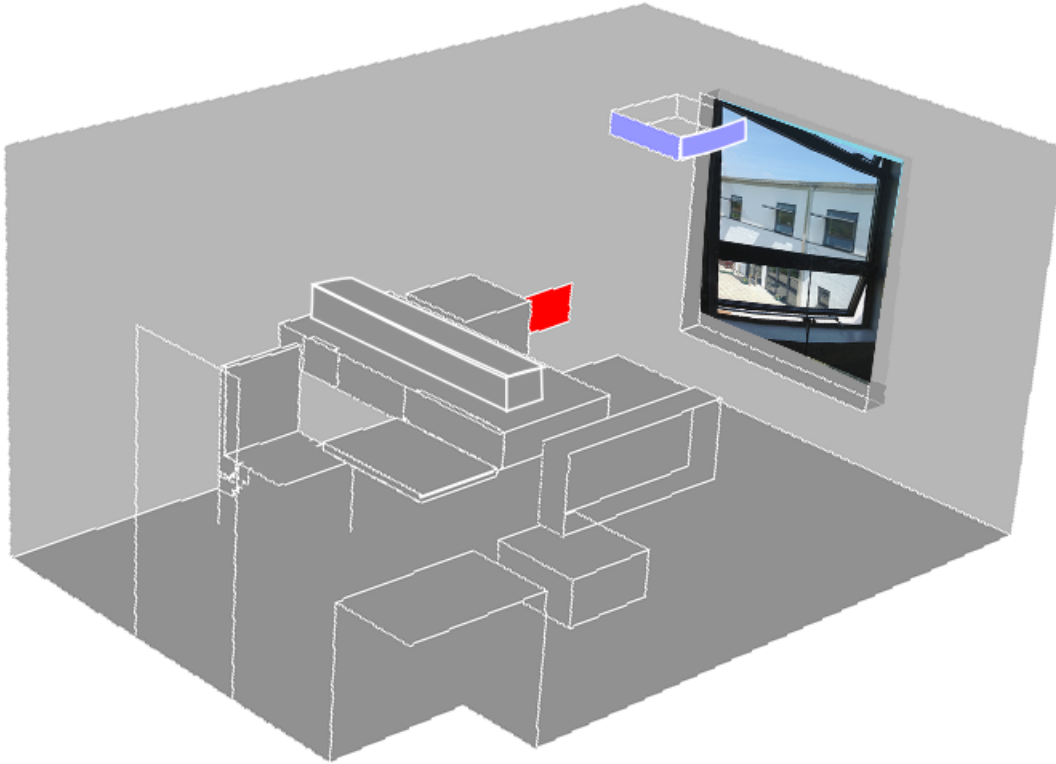


Figure 7.2: YAB single room layout and CFD geometry.

### 7.1.2 HBN04-01 Four-Bed Patient Room

The four-bed room used here is based on the Bradford Royal Infirmary (Bradford, UK) modular ward which includes two such multi-bed bays connected on one side to a central corridor. Dimensions are similar to the HBN04-01 specifications of 6.8m in height  $\times$  7.6m in width. This model will consider only one four-bed bay accommodation given the variability of activities within the ward itself. Figure 7.3 illustrates the positioning of the beds with respect to each other, where a mirrored copy of the beds sits behind the photographer. During the day the curtains remain open unless *personal care* is carried out within the cubicle.

#### 7.1.2.1 Model set-up

The ventilation within the four bed accommodation is assumed to be self-contained, where air is supplied within the room by two ceiling four-way diffusers (blue) and extracted (coloured red) at floor level on the wall to right of the door (see Figure 7.4).



Figure 7.3: Photo of Bradford Royal Infirmary 4-bed maternity ward.

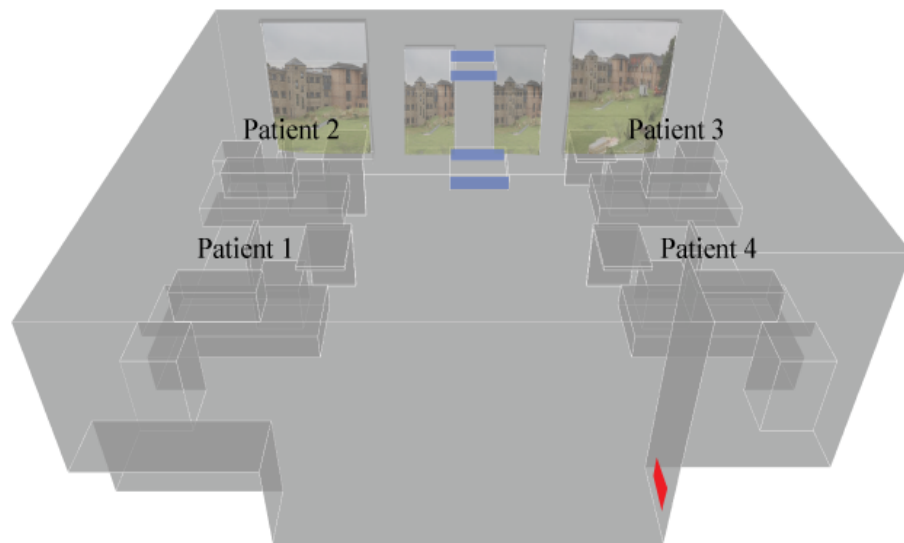


Figure 7.4: Bradford Royal Infirmary multi-bed room.

The model geometry for each of the four bed cubicles is comprised of a heated volume to represent a supine patient, bed, bedside table, over-bed movable tray and accompanying chair. As per HBN04-01 specifications, a sink is placed at the entrance to the room (wall closest) set within the nurses' workstation. In all cases the geometry of these items of furniture are models as simplified representative blocks as shown in Figure 7.4. Two window types (A and B) are located within the multi-bed room; these are modelled as being shut during the current study. Particle injections are performed in the same manner as within the single room 10cm above the patients' heads. Cases 3-10 perform the injections

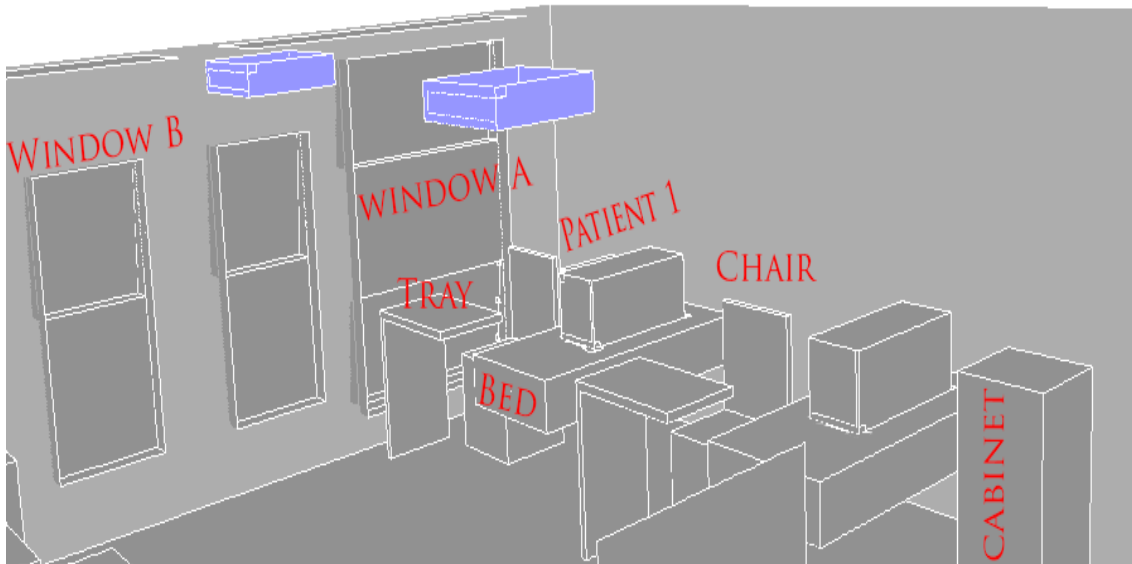


Figure 7.5: Close-up of surfaces within a patient cubicle in the multi-bed room.

Boundary name	Dimensions	Boundary value
Bed(s)	$4 \times (1.9\text{m} \times 1.1\text{m})$	Stationary
Inlet diffuser	$2 (\times 0.5\text{m} \times 0.5\text{m})$	$4$ or $6\text{ac.h}^{-1}$
Outlet transfer grille	$0.3\text{m} \times 0.5\text{m}$	$4$ or $6\text{ac.h}^{-1}$
Patients	$4 \times (1\text{m} \times 0.4\text{m})$	$56\text{W/m}^2$ each
Lighting	None	None
Windows type A $\times 2$	$1.3\text{m} \times 0.8\text{m}$	Closed
Windows type B $\times 2$	$1.0\text{m} \times 0.5\text{m}$	Closed
Door	Closed	Closed
Radiant panel	$2 \times 1.5\text{m} \times 0.4\text{m}$	Off

Table 7.3: Boundary conditions for the multi-bed room

sequentially at the locations shown in Table 7.1.

The meshing of the four bedded room consists entirely of hexahedral elements with a maximum volume of  $1.5625 \times 10^{-5} \text{m}^{-3}$  within the bulk of the domain and a minimum volume of  $1 \times 10^{-6} \text{m}^{-3}$  0.1m from horizontal surfaces. Total cell count is approximately 8 million.

## 7.2 CFD Results and Discussion

### 7.2.1 Airflow Pathways

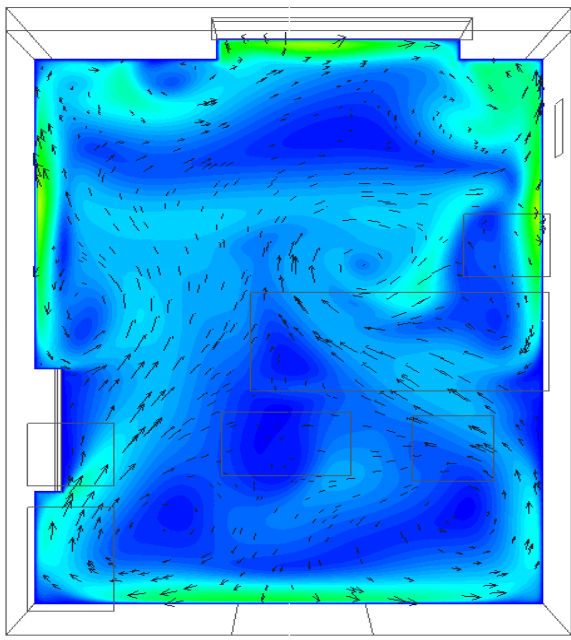
Figure 7.6 and Figure 7.7 show both the velocity vectors and velocity magnitude contours for each sub-scenario for each room type plotted along a meridional plane at breathing level ( $y=1.5\text{m}$ ). Airflow pathways and directions can be seen to be similar between both  $4 \text{ ac.h}^{-1}$  and  $6 \text{ ac.h}^{-1}$  for each case, whereas velocity magnitude does increase as expected. In certain positions the patient may experience a feeling of a draft due to currents higher than  $0.2 \text{ m/s}$  [73].

Airflow movement within the single room reveals that that a strong Coanda effect [68] forms on the ceiling from the inlet diffuser towards the doorway, particularly at the higher airspeeds. No large recirculation zones can be observed where stagnant air could sit, allowing constant fresh air supply to the patient.

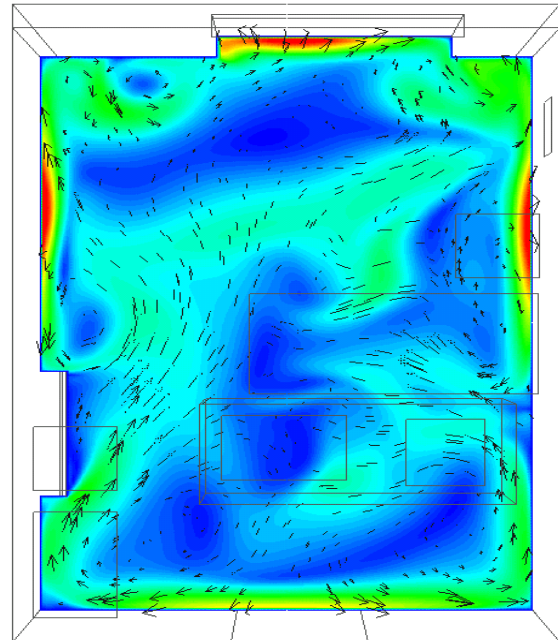
In the case of the multi-bed scenario in Figure 7.7, each area in the close vicinity of the bed-head displays relatively high velocity air movements (ca.  $0.05\text{-}0.08 \text{ m/s}$ ), particularly in the case of  $6 \text{ ac.h}^{-1}$ . This shows that although the patients are in a shared space, they each appear to benefit from a dedicated air stream. Despite this, large stagnant regions or areas of very low air speeds (dark blue colours) are seen throughout the room.

### 7.2.2 Bioaerosol Deposition

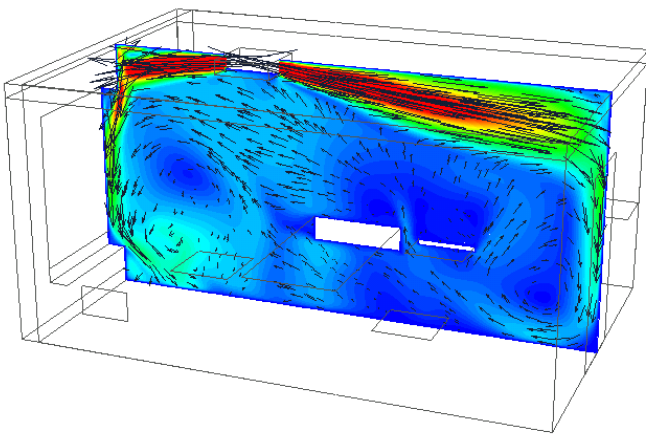
Figure 7.8 and Figure 7.9 show the tracks of a representative number of particles released within the single and multi-bed rooms respectively. Figure 7.9 *a-d* represent the cyclical location of an infectious patient 1 through 4.



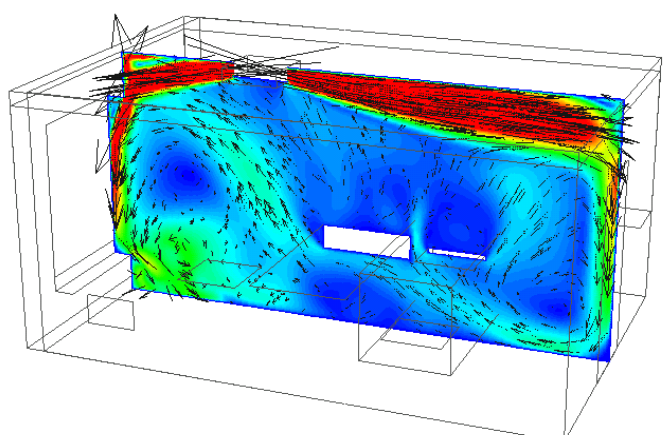
(a). YAB single bed: 4 ac.h<sup>-1</sup>, horizontal plane



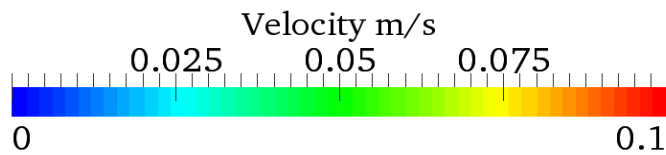
(b). YAB single bed: 6 ac.h<sup>-1</sup>, horizontal plane



(c). YAB single bed: 4 ac.h<sup>-1</sup>, vertical plane



(d). YAB single bed: 6 ac.h<sup>-1</sup>, vertical plane



(e). Velocity magnitude

Figure 7.6: Velocity magnitude contours and vectors on horizontal ( $y=1.5\text{m}$ ) and vertical ( $x=2\text{m}$ ) planes within the YAB single room.

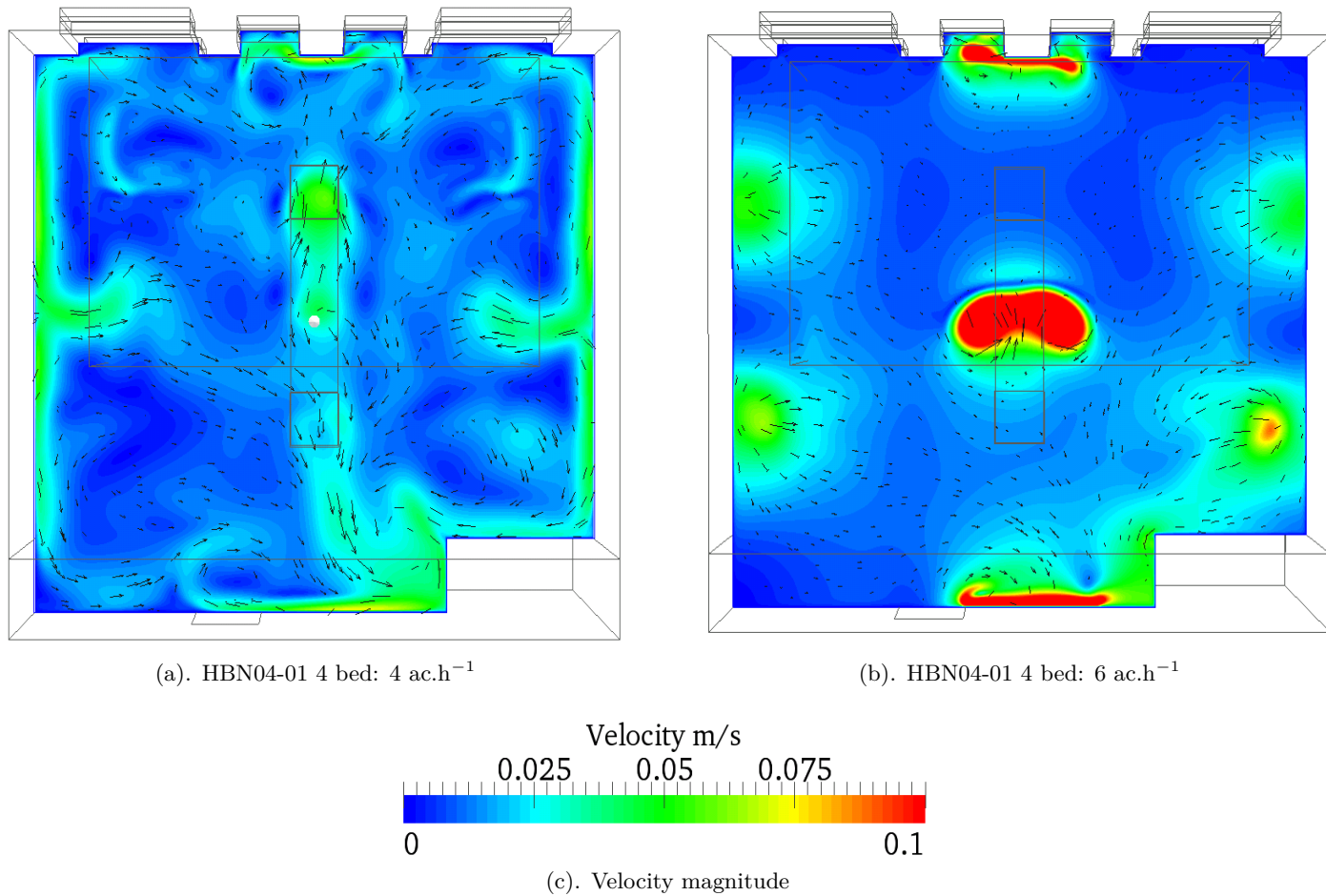


Figure 7.7: Velocity magnitude contours and vectors on horizontal plane ( $y=1.5\text{m}$ ) within HBN04-01 4-bed room.

Results are examined initially in terms of deposition percentage and subsequently in terms of  $\text{CFU}/\text{cm}^2$  where each particle trapped on a surface is considered to be equal to a bacterial colony. Note that in reality bacterial colonies are not necessarily single cells, but may represent a ‘clump’ which grows as a single indistinguishable colony [48].

Figure 7.10 shows total particle deposition percentages for both room scenarios and in the case of the four-bed room, each release position (or infectious patient). In the case of the single room (Figure 7.10a), only small spatial variations can be distinguished between the deposition at  $4\text{ ac.h}^{-1}$  and  $6\text{ ac.h}^{-1}$ . This concurs with Wong et al.’s [92] findings, where they establish that successively higher air changes rates only marginally reduced the deposition percentages. The four-bed room model (Figure 7.10b) shows greater difference with air change rate increase and also variation in deposition depending on release location. Wong et al.’s conclusions are borne out to some extent within the multi-bed scenario

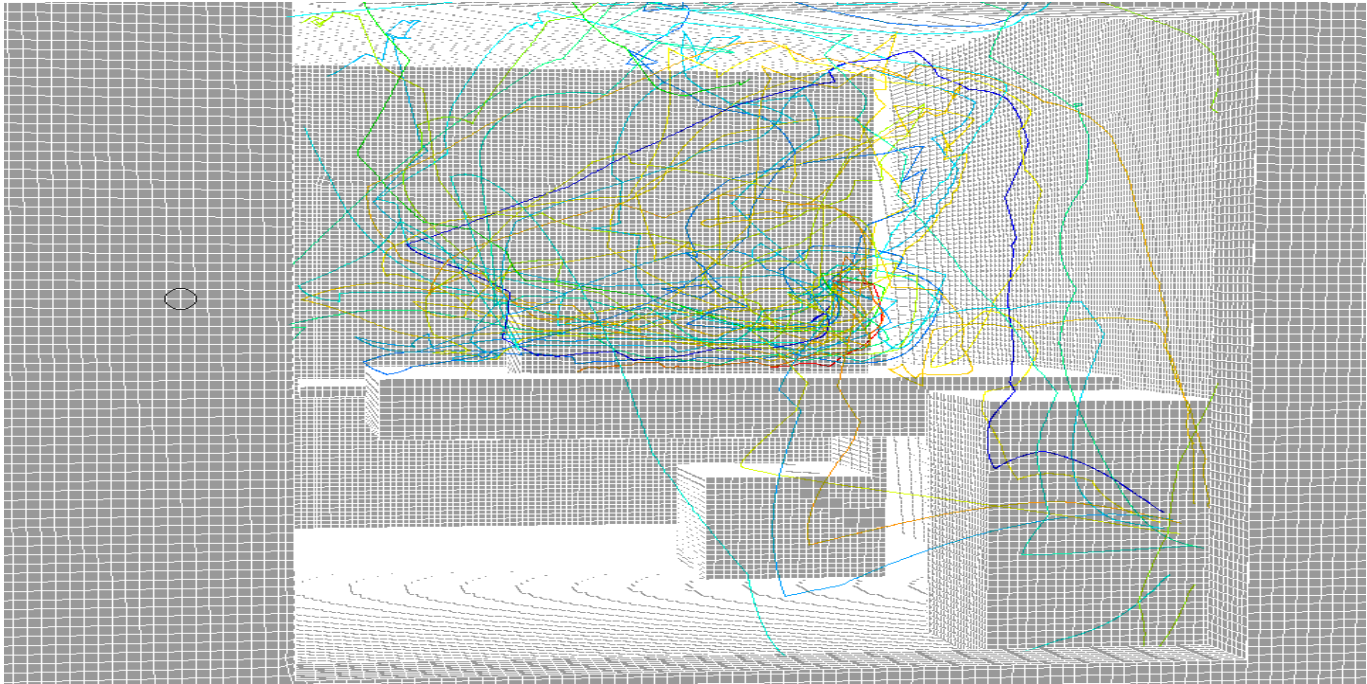
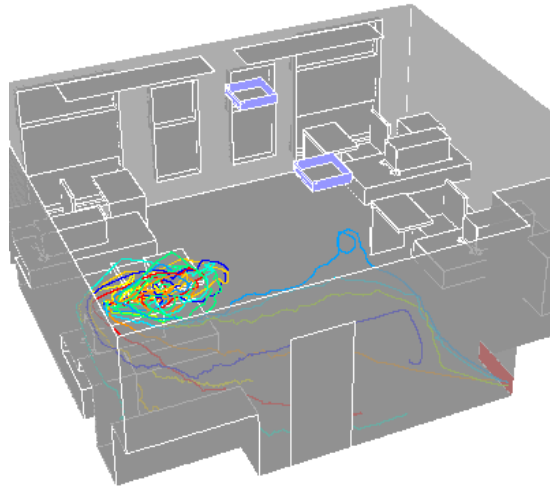
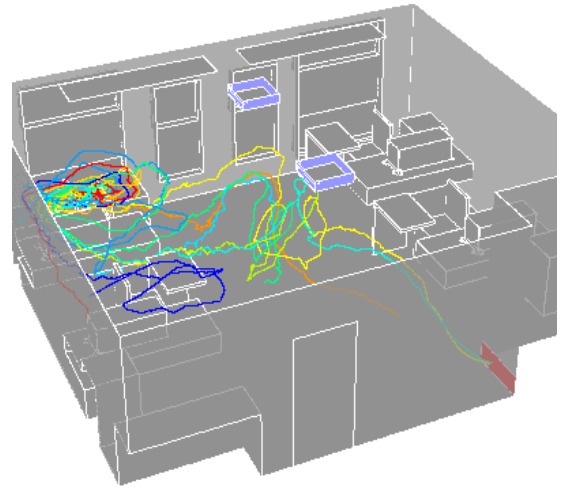


Figure 7.8: Particle tracks by colour ID within the single room.

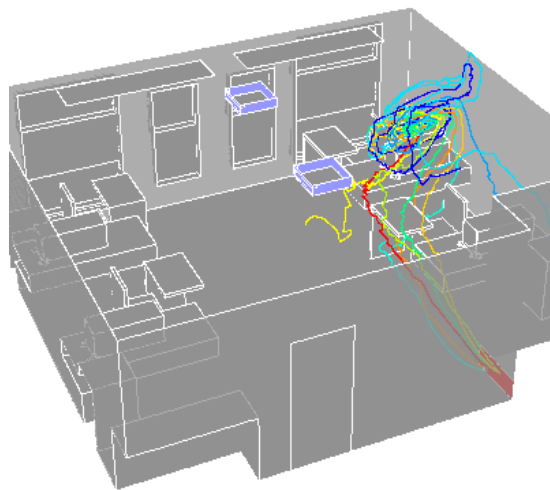
except in the last simulation where the release point was *patient 4*. Since *patient 4* is closest to the extract it might be logical to deduce that a higher  $\text{ac.h}^{-1}$  rate acts counter intuitively and incurs higher deposition percentages at this point. The reason for this could be that the outlet location being close to the ground is influencing particle direction whereby applying a stronger downward momentum and hence forcing them to deposit more readily. Consequently a high-level outlet would necessarily produce the opposite effect [55, 94, 95, 100]. If such is the case the implication is that higher  $\text{ac.h}^{-1}$  mainly affects particles within a reduced locus of the outlet. This may be why *cases 5 and 9* (or release position 3) do not exhibit this behaviour reversal.



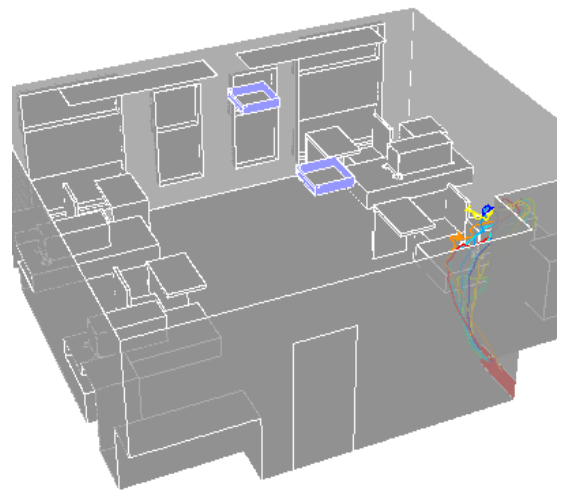
(a). Infectious patient 1



(b). Infectious patient 2

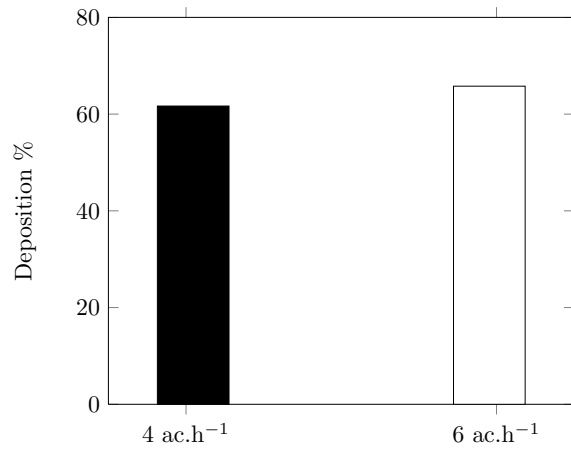


(c). Infectious patient 3

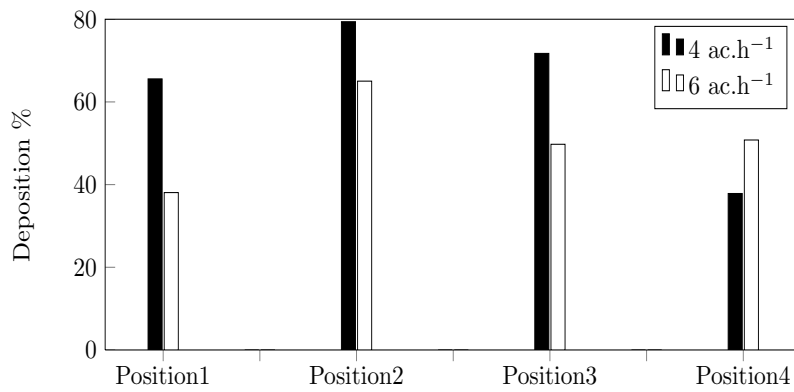


(d). Infectious patient 4

Figure 7.9: Particle tracks coloured by particle ID, when released from all infectious patients within the multi-bed room.



(a). YAB single room



(b). HBN04 01 multi-bed

Figure 7.10: Particle deposition on surfaces within both YAB single room and HBN04-01 4 bed accommodation. Displayed as percentage deposition. Multi-bed release positions 1-4. Comparison shown between 4 ac.h<sup>-1</sup> and 6 ac.h<sup>-1</sup> for each case.

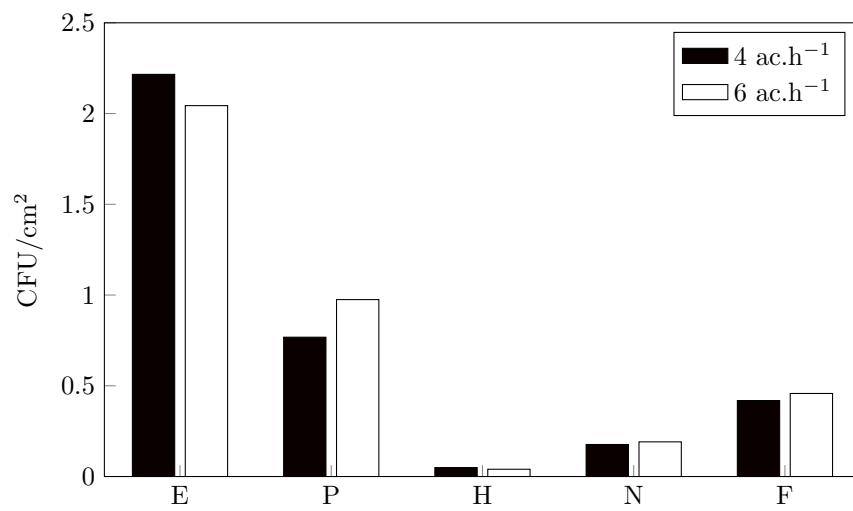
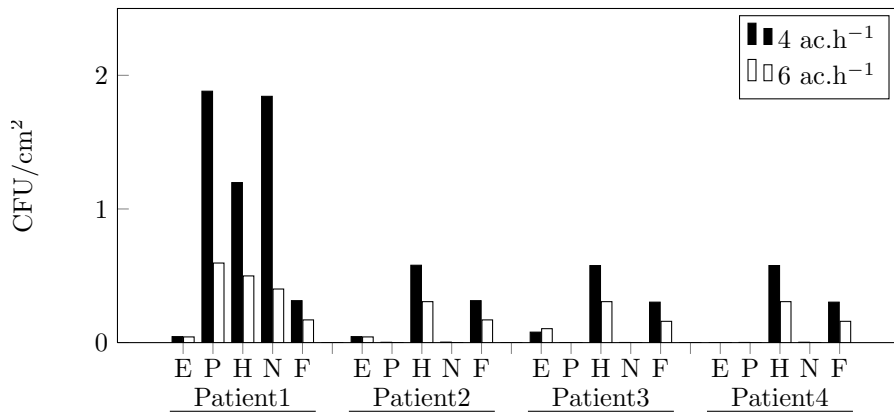
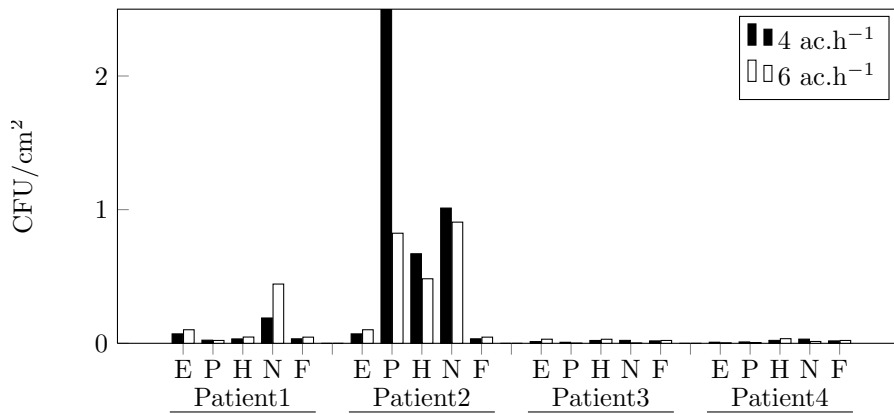


Figure 7.11: Particle deposition quantities on horizontal surfaces within the YAB single room displayed as CFU/cm<sup>2</sup>. Legend: E=Equipment, P=Patient, H=Hygiene Products, N=Near-bed surfaces, F=Far-bed surfaces.

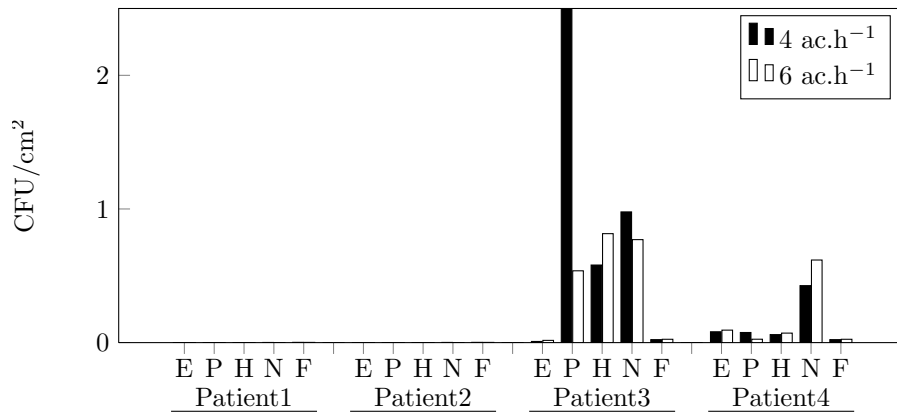


(a). HBN04 01 multi-bed release position 1

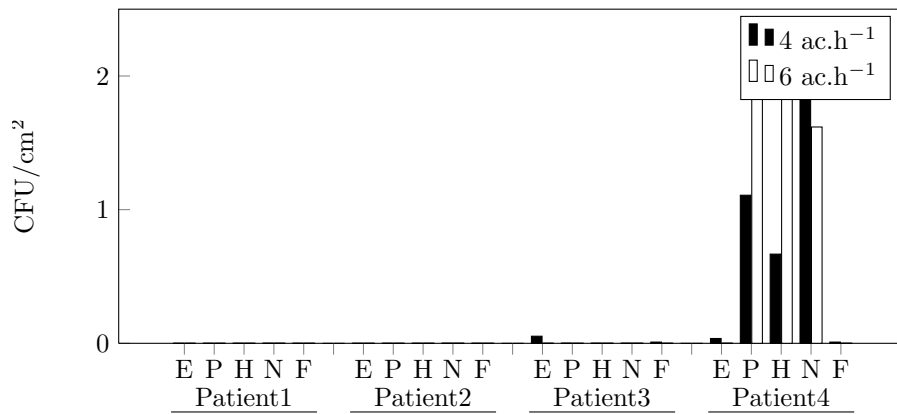


(b). HBN04 01 multi-bed release position 2

Figure 7.12: Particle deposition quantities on horizontal surfaces within the HBN04-01 4 bed accommodation. Displayed as CFU/cm<sup>2</sup>. Multi-bed release positions 1-4. Comparison shown between 4 ac.h<sup>-1</sup> and 6 ac.h<sup>-1</sup> for each case. Legend: E=Equipment, P=Patient, H=Hygiene Products, N=Near-bed surfaces, F=Far-bed surfaces



(c). HBN04 01 multi-bed release position 3



(d). HBN04 01 multi-bed release position 4

Figure 7.12: (continued) Particle deposition quantities on horizontal surfaces within both YAB single room and HBN04-01 4 bed accommodation. Displayed as CFU/cm<sup>2</sup>. Multi-bed release positions 1-4. Comparison shown between 4 ac.h<sup>-1</sup> and 6 ac.h<sup>-1</sup> for each case. Legend: E=Equipment, P=Patient, H=Hygiene Products, N=Near-bed surfaces, F=Far-bed surfaces

Figure 7.11 shows the total deposition quantities for all different surface categories within the single room. Differences induced due to between air change rates appear negligible for all categories except the patient, which shows an increase in contamination levels at  $6\text{ac.h}^{-1}$ . Equipment surfaces appear to accrue the highest deposition values and hence are most contaminated.

Figure 7.12 shows the breakdown of particle deposition by  $\text{CFU}/\text{cm}^2$  for the five different surface categories and for each infectious patient position in turn. Deposition percentages within areas opposite the source position demonstrate a sharp drop-off, where particles are maintained airborne and directed towards the extract. This is particularly the case when *patient 2* is the source where a seemingly dichotomous partition within the room can be observed, and few particles are deposited on *patient 1*. Equally when *patient 3* is the source negligible counts can be found in the vicinity of *patients 1* or *patient 2*. Wong and colleagues [92] also noticed that as the air change rate increased, the deposition quantities increased further from the source. A one-way non-parametric Wilcoxon signed-rank test is used to investigate this possibility within the small step increase from 4 to  $6\text{ac.h}^{-1}$  for each release position in turn. Table 7.4 shows that the distributions cannot be distinguished at the 5% level and hence Wong et al.'s conclusions are not necessarily borne out in this scenario. Nevertheless a Kruskal-Wallis test between all scenarios ( $p=0.04$ ) shows that release position does indeed provide a significant impact on deposition percentage.

Room type	Release point	p-value
YAB Single room	Patient	0.33
HBN04-01 4-bed	Patient 1	0.55
HBN04-01 4-bed	Patient 2	0.10 <sup>†</sup>
HBN04-01 4-bed	Patient 3	0.42
HBN04-01 4-bed	Patient 4	0.65

Table 7.4: Wilcoxon rank test p-values for particle deposition distribution comparison between  $4\text{ac.h}^{-1}$  and  $6\text{ac.h}^{-1}$ . <sup>†</sup> denotes significant difference at the 10% level

### 7.3 Application of PAM to YAB Single Room and HBN04-01 Multi-Bed Accommodation

The pathogen accretion model developed in Chapter 6 is subsequently applied in this section to both room settings. Since the four bed ward is roughly four times the volume of a single room and containing four times the surface numbers, releasing the same number of particles in both scenarios results in a natural discrepancy. Therefore in this section the concept of normalisation is introduced in order to compare room types in a consistent manner. Standard intentional nurse rounding in single rooms comprises mainly of *direct care*, a definition of which can be found on page 167 and as such will be used as a reference case. Since PAM requires surface contamination to be introduced as CFU/cm<sup>2</sup>, pathogen counts at this stage are raw values obtained from the CFD simulations (see Figure 7.12). Subsequently the results are normalised with respect to the mean contamination level on HCWs' hands after *direct care* in the single room at 6 ac.h<sup>-1</sup>. This can be considered the 'base case'.

#### 7.3.1 HCW Behaviour in the HBN04-01 Four-Bed Ward

HCW behaviour has to be assumed at this stage to be related at some level to that observed in the single room. Without this, comparison between accommodation types purely with respect to HCW hand pathogen contamination level would not make sense. Smith et al. [25] conducted an observational study of HCWs in a 4-bedded room applying the same surface category criteria as used here. In the ward however, they note that patient charts become near-bed objects as these are often at the foot of the patient's bed. Therefore this adjustment is made to the probability densities derived from the observations at YAB. Figure 7.13 shows that there exists no statistical difference at the 5% level ( $p=0.068$ ), highlighting that the only difference in HCW behaviour between single and multi-bed rooms is the positioning of patient charts. Consequently this demonstrates the similarity between nurse behaviour in single and multi-bed rooms. Subsequent models will use this adjusted behaviour in line with Smith et al. for all multi-bed simulations.

Potential differences may still exist however, in particular multi-bed cubicles are often surrounded by privacy curtains. Hathway et al. [46] found that following morning bathing

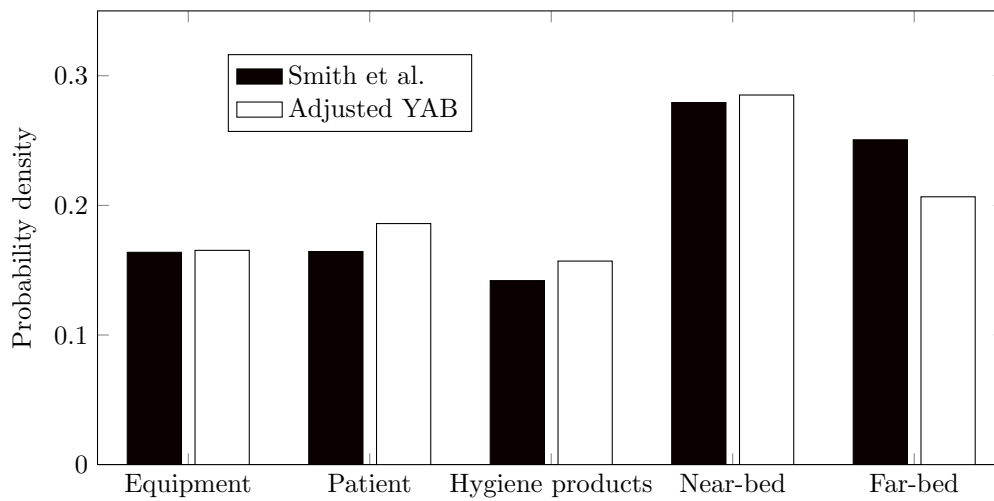


Figure 7.13: Adjusted HCW behaviour based on ward observations by Smith et al. ([25] and private communication). Patient charts become near-bed surfaces in the multi-bed scenario instead of the far-bed surfaces in the single room.

of bed-ridden patients, cubicle curtains on a standard ward typically remain open during the daytime. They are only drawn during further *personal care* whereby adding an extra surface contact opportunity. Here we will consider the curtain a *near-bed* porous surface and enforce the first contact to be with this category.

## 7.3.2 PAM Results and Discussion

### 7.3.2.1 Single bed room: YAB

Figure 7.14 shows the normalised CFU values ( $Y$  for simplicity) compared against the average of standard *direct care* for each subsequent type of care within the single room. Additionally, the comparison is made between a ventilation rate of  $4 \text{ ac.h}^{-1}$  and the standard HTM 03-01 prescribed  $6 \text{ ac.h}^{-1}$ . Initially there appears only to be a small reduction of CFU contamination from  $4$  to  $6 \text{ ac.h}^{-1}$  when comparing medians. This refers to the 50th percentile on the boxplot or the horizontal bar inside it. However comparison of extrema reveals that contamination levels under  $4 \text{ ac.h}^{-1}$  are consistently higher throughout ( $p < 0.05$ ). Only in the cases of *housekeeping* and *personal care* does there appear to be a noticeable difference in mean contamination levels ( $p = 0.019$  and  $p = 0.04$  respectively) between air change rates.

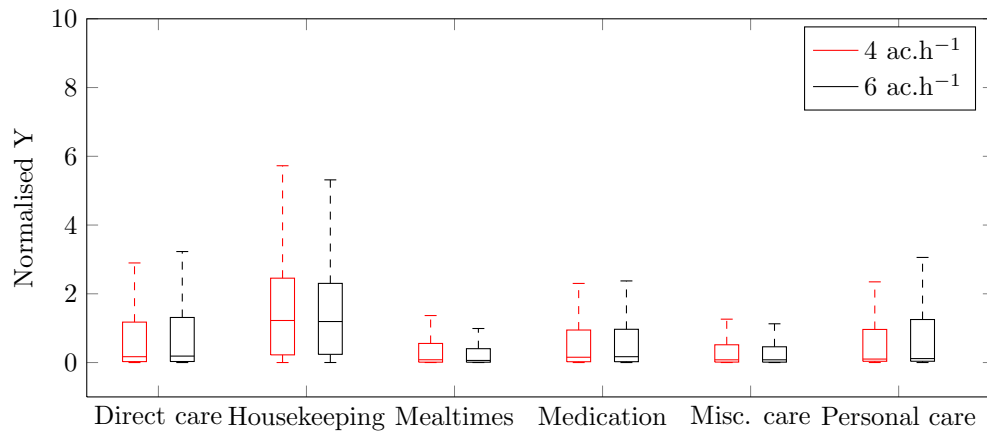


Figure 7.14: Boxplots showing normalised CFU values for YAB single room, comparing 4 and 6 ac.h<sup>-1</sup>.

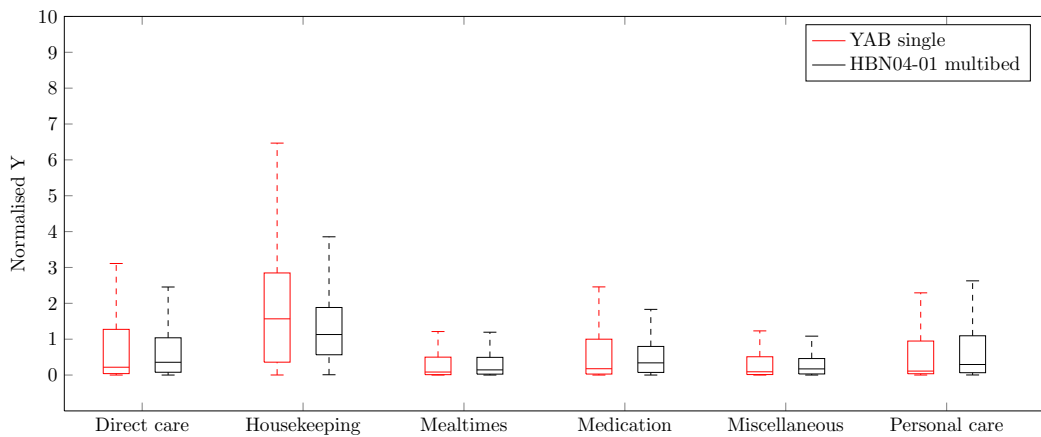
Comparing the resultant differences between the contamination levels reveals that the discrepancies appear to be magnified through the behaviour of the HCW (see Section 7.2.2 page 247). Table 7.5 shows the ranking of Y values based on care types within the single room. A non-parametric rank test is used to compare equal medians (or 50th percentiles) and results given as p-values. Inter-care type comparison reveals some fluctuation with only *mealtimes* and *miscellaneous care* showing on average lower contamination levels than *direct care* (p=0.001). A two-sided Kruskal-Wallis non-parametric test supports the conclusion that care type has a significant effect on final CFU values. This is consistent with results found in Chapter 6 Section 6.7.1. Ranking by mean and maximum values show that the distribution (see Figure 7.14) of pathogens shows only minor fluctuations with a concentration of the majority of the data within the lower quartiles (<50%).

Rank	Care type					
	Direct care	House-keeping	Mealtimes	Medication rounds	Misc. care	Personal care
by mean	3	5	2	4	6	1
by max.	3	2	5	4	6	1

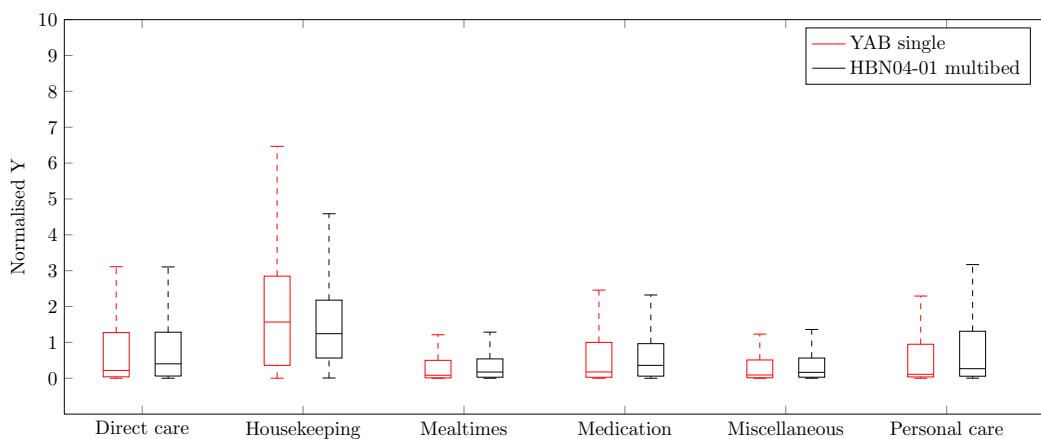
Table 7.5: Ranking by mean and maximum of care types (lower is better, meaning cleaner hands) after hand hygiene in YAB single room.

### 7.3.2.2 Combined single and multi-bed room comparison

Boxplots of normalised  $Y$  values are shown in Figure 7.15 comparing the single room scenario directly against the multi-bed room. These are broken down into care types throughout. Each set of boxplots shows the resultant contamination level of HCWs hands (normalised  $Y$  values) for sequential positioning of an infectious patient. In the four-bed room scenario values are cumulative over care for four patients. Care always starts at patient 1 and continues chronologically through 2, 3 and finally 4. The same surface contact sequence is repeated for each patient hence allowing for reproducibility of results.

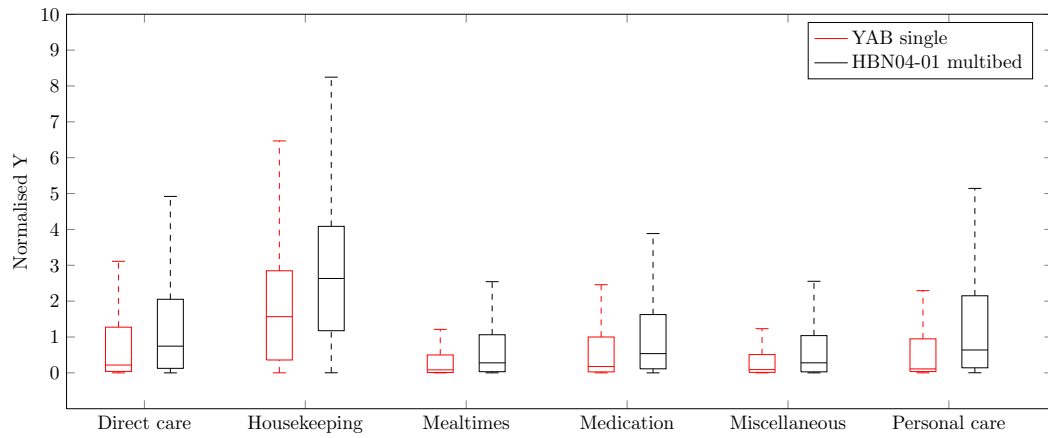


(a). Infectious patient=1

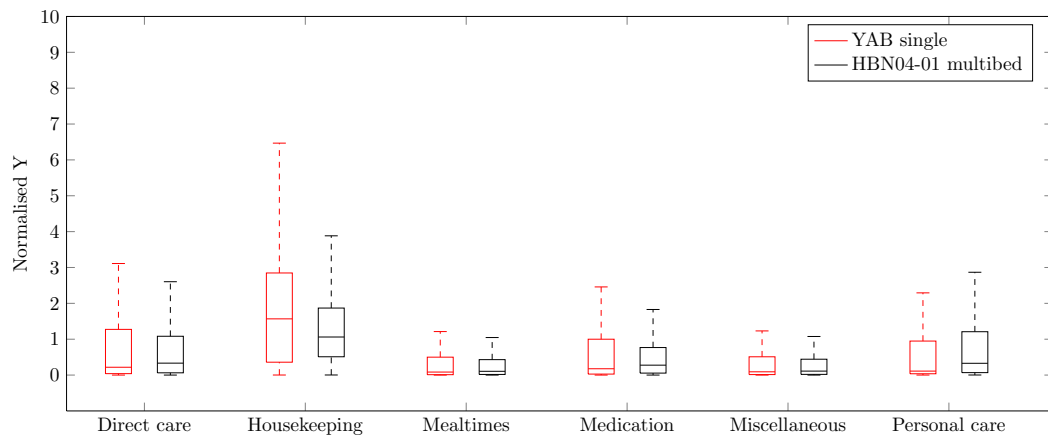


(b). Infectious patient=2

Figure 7.15: Comparison of normalised CFU values ( $Y$ ) against YAB single room *direct care* after hand hygiene: YAB single room vs HBN04-01 4-bed room.



(c). Infectious patient=3



(d). Infectious patient=4

Figure 7.15: (continued) Comparison of normalised CFU values (Y) against YAB single room *direct care* after hand hygiene: YAB single room vs. HBN04-01 4-bed room.

Results presented in boxplot form in Figure 7.15 show that hand contamination is similar in the two rooms, but that there are some differences between care type and in the case of the four-bed room, the location of infectious patient (see Table 7.6). Given that the care patterns are the same for each patient, differences between infector location are down to the airflow paths and the resulting surface contamination levels. To investigate the reality of this claim a one-sided Wilcoxon ranksum test is applied to each care type pair. Table 7.7 shows the p-values for the hypothesis that 50% of the care episodes carried out in the multi-bed room cause higher contamination than the equivalent care in the single room. This one-sided test rejects the null hypothesis at the 2.5% level (equivalent to two-sided 5%).

<b>Infectious patient</b>	Rank by			
	<b>Mean</b>	<b>Median</b>	<b>Max</b>	<b>Mean rank</b>
<b>1</b>	2	2 <sup>†</sup>	3	<b>2</b>
<b>2</b>	3	3 <sup>†</sup>	2	<b>3</b>
<b>3</b>	1	1	1	<b>1</b>
<b>4</b>	4	4	4	<b>4</b>

Table 7.6: Comparison of infectious patient location by ranking via mean, median and maximum. A higher rank is better. <sup>†</sup> indicates a tied rank.

Inspection of Figure 7.15 throughout all four scenarios reveals that differences are not dichotomous, where contamination levels are dependent on the location of the infectious patient ( $p=0.003$ ). This is supported by a Kruskal-Wallis non-parametric test which shows that in the case of *direct care* only release *position 4* yields systematically lower hand contamination than from all other locations including the single room. This conclusion is supported in Table 7.6 by ranking of pathogenic loading following care of an infectious patient in all four locations. It also shows that by comparison when the infectious patient is located in position 3 the resulting contamination levels are consistently higher over all scenarios and care types ( $p<0.0001$ ).

Figure 7.16 shows an individual boxplot comparison of the normalised Y values between the single and multi-bed room. These are further broken down by infectious patient position and care type. Comparison of the 50th percentile through a Kruskal-Wallis

test reveals that the single room can yield lower contamination spread during all care types ( $p=0.03$ ). Comparing the single room against the multi-bed scenario in Figure 7.16 emphasises that the former can yield lower contamination spread via median comparison during all types of care. The interquartile range for the single room may still be higher in many cases however. This is a representation of the overall surface contamination level of the multi-bed room being proportionally lower due to the higher volume.

Infectious patient	Care type					
	Direct care	House keeping	Mealtimes	Medication rounds	Misc. care	Personal-care
	p-value					
1	1	1	0.975	1	0.996	0.971
2	0.011*	0.048 <sup>†</sup>	0.0139*	0.021*	0.015*	0.02*
3	0*	0*	0*	0*	0*	0*
4	1	1	0.974	1	0.966	0.901

Table 7.7: Comparison of CFU values after hand hygiene between YAB single room and HBN04-01 4-bed room via a one-sided non-parametric Wilcoxon ranksum test hypothesising that 50% of the values obtained from the multi-bed room are higher than those from YAB while performing the same activities. \* denotes significant results at 2.5% level. <sup>†</sup> denotes significant values at 5% level.

## 7.4 Quantifying Patient Risk and Application of an Exponential Dose-Response Model

Chapter 3, page 80 highlight the intricacies of empirical feeding trials which estimate the risk of infection given a certain quantity of inoculum administered. At low doses the exponential dose-response model given in Equation (3.4.3) was deemed to be of adequate complexity to investigate the discrepancies between care and room type. The intention of this is to compare the HCW-patient contact count against the risk of infection for each type of care. The risk posed is that to the subsequent patients (after care carried is out on an infectious patient) undergoing HCW care. In the case of the single room this is assumed to be the patient in the contiguous room for all care types except *miscellaneous*. For *miscellaneous care* the next patient the HCW comes in contact with may potentially

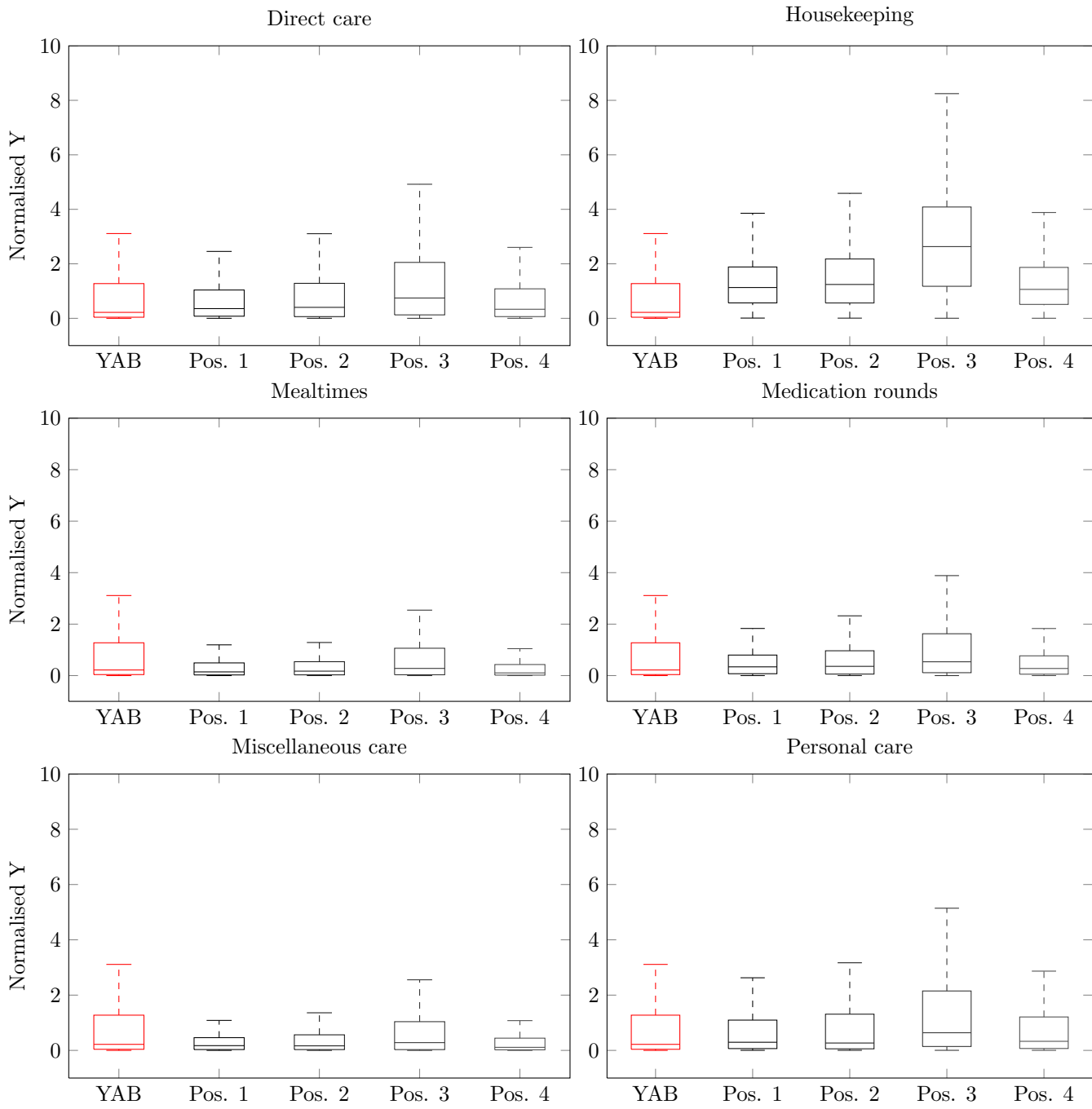


Figure 7.16: Comparison of normalised Y values between single room (red) and cumulative sum for each release location within the multi-bed room (black).

be in a non-random order. This is due to the care being reactionary (to a call bell) rather than pre-planned. This also holds for the multi-bed room, and therefore risk for *miscellaneous care* is calculated as if the HCW had not attended to any previous patient and hence had clean hands. Figure 7.17a depicts the sequential movement of the HCW from single room 1 through room 4. Figure 7.17b shows the equivalent route in the multi-bed accommodation.

Figure 7.18 shows the normalised contamination on health care worker hands (Y values) for progression through a series of four patients in single Figure 7.18a and multi-bed Figure 7.18b rooms.

In the absence of airborne cross-transmission between single rooms, CFU values can be seen (see Figure 7.18a) to be monotonically non-increasing as hand antisepsis and deposition onto surfaces removes contamination. Within the multi-bed scenario, however, the spread of microorganisms to neighbouring cubicles allows for subsequent accretion of pathogenic material by the HCW regardless of hand hygiene (see Figure 7.18b).

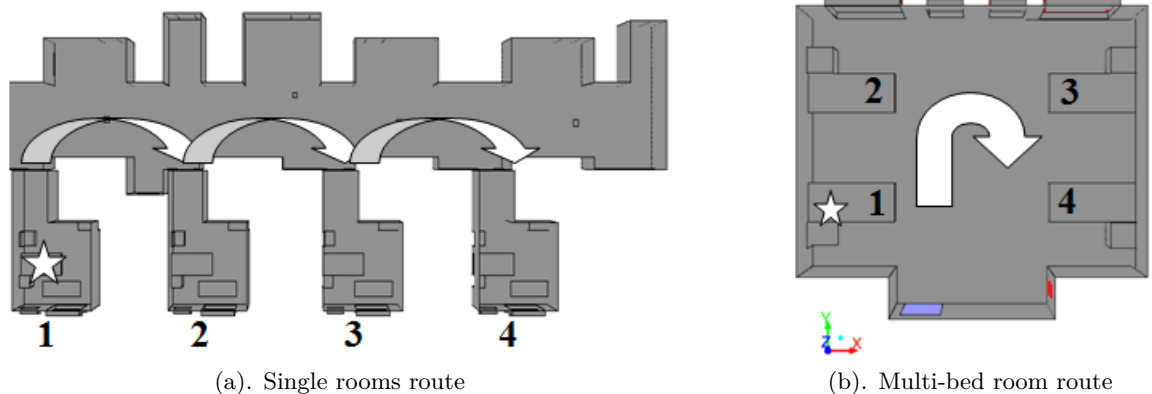
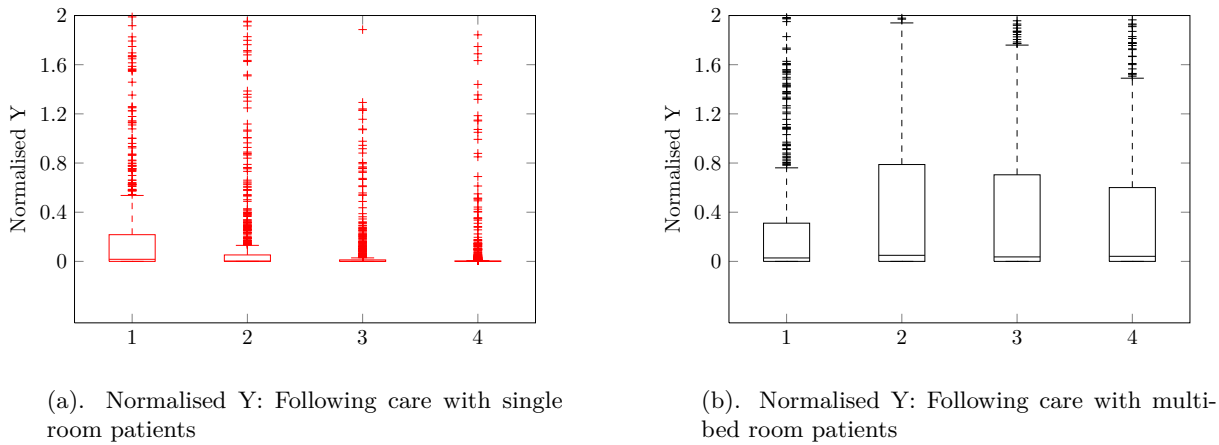


Figure 7.17: HCW route for all care types except *miscellaneous care* within both the YAB single room and HBN04-01 4 bed room. Star indicates infectious patient location in the first scenario.

### 7.4.1 Relative Risk

An exponential dose-response model is applied to the two scenarios investigated given by Equation (3.4.3) presented in Chapter 3, Section 3.4:

$$P(\text{infection} | \lambda) = 1 - \exp(-\alpha\lambda)$$



(a). Normalised Y: Following care with single room patients

(b). Normalised Y: Following care with multi-bed room patients

Figure 7.18: Boxplots show normalised Y values after an episode of *direct care* following care of one infected patient.

where  $\lambda$  represents the dose administered to a susceptible host.

Figure 7.19 shows the relative risk associated with patients in both single rooms and multi-bed accommodation. This is plotted against the number of times the HCW comes in contact with the patient. Standard deviations are also plotted at each data point. The term  $\alpha$  represents the probability of the HCW contact being with a patient's mucous membrane or other susceptible location. This also accounts for the likelihood of the pathogens overcoming the patients own immune defences. For example in this case a value of  $\alpha = 0.069$  [199] (e.g. influenza) was used to represent a relatively low probability or a pathogen of low virulence. Results are an average of episodes of the same type of care to three susceptible patients following interaction with an infectious patient. All risk is normalised with respect to typical *direct care* in the single room. Figure 7.19 actually highlights the similarity between accommodation types through this type of comparison. At a first glance a curious phenomenon occurs at higher patient contact rates, where in some cases a drop in risk is observed. This is explained by considering that high numbers of contacts are not necessarily proportional to high inocula. Consider the case where the value of overall HCW surface contacts may be high, amongst these are also high numbers of patient contacts. However the timing of the patient contacts is important, insofar that significant quantities of pathogenic material may have been shed or deposited onto other inanimate surfaces in the meantime. Consequently the dose of pathogens delivered through patient contact may, in this case, be quite small. Comparison of risk between the two accommodations is highlighted by the one-sided non-parametric Wilcoxon rank test

which shows that the multi-bed accommodation poses a higher risk at low ( $<4$ ) contact counts ( $p=0.04$ ). However this appears to be reversed at higher values ( $p=0.001$ ). This phenomenon holds throughout all care types except for the *medication round*, where on average multi-bed room shows significantly higher risk throughout. No difference is found, for *miscellaneous care* ( $p=0.89$ ).

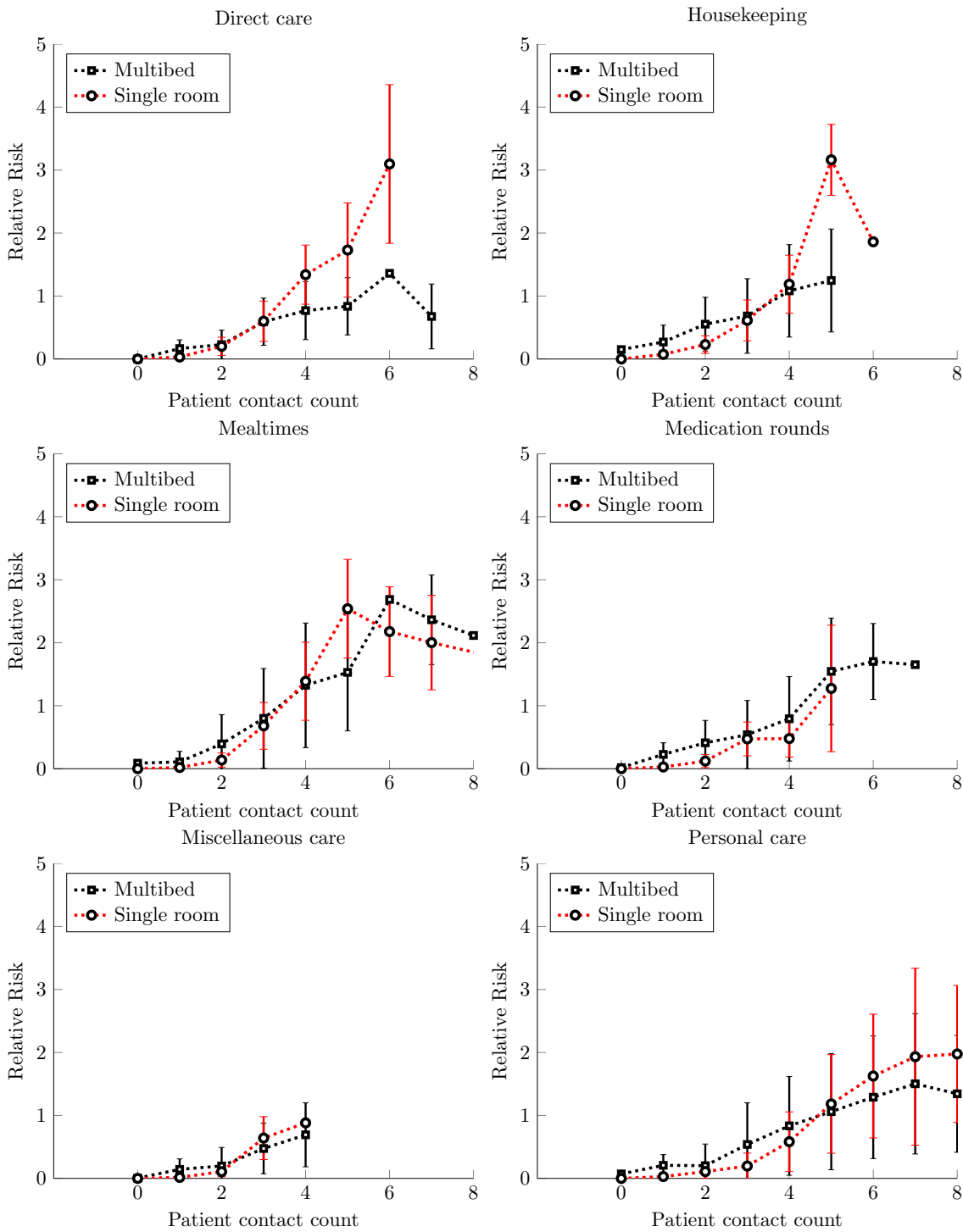


Figure 7.19: Comparing average risk during care to 3 uninfected patients within single and multi-bed room relative to *direct care*.  $\alpha = 0.069$ . Where infection status of all patients is unknown. Errorbars represent one standard deviation either side of the mean.

#### 7.4.1.1 Prior knowledge of infection

In the UK and many other EU countries, both planned admission and emergency patients are screened for MRSA [288], however the feedback time on results of this test vary and a patient may be placed into a multi-bed room before results become available. Therefore this incurs a latent risk to other patients via surface contamination and subsequent transmission via HCW hands. Figure 7.19 shows the situation in which the state of infection of the patient is unknown to the HCW and hence no extra quarantine precautions have been taken. This can be considered a *worst case* scenario. Conversely however if a patient is known to be infectious, then increased probability of antiseptics procedures is expected [28]. Let us consider this the *best case scenario* where some form of hand hygiene is necessarily undertaken after each episode of care with an infectious patient. Note however that the efficacy of the antiseptics will still vary as before. The HCW will then return to the original probability of antiseptics following care with subsequent other known uninfected patients.

Figure 7.20 represents the relative risk to three subsequent susceptible patients plotted against patient contact count. The HCW is aware of an infectious patient in both scenarios. Note however that hand hygiene is only obligatory after care concludes with the infected patient (e.g. patient 1), however the probability of further antiseptics returns to that observed at YAB for all subsequent care episodes for patients 2, 3 and 4. Comparison shows the multi-bed room to pose a greater risk ( $p \sim 0.038$ ) during all types of care except *miscellaneous*, where no difference is found ( $p = 0.78$ ). The latter may be explained by the low number of patient contacts during this type of care. Despite this, the risk observed within the single rooms is consistently within one standard deviation of that observed in the multi-bed counterpart.

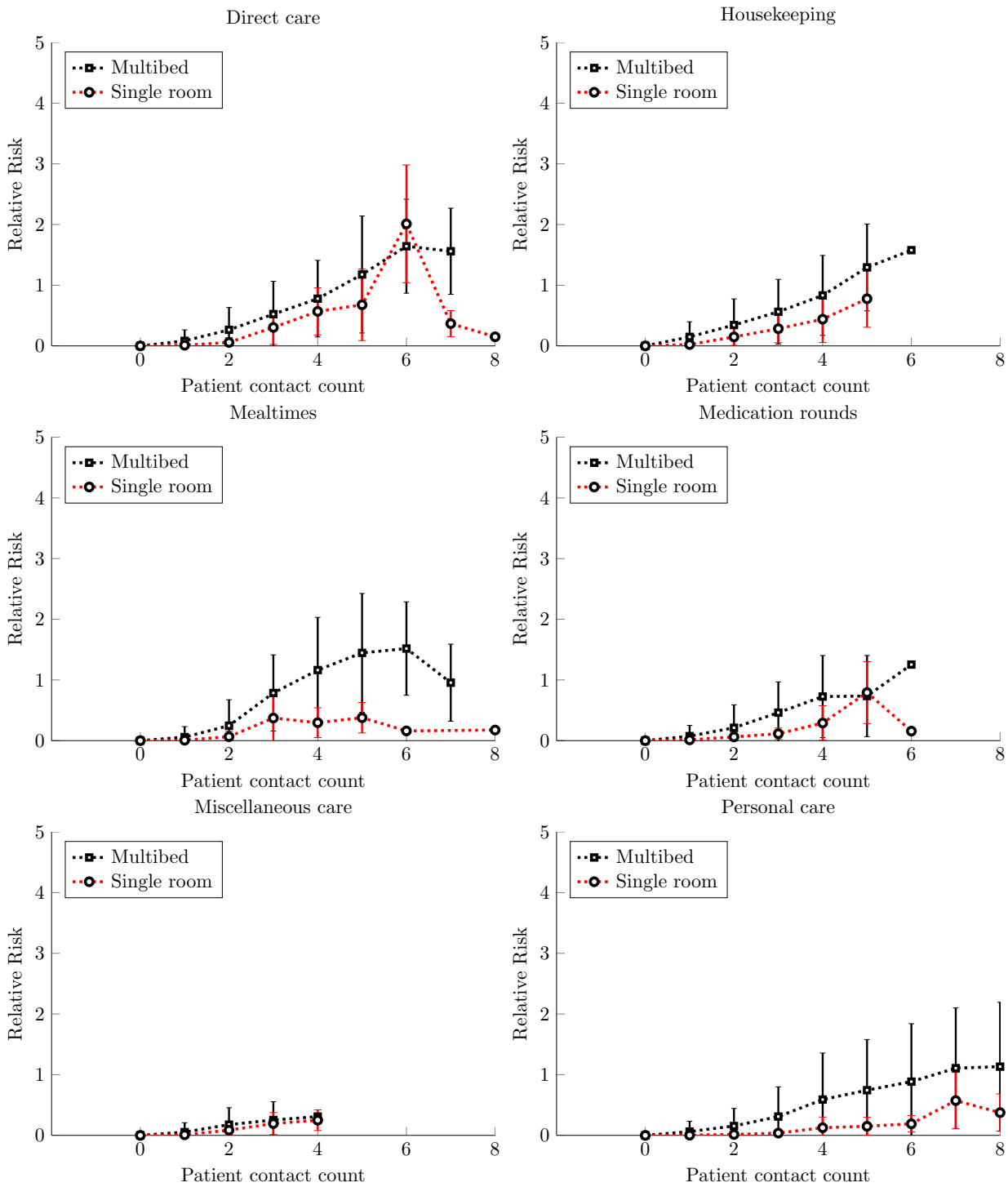


Figure 7.20: Comparing average risk during care to 3 uninfected patients within single and multi-bed room relative to *direct care*. Antisepsis is enforced after care with the infectious patient.  $\alpha = 0.069$ . When infectious patient is identified. Errorbars represent one standard deviation either side of the mean.

## 7.5 Summary

This chapter compares the single and multi-bed accommodation through three integral approaches: CFD, PAM and infection-risk modelling. Section 7.2.2 depicts the CFD is capable of the prediction of spatial deposition of particles within both environments, highlighting subtle differences between designs. A higher air change rate of 6 ac.h<sup>-1</sup> (vs 4 ac.h<sup>-1</sup>) showed to have little significant impact for three of the four considered scenarios in the multi-bed room on deposition quantity or spatial variation under controlled conditions. A decrease in spread locus was noticed however, when the infectious patient was placed closest to the outlet vent, highlighting the greater downward momentum on particles exerted by comparatively higher local air velocities at 6 ac.h<sup>-1</sup>.

PAM was then applied within both the single and multi-bed room successfully by using the surface contamination values accrued through the CFD models. Differences were not clear cut and the positioning of the infectious patient had most effect on the final results. Locating the infectious patient in a multi-bed room without an unobstructed air pathway from the bed to the ventilation outlet caused the highest level of surface contamination of all scenarios tested. Other positions (2 and 3) often led to comparable contamination levels as in a single room.

Quantification of the risk of the accrued pathogens to subsequent susceptible patients was investigated by an exponential dose-response model. Significant differences only became apparent between the two accommodation types when the existence of an infectious patient was known. Results suggested that CFU values on the hands of the HCWs decreased monotonically when single rooms were considered, however in the case of the multi-bed room the biological load either remained stable or increased during contact with subsequent patients. Overall, when hand hygiene was enforced due to the knowledge of an infectious patient, the single room became significantly less risk prone.

## Chapter 8

# Implications of results, conclusions and further research

### Contents

---

<b>8.1 Key Findings . . . . .</b>	<b>272</b>
<b>8.2 Future Research . . . . .</b>	<b>277</b>
<b>8.3 Implications of the Study and Conclusions . . . . .</b>	<b>279</b>

---

The focus of the research presented in this thesis is to provide a robust but flexible framework which evaluates and quantifies the risk of acquiring a secondary infection from contaminated surfaces within hospital single and multi-bed accommodation. This is achieved by forging a multidisciplinary analysis in numerical and experimental techniques coupled with extensive in-field clinical observation and mathematical modelling. The three main elements of the research and the key findings in each aspect are summarised below. A number of areas for future work are identified and discussed, and considerations are given to the implications of the research findings.

### 8.1 Key Findings

This multidisciplinary research potentially has global implications for architects, clinicians and infection control teams in hospital room design but ultimately for patient satisfaction.

### 8.1.1 Bioaerosol Deposition: Experimental and Numerical Approaches

Simulation approaches such as computational fluid dynamics (CFD) are increasingly used to model particle behaviour in indoor air, however previously there have only been tentative attempts at large scale validation of such methods in the open literature. In this study a total of four hospital room scenarios were recreated in an aerobiology test chamber to form a comparative experimental study which could be replicated in a CFD model.

This set of experiments and simulations was designed to assess the ability of CFD simulations to accurately predict spatial distributions of bioaerosol deposition in indoor environments and explored the influence that different room layouts have on deposition patterns. Spatial deposition of aerosolised *Staphylococcus aureus* was measured in the test room arranged in different layouts: an empty room, a single-bed and a two-bed hospital room. This was compared with CFD simulations that used a Lagrangian particle tracking method to simulate bioaerosol dispersion and deposition. This study concluded that:

- Realistic prediction of spatial deposition is feasible within a CFD model, and a Reynolds Stress (RSM) turbulence model yields significantly better results than the k- $\epsilon$  RNG turbulence model used in most published indoor air simulations.
- Experimental and CFD results for all layouts demonstrate that small particle bioaerosols are deposited throughout a room with no clear correlation between relative surface concentration and distance from the source.
- A physical partition separating patients is effective at reducing cross-contamination by up to 50% in neighbouring patient zones, particularly with ventilation upwind of the infected patient.

Across all scenarios it is noted that both experiments and simulations predict measurable deposition across the room space. While spatial variation depends on layout, the results suggest there is clear potential for small diameter ( $\sim 2.5 \mu\text{m}$ ) particles to play a role in transmission of infection through indirect contact routes. This is an important conclusion; such particles are routinely regarded as airborne and hence controlled through ventilation rather than cleaning. Moreover, these small particles are usually only considered of concern where the pathogen is classed as possibly capable of direct airborne transmission, for

example tuberculosis, measles or influenza. The deposition of culturable bioaerosols in this study adds support to the hypothesis that airborne dispersion may play a role in non-respiratory infections. This study formed the baseline validation for implementing CFD and Lagrangian particle tracking with confidence in single and multi-bed hospital accommodation in subsequent chapters. Consequently direct comparison could be made between the influence of design and room layout in each scenario.

### 8.1.2 HCW Behavioural and Observational Study

A gap in the literature for observational studies of HCWs as they perform episodes of patient care is recognised almost globally [13, 22, 25]. This element (objective 3) of the research therefore aimed to monitor HCW behaviour and characterise it in a quantitative manner that could be used in infection risk models. An observational study of some 400+ episodes of care was carried out in the Welsh hospital Ysbyty Aneurin Bevan (YAB). This hospital, as well as being one of the first to implement ‘*intentional rounding*’ with its patients, also features the first 100% single room accommodation provision within the UK. This milestone in NHS history provided the ideal setting to watch HCWs as they came in contact with surfaces within patients’ rooms. This first hand data is of fundamental importance for the modelling of human hand-to-surface contact events, allowing inclusive insight into the different types of care and how these also the behaviour of nurses and doctors. HCWs were observed as they performed standard patient care with particular interest in the frequency and the sequence of surfaces touched. This formed the basis for building directed probabilities graphs called Markov chains. The key findings from the evaluation of HCW behaviour were:

- Data revealed that care type influenced the HCW’s surface contact distribution to a large extent. *Direct care* is the mainstay of *intentional rounding*, forming the basis against which all other care types are compared. *Personal care* often contained the most numerous surface contacts, with *miscellaneous care* exhibiting the fewest. However length of care (time) was less influential and showed only weakly positive correlation with surface contact counts. Care types could not be distinguished with respect to patient contacts, however environmental surface contacts exhibited a statistically significant variation throughout.

- Hand hygiene choice at YAB shows a snapshot of a single dynamic modern Welsh hospital. Type of care influenced the choice of hand antiseptics, where HCWs performing short (<30s) episodes of *social care* showed a predilection for alcohol rub. *Direct care* and *miscellaneous care* split the usage of alcohol gel and handwashing almost 50-50. Over 90% of the observed episodes of *personal care* concluded with some form of hand hygiene. These are considered mostly either *hygienic* or *social care* and hence exhibited a 62% preference for handwashing.
- This data then formed the basis of a stochastic model of HCW behaviour as they moved from one surface to another, and consequently forms the driving force behind the subsequent model for pathogen accretion on their hands. Replicating hand-to-surface HCW frequencies for each care type was found to be most effective when considering directed probabilities through Markov chain modelling. There shows a statistically significant improvement of predicted surface contact sequences over simple undirected maximum likelihood estimators.

### 8.1.3 Quantification of Risk and Application of PAM

The Pathogen Accretion Model (PAM) is developed from the growing understanding of hand contamination from surface contacts. This model focuses on the physical process of accruing pathogens onto either the skin or gloved surfaces of HCWs' hands as they perform episodes of standard patient care.

The aim of this model, under objectives 4 and 5 is to provide a framework which allows for the quantitative comparison of hospital room design including single vs. multi-bed accommodation by means of HCW hand contamination. CFD prediction of bioaerosol deposition forms the basis for prediction of surface contamination within a test scenario on which a performance study of PAM can be made. Here the results obtained from the observational study at YAB and presented in Chapter 5 form the basis for the behaviour of the personnel tending to patients. The model represents the HCWs' surface contact patterns by the use of Markov chain modelling. Monte-Carlo sampling allowed a sensitivity analysis along with a parametric study to be carried out, comparing the effects of parameter modification within a test case scenario. This permitted the model to be calibrated and subsequently validated against published literature data.

The PAM methodology was then applied to a typical single and four-bed hospital room to explore the application and scope of the model. Quantification of the risk of the accrued pathogens to subsequent susceptible patients was investigated by an exponential dose-response model.

Key findings from this element of the study:

- Sensitivity analysis showed that the frequency of surface contacts was the dominant factor affecting the end contamination quantities. Other parameters showed only a mildly directly proportional effect. Hand hygiene incorporates the probability of compliance along with efficacy of the chosen antiseptics, which exhibits a clearly bimodal distribution with either neutral or positively linear effects. Total Sobol indices indicated that the mechanism of pathogen transfer was mildly non-linear indicating that bi-directional transfer from both surface-to-hand as well as hand-to-surface was important in the overall process. In order to allow for this variation, it was incorporated.
- CFD modelling of the application scenarios revealed that a ventilation rate of 6 ac.h<sup>-1</sup> showed little significant improvement over 4 ac.h<sup>-1</sup> on deposition percentages or spatial variation in three of the four considered scenarios in the multi-bed room. A decrease in spread locus was noticed particularly when the infectious patient was placed closest to the outlet vent, highlighting the greater downward momentum on particles exerted by comparatively higher local air velocities at 6 ac.h<sup>-1</sup>.
- Application of PAM to the scenario rooms showed that differences were not clear cut and the positioning of the infectious patient had most effect on the final results. Locating the infectious patient in a multi-bed room without an unobstructed air pathway from the bed to the ventilation outlet caused the highest level of surface contamination of all scenarios tested. Other positions often led to comparable contamination levels in a single room.
- Significant differences only became apparent between the two accommodation types when the existence of an infectious patient was known. Results suggested that CFU values on the hands of the HCWs decreased monotonically when single rooms were considered, however in the case of the multi-bed room the biological load either remained stable or increased during contact with subsequent patients. Overall, when

hand hygiene was enforced due to the knowledge of an infectious patient, the single room became significantly less risk prone.

- Hand hygiene compliance obligation significantly improved contamination levels in both cases, with particular effect in the single rooms.
- No airborne cross-contamination was considered in the single rooms due to the recommended corridor pressurisation characteristics. This means that pathogens cannot travel between rooms via air currents meaning that single patient accommodation acts as an effective passive infection control barrier.

## 8.2 Future Research

Each section of this research relies on the best data available as of today (2013), however there are still areas which will benefit from further investigation. Some of the most important are summarised as follows:

### 8.2.1 Experimental and Numerical Particle Deposition

**Particle release quantities** are unknown, à priori, when injecting bioaerosols into the PaCE chamber using the BGI colison nebuliser. Even with the use of a laser particle counter, exact values are far from certain and hence a normalisation metric is necessary to be able to compare different experiments and room layouts. One way to restrict uncertainty is to use silicon or latex particles of a known quantity [289]. The difficulty then lies in being able to capture and count these in the same way as live bacteria. Particle size distributions are also particularly important to characterise within indoor environments [18]. The distribution studied in Chapter 4 has a mean mass diameter of  $2.5\mu\text{m}$ , whereas sneezes or coughs may produce much larger particles [138]. It would be beneficial to investigate the effects of a larger size range on particle behaviour in the indoor environment.

**Surrogate tracers** Unpublished work showed that non-pathogenic tracer chemicals such as lithium chloride or lithium acetate provide an alternative way of tracking aerosols in the indoor environment. These chemicals can be diluted and nebulised in the same way as the *S. aureus* aliquot and captured on dry Petri dishes. Careful washing of

the plates in HCl aqueous solution provides an ideal medium from which atomic absorption spectrometry (AAS) can be performed [290]. In the same manner as the bioaerosols, a spatial concentration contour plot can be created, but without any of the contamination concerns associated with the use of live bacteria.

**Lagrangian particle tracking + DRW** currently appears to be a reliable method to achieve realistic deposition percentages within CFD models [67]. In the exclusion of turbophoresis (turbulence induced particle repulsion), the DRW model provides extra impetus to deposition velocities. In some cases this may be unphysically large, which probably accounts for some of the over-deposition observed. Lai et al. [213, 217] suggest the usage of empirical turbulent kinetic energy models for particles within boundary layers possibly being one solution. This method requires the length-scale of mesh cells to be in the order of millimetres. Therefore computational costs may become exaggerated for room-size domains.

## 8.2.2 Clinical Observational Studies

**Patient care** such as *personal care*, due to its intimate nature, was not observed entirely if the hospital room door was closed. Hence, risks attributed to this type of care may have been underestimated. Therefore to correctly estimate this, the NHS ethics committee deemed a qualified nurse or doctor would be required to observe this type of care [25]. This may be feasible as in the cases of Hayden et al. Duckro et al. and Smith et al. [13, 19, 25], where some form of care has been observed and recorded but not in sufficient detail.

**Surface contamination** is largely uncharacterised. Very few studies swab hospital surfaces for pathogen loads, mainly due to the ineffectiveness of sampling methods [51] but also due to the time-delayed effect of cleaning [166]. Effectively this may represent an oscillating time series which would require substantial sample quantities to correctly characterised.

**Transfer efficiency** of pathogens to hands requires full validation in the clinical setting. This would require glove juice sampling methods in connection with surface swabbing [19]. The very nature of sampling microorganisms from the HCWs' skin or gloves alters the results of future transfer efficiencies [25]. Adenosine triphosphate,

which is fluorescent under UV light has been used successfully in qualitatively tracking surface contacts around a hospital corridor and nurse station [169]. This could prove a useful and non-invasive procedure for use in a hospital patient room.

### 8.2.3 Pathogen Accretion Models

**Validation** of raw pathogen quantities accrued during surface contact is necessary to be able to apply this model without normalisation [22]. This is relatively straight forward in theory, however practice has shown that viable microorganism counts vary depending on the species, culture method and other environmental factors [279]. PAM has been validated against the only known published study containing CFU levels on HCWs' hands, but would benefit greatly from intensive laboratory testing. A preliminary study in the PaCE chamber could be used to evaluate certain sequences of surface contacts but in-vivo glove juice analysis coupled with surface swabbing and HCW surface contact pattern observation would be ultimately necessary.

**Transfer efficiency** may also be a function of contact time and pressure as well as contact method. Assessment of this through a parametric study using live bacteria in a laboratory setting would narrow the uncertainty of this variable [21].

## 8.3 Implications of the Study and Conclusions

In this research, a framework has been developed which enables surface contact risks to be related to room design and healthcare activities. The complementary nature of experimental and computational analysis has facilitated a detailed and systematic investigation into the deposition of bioaerosols within hospital accommodation, revealing that environmental surfaces many metres away from the infectious source may become contaminated. Coupling this with the observational study at YAB showed that, on average, every surface category was touched during a care procedure. Hereby, the extent of how important surfaces really are becomes apparent.

Ayeliffe's remark about the unimportance of hospital surfaces in the chain of infection transmission is becoming increasingly wide of the mark, as research is showing that

aerosolised pathogens are capable of travelling many metres away from the infectious source. Not only this but they are remaining viable for extended periods of time and depositing onto environmental surfaces, putting HCWs at the latent risk of cross-contamination.

This has profound implications for cleaning regimes. Current remits for the cleaning carried out by HCWs are based on ‘*high touch*’ surfaces [35] and equipment. These are to be cleaned twice daily, but according to findings of this research, this may need to be extended to the entire set of touchable surfaces in the vicinity of the patient. Consequently, this has important implications not only for healthcare staff and patients, but also for overall hospital costings [24].

In this golden-age of hospital design and retrofit we are at the foothills of a century of incremental climatic change, requiring hospital design teams, infection control teams, clinicians, housekeeping and the general public to continually adapt and become resilient to an ever changing environment.

Appendix A

Appendix A



**South East Wales Research Ethics  
Committee, Panel C  
Sixth Floor, Churchill House  
17 Churchill Way  
Cardiff CF10 2TW**

Telephone: 02920 3768 23  
Website : [www.nres.nhs.uk](http://www.nres.nhs.uk)

10 January 2012

Mr Marco-Felipe King  
PhD Student  
University of Leeds  
School of Civil Engineering  
Woodhouse Lane, Leeds  
**LS2 9JT**

Dear Mr King

**Study title: Evaluation of the risk of infection in hospital single and ward accommodation via mathematical modelling and computer simulation.**

**REC reference: 11/WA/0200**

Thank you for your letter of the 20 December 2011, responding to the Committee's request for further information on the above research, and for submitting revised documentation.

The further information has been considered on behalf of the Committee by the Chair.

### **Confirmation of ethical opinion**

On behalf of the Committee, I am pleased to confirm a favourable ethical opinion for the above research on the basis described in the application form, protocol and supporting documentation [as revised], subject to the conditions specified below.

### **Ethical review of research sites**

#### **NHS sites**

The favourable opinion applies to all NHS sites taking part in the study, subject to management permission being obtained from the NHS/HSC R&D office prior to the start of the study (see "Conditions of the favourable opinion" below).

### **Conditions of the favourable opinion**

The favourable opinion is subject to the following conditions being met prior to the start of the study.

- Management permission or approval must be obtained from each host organisation prior to the start of the study at the site concerned.
- Management permission ("R&D approval") should be sought from all NHS organisations involved in the study in accordance with NHS research governance arrangements.

- Guidance on applying for NHS permission for research is available in the Integrated Research Application System or at <http://www.rdforum.nhs.uk>.
- Where a NHS organisation's role in the study is limited to identifying and referring potential participants to research sites ("participant identification centre"), guidance should be sought from the R&D office on the information it requires to give permission for this activity.
- For non-NHS sites, site management permission should be obtained in accordance with the procedures of the relevant host organisation.
- Sponsors are not required to notify the Committee of approvals from host organisations
- The Information Sheets should be revised before use to make it clear which cohort they related to, e.g. '*Staff Information Sheet version 2.2 dated 20 December 2011*' and '*Patient Information Sheet version 2.2 dated 20 December 2011*'.
- The Chair recommended that the statement in the staff information sheet advising on possible observation of bad practice etc should also be inserted into the proposed patient information sheet.
- It is the responsibility of the sponsor to ensure that all the conditions are complied with before the start of the study or its initiation at a particular site (as applicable).
- You should notify the REC in writing once all conditions have been met (except for site approvals from host organisations) and provide copies of any revised documentation with updated version numbers. Confirmation should also be provided to host organisations together with relevant documentation.

### **Approved documents**

The final list of documents reviewed and approved by the Committee is as follows:

Document	Version	Date
Evidence of insurance or indemnity	University of Leeds	10 September 2010
Investigator CV	M F King	01 August 2011
Investigator CV	C Noakes	19 September 2011
Participant Information Sheet: Patient Information and Consent Form	2.2	20 December 2011
Participant Information Sheet: Staff Information and Consent Form	2.2	20 December 2011
Protocol	2.0	08 August 2011
Questionnaire: Healthcare Worker Questionnaire	2.0	18 August 2011
REC application		22 June 2011
Referees or other scientific critique report	Research Scrutiny Committee, Aneurin Bevan Health Board	11 May 2011
Referees or other scientific critique report	Research Scrutiny Committee, Aneurin Bevan Health Board	23 May 2011
Response to Request for Further Information	M-F King	01 August 2011

Response to Request for Further Information	2.0	11 November 2011
Response to Request for Further Information	M F King	11 November 2011

### **Statement of compliance**

The Committee is constituted in accordance with the Governance Arrangements for Research Ethics Committees (July 2001) and complies fully with the Standard Operating Procedures for Research Ethics Committees in the UK.

### **After ethical review - Reporting requirements**

The attached document "*After ethical review – guidance for researchers*" gives detailed guidance on reporting requirements for studies with a favourable opinion, including:

- Notifying substantial amendments
- Adding new sites and investigators
- Notification of serious breaches of the protocol
- Progress and safety reports
- Notifying the end of the study

The NRES website also provides guidance on these topics, which is updated in the light of changes in reporting requirements or procedures.

### **Feedback**

You are invited to give your view of the service that you have received from the National Research Ethics Service and the application procedure. If you wish to make your views known please use the feedback form available on the website.

Further information is available at National Research Ethics Service website > After Review

<b>11/WA/0200</b>	<b>Please quote this number on all correspondence</b>
-------------------	---

With the Committee's best wishes for the success of this project

Yours sincerely



Mrs J Jenkins  
**Chair, Panel C**  
**South East Wales Research Ethics Committees**  
Email: [Carl.phillips@wales.nhs.uk](mailto:Carl.phillips@wales.nhs.uk)

Enclosures: "After ethical review – guidance for researchers" SL-AR2

Copy to: R&D office for University of Leeds ([r.e.desouza@leeds.ac.uk](mailto:r.e.desouza@leeds.ac.uk))

R&D office for Aneurin Bevan Health Board ([abb.r&d@wales.nhs.uk](mailto:abb.r&d@wales.nhs.uk))



## Appendix B

## Appendix B

$$\tilde{P}_{\text{Direct care}} = \begin{pmatrix} 0.1842 & 0.3106 & 0.0759 & 0.1515 & 0.2779 \\ 0.4553 & 0.1166 & 0.0068 & 0.2569 & 0.1644 \\ 0.1854 & 0.2425 & 0.2210 & 0.1915 & 0.1595 \\ 0.2454 & 0.1854 & 0.0636 & 0.3248 & 0.1808 \\ 0.2452 & 0.1841 & 0.1219 & 0.1806 & 0.2683 \end{pmatrix}$$

$$\tilde{P}_{\text{Housekeeping}} = \begin{pmatrix} 0.3071 & 0.0001 & 0.0001 & 0.3953 & 0.2975 \\ 0.0004 & 0.0004 & 0.0004 & 0.6679 & 0.3310 \\ 0.0004 & 0.0004 & 0.1621 & 0.1770 & 0.6601 \\ 0.2408 & 0.0537 & 0.0000 & 0.5993 & 0.1061 \\ 0.2624 & 0.1343 & 0.2035 & 0.2625 & 0.1373 \end{pmatrix}$$

$$\tilde{P}_{\text{Mealtimes}} = \begin{pmatrix} 0.9999 & 0.0000 & 0.0000 & 0.0000 & 0.0000 \\ 0.2000 & 0.2000 & 0.2000 & 0.2000 & 0.2000 \\ 0.2000 & 0.2000 & 0.2000 & 0.2000 & 0.2000 \\ 0.2000 & 0.2000 & 0.2000 & 0.2000 & 0.2000 \\ 0.2000 & 0.2000 & 0.2000 & 0.2000 & 0.2000 \end{pmatrix}$$

(B.0.1)

$$\tilde{P}_{\text{Medication rounds}} = \begin{pmatrix} 0.0304 & 0.2767 & 0.2196 & 0.3421 & 0.1312 \\ 0.1560 & 0.0308 & 0.1151 & 0.5537 & 0.1443 \\ 0.0572 & 0.1660 & 0.1703 & 0.3688 & 0.2377 \\ 0.0700 & 0.3377 & 0.1208 & 0.2564 & 0.2152 \\ 0.1374 & 0.1369 & 0.1661 & 0.3567 & 0.2028 \end{pmatrix}$$

$$\tilde{P}_{\text{Miscellaneous}} = \begin{pmatrix} 0.0003 & 0.4185 & 0.0003 & 0.2927 & 0.2883 \\ 0.0002 & 0.0002 & 0.1245 & 0.7500 & 0.1252 \\ 0.0001 & 0.0763 & 0.2024 & 0.5235 & 0.1976 \\ 0.0302 & 0.1152 & 0.1412 & 0.3439 & 0.3695 \\ 0.2359 & 0.0822 & 0.1162 & 0.4063 & 0.1595 \end{pmatrix}$$

$$\tilde{P}_{\text{p. care}} = \begin{pmatrix} 0.167 & 0.167 & 0.167 & 0.331 & 0.167 \\ 0.073 & 0.073 & 0.215 & 0.352 & 0.284 \\ 0.041 & 0.198 & 0.479 & 0.121 & 0.159 \\ 0.059 & 0.196 & 0.114 & 0.435 & 0.195 \\ 0.050 & 0.099 & 0.147 & 0.461 & 0.241 \end{pmatrix}$$

# Bibliography

- [1] R.M. Klevens, J.R. Edwards, and C.L. Richards. Estimating health-care associated infections and deaths in U.S. hospitals. *Public Health Rep.*, 122(2):160–166, 2002.
- [2] S.J. Smith, V. Young, C. Robertson, and S.J. Dancer. Where do hands go? An audit of sequential hand-touch events on a hospital ward. *Microbiol. Mol. Biol. Rev.*, 74(3):417–433, 2010.
- [3] Centers for Disease Control and Prevention. Guidelines for environmental infection control in health-care facilities. *MMWR Morbidity Mortality Weekly*, 52(10), 2003.
- [4] OECD. Health at a glance: Europe 2012. Technical report, OECD Publishing, <http://www.oecd.org/health/healthataglance/europe> Accessed:05/2013, 2012.
- [5] Department of Health. *Health Building Note 04-01: Adult in-patient facilities*. The Stationery Office, 2005.
- [6] C.R. Alalouch and P. Aspinall. Spatial attributes of hospital multi-bed wards and preferences for privacy. *Facilities*, 25(9-10):345–362, 2008.
- [7] Phoenix Controls. Mechanical ventilation set-up in hospital isolation rooms. <http://www.phoenixcontrols.com/Collateral/Images/English-US/Isolation-Room.jpg>, Accessed: 18/05/13.
- [8] Arup. *Arup in Healthcare: Collaborating globally*, volume 1. Digest of the International Federation of Hospital Engineering, London, 2013.
- [9] K.J. Lomas and Y. Ji. Resilience of naturally ventilated buildings to climate change: Advanced natural ventilation and hospital wards. *Energy and Buildings*, 41(6):629 – 653, 2009.

- [10] I. Semmelweis. *Etiology, Concept and Prophylaxis of Childbed Fever*. University of Wisconsin Press, USA, September 1983. Translation.
- [11] J.D. Spengler. Approximate particle settling time. [http://www.lungusa.org/site/c.dvLUK900E/b.39314/k.DF00/Appendix\\_1\\_Table\\_Approximate\\_Particle\\_Setting\\_Time.htm](http://www.lungusa.org/site/c.dvLUK900E/b.39314/k.DF00/Appendix_1_Table_Approximate_Particle_Setting_Time.htm), Accessed:01/06/10.
- [12] X. Xie. *Evaporation and Movement of Respiratory Droplets in Indoor Environments*. PhD thesis, The University of Hong Kong, 2008.
- [13] A.N. Duckro, D.W. Blom, E.A. Lyle, R.A. Weinstein, and M.K. Hayden. Transfer of vancomycin-resistant enterococci via health care workers' hands. *Archive International Medicine*, 165(3) PAGES=302-307,, 2005.
- [14] L. J. S. Allen. An introduction to stochastic epidemic models. *Department of Mathematics and Statistics Texas Tech University*, I, 2008.
- [15] G. N. Sze To and C. Y. H. Chao. Review and comparison between the wells-riley and dose-response approaches to risk assessment of infectious respiratory diseases. *Indoor Air*, 20(1):2–16, 2010.
- [16] J.M. Pujol, J.E. Eisenberg, C.N. Haas, and J.S. Koopman. The effect of ongoing exposure dynamics in dose response relationships. *PLoS Comput Biol*, 5(6), 2009.
- [17] M-F. King. Protection provided by local uvgi intervention devices against influenza transmission within hospitals. Master's thesis, University of Leeds, 2009.
- [18] J.W. Tang, C.J. Noakes, P.V. Nielsen, I. Eames, A. Nicolle, Y. Li, and G.S. Settles. Observing and quantifying airflows in the infection control of aerosol and airborne-transmitted diseases: an overview of approaches. *Journal of Hospital Infection*, 7: 213–222, 2011.
- [19] M.K. Hayden, D.W. Blom, E.A. Lyle, C.G. Moore, and R.A. Weinstein. Risk of hand or glove contamination after contact with patient colonized with vre or the colonized patients' environment. *Infection Control and Hospital Epidemiology*, 29: 149–154, 2008.
- [20] D. Pittet, B. Allegranzi, H. Sax, S. Dharan, C. Lucia Pessoa-Silvia, L. Donaldson, and J. Boyce. Evidence-based model for hand transmission during patient care and the role of improved practices. *Lancet Infect Dis*, 6:641–652, 2006.

- [21] G. Lopez. *Transfer of Microorganisms from Fomites to Hands and Risk Assessment of Contaminated and Disinfected Surfaces*. PhD thesis, The University of Arizona, 2013 Unpublished.
- [22] D. Pittet, S. Dharan, S. Touveneau, V. Sauvan, and T.V. Perneger. Bacterial contamination of the hands of hospital staff during routine patient care. *Arch. Intern. Med*, 159:821–826, 1999.
- [23] R. Montville and D.W. Schaffner. A meta-analysis of the published literature on the effectiveness of antimicrobial soaps. *Journal of Food Protection*, 74(11):1875–1882, 2011.
- [24] S.J. Dancer. Mopping up hospital infection. *Journal of Hospital Infection*, 43:85–100, 1999.
- [25] S.J. Smith, V. Young, C. Robertson, and S.J. Dancer. Where do hands go? An audit of sequential hand-touch events on a hospital ward. *Journal of Hospital Infection*, 80:206–211, 2012.
- [26] York Health Economics Consortium. Cost-effectiveness of hospital design: Options to improve patient safety and wellbeing. Technical report, University of York, 2005.
- [27] C. Wendt, D. Knautz, and H. von Baum. Differences in hand hygiene behavior related to the contamination risk of healthcare activities in different groups of healthcare workers. *Infection Control and Hospital Epidemiology*, 3(25):203–206, 2004.
- [28] R. J. Pratt, C. M. Pellowe, J. A. Wilson, H. P. Loveday, P. J. Harper, S. R. L. J. Jones, C. McDougall, and M. H. Wilcox. epic2: National evidence-based guidelines for preventing healthcare-associated infections in nhs hospitals in england. *Journal of Hospital Infection*, 65(1):1–59, 2007.
- [29] National Audit Office. The management and control of hospital acquired infections in acute nhs trusts in england. *National Audit Office.*, 1, 2000.
- [30] B. Dowdeswell, J. Erskie, and M. Heasman. Hospital ward configuration determinants influencing single room provision: A report for nhs estates, england. *EU Health Property Network*, 2004.
- [31] G. Clark. *UK Budget 2013*. The stationery office ltd., 2013.

- [32] C.B. Beggs, C.J. Noakes, S.J. Shepherd, K.G. Kerr, P.A. Sleight, and K. Banfield. The influence of nurse cohorting on hand hygiene effectiveness. *AJIC*, 44:295–304, 2006.
- [33] C.B. Beggs, K.G. Kerr, J.K. Donnelly, P.A. Sleight, D.D. Mara, and G. Cairns. An engineering approach to the control of mycobacterium tuberculosis and other airborne pathogens: a uk hospital based pilot study. *Transactions of the Royal Society of Tropical Medicine and Hygiene*, 94(2):141–146, 2000.
- [34] C.B. Beggs. The airborne transmission of infection in hospital buildings: fact or fiction? *Indoor and Built Environment*, 12:1–10, 2003.
- [35] K. Huslage, W.A. Rutala, E. Sickbert-Bennett, and D.J. Weber. A quantitative approach to defining “high-touch” surfaces in hospitals. *Infection Control and Hospital Epidemiology*, 31(8):850–853, 2010.
- [36] R. Canales and J. Leckie. Application of a stochastic model to estimate children’s short-term residential exposure to lead. *Stochastic Environmental Research and Risk Assessment*, 21(6):737–745, 2007.
- [37] F. Nightingale. *Notes on Hospitals*. Harvard College Press, Massachusetts, 1883.
- [38] WebMD. Webster’s new world medical dictionary. 3, Accessed:2009.
- [39] World Health Organization. WHO guidelines on hand hygiene in health care. Technical report, WHO, 2009.
- [40] S. Harbarth, H. Sax, and P. Gastmeier. The preventable proportion of nosocomial infections:an overview of published reports. *Journal of Hospital Infection*, 54:258–266, 2003.
- [41] R.S. Ulrich, C. Zimring, X. Zhu, J. DuBose, H-B. Seo, Y-S. Choi, X. Quan, and A. Joseph. A review of the research literature on evidence-based healthcare design. *The center for health design*, 2008.
- [42] Chief Medical Officer. Winning way. Working together to reduce healthcare associated infection in englands. *Department of Health*, 2003.
- [43] Department of Health. *The Health Act 2006: Code of practice for the prevention and control of healthcare associated infections*. Department of Health, 2006.

- [44] Health Protection Agency. Results from the mandatory surveillance of methicillin resistant *Staphylococcus aureus* (mrsa) bacteraemia. Technical report, [http://www.hpa.org.uk/web/HPAweb&HPAwebStandard/HPAweb\\_C/1254510675444](http://www.hpa.org.uk/web/HPAweb&HPAwebStandard/HPAweb_C/1254510675444), Accessed:20/03/2013.
- [45] S. Harbarth. Nosocomial transmission of antibiotic-resistant microorganisms. *Current Opinion in Infectious Diseases*, 14:437–442, 2001.
- [46] E.A. Hathway. *CFD modelling of pathogen transport due to human activity*. PhD thesis, Civil Engineering, Leeds University, 2008.
- [47] E. J. Fendler, Y. Ali, B.S. Hammond M.K. Lyons, M.B. Kelley, and N.A. Vowell. The impact of alcohol hand sanitizer use on infection rates in an extended care facility. *American Journal of Infection Control*, 30(4):226–233, 2002.
- [48] G A J Ayliffe, A.P. Fraiese, and A.M. Geddes et al. *Control of hospital infection: a practical handbook*. Arnold, London, 4th edition, 2000.
- [49] J.M. Boyce. Environmental contamination makes an important contribution to hospital infection. *Journal of Hospital Infection*, 65:50–54, 2007.
- [50] L.F. White, S.J. Dancer, C. Robertson, J McDonald, and NHS. Are hygiene standards useful in assessing infection risk? *American Journal of Infection Control*, 36(5):381–384, 2008.
- [51] A. Bhalla and et al. Acquisition of nosocomial pathogens on hands after contact with environmental surfaces near hospitalized patients. *Infection control and hospital epidemiology*, 25(2):164–167, 2004.
- [52] N. Dimmock, A. Easton, and K. Leppard. *Introduction to Modern Virology*. Wiley-Blackwell, 6th edition, 2006.
- [53] D.J. Weber, W.A. Rutula, M.B. Miller, K. Huslage, and E. Sickbert-Bennett. Role of hospital surface in the transmission of emerging health care-associated pathogens: Norovirus, clostridium difficile and acinetobacter species. *American Journal of Infection Control*, 38(5 Suppl 1):25–33, 2010.
- [54] APIC. Apic text of infection control and epidemiology. Technical report, Association for Professionals in Infection Control and Epidemiology Inc, Washington, DC, 2005.

- [55] W.A.C. Zoon, M.G.L.C. Loomans, and J.L.M. Hensen. Testing the effectiveness of operating room ventilation with regard to removal of airborne bacteria. *Building and Environment*, 46(12):2050–2077, 2011.
- [56] C.A. Mitchell, L.F. Guerin, and J. Robillard. Decay of influenza a viruses of human and avian origin. *Can J Comp Med*, 32:544–6, 1968.
- [57] H. Qian. *Ventilation for Controlling airborne infection in hospital environments*. PhD thesis, The University of Hong Kong, 2007.
- [58] P.N. Hoffman, A.M. Bennett, and G.M. Scott. Controlling airborne infection. *Journal of Hospital Infection*, 43:203–210, 1999.
- [59] C.J. Noakes, P.A. Sleight, A.R. Escombe, and C.B. Beggs. Use of cfd analysis in modifying a tb ward in lima, peru. *Indoor and Built Environment*, 15(1):41–47, 2006.
- [60] E.C. Riley, G. Murphy, and R.L. Riley. Airborne spread of measles in a suburban elementary school. *American Journal of Epidemiology*, 107:421–432, 1978.
- [61] S. Francis and R. Glanville. Building a 2020 vision: Future health care environments. Technical report, Nuffield Trust and RIBA Future Studies, London: The Stationery Office, 2001.
- [62] Department of Health. High quality care for all. Technical report, NHS Next Stage Review Final Report, 2007.
- [63] J.M. Stockley, C.E. Constantine, and K.E. Orr. Building new hospitals: a uk infection control perspective. *Journal of Hospital Infection*, 62:285–289, 2006.
- [64] NHS Sustainable Development Unit. Nhs carbon reduction strategy for england: Saving carbon improving health. Technical report, NHS, Cambridge, 2009.
- [65] E.M. Sternberg. *Healing Spaces: the Science of Place and Well-Being*. Belknap Press: Cambridge, 2009.
- [66] B. Friberg, S. Friberg, and L.G. Burman. Correlation between surface and air counts of particles carrying aerobic bacteria in operating rooms with turbulent ventilation: an experimental study. *Journal of Hospital Infection*, 42(1):61 – 68, 1999.

- [67] L. Tian and G. Ahmadi. Particle deposition in turbulent duct flows- comparisons of different model predictions. *Journal of Aerosol Science*, 38:377–397, 2007.
- [68] Q.Chen and Glicksman. System performance evaluation and design guidelines for displacement ventilation. *ASHRAE*, 2003.
- [69] H. Chaudhury, A. Mahmood, and M. Valente. Advantages and disadvantages of single-versus multiple-occupancy rooms in acute care environments: a review and analysis of the literature. *Environment and Behavior*, 37(6):760–786, 2005.
- [70] P. Nedin. Planning today’s estate to meet tomorrow’s needs. *Digest of the International Federation of Hospital Engineering*, 1:14–18, 2013.
- [71] J. Marraccini and D. Patterson. *Development Study VA Hospital Building System by Building Systems Development and Stone*. U.S. Government Printing Office, John Wiley Sons Ltd England, 1977.
- [72] Leeds Teaching Hospitals NHSTrust. Leeds general infirmary. <http://www.leedsteachinghospitals.com/patients/aboutus/hospitals/lgi.php>, Accessed:02/07/09.
- [73] Department of health. Health technical memorandum 03-01: Specialised ventilation for healthcare premises. *Heating and Ventilation Systems*, A 03-01, 2013.
- [74] H.M. Pattison and C.E. Robertson. The effect of ward design on the well-being of post-operative patients. *Journal of Advanced Nursing*, 23(4):820–6, 1996.
- [75] C. Beggs, K.G. Kerr, C.J. Noakes, A. Hathway, and P.A. Sleight. The ventilation of multiple-bed hospital wards: Review and analysis. *American Journal for Infection Control*, 36(4):150–159, 2008.
- [76] N.H. O’Connell and H. Humphreys. Intensive care unit design and environmental factors in the acquisition of infection. *Journal of Hospital Infections*, 45, 2000.
- [77] D. Bracco, M-J. Dubois, R. Bouali, and P. Eggimann. Single rooms may help to prevent nosocomial bloodstream infection and cross-transmission of methicillin-resistant staphylococcus aureus in intensive care units. *Intensive Care Medical*, 33, 2007.

- 
- [78] F. Brauer. Mathematical epidemiology is not an oxymoron. *BMC Public Health*, 9, 2009.
- [79] W.O. Kermack and A.G. McKendrick. Contributions to the mathematical theory of epidemics. *Proc Roy Soc London*, 115:700–712, 1927.
- [80] W.O. Kermack and A.G. McKendrick. Contributions to the mathematical theory of epidemics, part ii. *Proc Roy Soc London*, 138:55–83, 1932.
- [81] W.O. Kermack and A.G. McKendrick. Contributions to the mathematical theory of epidemics, part iii. *Proc Roy Soc London*, 141:94–112, 1933.
- [82] D.J. Watts. *Small Worlds: The Dynamics of Networks Between Order and Randomness*. Princeton University Press, 1999.
- [83] Environmental Protection Agency. Dermal exposure assessment: Principles and applications. Technical report, Office of Health and Environmental Assessment U.S. Environmental Protection Agency, Washington D.C. 20460. USA, 1992.
- [84] P. Beamer, R.A. Canales, and J.O. Leckie. Developing probability distributions for transfer efficiencies for dermal exposure. *Journal of Exposure Science and Environmental Epidemiology*, 19:274–283, 2009.
- [85] V.A. Zartarian, H. Özkaynak, J.M. Burke, M.J. Zufall, M.L. Rigas, and E.J. Furtaw. A modeling framework for estimating children’s residential exposure and dose to chlorpyrifos via dermal residue contact and nondietary ingestion. *Environ Health Perspect*, 108:505–514, 2000.
- [86] W.F. Wells. *Airborne Contagion and Air Hygiene: an Ecological Study of Droplet Infection*. Harvard University Press, MA, 1955.
- [87] L. Gammaitoni and M.C. Nucci. Using a mathematical model to evaluate the efficacy of tb control measures. *Emerg. Infect. Dis*, 3:335–342, 1997.
- [88] C.B. Beggs, C.J. Noakes, P.A. Sleight, L.A. Fletcher, and K. Siddiqi. The transmission of tuberculosis in confined spaces: an analytical study of alternative epidemiological models. *International Journal of Tuberculosis Lung Disease*, 7:1015–1026, 2003.

- [89] H. Qian, Y.G. Li, P.V. Nielsen, and X.H. Huang. Spatial distribution of infection risk of sars transmission in a hospital ward. *Building and Environment*, 44:1651–1658, 2009.
- [90] C.J. Noakes and P.A. Sleigh. Mathematical models for assessing the role of airflow on the risk of airborne infection in hospital wards. *Journal of the Royal Society Interface*, 6, 2009.
- [91] Z.F. Tian, J.Y. Tu, G.H. Yeoh, and R.K.K. Yuen. On the numerical study of contaminant particle concentration in indoor air?ow. *Building and Environment*, 41(11):1504–1514, 2006.
- [92] L.T. Wong, W.Y. Chan, K.W. Mui, and A.C.K. Lai. An experimental and numerical study on deposition of bioaerosols in a scaled chamber. *Aerosol Science and Technology*, 44(2):117–128, 2010.
- [93] M-F. King, M.A. Camargo-Valero, C.J. Noakes, and P.A. Sleigh. Bioaerosol deposition in single and two-bed hospital rooms: A numerical and experimental study. *Building and Environment*, 59:436–447, 2013.
- [94] T.T. Chow and X.Y. Yang. Ventilation performance in the operating theatre against airborne infection: numerical study on an ultra-clean system. *Journal of Hospital Infection*, 59:138–147, 2005.
- [95] T-T. Chow and X-Yu. Yang. Performance of ventilation system in a non-standard operating room. *Building and Environment*, 38:1401–1411, 2003.
- [96] I. Eames, D. Shoaib, C.A. Klettner, and V. Taban. Movement of airborne contaminants in a hospital isolation room. *Journal of the Royal Society Interface*, 6, 2009.
- [97] F. Memarzadeh, Z. Jiang, and W. Xu. Analysis of efficacy of uvgi inactivation of airborne organisms using eulerian and lagrangian approaches. *Indoor Air Quality*, 2004.
- [98] S-C. Hu Y-C. Tung, Y-C. Shih. Numerical study on the dispersion of airborne contaminants from an isolation room in the case of door opening. *Applied Thermal Engineering*, 29, 2009.

- [99] H. Qian, Y. Li, P.V Nielsen, and C.E. Hyldgaard. Dispersion of exhalation pollutants in a two-bed hospital ward with a downward ventilation system. *Building and Environment*, 2008.
- [100] A. Hathway, L.A. Fletcher, C.J. Noakes, P.A. Sleight, M. Elliot, and I. Clifton. Bioaerosol production from routine activities within a hospital ward. In *Indoor Air 2008 : The 11th International Conference on Indoor Air Quality and Cl*, Copenhagen, Denmark, 17-22nd August 2008.
- [101] T.W. Wong and et al. Cluster of sars among medical students exposed to single patient. *Emerging Infectious Diseases*, 10, 2004.
- [102] Y. Li and X. Huang. Role of air distribution in sars transmission during the largest nosocomial outbreak in hong kong. *Indoor Air*, 15(2):83–95, 2005.
- [103] C.J. Noakes, P.A. Sleight, C.B. Beggs, and K.G. Kerr. Modelling the transmission of airborne infections in enclosed spaces. *Epidemiol. Infect*, 134, 2006.
- [104] S. Prasad, editor. *Changing hospital architecture*. Riba publishing, London, 2008.
- [105] C. Hendrickson and A. Tung. *Project Management for Construction*. Prentice Hall, 1989.
- [106] Department of Health. *Health Technical Memorandum 07-01: Safe Management of Healthcare Waste*. Department of Health, Stationery office, London, 2013.
- [107] NHS Estates. *Infection control in the built environment design and planning*. NHS Estates, London, 2001.
- [108] L. Morawska. Droplet fate in indoor environments, or can we prevent the spread of infection. *Indoor Air*, 16, 2006.
- [109] A.P.R. Wilson and G.L. Ridgway. Reducing hospital-acquired infection by design: the new university college london hospital. *Journal of Hospital Infection*, 62(3):264 – 269, 2006.
- [110] Nuffield Provincial Hospitals Trust. *Studies in the functions and design of hospitals: the report of an investigation sponsored by the nuffield provincial hospitals trust and the university of bristol*. Technical report, Oxford University Press, London, 1955.

- 
- [111] C.R. Alalouch. *Hospital ward design: implications for space and privacy*. PhD thesis, Heriot-Watt University Built Environment, 2009.
- [112] C.A. Gilkeson, M.A. Camargo-Valero, L.E. Pickin, and C.J. Noakes. Measurement of ventilation and airborne infection risk in large naturally ventilated hospital wards. *Building and Environment*, 65:35 – 48, 2013.
- [113] R.S. Ulrich. Research on building design and patient outcomes in exploring the patient environment: An nhs estates workshop. *London: The Stationery Office*, 2003.
- [114] M.S. Dettenkofer, S. Seegers, G. Antes, E. Motschall, and M. Schumacher. Does the architecture of hospital facilities influence nosocomial infection rates? a systematic review. *Infection Control and Hospital Epidemiology*, 25(1):21–25, 2004.
- [115] I. van de Glind, S. de Roode, and A. Goossensen. Do patients in hospitals benefit from single rooms? A literature review. *BMJ British Medical Journal*, 84(2):153–161, 2007.
- [116] M. Martinez and E. Tobari. Designing behaviour the influence of design on ward performance. Technical report, Space Syntax, London, 2008.
- [117] Department of Health. *Health Building Note 04-01: Sanitary spaces*. The Stationery Office, 2005.
- [118] C.J. Noakes, P.A. Sleight, and A. Khan. Appraising healthcare ventilation design from combined infection control and energy perspectives. *HVAC&R Research*, 18(4), 2012.
- [119] P. Ninomura and J. Bartley. New ventilation guidelines for health-care facilities. *ASHRAE*, 43:29–33, 2001.
- [120] J. Sundell, H. Levin, W.W. Nazaroff, W.S. Fish, W.J. Fish, and et al. Ventilation rates and health: multidisciplinary review of the scientific literature. *Journal of Hospital Infection*, 21:191–204, 2011.
- [121] D. Menzies, A. Fanning, L. Yuan, J.M. FitzGerald, and the Canadian Collaborative Group in Nosocomial Transmission of TB. Hospital ventilation and risk for tuberculous infection in canadian health care workers. *Ann. Intern. Med.*, 133:779–789, 2000.

- [122] Y. Li, X. Huang, I.T.S. Yu, T. W. Wong, and H. Qian. Role of air distribution of sars outbreak during largest nosocomial infection in hong kong. *Indoor air*, 15: 83–95, 2004.
- [123] W. Whyte, O.M. Lidwell, E.J.L. Lowbury, and R. Blowers. Suggested bacteriological standards for air in ultraclean operating room. *Journal of Hospital Infection*, 4:133–139, 1984.
- [124] O.M. Lidwell. Ultraviolet radiation and the control of airborne contamination the operating room. *Journal of Hospital Infection*, 28:245–248, 1994.
- [125] B. Drake. Infection control in hospitals. *Health-Care HVAC*, 13, June 2006.
- [126] W.J. Fisk, D. Faulkner, D. Sullivan, and F. Bauman. Air change effectiveness and pollutant removal efficiency during adverse mixing conditions. *Indoor Air*, 7, 1997.
- [127] CIBSE. *Guide B: Heating, Ventilating, Air Conditioning and Refrigeration*. Chartered Institute of Building Services Engineers, 2005.
- [128] Department of Health. Sustainable health and social care buildings. Technical report, The stationery office London, 2009.
- [129] K.J. Lomas and R. Giridharan. Thermal comfort standards, measured internal temperatures and thermal resilience to climate change of free-running buildings: A case-study of hospital wards. *Building and Environment*, 55(0):57 – 72, 2012.
- [130] C.A. Short, K.J. Lomas, R. Giridharan, and A.J. Fair. Building resilience to overheating into 1960’s {UK} hospital buildings within the constraint of the national carbon reduction target: Adaptive strategies. *Building and Environment*, 55(0):73 – 95, 2012.
- [131] Z.A. Adamu, A.D.F. Price, and M.J. Cook. Performance evaluation of natural ventilation strategies for hospital wards - a case study of great ormond street hospital. *Building and Environment*, 56(0):211–222, 2012.
- [132] National Health Service. *Heatwave plan for England, protecting health and reducing Harm from extreme heat and Heatwaves*. NHS, [http://www.nhs.uk/Livewell/Summerhealth/Documents/dh\\_HeatwavePlan2011.pdf](http://www.nhs.uk/Livewell/Summerhealth/Documents/dh_HeatwavePlan2011.pdf), May 2011.

- [133] C. Short and S. Almaiya. Design strategy for low-energy ventilation and cooling of hospitals. *Building Research & Information*, 37(3):264–292, 2009.
- [134] CIBSE. *CIBSE Guide A Environmental Design*. Chartered Institution of Building Services Engineers, 2007.
- [135] C. Alan Short, Malcolm Cook, Paul C. Cropper, and Sura Al-Maiyah. Low energy refurbishment strategies for health buildings. *Journal of Building Performance Simulation*, 3(3):197–216, 2010.
- [136] @MisterPeter. Children’s eye centre. <http://www.architravel.com/architravel/building/the-richard-desmond-childrens-eye-centre-moorfields-eye-hospital>, Accessed: 2013.
- [137] C. McCartney. Healthcare-associated infections in england: 2008-2009 report. *Health Protection Agency*, 2009.
- [138] J.W. Tang, Y. Li, I. Eames, P.K.S. Chan, and G.L. Ridgway. Factors involved in the aerosol transmission of infection and control of ventilation in healthcare premises. *Journal of Hospital Infection*, 64:100–114, 2006.
- [139] C-C. Tseng and C-S. Li. Inactivation of virus-containing aerosols by ultraviolet germicidal irradiation. *Aerosol Science and Technology*, 39(12):1136–1142, 2005.
- [140] M. Nicas and G. Sun. An integrated model of infection risk in a health-care environment. *Risk Analysis*, 26(4), 2006.
- [141] Kathrine Roberts. *The aerial dissemination of Clostridium difficile in the clinical environment*. PhD thesis, University of Leeds, 2008.
- [142] B.S Cooper, G.F. Medley, and G.M. Scott. Preliminary analysis of the transmission dynamics of nosocomial infections: stochastic and management effects. *Journal of Hospital Infection*, 43, 1999.
- [143] K.N. Huynh, Brian G. Oliver, Sacha Stelzer, William D. Rawlinson, and Euan R. Tovey. A new method for sampling and detection of exhaled respiratory virus aerosols. *CID*, 2007.

- [144] NICE. *Prevention and control of healthcare-associated infections in primary and community care*. National Institute for Health and Clinical Excellence: NICE clinical guideline 139, NHS, 2012.
- [145] I. Eames, J. W. Tang, Y. Li, and P. Wilson. Airborne infection transmission of disease in hospitals. *Journal of the Royal Society Interface*, 6, 2009.
- [146] C.S Cox. *Physical aspects of bioaerosol particles*, chapter Chapter 3, pages 15–25. Lewis Publishers, New York, 1995.
- [147] W.F. Wells. On air-borne infection. ii. droplets and droplet nuclei. *American Journal of Hygiene*, 20:611–618, 1934.
- [148] N.A. Fuks. *The mechanics of aerosols*. Dover Publications, New York, 1989.
- [149] J.P. Duguid. The size and distribution of air-carriage of respiratory droplets and droplet-nuclei. *Journal of Hygiene*, 4, 1946.
- [150] J.W. Tang, G.C. Koh, A.D. Nicolle, C.A. Klettner, J. Pantelic, and L. Wang et al. Lack of influenza transmission via aerosol during various human respiratory activities. In *Bioaerosols and the Built Environment Conference*. University of Leeds, June 2013.
- [151] P.R. Chadwick and R. McCann. Transmission of a small round structured virus during an hospital outbreak of gastroenteritis. *Journal of Hospital Infection*, 26, 1994.
- [152] W.C. Noble. Dispersal of bacteria from human skin. *Proceedings of the International Symposium on Contamination Control, Copenhagen, Denmark*, pages 16–24, 1976.
- [153] R. Sheretz and et al. A cloud adult: The staphylococcus aureus virus-interaction revisited. *Annals of internal medicine*, 126(6):539–547, 1996.
- [154] S.W. Kembel, E. Jones, J. Kline, D. Northcutt, J. Stenson, A.M. Womack, B.J.M. Bohannan, G.Z. Brown, and J.L. Green. Architectural design influences the diversity and structure of the built environment microbiome. *The ISME Journal*, 6:1469–1479, 2012.
- [155] T. Rinttilä, A. Kassinen, E. Malinen, L. Krogius, and A. Palva. Development of an extensive set of 16s rdna-targeted primers for quantification of pathogenic and

- indigenous bacteria in faecal samples by real-time pcr. *J Appl Microbiol*, 97:1166–1177, 2004.
- [156] A. Kramer, I. Schwebke, and G. Kampf. How long do nosocomial pathogens persist on inanimate surfaces? a systematic review. *BMC Infectious Diseases*, 130(6), 2006.
- [157] L. Curtis. Prevention of hospital-acquired infections: review of non-pharmacological interventions. *Journal of Hospital Infection*, 69, 2008.
- [158] Z. D. Bolashikovt and A. K. Melikov. Methods for indoor disinfection and purification from airborne pathogens for application in hvac systems. *International Centre for Indoor Environment and Energy, Department of Mechanical Engineering, Technical University of Denmark*, 1, 2008.
- [159] A.R. Escombe, L. Huaroto, E. Ticona, M. Burgos, I. Sanchez, L. Carrasco, E. Farfan, F. Flores, and D.A.J. Moore. Tuberculosis transmission risk and infection control in a hospital emergency department in lima, peru. *The International Journal of Tuberculosis and Lung Disease*, 14(9):1120–1126, 2010.
- [160] J. H. Vincent. *Aerosol Sampling; Science, Standards, Instrumentation and Application*. John Wiley and Sons Ltd, John Wiley & Sons Ltd, The Atrium, Southern Gate, Chichester, West Sussex PO19 8SQ, England, 2007.
- [161] X.Wen and S.J. Dunnett. A numerical study of the sampling efficiency of a tube sampler operating in calm air facing both vertically upwards and downwards. *Journal Aerosol Sci*, 33:1663–1665, 2002.
- [162] Y. Thomas, G. Vogel, W. Wunderli, P. Suter, M. Witschi, D. Koch Caroline Tapparel, and Laurent Kaiser. Survival of influenza virus on banknotes. *Applied and Environmental Microbiology*, 74(10):3002–2007, May 2008.
- [163] J.D. Noti, F.M. Blachere, C.M. McMillen, W.G. Lindsley, M.L. Kashon, D.R. Slaughter, and D.H. Beezhold. High humidity leads to loss of infectious influenza virus from simulated coughs. *PLoS ONE*, 8:Not yet published in print. <http://dx.doi.org/10.1371/journal.pone.0057485> e57485, Accessed:07/07/2013, 2013.
- [164] A.M. Savage and R.H. Alford. Nosocomial spread of *Clostridium difficile*. *Infection Control*, 4:31–33, 1983.

- [165] J.S. Garner. Guideline for isolation precautions in hospitals. part ii. recommendations for isolation precautions in hospitals. *American Journal of Infection Control*, 24(1):32–52, 1997.
- [166] A. Bogusz, M. Stewart, J. Hunter, B. Yip, D. Reid, C. Robertson, and S.J. Dancer. How quickly do hospital surfaces become contaminated after detergent cleaning? *Healthcare Infection*, 18(1):3–9, 2013.
- [167] S.J. Dancer. The role of environmental cleaning in the control of hospital-acquired infection. *Journal of Hospital Infection*, 73 (4):378–85, 2009.
- [168] T. Lewis, C. Griffith, M. Gallo, and M. Weinbren. A modified {ATP} benchmark for evaluating the cleaning of some hospital environmental surfaces. *Journal of Hospital Infection*, 69(2):156 – 163, 2008.
- [169] C.J. Griffith, P. Obee, R.A. Cooper, N.F. Burton, and M. Lewis. The effectiveness of existing and modified cleaning regimens in a welsh hospital. *Journal of Hospital Infection*, 66(4):352 – 359, 2007.
- [170] T.D. Hollingsworth. Controlling infectious disease outbreaks: Lessons from mathematical modelling. *Journal Public Health Policy*, 30(3):328–341, 2009.
- [171] N. T. J. Bailey. *The Mathematical Theory of Infectious Diseases and Its Applications*. Griffin, London, 1975.
- [172] P. V. Nielsen, F. Allard, H.B. Awbi, L. Davidson, and A. Schälin. *CFD in Ventilation Design a new REHVA Guide Book*. Aalborg University, 2009.
- [173] D. Bernoulli. *Essai d’une nouvelle analyse de la mortalité causée par la petite vérole et des avantages de l’inoculation pour la prévenir*, chapter Mémoires de Mathématiques et de Physique, pages 1–45. Académie Royale des Sciences, Paris, 1760.
- [174] W. H. Hamer. Epidemic disease in england. *Lancet*, 1:733–739, 1906.
- [175] H. W. Hethcote. The mathematics of infectious diseases. *Society for Industrial and Applied Mathematics*, 42(4), 2000.
- [176] G. Macdonald. The analysis of sporozoite rate. *Tropical Disease Bulletin*, 49:569–585, 1952.

- [177] K. MacKenzie and S. C. Bishop. Developing stochastic epidemiological models to quantify the dynamics of infectious diseases in domestic livestock. *Tropical Disease Bulletin*, 79:2047–2056, 2001.
- [178] Nikolaos Demiris. *Bayesian Inference for Stochastic Epidemic Models using Markov chain Monte Carlo Methods*. PhD thesis, University of Nottingham, 2004.
- [179] J. Vanderpas, J.Louis, M.Reynders, G.Mascart, and O. Vandenberg. Mathematical model for the control of nosocomial norovirus. *Journal of Hospital Infection*, 71, 2009.
- [180] J. Mena-Lorca, J. X. Velasco-Hernandez, and C. Castillo-Chavez. Density-dependent dynamics and superinfection in an epidemic model. *IMA Journal of Mathematical and Applied Medical Biology*, 16:307–317, 1999.
- [181] R. M. Anderson and R. M. May. *Population Biology of Infectious Diseases*. Springer-Verlag, Berlin Heidelberg New York,, 1982.
- [182] E. Renshaw. *Modelling Biological Populations in Space and Time*. Cambridge studies in mathematical biology, 1991.
- [183] M. Nicas and R.M. Jones. Relative contributions of four exposure pathways to influenza infection risk. *Risk Analysis*, 29(9), 2009.
- [184] D.J. Wilkinson. *Stochastic modelling for systems biology*. Mathematical and Computational Biology Series. Chapman Hall, 2006.
- [185] H.C. Tijms. *A First Course in Stochastic Models*. Wiley, 2003.
- [186] P. E. Greenwood and L.F. Gordillo. *Stochastic Epidemic Modelling*, chapter Mathematical and Statistical Estimation Approaches in Epidemiology. Springer Science + Business, 2009.
- [187] K. Borovkov. *Elements of Stochastic modeling*. World Scientific Publishing, Singapore, 2003.
- [188] S.N. Rudnick and D.K. Milton. Risk of indoor airborne infection transmission estimated from carbon dioxide concentration. *Indoor Air*, 13:237–245, 2003.

- [189] T. Smieszek. A mechanistic model of infection: why duration and intensity of contacts should be included in models of disease spread. *Theoretical Biology and Medical Modelling*, 6(25), 2009.
- [190] C-M Liao and C-F Chang ABD H-M Liang. A probabilistic transmission dynamic model to assess indoor airborne infection risks. *Risk Analysis*, 25(5), 2005.
- [191] A.D. Lemaire and M. Loomans. Particle concentration calculations using cfd - a comparison-. *Modelling Techniques*, 2000.
- [192] D.M. Lorenzetti. Predicting indoor pollutant concentrations and applications to air quality management. *Lawrence Berkeley National Laboratory*, 2002.
- [193] B. Jayaraman, E.U. Finlayson, E.E. Wood, T.L. Thatcher, M.D. Sohn, P.N. Price, R.G. Sextro, and A.J. Gadgil. Comparison between experiments and cfd predictions of mixed convection flows in an atrium. *Indoor Environment Department, Lawrence Berkeley National Laboratory, Berkeley, CA 94720, USA.*, 2005.
- [194] Z. Zhang and Q. Chen. Comparison of the eulerian and lagrangian methods for predicting particle transport in enclosed spaces. *Atmospheric Environment*, 41, 2007.
- [195] E.A. Nardell, J. Keegan, S.A. Cheney, and S.C. Etkind. Airborne infection : theoretical limits of protection achievable by building ventilation. *American Review of Respiratory Disease*, 144:302–306, 1991.
- [196] D. Vose. *Risk Analysis: A quantitative guide*. John Wiley & Sons, Chichester, 3rd edition, 2008.
- [197] P.F.M. Teunis and A.H. Havelaar. The beta poisson dose-response model is not a single-hit model. *Risk Analysis*, 20(4), 2000.
- [198] World Health Organization. Risk assessment of cryptosporidium in drinking water. Technical report, WHO, 2009.
- [199] P.F.M. Teunis and et al. Norwalk virus: How infectious is it? *Journal of Medical Virology*, 80:1468–1476, 2008.
- [200] J. Tu, G-H. Yeoh, and C. Liu. *Computational Fluid Dynamics: A practical approach*. Butterworth-Heinemann, 2005.

- [201] M. Loomans and T. Lemaire. Particle concentration calculations using cfd: a comparison. *TNO Building and Construction Research*, 2000.
- [202] E.A. Hathway, C.J. Noakes, P.A. Sleigh, and L.A. Fletcher. Cfd simulation of airborne pathogen transport due to human activities. *Building and Environment*, 46(12):2500–2511, 2011.
- [203] *CFD Validation Of Controlled Bioaerosol Release For Simulating Droplet Transmission Of Live Pathogens*, 2011. ISIAQ Indoor Air Quality and Climate Conference.
- [204] S.C. Sekhar and H.C. Willem. Impact of airflow profile on indoor air quality - a tropical study. *Building and Environment*, 39(3):255–266, 2004.
- [205] M. Loomans and A.D. Lemaire. Performance assessment of an operating theatre design using cfd simulation and tracer gas measurements. *Indoor and Built Environment*, 17:299–312, 2008.
- [206] I.T.S. Yu, Y. Li, T.W. Wong, W. Tam, A.T. Chan, J.H.W Lee, D.Y.C. Leung, and T. Ho. Evidence of airborne transmission of the severe acute respiratory syndrome virus. *New England Journal of Medicine*, 350(17):1731–1739, 2004.
- [207] T. Zhang and Q. Chen. Novel air distribution systems for commercial aircraft cabins. *Building and Environment*, 42(4):1675–1684, 2007.
- [208] C.P. Karthikeyan and A. Samuel. Co<sub>2</sub>-dispersion studies in an operation theatre under transient conditions. *Energy and Buildings*, 40, 2008.
- [209] C. Jin. A numerical simulation of particle deposition in turbulent pipe flow. *The school of Mechanical and Systems Engineering, Newcastle University*, 2000.
- [210] C. Narayanan and D. Lakehal. Mechanisms of particle deposition in a fully developed turbulent open channel flow. *Physics of Fluids*, 15(3), 2003.
- [211] T.J. Chang Y.F Hsieh H.M. Kao. Numerical study of the effect of ventilation pattern on coarse, fine and very fine particulate matter removal in partitioned indoor environment. *JAPCA J Air Waste Ma*, 57:179–189, 2007.
- [212] B. Zhao, Y. Zhang, X.T. Li, X.D. Yang, and D.T. Huang. Comparison of indoor aerosol particle concentration and deposition in different ventilated rooms by numerical method. *Building and Environment*, 39:1–8, 2004.

- [213] A. Lai and F. Chen. Modeling particle deposition and distribution in a chamber with a two-equation reynolds-averaged navier-stokes model. *Journal of Aerosol Science*, 37:1770–1780, 2006.
- [214] E. Bjørn and P.V. Nielsen. Dispersal of exhaled air and personal exposure in displacement ventilated rooms. *Indoor Air*, 12(3):147–164, 2002.
- [215] C.A. Gilkeson, C.J. Noakes, P.A. Sleight, A.I. Khan, and M.A. Camargo-Valero AND. Simulating pathogen transport within a naturally ventilated hospital ward. *World Academy of Science, Engineering and Technology*, 55:119–125, 2011.
- [216] Luke D. Knibbs, Lidia Morawska, Scott C. Bell, and Piotr Grzybowski. Room ventilation and the risk of airborne infection transmission in 3ăhealth care settings within a large teaching hospital. *American Journal of Infection Control*, 39(10):866 – 872, 2011.
- [217] A.C.K. Lai and W.W. Nazaroff. Modelling indoor particle deposition from turbulent flow onto smooth surface. *Indoor Environment Department*, 51(4):463–473, 2000.
- [218] C.C. Kibbler, A. Quick, and A.M. O’Neill. The effect of increased bed numbers on mrsa transmission in acute medical wards. *Journal of Hospital Infection*, 39: 213–219, 1998.
- [219] C.J. Noakes, L.A. Fletcher, C.B. Beggs, P.A. Sleight, and K.G. Kerr. Development of a numerical model to simulate the biological inactivation of airborne micro-organisms in the presence of ultraviolet light. *Journal Aerosol Science*, 35:489–507, 2004.
- [220] C. Wilcox. *Turbulence Modeling for CFD*. D C W Industries, 2nd edition edition, December 2002.
- [221] B. E. Launder and D. B. Spalding. Mathematical models of turbulence. *Journal of Sound and Vibration*, 25(4):651–651, 1972.
- [222] J. Boussinesq. Theorie de l’ecoulement toubillant. *Mem. Acad. Sci.*, 23(46), 1877.
- [223] ANSYS Inc. *ANSYS Theory Guide*, 2011.
- [224] J. Tu, G.H. Yeoh, and L. Chaoqun. *Computational Fluid Dynamics; A Practical Approach*. Butterworth-Heinemann, 2003.

- [225] D.C. Wilcox. *Turbulence Modeling for CFD*. DCW Industries, 1994.
- [226] J. Kim, P. Moin, and R.D. Moser. Turbulent statistics in fully developed channel flow at low reynolds-number. *J. of Fluids Mechanics*, 177:133–166, 1987.
- [227] *ANSYS Fluent-Solver Theory Guide*. ANSYS Europe, Ltd., ansys fluent release 12.0 edition, 1996-20010.
- [228] ANSYS Inc. *ANSYS User Manual*, 2011.
- [229] J.W. Gibbs. Fourier series. *Nature*, 59(200), 1898.
- [230] F. Bauman and A. Daly. Underfloor air distribution. (*UFAD*) *design guide ASHRAE*, 2003.
- [231] J. Srebric, V. Vukovic, G. He, and X. Yang. Cfd boundary conditions for contaminant dispersion, heat transfer and airflow simulations around human occupants in indoor environments. *Building and Environment*, 43(3):294 – 303, 2008. Indoor Air 2005: Modeling, Assessment, and Control of Indoor Air Quality.
- [232] Q. Chen and J. Srebric. Simplified diffuser boundary conditions for numerical room airflow models. Technical report, ASHRAE, 2001.
- [233] T. Zhang, K.S. Lee, and Q. Chen. A simplified approach to describe complex diffusers in displacement ventilation for cfd simulations. *Indoor Air*, 19(3), 2009.
- [234] F.E. Jorgensen. *How to measure turbulence with hot-wire anemometers - a practical guide*. Dantec Dynamics A/S, 2002.
- [235] J. Taylor. *An introduction to Error Analysis: The study of uncertainties in Physical Measurements*. University Science Books, 1977.
- [236] A. Dehbi. Assessment of a new fluent model for particle dispersion in turbulent flows. *OECD Technical Report*, 39, 2007.
- [237] P.J. Roache. Quantification of uncertainty in computational fluid dynamics. *Annual Rev. Fluid. Mech.*, 29:123–60, 1999.
- [238] W. Lach. Performance of the surface air system air samplers. *Journal of Hospital Infection*, 6:102–107, 1985.

- [239] W.H. Ching, M.K.H. Leung, D.Y.C. Leung, and Y. Li. Reducing risk of airborne transmitted infection in hospitals by use of hospital curtains. *Indoor and Built Environment*, 17(3):252–259, 2008.
- [240] K. Roberts. *The aerial dissemination of Clostridium difficile in the clinical environment*. PhD thesis, Civil Engineering, Leeds University, 2008.
- [241] B. Allegranzi and D. Pittet. Role of hand hygiene in healthcare-associated infection prevention. *Journal of Hospital Infection*, 73:305–315, 2009.
- [242] C. Fuller, J. Savage, and et al. The dirty hand in the latex glove: A study of hand hygiene compliance when gloves are worn. *Infection Control and Hospital Epidemiology*, 32(12):1194–1199, 2011.
- [243] Erol Kohli, Judy Ptak, Randall Smith, Eileen Taylor, Elizabeth A. Talbot, and Kathryn B. Kirkland. Variability in the Hawthorne effect with regard to hand hygiene performance in high and low performing inpatient care units. *Infection Control and Hospital Epidemiology*, 30(3):222–225, 2009.
- [244] J.P. Haas and E.L. Larson. Measurement of compliance with hand hygiene. *Journal of Hospital Infection*, 66(1):6 – 14, 2007.
- [245] M. McGuckin. Hand hygiene compliance rates in the United States—a one-year multi-center collaboration using product/volume usage measurement and feedback. *American Journal of Medical Quality*, 24(205):205–213, 2009.
- [246] B. Fitzsimons and A. Bartley J. Cornwell. Intentional rounding: its role in supporting essential care. *Nursing Times*, 107(27):18–19, 2011.
- [247] J.D. Gibbons. *Nonparametric Statistical Inference*. Marcel Dekker, New York, 1985.
- [248] M.D.A. Carlson and R.S. Morrison. Study design, precision, and validity in observational studies. *J Palliat Med*, 12(1):77–82, 2009.
- [249] E. Larson. Effects of handwashing agent, handwashing frequency, and clinical area on hand flora. *American Journal of Infection Control*, 12(2):76 – 82, 1984.
- [250] Pessoa-Silva, Carmem, Sasi Dharan, Stéphane Hugonnet, Sylvie Touveneau, Posfay-Barbe, Klara, Riccardo Pfister, and Didier Pittet. Dynamics of bacterial hand contamination during routine neonatal care. *Infection control and hospital epidemiology*:

- The official journal of the Society of Hospital Epidemiologists of America*, 25(3):192–197, 2004.
- [251] A. Hay. The evolution of human influenza viruses. *Philos Trans R Soc Lond B Biol Sci*, 356 (1416):1861–70, 2001.
- [252] E. McBryde, AND L. Bradley, M. Whitby, and D. McElwain. An investigation of contact transmission of methicillin-resistant staphylococcus aureus. *The Journal of hospital infection*, 58(2):104–108, 2004.
- [253] S.A. Sattar, S. Springthorpe, S. Mani, M. Gallant, R.C. Nair, E. Scott, and J. Kain. Transfer of bacteria from fabrics to hands and other fabrics: development and application of a quantitative method using staphylococcus aureus as a model. *Journal of Applied Microbiology*, 90(6):962–970, 2001.
- [254] G. Glen, V. Zartarian, L. Smith, and J. Xue. *The Stochastic Human Exposure and Dose Simulation Model for Multimedia, Multipathway Chemicals (SHEDS-Multimedia): Residential Module SHEDS-Residential version 4*. US Environmental Protection Agency Office of Research and Development, National Exposure Research Laboratory, 2012.
- [255] T. Schneider, R. Vermeulen, D.H. Brouwer, J.W. Cherrie, H. Kromhout, and C.L. Fogh. Conceptual model for assessment of dermal exposure. *Occup Environ Med*, 56:765–773, 1999.
- [256] B. Van-Wendel-de-Joode, D.H. Brouwer, R. Vermeulen, D. Heenderik J.J. van Hemmen, and H. Kromhout. Dream: A method for semi-quantitative dermal exposure assessment. *Ann Occup Hyg*, 47(1):71–87, 2003.
- [257] D. W. Schaffner. *Models: what comes after the next generation?* CRC Press Inc., Boca Raton FL, 2003.
- [258] V. Sébille and A. Valleron. A computer simulation model for the spread of nosocomial infections caused by multidrug-resistant pathogens. *Computers and biomedical research, an international journal*, 30(4):307–322, 1997.
- [259] F. Perez-Rodriguez, A. Valero, E. Carrasco, R.Ma. Garcia, and G. Zurera. Understanding and modelling bacterial transfer to foods: a review. *Trends in Food Science & Technology*, 19(3):131 – 144, 2008.

- [260] E.D. den Aantrekker, R.M Boom, and M.H. Zwietering M. van Schothorst. Quantifying recontamination through factory environments: a review. *International Journal of Food Microbiology*, 80(2):117 – 130, 2003.
- [261] V.A. Zartarian, J. Xue, H. Özkaynak, D. Winston, G. Graham, L. Smith, and C. Stallings. A probabilistic arsenic exposure assessment for children who contact cca-treated playsets and decks, part 1: Model methodology, variability results, and model evaluation. *Risk Analysis*, 26(2):515–531, 2006.
- [262] V.A. Zartarian, J. Xue, H. Özkaynak, D. Winston, G. Graham, L. Smith, and C. Stallings. A probabilistic arsenic exposure assessment for children who contact chromated copper arsenate (cca)-treated playsets and decks, part 2: Sensitivity and uncertainty analyses. *Risk Analysis*, 26(2):533–541, 2006.
- [263] Exposure Modelling Subcommittee of the IPCS Harmonization Project Exposure Assessment. *Principles of characterizing and applying human exposure models*. World Health Organization, Geneva, 2004.
- [264] A. Saltelli et al. *Global Sensitivity Analysis: The Primer*. John Wiley & Sons, 2008.
- [265] Mathworks Inc. Runttest. <http://www.mathworks.co.uk/help/stats/runstest.html>, Accessed:05/04/13.
- [266] B. Efron and R. Tibshirani. *An Introduction to the Bootstrap*. Chapman and Hall, London, 1993.
- [267] C.D. Manning, P. Raghavan, and M. Schütze. *Introduction to Information Retrieval*. Cambridge University Press, 2008.
- [268] I. Teodorescu. Maximum likelihood estimation for markov chains. Report, <http://arxiv.org/abs/0905.4131v1>, Cornell University, May 2009.
- [269] R. Montville and D.W. Schaffner. Inoculum size influences bacterial cross contamination between surfaces. *Applied and Environmental Microbiology*, 69(12):7188–7193, 2003.
- [270] R. Canales and J. Leckie. Algorithm for using contact specific surface area estimates in dermal exposure models. *Journal of Child Health*, 2(3-4):345–362, 2004.

- [271] D.H. Brouwer, R. Kroese, and J.J. Van Hemmen. Transfer of contaminants from surface to hands: Experimental assessment of linearity of the exposure process, adherence to the skin, and area exposed during fixed pressure and repeated contact with surfaces contaminated with a powder. *Applied Occupational and Environmental Hygiene*, 14:231–239, 1999.
- [272] J. A. Otter, S.Yezli, and G.L.French. The role played by contaminated surfaces in the transmission of nosocomial pathogens. *Infection Control and Hospital Epidemiology*, 32(7):687–699, 2011.
- [273] N. Neely and M.P. Maley. Survival of enterococci and staphylococci on hospital fabrics and plastics. *J Clin Microbiol*, 38(4):724–726, 2003.
- [274] G.A. Noskin, V. Stosor, I. Cooper, and L.R. Peterson. Recovery of vancomycin-resistant enterococci on fingertips and environmental surfaces. *Infection control and epidemiology*, 16(10):577–581, 1995.
- [275] P. Rusin, S. Maxwell, and C. Gerba. Comparative surface-to-hand and fingertip-to-mouth transfer efficiency of gram-positive bacteria, gram-negative bacteria, and phage. *Journal of Applied Microbiology*, 93(4):585–592, 2002.
- [276] A.F. Widmer. Replace hand washing with use of a waterless alcohol hand rub? *Clinical Infectious Disease*, 31:136–143, 2000.
- [277] N.P. Boks, W. Norde, H.C. van der Mei, and H.J. Busscher. Forces involved in bacterial adhesion to hydrophilic and hydrophobic surface. *Microbiology*, 154(10):3122–3133, 2008.
- [278] A. McDonagh, R.G. Sextro, and M.A.Byrne. Mass transport of deposited particles by surface-to-surface contact. *Journal of Hazardous Materials*, 227:370–377, 2012.
- [279] R. Montville, Y. Chen, and D.W. Schaffner. Glove barriers to bacterial cross-contamination between hands to food. *Journal of Food Protection*, 64(6):845–849, 2001.
- [280] E. J. Fendler, M. J. Dolan, R. A. Williams, and D. S. Paulson. Handwashing and gloving for food protection. part ii. effectiveness. *Dairy Food Environ. Sanit.*, 18:824–829, 1998.

- [281] E.E. Sickbert-Bennett, D.J. Weber, M.F. Gergen-Teague, M.D. Sobsey, G.P. Samsa, and W.A. Rutala. Comparative efficacy of hand hygiene agents in the reduction of bacteria and viruses. *American Journal of Infection Control*, 33(2):67 – 77, 2005.
- [282] E. Girou, S. Loyeau, P. Legrand, F. Oppein, and C. Brun-Buisson. Efficacy of hand-drubbing with alcohol based solution versus standard handwashing with antiseptic soap: randomised clinical trial. *BMJ British Medical Journal*, 325(7360):362–367, 2002.
- [283] M. Rotter. *Hand washing and hand disinfection*. Williams and Wilkins, Baltimore, 2 edition, 1999.
- [284] D.J. Weber, W.A. Rutula, M.B. Miller, K. Huslage, and E. Sickbert-Bennett. Efficacy of selected hand hygiene agents used to remove *Bacillus atrophaeus* (a surrogate of *Bacillus anthracis*) from contaminated hands. *Journal of the American Medical Association*, 289(10):1274–1277, 2003.
- [285] J.-C. Lucet, M.-P. Rigaud, F. Mentrey, N. Kassisz, C. Deblangy, A. Andremontzx, and E. Bouvet. Hand contamination before and after different hand hygiene techniques: a randomized clinical trial. *Journal of Hospital Infection*, 50:276–280, 2002.
- [286] I. Dimov and R. Georgieva. Monte carlo algorithms for evaluating sobol sensitivity indices. *Mathematics and Computers in Simulation*, 81(3):506 – 514, 2010.
- [287] A. Saltelli and P. Annoni. How to avoid a perfunctory sensitivity analysis. *Environmental Modelling & Software*, 25(12):1508 – 1517, 2010.
- [288] NHS Choices. Mrsa infection - screening. <http://www.nhs.uk/Conditions/MRSA/Pages/MRSAscreeningwhattoexpect.aspx>, Accessed:14/05/2013.
- [289] J. P. Mitchell. *Aerosol Generation for Instrument calibration: Bioaerosols handbook*. Lewis Publishers, New York, 1995.
- [290] B. Welz and M. Sperling. *Atomic Absorption Spectrometry*. Wiley-VCH, Weinheim, Germany, 1999.